GEOCHEMISTRY OF THE MURRUMBIDGEE BATHOLITH

by

A.S. Joyce

February, 1970

A thesis submitted as a requirement for admission to the Degree of Doctor of Philosophy of the Australian National University.

The assistance and guidance given to the author by various people are detailed in the acknowledgements. Except where otherwise indicated, all results presented in this thesis are the author's own, as are all conclusions drawn from the data.

Signed .....A.S.Joyce.....
(A.S. Joyce)

ACKNOWLEDGEMENTS

The author gratefully acknowledges the guidance of his supervisor, Dr B.W. Chappell, particularly with X-ray fluorescence techniques.

Dr A.J.R. White provided assistance and encouragement during this study and discussed the final draft extensively. He also provided the opportunity for the author to examine inaccessible areas of the batholith from a light aircraft.

Mr J. Wasik provided instruction and assistance in mineral separation and assisted at various times with procedures of wet chemical analysis.

Mr J. Pennington provided instruction and assistance with X-ray fluorescence and diffraction techniques.

The competence and co-operation of Mr R.A. Cliff and the technical staff in providing technical facilities are appreciated.

Mr T. Quinlan provided a computer program written by W.R. Morgan to calculate CIPW norms and this was adapted by the author for use on the Australian National University computer.

The author's fellow research students provided much discussion on topics of mutual interest. Mr J.M. Rhodes introduced the author to computer programming and provided several of the computer programs used in the preparation of this thesis. Mr I.A. Crain solved some programming problems.

My wife provided invaluable assistance at all stages of the work in calculating results, compiling tables and diagrams, and typing the

initial and final drafts of the thesis.

This research has been conducted in the Department of Geology at the Australian National University, and the author gratefully acknowledges Professor D.A. Brown for providing excellent facilities.

Financial support was provided by a Commonwealth Post-graduate Award and by supplementary allowances from the Australian National University.

CONTENTS

A geological map is in a folder at the back of the thesis.

1. INTRODUCTION

Nature and scope of investigation

Many granites* contain dark xenoliths which are thought to have been responsible for at least some of the compositional variation of their host rocks. Many of these xenoliths seem to be derived from basic igneous material and Chappell (1966) has interpreted their world-wide distribution and general similarities as implying that they are derived from a common source and represent cognate, relict material with direct bearing on the ultimate source of granitic magmas. In contrast, large volumes of other granites (Brammall & Harwood, 1932; Vallance, 1969) contain xenoliths apparently derived from a sedimentary source.

In addition to quartz and feldspar, the granites containing basic igneous xenoliths are characterised by biotite, hornblende and pyroxene, whereas granites containing sedimentary xenoliths typically contain biotite and muscovite and are notably deficient in hornblende and pyroxene. Aluminous minerals such as andalusite, cordierite and garnet are common trace constituents of the latter granites but rare in the former type. In view of the distinctions between these two granite types, the question arises whether they originated in different ways.

One example of granites containing abundant sedimentary xenoliths is provided by the Murrumbidgee Batholith which crops out over an area of about 1400 km^2, south-west of Canberra, A.C.T. It consists of many

* In this thesis, the term 'granite' is used in the broad sense (c.f. Hatch *et al.*, 1961) to refer to the whole family of granitoid rocks, except where the context indicates otherwise.

discrete granitic intrusions ranging from tonalite to leucogranite and Snelling (1957, 1960) delineated nine separate components in excess of 5 km^2 and noted numerous minor intrusions. He divided the rocks into three groups, "uncontaminated granites", "contaminated granites" and "potassic leucogranites", but considered them all to be petrogenetically related. The aim of this investigation has been to define the nature and extent of chemical, modal and mineralogical variation within this batholith and to assemble significant features which may be used as controls in examining the petrogenesis of the rocks.

The batholith shows a close spatial and temporal association with the Cooma granite (Browne, 1943; Pidgeon & Compston, 1965) which also contains metasedimentary xenoliths, but which occurs in a localised, high-grade metamorphic environment in contrast to the low-grade environment of the Murrumbidgee Batholith. The Cooma granite has been interpreted as being consistent with generation essentially in situ by the melting of high-grade metasedimentary material (Pidgeon & Compston, 1965). Its significance in relation to the Murrumbidgee Batholith is examined in the final chapter.

Previous information

Investigations prior to 1957 were summarised by Snelling (1957, 1960). The most significant contributions were those of Browne (1914, 1943), supplemented by Joplin (1943), concerning the south-eastern extremity of the batholith. A map showing the full extent of the batholith was first prepared by Legge (1937) and modifications are shown on subsequent Bureau of Mineral Resources 1:250,000 geological

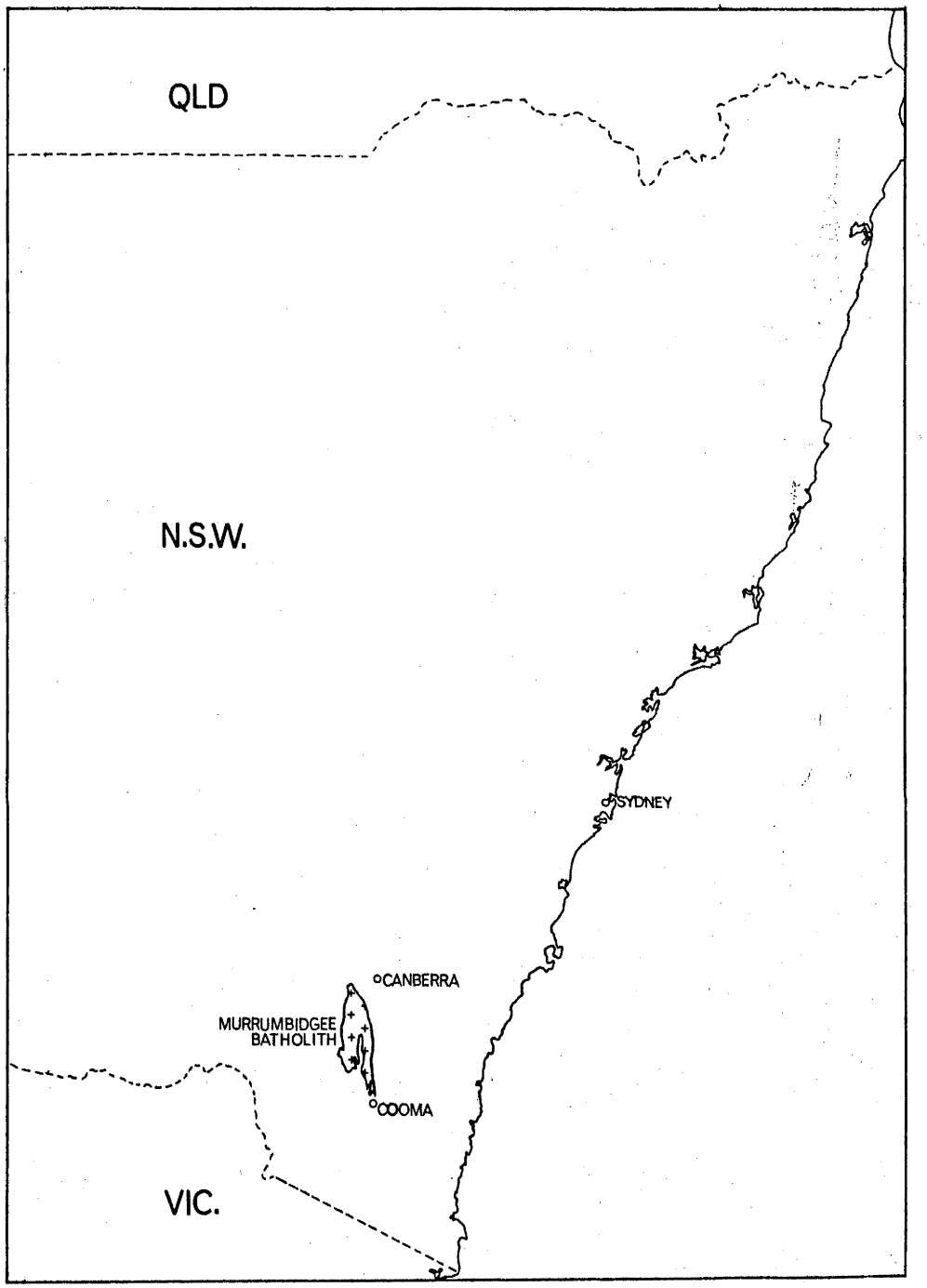

Figure 1. Locality Map

sheets.

Snelling (1957, 1960) provided the most extensive contribution on the batholith as a whole by mapping internal as well as external contacts of the batholith and examining details of petrology.

Subsequent contributions have been concerned with radiometric dating of the batholith (Evernden & Richards, 1962; Joplin, 1962; Pidgeon & Compston, 1965).

One of the leucogranites of the batholith is included in a geochemical study by Kolbe & Taylor (1966).

2. FIELD RELATIONSHIPS

Setting

The Murrumbidgee Batholith is set in the Palaeozoic Lachlan Geosyncline, the southern portion of the Tasman Orthogeosyncline (Packham, 1960) extending along the eastern side of Australia. Within the Tasman Geosyncline the main area of sedimentary deposition appears to have migrated with time to the north-north-east and Brown (1933) was the first to suggest a progression of igneous activity also in this direction with time.

Browne (1929 and in David, 1950) divided the granites in N.S.W. into three types on the basis of field characteristics and associated metamorphism, and interpreted them as representing Ordovician, Silurian and post-Silurian activity. Evernden & Richards (1962) and Joplin (1962) agreed that "gneissic", "foliated" and "massive" types are recognisable but K/Ar geochronology by Evernden & Richards indicated that the three types overlap in time and were emplaced in the time interval Middle Silurian to Middle Devonian. There is an apparent eastward movement of the axis of intrusion with time and Joplin (1962) has integrated the three-fold division of the granites with their geochronology into an hypothesis of a magmatic cycle within the Tasman Geosyncline.

The Murrumbidgee Batholith intrudes Upper Ordovician and Silurian rocks (Browne, 1943) and is overlain by Tertiary basalts and Pleistocene deposits. The Ordovician rocks consist of low grade metamorphic shales and sandstones and the Silurian rocks of calcareous shales, sandstones, and acid volcanic types.

Age of the batholith and its components

The batholith is intrusive into low grade regionally metamorphosed sandstones and shales near Cooma identified as Upper Ordovician on the basis of graptolites, including Diplograptus bicornis Hall (Browne, 1931). Comparable sandstones and shales, apparently unfossiliferous, crop out in the axis of the batholith and along its western margin. The eastern margin of the batholith is in faulted contact with acid volcanic rocks, fine sandstones, calcareous shales and pods of limestone. Fossils recorded by Browne (1943) indicate a Silurian age for these rocks (Encrinurus mitchelli Eth. fil., Alveolites sp., Favosites sp., Heliolites sp., Hercophyllum shearsbyi Sussmilch, "Cystiphyllum" sp., Mucophyllum crateroides Eth. fil., and Favosites allani Jones).

Pleistocene lake deposits and alluvium and several small outcrops of Tertiary basalt overly the batholith. Browne (1943) concluded that the batholith was intruded at the close of the Silurian and Snelling (1960), by comparison with detailed stratigraphic studies by Opik (1958) in the Canberra region, deduced that emplacement occurred during or immediately after the Bowning orogeny (lower Ludlow).

Using K/Ar dating methods on biotites Evernden & Richards (1962) obtained ages of 348 and 376 million years on two samples of Tharwa Adamellite and 396 million years on a sample of Shannons Flat Adamellite. The age of 396 million years was considered by them to be the more reliable estimate of the age of the batholith since both of the Tharwa Adamellite samples showed obvious shearing, related to the Murrumbidgee Fault, and were thus subject to argon loss.

Additional geochronology was carried out by Pidgeon & Compston (1965), who obtained an age of 417 million years for a sample of Shannons Flat Adamellite using Rb/Sr methods on total rock, microcline and biotite. For comparison purposes Pidgeon & Compston (1965) published a set of biotite and muscovite ages determined by them using Rb/Sr methods and by Richards using K/Ar methods. One sample was the biotite from the Shannons Flat Adamellite and the ages obtained were 404 million years by K/Ar and between 415 and 404 million years (depending on an assumed range of the initial ratio Sr^{87}/Sr^{86}) by Rb/Sr. Thus, an age of around 417 million years for the Shannons Flat Adamellite appears reliable. This is comparable to the age of 415±12 million years determined for the Cooma granite (Pidgeon & Compston, 1965) which was previously considered to be notably older than the Murrumbidgee Batholith and which, in fact, is intruded by it. Those authors place these ages as lower or middle Devonian in terms of the geological time scale.

Within the batholith (defining its limits as the Cotter, Winslade and Murrumbidgee faults and the vicinity of the Murrumbidgee River in the south) nine named intrusions have been mapped, as well as stocks, bosses and dykes of unnamed microgranites. Their distribution is shown on the accompanying geological map and their outcrop areas and apparent order of intrusion are summarised below:

Youngest

Stewartsfield Granodiorite (about 5 km^2)	Stocks, bosses and dykes of microgranite (total about 55 km^2)

Yaouk Leucogranite (145 km.^{2})

Tharwa Adamellite (45 km.^{2})

Westerly Muscovite Granite (6 km.^{2})

Bolairo, Callemondah and Clear Range granodiorites (8 km.^{2}) (22 km.^{2}) (440 km.^{2})

Willoona Tonalite (8 km^2)

Shannons Flat Adamellite (655 km.^{2})

Oldest

Although contacts between intrusions can be located typically to within a few metres, actual intrusive relationships between the medium or coarse-grained granites are usually obscured by weathering (much more so than granite/hornfels or microgranite/coarser granite contacts). Thus, age relationships must be inferred mainly from the general shapes of the intrusions and the curvature of their mutual boundaries. The deduced sequence of emplacement is based on the following evidence:

1. the gently curving eastern margin of the Shannons Flat Adamellite is disrupted by the convex north-western margin of the Callemondah Granodiorite.

2. the dyke-like Willoona Tonalite intrudes the outcrop pattern of the Shannons Flat Adamellite and truncates its faulted southern boundary.

3. the north-western margin of the Clear Range Granodiorite is convex towards the Shannons Flat Adamellite.

4. in an outcrop west of 'Long Flat' Homestead the Clear Range Granodiorite is finer grained than usual where it is within several feet of its contact with porphyritic, coarse-grained Shannons Flat

Adamellite which, in turn, contrasts with the finer nature of the marginal Shannons Flat Adamellite observed near its contact with hornfels at the entrance to Orroral Valley and near 'Gudgenby' Homestead (such grainsize variation alone must be regarded with caution because some marginal, unfaulted areas of Shannons Flat Adamellite are coarse-grained immediately adjacent to hornfels).

5. the dyke-like Tharwa Adamellite distinctly interrupts the shape of both the Shannons Flat Adamellite and the Clear Range Granodiorite.

6. an outcrop of Tharwa Adamellite intruding Clear Range Granodiorite has been observed in the Naas River.

7. the dyke-like Westerly Muscovite Granite truncates the curving shape of the Bolairo Granodiorite.

8. the Yaouk Leucogranite interrupts the shape of the Shannons Flat Adamellite and truncates the fault which forms the northern margin of both the Westerly Muscovite Granite and the Bolairo Granodiorite. In contrast to the Yaouk Leucogranite and other intrusions, the Westerly Muscovite Granite is essentially unfoliated, possibly implying that it belongs to a later period of emplacement. However, the absence of foliation may find an explanation in the tough, aplitic texture of the intrusion.

9. unlike most other components of the batholith, and despite its proximity to the Cotter Fault, the medium-grained Stewartsfield Granodiorite has little consistent foliation or shearing, thereby implying that it succeeded the period of compression operating

during emplacement of most of the intrusions.

10. stocks, bosses and dykes of microgranite clearly intrude all components of the batholith (especially the Shannons Flat Adamellite and the Tharwa Adamellite).

Metamorphism

The Ordovician country rocks in the vicinity of the batholith have undergone low grade regional metamorphism prior to emplacement of the batholith and consist of slates, phyllites and recrystallised fine quartz sandstones containing chlorite and muscovite. Adjacent to intrusive borders of the batholith a zone of thermal metamorphism about 100 metres in width is evident from the presence of biotite and a recrystallised texture which is fairly resistant to weathering.

The north-eastern margin of the Shannons Flat Adamellite intrudes volcanic rocks with interbedded pods of limestones and sedimentary rocks. Reaction between these limestones and the adjacent intrusion has given rise to several skarn deposits, the largest of which is located near the junction of the Cotter and Paddys rivers.

The south-eastern end of the batholith intrudes the higher grade regional metamorphic rocks of the Cooma Complex and its effect there has been minor retrogressive metamorphism of the highest grade rocks (Joplin 1943).

Foliation

Foliation is a characteristic feature of all components of the batholith with the exception of the aplitic leucogranite stocks and dykes. It is most conspicuous in the contaminated granites, because of their high biotite content, but is nevertheless recognisable throughout

the less mafic Shannons Flat Adamellite. The Tharwa Adamellite is heavily sheared.

The foliation is roughly constant throughout the batholith, striking just west of north and dipping steeply eastwards. Many discoid xenoliths within the contaminated granites are aligned parallel to the foliation indicating a primary origin. However, the stresses responsible for the foliation continued after crystallisation of the rocks, since all show conspicuous evidence of shearing and strain in their component minerals (e.g. the blue quartz of the contaminated granites). There is a clear relationship between the foliation and the Cotter and Murrumbidgee faults since its orientation is subparallel to the fault planes and its intensity increases very markedly east and west from the centre of the batholith towards the faults. The eastern margins of the Tharwa Adamellite and the Clear Range Granodiorite are conspicuously sheared, as is the western margin of the Shannons Flat Adamellite in the vicinity of its contact with the Yaouk Leucogranite, which is itself foliated.

Mechanics of emplacement

Browne (1943) first pointed out that the batholith is clearly unrelated to the widespread regional metamorphism of the Ordovician rocks and was evidently emplaced much later, as has been substantiated by Snelling (1957, 1960) and Pidgeon & Compston (1965). The batholith was seen as a synchronous type by Browne (1943) and both he and Snelling (1960) have interpreted the internal structures of the batholith as products of east-west compression.

Faulting has played a major role in the emplacement of the batholith. The western margins of the eastern tongue of the batholith dip eastwards, a feature discussed by Browne (1943) who concluded 'that the shape assumed by the intrusion was conditioned by either folding or faulting'. Conspicuous major faults define the eastern, western and northern limits of the batholith and regular large fault systems are conspicuous within the batholith itself. The Murrumbidgee Fault, which determines the eastern limits of the Tharwa Adamellite and the Clear Range Granodiorite, extends the full length of the batholith and is a steep easterly dipping normal fault with a sinistral transcurrent component. It was active during and after consolidation of the batholith. The Cotter Fault to the west appears to be essentially vertical and shows a nine kilometre apparent dextral offset of leucogranites near the Cotter Rangers Hut. Prominent regular patterns of faults within the batholith strike south-east on the western side and south-west on the eastern side of the batholith.

Nevertheless, unequivocable intrusive contacts are exposed against the Ordovician metasedimentary septum between the Clear Range Granodiorite and the Shannons Flat Adamellite, against Ordovician metasediments and Silurian volcanics in the northern part of the batholith, and against Ordovician metasediments in the south-western region. These contacts are locally discordant with the structures of the country rocks but on a regional scale the major components of the batholith are elongate bodies concordant with the regional strike of the country rocks. Contacts curve gently over long distances with no

evidence of marginal shattering and veining. These features are consistent with forcible emplacement by wedging upwards along weaknesses, such as fold axes in the metasediments. Probably this upward thrust initiated the Cotter and Murrumbidgee faults which parallel the primary foliation of the batholith and upward movement continued by block faulting on these planes after crystallisation of the intrusions, leading to development of a cataclastic foliation parallel to the primary foliation. In occasional specimens, for example in the Tharwa Adamellite near Castle Hill, two subparallel foliations can be recognised but, in any case, the coincidence of primary foliation, defined by discoid xenoliths (with unsheared margins), and cataclastic foliation testifies to the existence of essentially the same stress field before and after crystallisation. Lack of regular cataclastic foliation in the aplitic leucogranites need not imply that they succeed the faulting since they are restricted mainly to the centre of the batholith, away from the major shearing stresses, and also because their fine equigranular texture constitutes a tougher rock type than the enclosing coarse grained Shannons Flat Adamellite.

3. PETROGRAPHY

The petrography of the batholith has been discussed by Snelling (1957, 1960) and its treatment here will be restricted to a brief summary of the pertinent features and comments on peculiarities not recorded or not emphasised by Snelling.

On the basis of field characteristics and inferred genetic relationships, Snelling divided the rocks into three groups - uncontaminated granites, contaminated granites and potassic leucogranites. Whilst inferred genetic relationships are undesirable for descriptive classification, the features of the groups are sufficiently distinctive to warrant their use. Therefore, Snelling's grouping and terminology is retained but with the proviso that the terms "uncontaminated" and "contaminated" are taken to mean respectively poor in sedimentary xenoliths and rich in sedimentary xenoliths (and in that sense contaminated regardless of whether significant reaction has occurred between xenoliths and magma).

The uncontaminated granites

This group consists of the Shannons Flat Adamellite and the Tharwa Adamellite, both of which are coarse-grained and poor in xenoliths.

The Shannons Flat Adamellite is a coarse-grained adamellite conspicuously porphyritic in microcline crystals up to 4 cm in length. Snelling regarded the rock as typically massive but most areas are recognisably foliated despite the fact that this feature is less conspicuous than in the contaminated granites, where it is emphasised by the abundant dark xenoliths and biotite. The primary minerals are

quartz, microcline, plagioclase and brown biotite, all showing strain effects to varying degrees from one specimen to another. The chemistry of these minerals will be discussed subsequently. Minor accessory minerals are apatite, pyrite and zircon. Secondary minerals formed by breakdown of plagioclase and biotite are common. The cores of many plagioclase grains are altered to sericite and epidote whilst some biotite is altered to chlorite and epidote. A common type of biotite alteration, especially in the most sheared specimens, consists of marginal alteration to fine-grained muscovite, magnetite, ilmenite and quartz. Such production of muscovite may be related to the high aluminium content of the Shannons Flat Adamellite biotites and will be discussed more fully in the section on mineral chemistry. A few samples (e.g. 20505, 20508) appear to contain rare, large flakes of primary muscovite.

The Tharwa Adamellite differs from the Shannons Flat Adamellite primarily in having a greater abundance of microcline and a conspicuously sheared texture.

Xenoliths occur sparsely in the Tharwa Adamellite but are rare in the Shannons Flat Adamellite.

The contaminated granites

The contaminated granites are a group of fine to medium grained rocks consisting mainly of quartz, feldspar and brown biotite and characterised by conspicuous foliation, blue quartz and abundant finer grained biotite-rich xenoliths. Overall they range from granodiorite to tonalite but individual intrusions have fairly restricted compositions.

Muscovite is a notable constituent of these rocks, occurring as an apparently primary mineral as well as an alteration product of both biotite and plagioclase in the same manner as in the uncontaminated granites. Muscovite is a mineral more frequently encountered in acid granites than tonalites and granodiorites and its presence is a reflection of the rather high aluminium content of all the components of the batholith.

The south-eastern extremity of the batholith, designated by Snelling (1957, 1960) as Murrumbucka Tonalite, is similar to the other contaminated granodiorites and tonalites, but unique in possessing hornblende-rich xenoliths, in addition to the biotite rich xenoliths typical of the other intrusions, together with accessory hornblende.

Leucogranites

Rocks included in this group differ widely in texture but are generally granites in the strict sense and are poor in mafic minerals.

The largest leucogranite, the Yaouk Leucogranite, consists of tabular microcline phenocrysts up to 6 cm in length set in a coarse groundmass of quartz, microcline, plagioclase, biotite and muscovite. The rock possesses a cataclastic foliation. Smaller bodies of porphyritic microgranite and aplitic leucogranites form dykes and small stocks mainly in the uncontaminated granites. These granites differ from the Yaouk Leucogranite in being massive and having a finer aplitic texture but possess the same mineralogy. The aplitic Westerly Muscovite Granite adjacent to the Adaminaby road contains about one per cent of garnet, a mineral not previously recorded in the Murrumbidgee Batholith. An unnamed leucogranite (20573) also contains garnet.

Modes and classification of the rocks

There are shortcomings in several formation names applied by Snelling (1957, 1960) and it is regarded as important to revise his terminology in order to place proper emphasis on the various mineralogical and chemical features of the batholith. The existing formation names imply that granodiorite dominates the batholith whereas, in fact, adamellite dominates over granodiorite and tonalite is also more abundant than previously inferred.

The most important discrepancy in terminology refers to the Shannons Flat Granodiorite which accounts for about 675 of the total 1400 square kilometres of the batholith. Snelling (1960) recorded an average of 19 modes as quartz 36.0 per cent, microcline 21 per cent, plagioclase 34.7 per cent and biotite 8.3 per cent. This mode has a microcline to total feldspar ratio of 37.7, thereby qualifying as granodiorite according to Nockolds (1954) classification but as adamellite according to others (e.g. Hatch et al., 1961). Snelling (1960) commented, on the basis of chemical analyses, that the 'Shannons Flat granodiorite is more acid than the average composition of biotite granodiorite (Nockolds, 1954) and is also characterised by a higher ratio of potash to soda' and that its composition closely resembles that of the Tharwa Adamellite which in turn compares fairly well with Nockolds' (1954) average biotite adamellite. New modal data recorded in table 3 indicate that Snelling underestimated the microcline content and the rocks clearly should be classified as adamellite, so throughout this thesis the name "Shannons Flat Granodiorite" has been replaced by

"Shannons Flat Adamellite".

The classification and nomenclature of all intrusions have been reassessed according to Nockolds' (1954) mineralogical criteria, and the name "Willoona Granodiorite" has been changed to "Willoona Tonalite". In defence of this particular revision, since some other classifications would equate this usage of "tonalite" with granodiorite (e.g. Hatch et al., 1961), it should be noted that Snelling applied the term "tonalite" to other rocks of the batholith containing comparable proportions of quartz and feldspars. In any case, the paucity of potassium feldspar is considered sufficiently distinctive to warrant separation of these rocks from the granodiorites.

The formation name "Stewartsfield Adamellite" has been replaced by "Stewartsfield Granodiorite". Snelling (1960) based the name on a single mode which qualified as adamellite but the modes recorded in table 4 are granodiorites according to Nockolds (1954) classification and, furthermore, chemical analyses to be presented in table 8 closely resemble those of other granodiorites of the batholith.

Average modes of the intrusions are presented in table 1 and individual modes in tables 3 to 5. Modal analyses were performed with a modified Swift point counter on large slides stained with sodium cobaltinitrite to aid identification of potassium fledspar. For the medium to coarse-grained uncontaminated granites an area of about 40 cm^2 and a point grid of 0.9mm was used, for the finer contaminated granites and leucogranites an area of about 20 cm^2 and a point grid of 0.9mm, and for xenoliths smaller areas, of the order of 5 cm^2, and a point grid

of 0.3 or 0.6mm depending on their grainsize. Estimates of the precision are recorded in table 2. The standard deviations of mineral estimates in replicate areas of about 20 cm^2 from a single specimen of the coarsest uncontaminated granite range from about one to three times those of replicate estimates of a single area. However, estimates based on averages of two 20 cm^2 areas (i.e. a total of 40 cm^2) would give standard deviations of the same order as those obtained for replicates of a single area and indicate that 40 cm^2 is an adequate sample area for the coarse samples. The contaminated granites are finer grained than the uncontaminated granites and their modes were estimated on areas of 20 cm^2 so the precision should be equal to or better than that recorded in table 2 for 20 cm^2 areas of the coarse uncontaminated granites.

Most modes of Shannons Flat Adamellite, and all of Tharwa Adamellite, Stewartsfield Granodiorite, Bolairo Granodiorite and Willoona Tonalite recorded in tables 3 to 5 conform strictly with the appropriate classification incorporated in their formation names. The Callemondah Granodiorite is more variable; of the six modes, four qualify as tonalite, one as granodiorite and one as adamellite. Two previous modes by Snelling (1957) qualify as granodiorite. The terminology "Callemondah Granodiorite" is justified on the basis that potassium feldspar, although only a trace constituent of some samples, attains significant amounts in others in contrast to the consistently low contents typical of the other tonalite intrusions. Samples of Clear Range Granodiorite also range from granodiorite to tonalite but

Table 1 Average modes of the intrusions

	Qz	Kf.	Pl.	Musc. Seric.	Bi.	Chl.	Amph.	Ep. Gp.	Op.	Others
1	32.8	17.2	31.1	1.3	3.5	11.4		1.8	0.3	0.6
2	37.2	5.4	33.1	0.8	21.4	0.3	0.9	0.9	0.1	0.2
3	36.6	3.8	27.7	7.6	14.0	5.9		3.6	0.6	0.2
4	35.5	6.1	28.3	5.9	22.0	0.9		1.1	0.1	0.1
5	37.6	0.2	26.1	11.7	19.4	2.2		1.9	0.6	0.4
6	34.1	25.7	26.4	2.1	7.1	1.6		2.6	0.3	0.1
7	38.4	25.5	23.1	1.9	8.2	1.0		1.6	0.4	0.1
8	37.1	33.9	19.8	6.2	1.8					1.2*
9	31.8	39.5	20.7	5.7	2.1	0.3				

* includes 0.7 per cent garnet

1. Stewartsfield Granodiorite (2 modes)
2. Clear Range Granodiorite (14 modes)
3. Callemondah Granodiorite (6 modes)
4. Bolairo Granodiorite (5 modes)
5. Willoona Tonalite (5 modes)
6. Shannons Flat Adamellite (25 modes)
7. Tharwa Adamellite (5 modes)
8. Westerly Muscovite Granite (1 mode)
9. Yaouk Leucogranite (2 modes)

Table 2 Precision of modal analyses

	Qz.	Pl.	Kf.	Bi.	Musc.	Chl.	Op.	Ep.	Other
1. Five analyses of a single area of approx. 20 cm^2 of coarse uncontaminated granite									
Mean	37.53	30.48	20.20	8.44	0.66	0.56	0.63	1.27	0.21
Pop. Std. Dev.	1.04	1.00	0.82	0.93	0.58	0.44	0.16	0.42	0.19
2. Analyses of six areas of approx. 20cm^2 from a single hand specimen of uncontaminated granite									
Mean	37.11	22.41	26.37	5.49	2.43	1.62	0.27	4.27	
Pop. Std. Dev.	1.55	1.80	3.71	1.41	0.58	0.59	0.20	1.07	
3. Calculated standard deviation of analyses of areas of 40cm^2 obtained by averaging analyses of two 20cm^2 areas ($\sigma_{40} = \sigma_{20}/\sqrt{2}$)									
Pop. Std. Dev.	1.09	1.28	2.62	1.00	0.41	0.42	0.14	0.76	

Table 3 Modal analyses of the uncontaminated granites

	Qz	Kf	Pl	Musc. Seric.	Bi	Chl	Ep.Gp.	Op	Others
Shannons Flat Adamellite									
20501	35.5	19.6	25.3	3.2	11.7	1.2	3.2	0.1	0.2
20502	36.0	20.6	30.8	1.3	9.8	0.3	0.4	0.2	0.2
20503	31.4	23.4	32.0	0.2	12.3	0.3	0.1	0.1	0.3
20504	30.9	28.8	24.6	2.6	7.5	1.0	4.0	0.4	0.2
20505	34.7	22.7	26.8	1.9	10.1	1.1	2.3	0.2	0.1
20506	31.7	21.7	31.1	1.3	10.6	1.7	1.3	0.5	0.1
20507	39.0	21.0	31.7	0.7	8.8	0.6	1.3	0.6	0.2
20508	34.6	21.6	26.4	3.6	9.8	1.3	2.5	0.2	tr
20509	29.1	31.1	26.9	2.4	6.8	1.1	2.3	0.1	0.2
20510	32.8	28.0	25.7	1.7	8.2	1.7	1.5	0.4	0.1
20511	33.0	24.4	20.9	5.4	2.0	3.2	10.7	tr	0.4
20512	37.6	19.7	29.5	0.9	8.2	1.6	1.9	0.5	0.1
20513	36.7	24.7	25.5	2.3	7.2	1.4	2.0	0.1	0.1
20514	34.8	23.8	26.2	2.7	6.0	2.3	3.9	0.3	tr
20515	33.8	27.1	27.6	0.1	9.4	0.9	0.4	0.4	0.1
20516	39.7	21.0	27.5	1.3	8.1	0.6	1.5	0.1	0.2
20517	31.4	30.0	33.0	0.7	0.2	4.0	0.1	0.5	0.1
20518	33.9	28.2	25.1	2.4	4.6	1.4	4.2	tr	0.2
20519	30.9	28.3	21.8	3.8	6.6	1.7	6.2	0.6	0.1
20520	33.4	26.4	23.8	1.5	8.8	1.1	4.0	0.4	0.6
20521	35.9	28.7	26.0	2.4	3.9	1.5	1.0	0.1	0.5
20522	32.7	27.3	28.5	1.4	7.0	1.4	1.0	0.5	0.2
20523	33.4	25.5	29.6	0.9	7.5	1.6	1.3	0.1	0.1
20524	34.7	30.2	21.6	2.5	4.1	1.6	5.2	0.1	tr
20525	35.5	19.6	25.3	3.2	11.7	1.2	3.2	0.1	0.2
Tharwa Adamellite									
20526	29.6	30.8	25.3	0.5	11.9	0.2	1.4	0.1	0.2
20527	34.4	28.9	20.6	2.4	10.0	0.7	2.2	0.4	0.4
20528	43.3	20.5	20.3	1.4	9.3	1.5	2.7	0.9	
20529	46.4	26.5	18.5	1.0	6.3	0.6	0.6	0.3	
20530	38.4	20.6	30.7	4.1	3.5	1.8	0.9	0.1	

Table 4 Modal analyses of the contaminated granites

	Qz	Kf	Pl	Musc. Seric.	Bi	Chl	Ep.Gp.	Op	Others
Stewartsfield Granodiorite									
20558	30.1	19.5	31.1	0.5	2.9	12.6	1.6	0.4	1.0
20559	35.4	14.9	31.1	2.0	4.1	10.1	2.0	0.2	0.1
Callemondah Granodiorite									
20542	35.5		31.2	2.4		19.0	11.0	0.3	0.7
20543	34.4	2.1	33.6	0.7	22.5	1.1	5.1	0.2	0.3
20544	39.6		25.5	13.2	7.6	10.8	1.6	1.8	
20545	37.7	0.3	25.1	15.6	20.2	0.3		0.7	0.1
20546	38.2	4.8	24.1	11.2	20.2	0.4	0.2	0.7	0.2
20547	34.1	15.4	26.8	2.7	13.6	4.0	3.4	0.1	
Bolairo Granodiorite									
20548	34.7	5.7	28.2	4.8	25.2	0.7	0.7		0.1
20549	35.8	5.3	27.4	6.4	22.4	1.0	1.4	0.2	0.1
20551	37.2	8.8	29.4	3.1	20.0	0.9	0.4	0.1	0.1
20552	34.4	4.6	28.1	9.3	20.4	1.0	1.9	0.2	
Clear Range Granodiorite									
20562	31.2		33.7		29.1	1.0	0.1	0.9	4.1[1]
20563	34.6		33.2		21.5	0.3	0.3		10.3[2]
20464	38.3	1.1	33.8		26.4		0.1		0.2
20565	37.1	3.3	35.4	0.6	23.7				
20566	41.8	0.7	35.9		18.8	0.1	0.2		0.3
20531	40.4	6.4	34.6	0.2	17.3		0.9	0.2	
20532	37.9	0.9	34.2		25.2		1.6		0.3
20533	31.9	4.7	37.2	0.5	23.4		2.0	0.1	0.2
20534	37.5	11.9	31.8	1.2	16.7	0.3	0.1	0.2	0.3
20536	44.5	4.2	26.8	2.1	21.9	0.2		0.3	
20537	37.5	5.8	31.2	0.7	19.9		4.6	0.2	0.2[3]
20538	34.3	10.0	31.6	1.9	21.6	0.1	0.1	0.4	0.1
20539	37.0	9.2	30.8	0.6	19.1	1.2	1.6	0.4	0.2
20540	36.5	8.1	33.2	4.5	15.8	0.5	1.0	0.3	0.9
Willoona Tonalite									
20553	35.1	0.3	25.7	11.6	24.4	1.5	0.7	0.7	0.1
20554	39.9		26.5	10.8	20.2	0.3	0.2	1.1	1.2
20555	35.8	0.9	28.2	11.6	20.4	0.4	2.4		0.3
20556	37.7		28.3	10.3	12.0	7.1	3.8	0.7	0.2
20557	39.3	tr	21.9	14.3	19.9	1.6	2.2	0.5	0.4

1 includes 3.5 per cent amphibole
2 includes 10.2 per cent amphibole
3 includes 0.2 per cent amphibole

Table 5 Modal analyses of leucogranites

	Qz	Kf	Pl	Seric	Bi	Chl	Op	Others
Westerly Muscovite Granite								
20569	37.1	33.9	19.8	6.2	1.8			1.2[1]
Yaouk Leucogranite								
20567	29.7	43.2	18.7	5.5	2.2	0.7		
20568	33.8	35.7	22.6	5.9	1.9			
Miscellaneous								
20571	35.5	36.3	20.2	4.4	1.6	1.0	0.4	0.6
20572	36.8	42.0	15.7	1.4	0.4	1.7	0.4	1.6
20573	35.0	29.3	28.6	6.0	0.2	0.1	tr	0.7[2]
20574	39.9	44.6	13.1	0.3	0.2	1.3	0.3	0.2

1 includes 0.7 per cent garnet.

2 includes trace of garnet.

granodiorite is areally more abundant. Modes of the various "leucogranites" all qualify strictly as granite except for sample 20573 which is an adamellite.

The modal relationships and variation of the batholith as a whole are summarised in figures 2 and 3.

KEY TO FIGURES 2, 3, 10 to 19, 22, 24 to 27.

Xenoliths

Stewartsfield Granodiorite

Clear Range Granodiorite

Callemondah Granodiorite

Bolairo Granodiorite

Willoona Tonalite

Shannons Flat Adamellite

Tharwa Adamellite

Leucogranites and minor intrusions

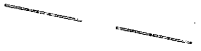

Regression trend for contaminated granites

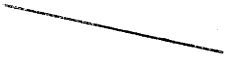

Regression trend for uncontaminated granites

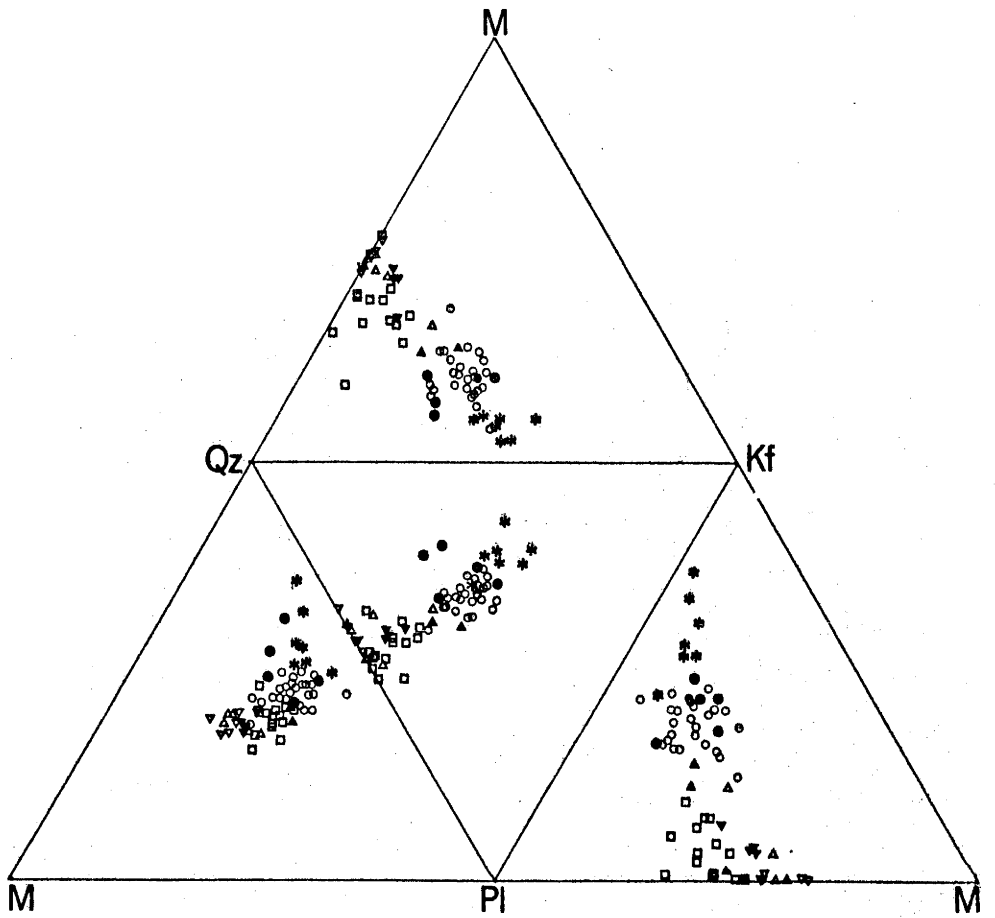

M = Mafic minerals
Qz = Quartz
Kf = Microcline
Pl = Plagioclase

Figure 2. Modal variation of the granites

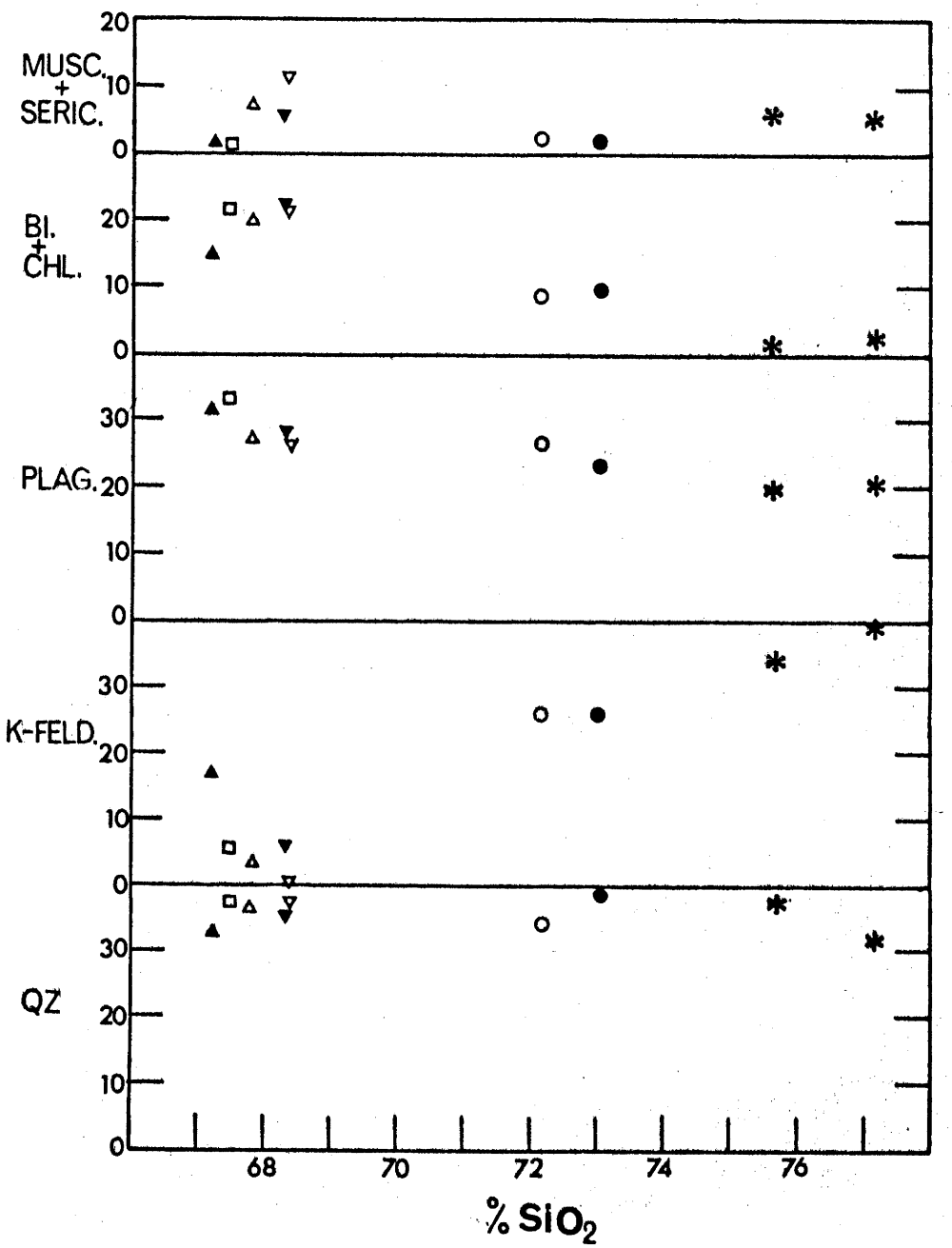

Figure 3. Variation of average modal composition of the granites in relation to average SiO_2 content

4. XENOLITHS

Dark, fine to medium-grained xenoliths are a conspicuous feature of all outcrops of the contaminated granites. They are invariably rounded, usually discoid and show a tendency to be aligned with the prominent foliation of the contaminated granites. Their size varies from aggregates of a few grains up to about 40cm. in diameter but rarely exceeds this. Some contrast sharply in grainsize with their hosts and have sharp boundaries but many are intimately veined and corroded by the enclosing rock so that their boundaries become diffuse and they appear as finer grained, dark streaks and patches in the granodiorites and tonalites.

Most of the xenoliths consist of foliated or schistose aggregates of plagioclase, biotite and quartz, many with streaky, finer grained areas of muscovite and biotite, but some consist entirely of fine muscovite and biotite, others contain actinolite, biotite, plagioclase and quartz and rarer types consist principally of quartz with lesser amounts of biotite or plagioclase. Several microxenoliths, 1 - 2 cm in length, in the Bolairo Granodiorite (sample 20552) contain grains of garnet, as large as 0.5mm in diameter, set in finer schistose aggregates of biotite and muscovite. Garnet has not been recorded previously in these xenoliths.

All minerals in all the xenoliths reveal evidence of strain; grain boundaries are ragged and bending, fracturing and undulose extinction of mineral grains are typical. The biotite is usually brown, like that of the host granites, but some grains, especially those within the finest

aggregates of muscovite and biotite, are green. Plagioclase is unzoned or weakly zoned and varies widely in composition from one xenolith to another between albite and bytownite; multiple twinning is abundant and commonly wedge shaped, indicative of deformation twinning (Vogel & Seifert, 1965).

The mineralogy, textures and modes of many xenoliths indicate a metasedimentary origin. Some xenoliths consisting of plagioclase, biotite and quartz have more igneous aspects, the biotite being identical in colour with the enclosing granite, though somewhat finer grained, whilst the plagioclase shows moderate zoning, a feature incompatible with a simple metamorphic origin. However, it is believed that these xenoliths are probably products of more extensive reaction by diffusion and penetration of magma into sedimentary xenoliths since traces of actinolite and streaks of fine muscovite and green biotite (in contrast to the brown biotite of the host granites) are present in many of them.

Modal analyses of xenoliths in table 6 and chemical analyses in table 7 serve to illustrate the range of compositions encountered. The quartz-rich, feldspar-poor assemblages of rounded xenoliths [illegible] 20599 from the Clear Range Granodiorite and 20578 from the Callemondah Granodiorite clearly reflect a psammitic or psammopelitic origin and the mica-rich assemblages of 20589 and 20549X and the garnet-mica assemblage of 20552X imply a pelitic origin. On the other hand, xenoliths 20576, 20592, 20577, 20591 and 20590 are similar in mode to tonalites from the south-eastern end of the batholith except that they are somewhat richer in biotite and are devoid of hornblende. However,

Table 6 Modal analyses of xenoliths

	Qz	Pl.	Kf.	Bi.	Amph.	Musc. Seric.	Chl.	Op.	Ep. Gp.	Other
Xenoliths from uncontaminated granites										
20585	27.0	26.0	35.1	8.9		0.8			1.3	
20586	29.2	19.1	32.8	11.3		1.2	2.5	1.3	2.6	
20587	39.2	25.0	24.5	8.7		0.6		1.0	1.0	
Xenoliths from contaminated granites										
20576	34.6	24.8		30.4	4.1		0.3	3.4	1.1	1.3
20577	33.8	31.1	0.9	32.9		0.6	0.2	0.2		0.3
20589	3.9	37.7		44.4		12.8	0.2	0.8		0.4
20590	33.0	37.6		28.1		0.1			0.9	0.4
20591	30.6	33.5	0.5	30.6		1.4	1.2	0.5	1.4	0.3
20592	32.7	28.7		38.8				0.1		0.1
20593	24.0	41.0		16.5	17.8		0.3		0.4	
20594	30.2	39.9		12.6	16.7					
20595	29.5	37.3		12.1	20.6					
20596	21.3	26.6		10.6	40.6			0.4	0.5	
20597	30.4	23.7		6.8	38.3					
20598	24.2	19.3		8.5	47.3		0.1	0.1	0.2	0.2
20599	76.7	11.2		11.8					0.4	
20578	58.2	19.7	0.1	19.8		0.3	0.7	0.7		0.6
20549X*	2	5		40		51		2		
20552X*				78		15		2		5+

* Microxenoliths - visual estimates of mode
\+ Garnet

Table 7 Chemical analyses of xenoliths from the Murrumbidgee Batholith

	1	2	3	4	5	6	7	8	9
SiO_2	49.07	50.76	60.43	61.61	61.66	64.28	67.59	65.49	78.93
TiO_2	0.69	0.80	0.55	1.19	0.60	1.27	0.62	0.84	0.51
Al_2O_3	21.76	23.10	14.53	14.81	13.91	15.00	14.40	13.85	9.51
Fe_2O_3	3.44	1.66	1.66	2.59	1.22	0.49	0.50	0.92	0.28
FeO	8.74	5.27	5.00	5.98	5.20	5.67	5.00	4.87	2.89
MnO	n.d.	0.08	0.10	0.11	0.09	0.10	0.08	0.07	0.05
MgO	3.65	3.01	6.71	1.95	5.94	2.81	2.63	3.06	1.39
CaO	10.32	5.85	5.56	4.99	4.85	5.17	2.89	2.88	2.16
Na_2O	1.03	3.63	2.12	2.94	0.48	2.18	2.21	2.53	1.92
K_2O	0.37	3.64	1.74	1.59	3.29	2.35	2.82	3.16	1.50
H_2O+	0.62	1.48	1.49	1.40	2.40	0.92	1.21	1.56	0.72
H_2O-	0.14	0.09	0.10	0.09	0.18	0.13	0.05	0.06	0.13
P_2O_5	tr	0.10	0.11	0.53	0.04	0.23	0.14	0.13	0.14
CO_2	n.d.	0.03	nil	0.03	0.05	0.16	0.02	0.01	0.07
Total	99.83	99.50	100.10	99.81	99.91	100.76	100.16	99.43	100.20
Ba						485	490		135
Rb						112	196		91
Sr						210	142		123
Pb						21	18		26
Th						16	16		14
U						4	3		2
Zr						270	170		235
Nb						15	18		19
Y						48	24		31
La						15	18		24
Ce						55	52		67
Pr						4	5		10
Nd						17	17		28
V						151	94		47
Cr						52	92		50
Mn						610	560		355
Ni						21	28		15
Cu						15	10		1
Zn						85	84		62
Ga						17	17		11

Oxides in per cent, elements in parts per million

1. Xenolith from 'Murrumbucka tonalite' (Anal.2,Table V, Snelling, 1960)
2. Xenolith from Clear Range Granodiorite (Anal.6,Table V, Snelling, 1960)
3. Xenolith from 'Murrumbucka tonalite' (Anal.1,Table V, Snelling, 1960)
4. Xenolith from Clear Range Granodiorite (Anal.5,Table V, Snelling, 1960)
5. Xenolith from Clear Range Granodiorite (Anal.4,Table V, Snelling, 1960)
6. Xenolith from Clear Range Granodiorite (Sample 20576)
7. Xenolith from Clear Range Granodiorite (Sample 20577)
8. Xenolith from Callemondah Granodiorite (Anal.3,Table V, Snelling, 1960)
9. Xenolith from Callemondah Granodiorite (Sample 20578)

traces of actinolite, schistose areas of fine-grained muscovite and green biotite and high contents of biotite relative to quartz combine to suggest an origin by modification of psammopelitic material rather than an igneous origin. The chemical analyses of table 7 support the modal data. Analyses 4, 6, 7, and 8 are similar to analyses of the contaminated granites (the high zirconium content in analysis 6 perhaps may reflect a sedimentary origin), but analyses 2, 5, and 9 are not consistent with igneous origins. Analysis 5, with 61.66 per cent SiO_2, has high CaO and MgO but only 0.48 per cent Na_2O and, thus, the xenolith probably originated from a calcareous shale; analysis 2 has a high aluminium content implying a pelitic origin but its alkali content testifies to considerable reaction with the enclosing granite; analysis 9, with low Al_2O_3 and high SiO_2 and Zr, resembles the composition of a psammite.

Many xenoliths in the Murrumbucka area differ from those elsewhere in the contaminated granites in possessing abundant hornblende and generally more calcic plagioclase (labradorite). Commonly they consist of plagioclase, hornblende, quartz, biotite, epidote and opaque minerals. Two analyses are shown in table 7. Snelling (1960) regarded these xenoliths as probably derived from basic or ultrabasic intrusions similar to those exposed in the Ordovician rocks of the Cooma area. The types of basic rocks in the Cooma area described and analysed by Joplin (1942) are "hornblende-pyroxene-granulites" (thought to have originated as sills or lava flows), amphibolites (probably derived from gabbros or norites) and chlorite amphibolites (probably derived from small basic or

ultrabasic intrusions). The xenoliths do not correspond closely with any of the analyses but there is a general similarity with those of the "granulites".

Xenoliths are rare in the uncontaminated granites, being sparsely distributed in the Tharwa Adamellite and almost absent from the Shannons Flat Adamellite. They have a grainsize of less than 0.5mm and consist of quartz, plagioclase, brown biotite and microcline. All minerals are strained and grain boundaries are ragged. The plagioclase is abundantly twinned and conspicuously zoned. Modally the xenoliths are granites and adamellites but the abundance of feldspar and quartz porphyroblasts testifies to extensive modification and the original nature of the xenoliths is uncertain.

5. CHEMISTRY OF THE ROCKS

New chemical analyses of 75 intrusive rocks and three xenoliths from the Murrumbidgee Batholith are presented in tables 7-16, together with some previous analyses. The analytical methods are recorded in Appendix A. The tables of individual intrusions are arranged in order of increasing average SiO_2 content, namely, Stewartsfield Granodiorite (table8), Clear Range Granodiorite (table 9), Callemondah Granodiorite (table 10), Bolairo Granodiorite (table 11), Willoona Tonalite (table 12), Shannons Flat Adamellite (table 13), Tharwa Adamellite (table 14), Westerly Muscovite Granite and Yaouk Leucogranite (table 15). Table 16 contains analyses of miscellaneous unnamed and minor intrusions. Within each table analyses are arranged in order of increasing SiO_2 content. Analyses of xenoliths arranged in groups according to their host rock were presented earlier (table 7).

The nature and extent of the variation recorded is discussed in the context of analytical variance, variation within outcrop, variation within intrusions, and variation within the batholith as a whole. In order to avoid the problem of differences in analytical precision and accuracy, only analyses performed by the author are incorporated in subsequent statistical treatment of the results; all rock analyses represent averaged duplicate determinations except for H_2O+, H_2O- and CO_2.

Analytical variance

Table 17 presents estimates of analytical variance based on the results of duplicate analyses of 25 samples of Shannons Flat Adamellite.

Table 8 Chemical analyses of the Stewartsfield Granodiorite

	20558	20559	20560	20561
SiO_2	65.62	67.58	67.79	67.85
TiO_2	0.62	0.60	0.62	0.64
Al_2O_3	14.19	14.30	14.59	14.34
Fe_2O_3	0.51	0.26	0.18	0.81
FeO	3.87	4.08	4.03	4.05
MnO	0.06	0.07	0.07	0.07
MgO	2.46	2.41	2.42	2.50
CaO	2.80	2.79	2.96	3.29
Na_2O	2.27	2.08	2.21	2.43
K_2O	3.78	3.30	3.48	1.41
P_2O_5	0.15	0.14	0.13	0.14
H_2O+	1.94	1.80	1.55	1.57
H_2O-	0.05	0.12	0.09	0.10
CO_2	0.09	0.11	0.13	0.05
Total	98.41	99.64	100.25	99.25
Ba			545	380
Rb	195	159	168	49
Sr	191	177	182	236
Pb	18	2	23	16
Th	17	23	17	19
U	3	3	4	3
Zr	170	170	170	190
Nb	17	17	17	20
Y	28	29	28	31
La			14	20
Ce			63	68
Pr			8	9
Nd			19	23
V			92	90
Cr			64	83
Mn			502	488
Ni			22	18
Cu			8	30
Zn			72	56
Ga	18	17	18	17

Oxides in per cent, elements in parts per million.

Table 9 Chemical analyses of the Clear Range Granodiorite
(continued on next page)

	20562	20563	20531	20564	20532	20565	20533	20566
SiO_2	62.19	64.32	65.43	66.14	66.43	66.87	67.33	67.60
TiO_2	0.80	0.58	0.53	0.68	0.67	0.66	0.57	0.57
Al_2O_3	15.56	14.88	15.08	14.59	14.96	14.57	14.21	14.63
Fe_2O_3	1.00	1.37	1.07	0.88	1.06	1.23	0.71	0.67
FeO	6.12	4.28	4.19	4.37	4.39	3.84	3.91	3.94
MnO	0.12	0.09	0.08	0.04	0.09	0.09	0.08	0.07
MgO	3.84	3.88	3.06	2.79	3.02	2.64	2.53	2.46
CaO	5.09	5.36	3.78	3.75	4.21	3.40	3.57	3.19
Na_2O	1.14	1.85	1.94	1.85	1.96	1.96	2.11	1.96
K_2O	2.53	2.20	3.49	2.91	2.74	3.00	3.08	2.76
P_2O_5	0.17	0.11	0.16	0.44	0.13	0.17	0.12	0.14
H_2O+	1.31	1.06	1.06		1.14		0.88	
H_2O-	0.21	0.21	0.18		0.13		0.08	
CO_2	0.20	0.11	0.06		0.06		0.06	
Total	100.28	100.30	100.11		100.99		99.24	
Ba	555	485	600		525		495	
Rb	130	125	177	139	139	149	149	139
Sr	194	229	200	177	180	145	155	155
Pb	14	17	21	21	18	19	20	24
Th	13	12	25	22	14	21	14	19
U	2	1	5	2	3	1	1	3
Zr	190	125	170	150	150	185	140	145
Nb	19	15	20	19	17	17	15	15
Y	17	19	22	30	25	15	26	25
La	30	23	30		29		17	
Ce	67	54	83		74		49	
Pr	6	6	11		13		3	
Nd	23	18	29		23		17	
V	163	129	111		123		106	
Cr	112	152	122		93		76	
Mn	440	640	560		640		585	
Ni	24	32	32		22		19	
Cu	18	16	20		18		7	
Zn	110	77	85		83		77	
Ga	20	16	17	18	18	16	17	16

Oxides in per cent, elements in parts per million.

Table 9 Chemical analyses of the Clear Range Granodiorite
(continued from previous page)

	20534	20535	20536	20537	20538	20539	20540	20541
SiO_2	68.73	68.73	68.77	68.93	69.10	69.12	69.72	70.61
TiO_2	0.58	0.58	0.67	0.50	0.59	0.55	0.50	0.51
Al_2O_3	14.54	14.49	14.40	13.78	14.41	14.20	14.49	14.06
Fe_2O_3	0.44	0.54	0.62	1.68	0.48	0.42	0.60	0.46
FeO	3.79	3.73	4.25	2.48	3.90	3.58	3.23	3.09
MnO	0.07	0.06	0.08	0.08	0.07	0.07	0.07	0.05
MgO	1.99	2.21	2.30	1.66	2.51	1.86	1.86	1.59
CaO	3.06	2.75	3.05	4.10	2.96	2.87	2.37	2.41
Na_2O	2.23	2.24	2.17	2.35	2.15	2.29	2.20	2.32
K_2O	3.53	3.56	2.79	2.45	3.45	3.52	3.80	3.81
P_2O_5	0.13	0.14	0.13	0.14	0.14	0.12	0.15	0.13
H_2O+	1.19	1.04	0.86		0.58	0.97		0.97
H_2O-	0.11	0.07	0.17		0.09	0.20		0.21
CO_2	0.06	0.17	0.09		0.12	0.14		0.11
Total	100.45	100.31	100.35		100.45	99.91		100.33
Ba	545	545	360		535	540		565
Rb	164	185	171	90	177	172	173	194
Sr	144	153	155	262	151	147	122	145
Pb	28	26	20	14	24	30	30	27
Th	15	17	18	19	16	16	19	15
U	3	4	1	4	3	3	5	3
Zr	165	155	190	160	170	155	150	160
Nb	18	18	20	13	17	17	14	18
Y	31	26	30	23	24	35	30	28
La	17	15	32		20	21		21
Ce	51	46	69		55	54		53
Pr	7	4	8		7	7		7
Nd	15	15	24		14	17		15
V	88	87	101		92	81		72
Cr	57	63	66		67	52		42
Mn	490	490	550		515	480		385
Ni	19	20	19		21	18		15
Cu	6	10	16		12	12		9
Zn	70	70	86		72	66		49
Ga	17	16	17	14	16	17	16	16

Oxides in per cent, elements in parts per million.

Table 10 Chemical analyses of the Callemondah Granodiorite

	20542	20543	20544	20545	20546	20547
SiO_2	65.29	66.68	68.36	68.74	68.92	69.27
TiO_2	0.60	0.58	0.70	0.68	0.66	0.47
Al_2O_3	14.85	14.66	14.49	14.59	14.49	14.19
Fe_2O_3	1.16	0.80	0.71	0.55	0.52	0.64
FeO	4.13	4.17	4.06	4.15	4.06	3.09
MnO	0.08	0.08	0.06	0.07	0.07	0.05
MgO	2.80	2.82	2.19	2.04	2.04	2.03
CaO	4.81	4.06	3.03	2.25	2.23	2.40
Na_2O	2.49	2.08	2.38	2.01	2.08	2.48
K_2O	0.71	2.83	1.45	3.24	3.46	3.44
P_2O_5	0.13	0.13	0.17	0.16	0.15	0.13
H_2O+	2.15	0.85	1.96	0.85	0.93	
H_2O-	0.10	0.19	0.07	0.17	0.15	
CO_2	0.03	0.02	0.05	0.14	0.03	
Total	99.33	99.95	99.68	99.64	99.79	
Ba	130	470	295	590	600	
Rb	27	128	56	169	160	129
Sr	350	172	302	141	145	146
Pb	11	22	19	30	29	24
Th	13	13	19	18	18	19
U	2	3	4	4	4	2
Zr	150	140	200	185	185	135
Nb	16	16	20	19	18	15
Y	25	30	35	34	34	27
La	12	14	27	26	25	
Ce	45	48	71	69	64	
Pr	5	3	5	8	9	
Nd	22	17	25	21	23	
V	109	110	88	87	89	
Cr	78	77	64	61	60	
Mn	560	600	400	490	490	
Ni	13	18	19	23	20	
Cu	2	15	2	15	16	
Zn	46	77	62	86	82	
Ga	16	16	18	19	17	16

Oxides in per cent, elements in parts per million.

Table 11 Chemical analyses of the Bolairo Granodiorite

	20548	20549	20550	20551	20552
SiO_2	67.63	67.97	68.18	68.73	69.26
TiO_2	0.63	0.60	0.63	0.63	0.53
Al_2O_3	14.45	14.38	14.79	14.37	14.07
Fe_2O_3	0.46	0.61	0.58	0.56	0.91
FeO	4.20	3.79	3.99	3.98	3.07
MnO	0.07	0.07	0.08	0.07	0.07
MgO	2.54	2.47	2.31	2.38	2.32
CaO	2.91	2.69	2.50	2.80	2.14
Na_2O	2.02	2.06	2.23	2.04	2.22
K_2O	3.34	3.40	3.36	3.48	3.66
P_2O_5	0.14	0.13	0.15	0.14	0.15
H_2O+	1.18	1.38	1.35	1.17	
H_2O-	0.06	0.07	0.15	0.17	
CO_2	0.26	0.08	0.10	0.10	
Total	99.89	99.70	100.40	100.62	
Ba			575	630	
Rb	167	164	197	165	114
Sr	169	159	145	145	139
Pb	29	28	22	29	26
Th	17	16	18	16	19
U	3	4	3	2	2
Zr	180	175	175	175	160
Nb	17	16	16	17	15
Y	28	28	37	33	37
La			24	21	
Ce			57	51	
Pr			4	11	
Nd			15	18	
V			94	83	
Cr			78	78	
Mn			605	510	
Ni			27	24	
Cu			1	16	
Zn			104	77	
Ga	18	16	18	17	16

Oxides in per cent, elements in parts per million.

Table 12 Chemical analyses of the Willoona Tonalite

	20553	20554	20555	20556	20557
SiO_2	68.05	68.11	68.49	68.66	68.69
TiO_2	0.67	0.66	0.67	0.61	0.67
Al_2O_3	14.25	14.36	14.53	14.48	14.59
Fe_2O_3	0.56	0.71	0.56	0.81	0.61
FeO	4.00	3.81	4.05	3.57	3.98
MnO	0.07	0.09	0.07	0.05	0.07
MgO	2.35	2.33	2.06	2.17	2.00
CaO	2.28	2.03	2.53	2.91	2.24
Na_2O	2.15	1.91	2.18	2.49	2.14
K_2O	3.15	3.36	2.98	1.74	2.99
P_2O_5	0.17	0.15	0.16	0.16	0.15
H_2O+	1.56	1.53	1.55		0.88
H_2O-	0.05	0.09	0.18		0.16
CO_2	0.08	0.07	0.11		0.05
Total	99.39	99.21	100.12		99.22
Ba	575	595	630		590
Rb	174	207	152	95	143
Sr	167	158	163	202	159
Pb	28	18	20	14	16
Th	18	20	18	23	21
U	3	4	4	3	3
Zr	190	185	180	175	180
Nb	17	18	18	16	17
Y	28	27	34	31	33
La	19	26	26		25
Ce	68	62	62		64
Pr	9	7	6		9
Nd	20	20	22		19
V	87	84	92		85
Cr	60	59	60		59
Mn	530	655	495		490
Ni	22	27	22		22
Cu	15	5	13		8
Zn	91	77	78		78
Ga	17	18	17	18	17

Oxides in per cent, elements in parts per million.

Table 13 Chemical analyses of the Shannons Flat Adamellite
(continued on the next two pages)

	20501	20502	20503	20504	20505	20506	20507	20508	20509
SiO_2	70.66	70.71	71.03	71.29	71.46	71.65	71.68	71.77	71.82
TiO_2	0.39	0.41	0.43	0.41	0.37	0.41	0.37	0.35	0.41
Al_2O_3	14.34	14.01	14.07	14.20	13.62	14.16	13.68	13.39	14.13
Fe_2O_3	0.56	0.70	0.79	0.70	0.67	0.55	0.58	0.65	0.62
FeO	2.05	2.05	2.03	2.07	2.19	2.10	1.98	2.24	2.12
MnO	0.05	0.05	0.05	0.05	0.05	0.05	0.04	0.07	0.05
MgO	1.06	0.88	0.94	0.94	1.06	0.92	0.87	1.03	0.91
CaO	2.40	2.59	2.62	2.63	2.51	2.75	2.43	2.17	2.63
Na_2O	2.65	2.72	2.61	2.66	2.42	2.62	2.51	2.49	2.60
K_2O	4.55	4.21	4.20	4.31	4.06	4.11	4.37	4.36	4.24
P_2O_5	0.09	0.10	0.11	0.10	0.09	0.09	0.09	0.09	0.10
H_2O+	0.85	0.67	0.57	0.83	0.80	0.70	0.66	0.81	0.67
H_2O-	0.08	0.13	0.06	0.11	0.07	0.13	0.07	0.07	0.03
CO_2	0.05	0.09	0.06	0.09	0.07	0.05	0.05	0.08	0.06
Total	99.78	99.32	99.57	100.39	99.44	100.29	99.38	99.57	100.39
Ba	540	575	680	645	475	605	645	395	605
Rb	262	224	204	204	218	193	224	288	206
Sr	150	158	167	150	163	159	163	134	137
Pb	25	26	23	30	31	29	23	30	28
Th	22	19	18	23	20	20	18	25	21
U	3	4	7	4	9	4	4	6	4
Zr	160	165	160	155	145	155	150	125	160
Nb	19	20	18	19	18	21	21	20	20
Y	42	30	37	41	51	39	200	56	40
La	22	21	31	20	34	27	27	30	27
Ce	63	61	60	67	70	65	64	73	65
Pr	9	9	11	7	8	7	8	9	6
Nd	18	21	25	22	32	20	27	28	23
V	49	52	54	47	56	49	45	52	51
Cr	18	18	23	19	25	19	17	22	19
Mn	350	345	355	380	390	360	260	480	345
Ni	15	10	12	12	14	9	12	19	11
Cu	<1	1	<1	3	1	3	<1	<1	4
Zn	36	39	41	50	45	46	26	46	41
Ga	16	15	17	16	15	14	15	16	16

Oxides in per cent, elements in parts per million.

Table 13 Chemical analyses of the Shannons Flat Adamellite
(see also preceding and following pages)

	20510	20511	20512	20513	20514	20515	20516	20517
SiO_2	71.86	71.93	72.03	72.04	72.14	72.29	72.38	72.44
TiO_2	0.37	0.35	0.39	0.42	0.34	0.39	0.36	0.34
Al_2O_3	13.76	13.88	13.73	13.84	13.92	14.20	14.08	13.89
Fe_2O_3	0.62	0.66	0.53	0.66	0.58	0.54	0.31	0.67
FeO	1.88	1.80	2.00	2.07	1.96	2.06	2.23	1.77
MnO	0.06	0.04	0.05	0.05	0.04	0.04	0.05	0.04
MgO	0.80	0.71	0.84	1.01	0.91	0.89	0.83	1.14
CaO	2.31	2.63	2.47	2.48	2.39	2.42	2.72	1.83
Na_2O	2.58	2.55	2.56	2.64	2.55	2.50	2.63	2.79
K_2O	4.50	4.31	4.28	4.32	4.35	4.85	3.91	4.15
P_2O_5	0.09	0.09	0.10	0.10	0.08	0.10	0.08	0.08
H_2O+	0.75	0.72	0.70	0.65	0.63	0.42	0.71	1.23
H_2O-	0.06	0.13	0.07	0.12	0.15	0.04	0.04	0.19
CO_2	0.02	0.03	0.03	0.05	0.02	0.05	0.07	0.11
Total	99.66	99.83	99.78	100.45	100.06	100.79	100.40	100.67
Ba	600	765	555	620	480	740	635	540
Rb	229	179	208	228	207	211	178	162
Sr	143	167	149	137	141	145	169	138
Pb	26	28	25	28	32	32	28	25
Th	19	26	20	24	19	18	25	26
U	3	3	3	4	4	3	5	3
Zr	160	140	160	195	120	160	160	160
Nb	20	19	18	21	17	22	20	20
Y	42	41	43	43	41	38	44	47
La	21	32	26	29	23	23	34	35
Ce	59	83	66	74	58	64	80	84
Pr	10	8	6	7	7	9	7	7
Nd	19	27	23	25	18	19	29	28
V	43	41	47	53	49	47	43	39
Cr	15	17	18	21	19	18	13	16
Mn	405	320	380	350	320	320	350	320
Ni	11	7	11	11	10	9	8	9
Cu	2	2	1	5	14	4	2	<1
Zn	41	37	43	44	35	34	39	31
Ga	15	15	15	15	14	14	15	14

Oxides in per cent, elements in parts per million.

Table 13 Chemical analyses of the Shannons Flat Adamellite
(continued from the two previous pages)

	20518	20519	20520	20521	20522	20523	20524	20525
SiO_2	72.51	72.59	72.60	73.08	73.16	73.34	73.91	74.89
TiO_2	0.30	0.38	0.33	0.30	0.32	0.36	0.27	0.23
Al_2O_3	14.30	14.01	13.98	13.90	13.77	13.60	13.80	13.32
Fe_2O_3	0.65	0.49	0.57	0.59	0.68	0.50	0.53	0.36
FeO	1.47	1.98	1.70	1.54	1.56	1.85	1.41	1.32
MnO	0.04	0.04	0.04	0.04	0.04	0.04	0.04	0.04
MgO	0.68	0.85	0.69	0.67	0.68	0.83	0.57	0.52
CaO	2.73	2.62	2.64	2.45	2.63	2.15	2.16	1.32
Na_2O	2.72	2.78	2.69	2.73	2.61	2.73	2.80	2.80
K_2O	4.22	3.93	4.13	4.40	3.96	4.67	4.54	4.75
P_2O_5	0.07	0.11	0.08	0.07	0.07	0.09	0.07	0.06
H_2O+	0.67	0.67	0.57	0.69	0.74	0.56	0.47	0.80
H_2O-	0.11	0.12	0.12	0.06	0.05	0.12	0.10	0.15
CO_2	0.06	0.06	0.06	0.07	0.07	0.10	0.08	0.07
Total	100.53	100.63	100.20	100.59	100.34	100.94	100.75	100.63
Ba	670	555	680	640	605	585	475	365
Rb	173	201	174	188	169	228	212	235
Sr	174	150	167	155	162	121	123	92
Pb	30	25	27	29	28	28	33	29
Th	24	18	23	25	23	22	20	18
U	3	3	4	3	3	5	4	2
Zr	130	140	150	135	145	165	130	105
Nb	18	20	20	20	25	18	20	18
Y	38	21	44	42	41	45	50	50
La	30	27	31	35	28	30	27	24
Ce	73	63	78	78	83	67	64	52
Pr	4	7	9	7	15	8	7	3
Nd	23	19	27	26	27	23	22	18
V	23	47	36	33	42	44	27	25
Cr	10	21	15	14	14	19	12	10
Mn	290	320	255	280	315	290	250	280
Ni	6	7	8	6	8	11	9	10
Cu	2	<1	1	<1	2	6	1	<1
Zn	35	31	25	27	35	34	24	20
Ga	14	15	14	15	14	15	14	14

Oxides in per cent, elements in parts per million.

Table 14 Chemical analyses of the Tharwa Adamellite

	20526	20527	20528	20529	20530
SiO_2	71.55	72.02	72.05	73.44	75.99
TiO_2	0.40	0.43	0.42	0.33	0.14
Al_2O_3	13.32	13.92	13.69	13.70	13.63
Fe_2O_3	0.74	0.70	0.58	0.56	0.23
FeO	2.01	2.09	2.21	1.83	1.36
MnO	0.05	0.05	0.05	0.01	0.03
MgO	1.13	0.98	0.92	0.82	0.30
CaO	2.59	2.44	2.35	1.92	1.91
Na_2O	2.50	2.59	2.53	2.55	3.54
K_2O	4.13	4.42	4.36	4.33	2.95
P_2O_5	0.10	0.09	0.10	0.11	0.08
H_2O+		0.56	0.62	0.62	0.51
H_2O-		0.14	0.15	0.14	0.13
CO_2		0.05	0.07	0.07	0.07
Total		100.48	100.10	100.43	100.87
Ba		590	630	455	505
Rb	193	217	212	229	143
Sr	134	131	131	129	265
Pb	23	29	28	29	24
Th	25	20	21	16	15
U	4	4	4	8	3
Zr	160	170	180	130	105
Nb	16	19	20	18	20
Y	32	43	42	33	35
La		29	29	9	26
Ce		70	66	45	60
Pr		5	7	8	8
Nd		22	22	13	21
V		54	55	41	7
Cr		23	22	23	5
Mn		340	390	380	185
Ni		12	10	10	1
Cu		2	5	<1	<1
Zn		45	42	37	20
Ga	15	14	15	14	15

Oxides in per cent, elements in parts per million.

Table 15 Chemical analyses of the Westerly Muscovite Granite and the Yaouk Leucogranite

	Westerly Muscovite Granite		Yaouk Leucogranite			
	20569	24[1]	20567	20568	23[2]	10[3]
SiO_2	75.68	75.61	77.02	77.36	78.33	75.56
TiO_2	0.04	0.11	0.08	0.07	0.08	0.08
Al_2O_3	13.20	13.52	12.68	12.74	12.14	13.81
Fe_2O_3	0.32	0.51	0.24	0.25	0.33	0.96
FeO	0.97	0.51	0.66	0.68	0.47	as FeO
MnO	0.07	0.04	0.04	0.05	0.03	
MgO	0.11	0.93	0.20	0.22	0.08	0.20
CaO	0.34	0.21	0.69	0.58	0.42	0.78
Na_2O	2.72	3.31	3.08	3.02	2.98	3.07
K_2O	5.41	4.57	4.67	4.69	5.00	4.87
P_2O_5	0.10	0.13	0.06	0.07	0.04	
H_2O+	0.78	0.88	0.58		0.55	
H_2O-	0.02	0.05	0.03		0.07	
CO_2	0.06	0.05	0.05		nil	
Total	99.82	100.43	100.08		100.52	99.33
Ba	<4		75			115
Rb	501		388	350		465
Sr	45		33	30		46
Pb	23		30	33		28
Th	12		10	17		14.4
U	18		11	14		8.7
Zr	35		55	55		52
Nb	33		23	22		
Y	14		34	40		29
La	<2		2			10
Ce	11		21			
Pr	3		4			
Nb	<3		6			
V	1		4			5
Cr	6		6			4.7
Mn	505		350			420
Ni	<1		<1			<1
Cu	<1		<1			<1
Zn	34		31			
Ga	18		15	14		13

Oxides in per cent, elements in parts per million

1. Anal. 24, Table II (Snelling, 1960) - Westerly Muscovite Granite
2. Anal. 23, Table II (Snelling, 1960) - Yaouk Leucogranite
3. Anal. 10, Table III (Kolbe & Taylor, 1966) - Yaouk Leucogranite

Table 16 Chemical analyses of miscellaneous unnamed and minor intrusions in the Murrumbidgee Batholith

	20570	27	28	20571	20572	20573	20574
SiO_2	72.73	75.14	75.66	76.45	76.80	77.11	77.45
TiO_2	0.50	0.21	0.25	0.11	0.14	0.03	0.08
Al_2O_3	13.70	12.42	12.72	13.36	12.35	13.21	12.37
Fe_2O_3	0.46	0.61	0.60	0.13	0.50	0.14	0.09
FeO	2.24	0.68	0.64	0.79	0.61	0.46	0.43
MnO	0.05	0.02	0.01	0.04	0.02	0.12	0.01
MgO	0.82	0.57	0.23	0.27	0.06	0.05	0.11
CaO	2.08	1.55	0.82	0.92	0.84	0.32	0.61
Na_2O	2.70	3.18	2.90	3.25	2.63	3.76	2.64
K_2O	4.36	4.74	4.89	4.82	5.78	4.62	5.73
P_2O_5	0.12	0.09	0.06	0.11	0.03	0.04	0.02
H_2O+	0.55	0.54	0.63	0.56	0.26	0.48	0.29
H_2O-	0.07	0.05	0.06	0.08	0.13	0.12	0.15
CO_2	0.08	0.03	nil	0.07	0.06	0.05	0.06
Total	100.46	99.83	99.47	100.96	100.21	100.51	100.04
Ba	590			210	570	< 4	60
Rb	229			302	259	469	249
Sr	133			58	63	4	36
Pb	28			37	33	29	44
Th	22			10	26	12	11
U	5			9	5	22	7
Zr	210			50	110	30	65
Nb	20			20	19	37	14
Y	38			34	53	47	55
La	30			9	31	6	9
Ce	74			22	73	25	26
Pr	9			3	7	3	4
Nd	29			8	27	8	12
V	52			9	4	< 1	2
Cr	16			8	4	4	5
Mn	330			305	110	815	60
Ni	2			< 1	< 1	< 1	< 1
Cu	5			11	< 1	< 1	4
Zn	49			13	9	10	8
Ga	15			14	13	17	12

Oxides in per cent, elements in parts per million

20570 Fine-grained adamellite dyke, Honeysuckle Valley.
27 Granite porphyry, Tharwa (Snelling, 1960).
28 Aphyric microgranite, 3 miles north-west of Boorroomba H.S. (Snelling, 1960).
20571 Fine-grained leucogranite, Corin Dam road.
20572 Aplite dyke, 1½ miles south-west of Paddys River H.S.
20573 Fine-grained leucogranite, Corin Dam road.
20574 Porphyritic leucogranite, Honeysuckle Valley.

The population standard deviations of single measurements of each chemical constituent were estimated using the relationship -

mean sample range = d x population standard deviation...(1)

where d = 1.128 for 2 samples

= 1.693 for 3 samples

(Moroney, 1958)

From the standard deviation of single determinations, the standard deviation of analyses representing means of duplicate determinations, were estimated from the relationship -

$$\sigma_n = \frac{\sigma}{\sqrt{n}}$$

where n = no of values averaged

σ_n = standard deviation of means of n values

σ = standard deviation of single values

(Moroney, 1958)

The variances of averaged duplicate determinations (σ_A^2) were obtained by squaring the standard deviations of averaged duplicate analyses.

Variation within outcrop

Analyses of three samples of Shannons Flat Adamellite collected over a distance of 250 metres in a continuous roadside outcrop are recorded in table 18; each analysis represents averaged duplicate determinations of each constituent. Using the relationship (1), referred to above, the population standard deviations (σ_0) and variances (σ_0^2) within the outcrop have been estimated (table 18); in addition, the coefficients of variation and the ratios outcrop variance/analytical variance are shown. The major element variances

Table 17 Estimates of analytical variance based on duplicate analyses of 25 samples of Shannons Flat Adamellite

	Pop. std. dev. of single determinations	Std. dev. of averaged duplicate determinations	Variance of averaged duplicate determinations
SiO_2	0.123	0.087	0.0076
TiO_2	0.0012	0.0009	0.0000008
Al_2O_3	0.082	0.058	0.0034
Total Fe as Fe_2O_3	0.017	0.012	0.00014
FeO	0.027	0.019	0.00038
MnO	0.0017	0.0012	0.0000015
MgO	0.037	0.026	0.0007
CaO	0.013	0.009	0.00009
Na_2O	0.081	0.057	0.0033
K_2O	0.053	0.038	0.0014
P_2O_5	0.0037	0.0026	0.0000068
Ba	9.15	6.47	41.85
Rb	0.68	0.48	0.23
Sr	0.40	0.28	0.08
Pb	0.97	0.69	0.47
Th	0.78	0.55	0.30
U	1.15	0.81	0.66
Zr	6.92	4.89	23.91
Nb	0.45	0.32	0.10
Y	0.77	0.55	0.30
La	2.98	2.10	4.43
Ce	3.53	2.50	6.24
Pr	2.03	1.44	2.06
Nd	1.84	1.30	1.69
V	2.41	1.71	2.91
Cr	2.31	1.64	2.67
Mn	4.44	3.14	9.86
Ni	0.59	0.42	0.17
Cu	1.12	0.79	0.63
Zn	1.43	1.01	1.02
Ga	0.70	0.49	0.24

Table 18 Variation within an outcrop of Shannons Flat Adamellite

	Analyses of individual samples 20504	20506	20509	MEAN	σ_0	σ_0^2	v	σ_0^2/σ_A^2
SiO_2	71.29	71.65	71.82	71.59	0.313	0.0980	0.4	12.9
TiO_2	0.41	0.41	0.41	0.41	0.000	0.0000	0.0	0.0
Al_2O_3	14.20	14.16	14.13	14.15	0.041	0.0017	0.3	0.5
Fe_2O_3	0.70	0.55	0.62	0.62	0.089	0.0079	14.3	
FeO	2.07	2.10	2.12	2.10	0.030	0.0009	1.4	2.4
MnO	0.05	0.05	0.05	0.05	0.000	0.0000	0.0	0.0
MgO	0.94	0.92	0.91	0.92	0.018	0.0003	2.0	0.4
CaO	2.63	2.75	2.63	2.67	0.071	0.0050	2.7	58.8
Na_2O	2.66	2.62	2.60	2.63	0.035	0.0012	1.3	0.4
K_2O	4.31	4.11	4.24	4.22	0.118	0.0139	2.8	9.9
P_2O_5	0.10	0.09	0.10	0.10	0.005	0.00003	5.2	3.7
Ba	646	603	604	618	25.40	645.2	4.1	15.4
Rb	204	193	206	201	7.68	58.98	3.8	256.4
Sr	150	159	137	149	12.99	168.7	8.7	2109
Pb	30	29	28	29	1.18	1.39	4.1	3.0
Th	23	20	21	21	1.77	3.13	8.3	10.4
U	4	4	4	4	0.00	0.00	0.0	0.0
Zr	154	155	162	157	4.73	22.33	3.0	0.9
Nb	19	21	20	20	1.18	1.40	0.1	14.0
Y	41	39	40	40	1.18	1.39	3.0	4.6
La	20	27	27	25	4.13	17.06	16.7	3.9
Ce	67	65	65	66	1.18	1.39	1.8	0.2
Pr	7	7	6	7	0.59	0.35	8.9	0.2
Nd	22	20	23	22	1.77	3.13	8.2	1.9
V	47	49	51	49	2.36	5.57	4.8	1.9
Cr	19	19	19	19	0.00	0.00	0.0	0.0
Mn	377	358	343	359	20.08	403.2	5.6	40.9
Ni	12	9	11	11	1.77	3.13	16.6	18.4
Cu	3	3	4	3	0.59	0.35	17.7	0.6
Zn	50	46	41	46	5.32	28.30	11.7	27.7
Ga	16	14	16	15	1.18	1.39	7.7	5.8

Oxides in per cent, elements in parts per million.

within outcrop are less than about ten times the estimated analytical variances for all constituents except CaO which has a variance over 50 times greater than the analytical variance.

However, the variation of CaO in relation to the other constituents is not as great as this ratio may imply and the high ratio is partly due to the very low value of the analytical variance of CaO. The coefficient of variation of CaO within the outcrop is only 2.7 per cent compared with coefficients of variation of 2.8 and 5.2 per cent for K_2O and P_2O_5, respectively. The trace elements show similarly small variation within outcrop, the highest ratios of outcrop variance to analytical variance being for Sr (2109), Rb (256.4) and Mn (40.9), but their respective coefficients of variation within the outcrop are only 8.7, 3.8 and 5.6 per cent. Zn and Ni have outcrop variances 28 times and 18 times their respective analytical variances coupled with coefficients of variation of 11.7 and 16.6 per cent.

Comparison of the absolute values of variances within the outcrop of Shannons Flat Adamellite (including analytical variance) recorded in table 18 may be made with outcrop variances measured by Baird et al. (1967) in five mappable units of the Rattlesnake Mountain pluton and reproduced in modified form in table 20. The original data of Baird et al.(1967) are listed as components of variance for eight elements and these have been used to calculate total outcrop variances (including analytical variance) for the elements expressed as oxides in table 20. The estimated outcrop variances of all eight oxides in the Shannons Flat Adamellite are much lower than those in all five rock

units examined by Baird et al. (1967) except for K_2O in the diorite which has 1.96 per cent average K_2O and a total outcrop variance of 0.0032 compared with an average of 4.22 per cent K_2O and and outcrop variance of 0.0139 in the Shannons Flat Adamellite.

Variation within intrusions

The variation of seven intrusions is summarised in table 19. The total variances of individual chemical constituents within the Shannons Flat Adamellite can be compared directly with the variances within outcrop recorded in table 18 and with the analytical variances in table 17. Of the major and minor constituents, TiO_2, CaO and FeO show the greatest variation, with total variances of 2500, 1180 and 182 times their respective analytical variances, together with coefficients of variation each of approximately 13 per cent. Na_2O shows remarkably little variation, the total variance being only three times greater than the analytical variance and the coefficient of variation being four per cent. The extent of variation of the trace elements in terms of coefficients of variation and ratios of total variance to analytical variance is similar to that of the major and minor constituents.

The extent of variation of the other intrusions recorded in table 19 can be assessed by comparison between the individual intrusions and with the analytical variance calculated for the Shannons Flat Adamellite. It may also be compared with the total variances of the same five mappable units in the Rattlesnake Mountain pluton (Baird et al., 1967) to which reference was made above. Data shown for these intrusions in table 20 have been recalculated from the original data into total

Table 19 Statistical data for seven intrusions of the Murrumbidgee Batholith

	Stewartsfield Granodiorite					Clear Range Granodiorite				
	$\bar{x}$	σ_T	σ_T^2	v	σ_T^2/σ_A^2	$\bar{x}$	σ_T	σ_T^2	v	σ_T^2/σ_A^2
SiO_2	67.21	1.07	1.137	1.6	149.6	67.50	2.20	4.840	3.3	637.0
TiO_2	0.62	0.02	0.000	2.6	375.0	0.60	0.08	0.006	13.3	7500
Al_2O_3	14.36	0.17	0.029	1.2	8.5	14.55	0.42	0.176	2.9	5.2
Fe_2O_3	0.44	0.28	0.081	64.6		0.83	0.38	0.144	42.7	
FeO	4.01	0.09	0.009	2.4	23.7	3.94	0.77	0.593	19.5	1560
MnO	0.07	0.01	0.000	7.5	16.7	0.08	0.02	0.000	25.0	200.0
MgO	2.45	0.04	0.002	1.7	2.9	2.51	0.69	0.476	27.5	680.0
CaO	2.96	0.23	0.055	7.9	647.1	3.50	0.086	0.740	24.6	8222
Na_2O	2.25	0.15	0.021	6.5	6.4	2.05	0.29	0.084	14.2	25.4
K_2O	2.99	1.07	1.152	35.9	822.9	3.10	0.50	0.25	16.1	178.5
P_2O_5	0.14	0.01	0.000	5.7	9.4	0.16	0.08	0.006	50.0	882
Ba	462.5					522.5	62.1	3853.87	11.9	92.2
Rb	142.8	64.3	4140.25	45.0	18001	154.6	27.0	729.00	17.5	3170
Sr	196.5	27.0	727.00	13.7	9087	169.6	36.2	1310.44	21.3	16381
Pb	14.8	9.0	80.92	60.8	172.2	22.1	5.2	27.04	23.5	57.5
Th	19.0	2.8	8.00	14.7	26.7	17.2	3.5	12.25	20.3	40.9
U	3.3	0.5	0.25	15.2	0.4	2.5	1.5	2.25	60.0	34.1
Zr	174.3	9.3	85.58	5.3	3.6	159.8	17.9	320.41	11.2	13.4
Nb	17.8	1.5	2.25	8.4	22.5	17.0	2.1	4.41	12.4	44.1
Y	29.0	1.4	2.00	4.8	6.7	25.4	5.4	29.16	21.3	97.2
La	17.0					23.2	6.1	36.76	26.3	8.3
Ce	65.5					59.5	11.8	139.67	19.9	22.4
Pr	8.5					7.2	2.8	7.96	38.9	3.9
Nd	21.0					19.1	4.9	23.89	25.6	14.1
V	91.0					104.8	26.0	676.4	24.8	232.1
Cr	73.5					82.0	33.9	1152.40	41.3	431.5
Mn	495.0					524.5	79.4	6308.07	15.1	640.0
Ni	20.0					21.9	5.5	30.09	25.1	177.0
Cu	19.0					13.1	4.8	22.89	37.6	36.4
Zn	64.0					76.8	15.2	229.76	19.8	225.0
Ga	17.5	0.6	0.30	3.4	1.3	16.7	1.3	1.69	7.8	7.4

	Callemondah Granodiorite					Bolairo Granodiorite				
	$\bar{x}$	σ_T	σ_T^2	v	σ_T^2/σ_A^2	$\bar{x}$	σ_T	σ_T^2	v	σ_T^2/σ_A^2
SiO_2	67.88	1.60	2.553	2.4	335.9	68.35	0.65	0.416	1.0	54.7
TiO_2	0.62	0.08	0.007	12.9	8750	0.60	0.04	0.002	6.7	2500
Al_2O_3	14.54	0.21	0.045	1.4	13.2	14.41	0.26	0.066	1.8	19.4
Fe_2O_3	0.74	0.24	0.058	32.4		0.62	0.17	0.029	27.4	
FeO	3.94	0.42	0.174	10.7	457.9	3.81	0.44	0.190	11.6	500
MnO	0.07	0.01	0.000	14.3	666.6	0.07	0.00	0.000	3.4	16.7
MgO	2.32	0.38	0.146	16.4	208.6	2.40	0.10	0.010	4.2	14.3
CaO	3.13	1.08	1.156	34.5	13600	2.61	0.30	0.091	11.5	1070
Na_2O	2.25	0.22	0.049	9.8	14.8	2.11	0.10	0.011	4.7	3.3
K_2O	2.52	1.16	1.353	46.0	966.4	3.45	0.13	0.017	3.7	12.1
P_2O_5	0.15	0.02	0.000	13.3	58.8	0.14	0.01	0.000	7.1	14.7
Ba	415.4	202.5	40994.28	48.7	979.6	300.8	348.0	121104.88	115.7	2894
Rb	111.5	57.4	3291.50	51.5	14311	161.4	29.9	891.30	18.5	3875
Sr	209.3	92.3	8517.46	44.1	106468	151.4	12.3	150.80	8.1	1885
Pb	22.5	7.0	49.10	31.1	104.5	26.8	2.9	8.70	10.8	18.5
Th	16.7	2.9	8.27	17.4	27.6	17.2	1.3	1.70	7.6	5.7
U	3.5	0.8	0.70	22.9	1.1	2.8	0.8	0.70	28.6	1.1
Zr	165.8	27.5	757.77	16.6	31.7	172.6	6.8	46.30	3.9	1.9
Nb	17.3	2.0	3.87	11.6	38.7	16.2	0.8	0.70	4.9	7.0
Y	30.8	4.2	17.37	13.6	57.9	32.6	4.5	20.30	13.8	67.7
La	20.8	7.2	51.70	3.4	11.7	11.3	13.0	170.25	115.0	38.4
Ce	59.4	12.1	146.30	20.4	23.4	27.0	31.3	978.00	115.9	156.7
Pr	6.0	2.4	6.00	40.0	2.9	3.8	5.2	26.92	136.8	13.1
Nd	21.6	3.0	8.80	13.9	5.2	8.3	9.6	92.25	115.7	54.6
V	96.6	11.8	139.30	12.2	47.9	44.3	51.3	2630.92	115.8	904.1
Cr	68.0	8.8	77.50	12.9	29.0	39.0	45.0	2028.00	115.4	759.6
Mn	507.8	77.7	6044.70	15.3	613.1	278.8	324.1	105043.56	116.2	10654
Ni	18.6	3.6	13.30	19.4	78.2	12.8	14.8	218.25	115.6	1284
Cu	10.0	7.3	53.50	73.0	84.9	4.3	7.8	61.58	181.4	97.7
Zn	70.6	16.5	271.80	23.4	266.5	45.3	53.4	2851.58	117.9	2796
Ga	17.0	1.3	1.60	7.6	6.7	17.0	1.0	1.00	5.9	4.2

	Willoona Tonalite					Shannons Flat Adamellite				
	$\bar{x}$	σ_T	σ_T^2	v	σ_T^2/σ_A^2	$\bar{x}$	σ_T	σ_T^2	v	σ_T^2/σ_A^2
SiO_2	68.40	0.30	0.092	0.4	12.1	72.21	0.96	0.923	1.3	121.4
TiO_2	0.66	0.03	0.001	4.5	1250	0.36	0.05	0.002	13.6	2500
Al_2O_3	14.44	0.14	0.019	1.0	5.6	13.90	0.26	0.068	1.9	20.0
Fe_2O_3	0.65	0.11	0.012	16.9		0.59	0.11	0.011	17.8	
FeO	3.88	0.20	0.039	5.2	102.6	1.90	0.26	0.069	13.8	181.6
MnO	0.07	0.01	0.000	14.3	133.3	0.05	0.01	0.000	17.4	42.6
MgO	2.18	0.16	0.025	7.3	35.7	0.85	0.16	0.025	18.4	35.7
CaO	2.40	0.34	0.114	14.2	1341	2.43	0.32	0.101	13.1	1188
Na_2O	2.17	0.22	0.047	10.1	14.2	2.64	0.11	0.011	4.0	3.3
K_2O	2.84	0.64	0.405	22.5	289.3	4.31	0.24	0.058	5.6	41.4
P_2O_5	0.16	0.01	0.000	6.3	14.7	0.09	0.01	0.000	14.8	24.9
Ba	596.5	22.7	513.67	3.8	12.3	586.2	96.3	9272.84	16.4	221.6
Rb	154.2	41.3	1703.70	26.8	7407	208.2	29.1	849.66	14.0	3694
Sr	169.8	18.4	336.70	10.8	4209	148.6	18.5	343.01	12.5	4288
Pb	19.2	5.4	29.20	28.1	62.1	27.9	2.7	7.33	9.7	15.6
Th	20.0	2.1	4.50	10.5	15.0	21.4	2.8	7.76	13.1	25.9
U	3.4	0.6	0.30	17.6	0.5	4.0	1.5	2.25	37.5	3.4
Zr	182.4	5.7	32.80	3.1	1.4	148.7	18.3	335.46	12.3	14.0
Nb	17.2	0.8	0.70	4.7	7.0	19.7	1.7	2.73	8.6	27.3
Y	30.6	3.1	9.30	10.1	31.0	48.2	32.3	1045.77	67.0	3486
La	24.0	3.4	11.33	14.2	2.6	27.8	4.5	20.36	16.2	4.6
Ce	64.0	2.8	8.00	4.4	1.3	68.6	8.7	75.17	12.7	12.0
Pr	7.8	1.5	2.25	19.2	1.1	7.8	2.3	5.17	29.5	2.5
Nd	20.3	1.3	1.58	6.4	0.9	23.6	4.0	15.76	17.0	10.0
V	87.0	3.6	12.67	4.1	4.4	43.8	9.0	80.36	20.6	27.6
Cr	59.5	0.6	0.33	1.0	0.1	17.3	3.8	14.38	22.0	5.4
Mn	542.0	76.0	5774.66	14.0	585.7	331.3	52.6	2762.22	15.9	1.6
Ni	23.3	2.5	6.25	10.7	36.8	10.8	4.6	21.14	42.6	124.4
Cu	10.3	4.6	20.93	44.7	33.2	2.2	3.0	8.97	136.4	14.2
Zn	81.0	6.7	44.67	8.3	43.8	36.2	7.8	60.25	21.6	59.1
Ga	17.4	0.6	0.30	3.4	1.3	14.9	0.8	0.69	5.4	2.9

	Tharwa Adamellite				
	$\bar{x}$	σ_T	σ_T^2	v	σ_T^2/σ_A^2
SiO_2	73.01	1.81	3.275	2.5	430.9
TiO_2	0.34	0.12	0.015	35.3	18750
Al_2O_3	13.65	0.22	0.047	1.6	13.8
Fe_2O_3	0.56	0.20	0.040	35.7	
FeO	1.90	0.33	0.110	17.4	289.5
MnO	0.04	0.02	0.000	50.0	240.3
MgO	0.83	0.32	0.100	38.6	142.9
CaO	2.24	0.31	0.097	13.8	1141
Na_2O	2.74	0.45	0.200	16.4	60.6
K_2O	4.04	0.62	0.382	15.4	272.9
P_2O_5	0.10	0.01	0.000	10.0	14.7
Ba	545.5	80.4	6456.33	14.7	154.3
Rb	198.8	33.8	1141.20	17.0	4962
Sr	158.0	59.8	3581.60	37.8	44763
Pb	26.6	2.9	8.30	10.9	17.7
Th	19.4	4.0	16.30	20.6	54.3
U	4.6	1.9	3.80	41.3	5.8
Zr	147.8	32.0	1024.70	21.7	42.9
Nb	18.6	1.7	2.80	9.1	28.0
Y	37.0	5.1	26.50	13.8	88.3
La	23.3	9.6	92.25	41.2	20.8
Ce	60.3	11.0	120.25	18.2	19.3
Pr	7.0	1.4	2.00	20.0	1.0
Nd	19.5	4.4	19.00	22.6	11.2
V	39.3	22.4	502.92	57.0	172.8
Cr	18.3	18.9	78.25	48.6	29.3
Mn	324.0	94.7	8964.66	29.2	909.2
Ni	8.3	4.9	24.25	59.0	142.6
Cu	1.8	2.4	5.58	133.3	8.9
Zn	36.0	11.2	124.67	31.1	122.2
Ga	14.6	0.5	0.30	3.4	1.3

Table 20 Variance data for five units in the Rattlesnake Mountain Pluton, Southern California - adapted from Baird et al. (1966)

a) Total outcrop variances

	1	2	3	4	5
SiO_2	1.5049	2.8451	0.7325	3.6101	3.2911
TiO_2	0.0022	0.0136	0.0003	0.0022	0.0039
Al_2O_3	0.2664	0.4103	0.1253	0.4303	0.5023
FeO	0.0212	0.4688	0.0021	0.3934	0.2218
MgO	0.0234	0.1585	0.0041	0.0269	0.0242
CaO	0.0274	0.1930	0.0145	0.1063	0.1345
Na_2O	0.0134	0.0429	0.0278	0.0154	0.4345
K_2O	0.0711	0.0197	0.0032	0.0485	0.2181

b) Total unit variances

	1	2	3	4	5
SiO_2	1.5049	14.9803	4.5755	3.6101	6.7891
TiO_2	0.0145	0.0963	0.0047	0.0022	0.0078
Al_2O_3	0.6966	1.3640	0.1253	0.4303	1.0465
FeO	0.0212	4.2784	0.1479	0.3934	0.2218
MgO	0.0234	2.1373	0.0297	0.0269	0.0242
CaO	0.2232	4.1796	0.0701	0.1063	0.1345
Na_2O	0.0672	0.5945	0.0278	0.0425	0.4345
K_2O	0.2201	0.2812	0.0064	0.1572	0.2181

1. Porphyritic biotite-quartz monzonite (average SiO_2 67.17 per cent)
2. Hornblende-quartz diorite (average SiO_2 51.55 per cent)
3. Diorite . (average SiO_2 56.04 per cent)
4. Hornblende-quartz monzonite (average SiO_2 60.11 per cent)
5. Biotite-quartz monzonite (average SiO_2 67.59 per cent)

variances for the elements expressed as oxides to allow direct comparison with table 19. The range of variances of the Murrumbidgee intrusions are similar to those of four of the Rattlesnake Mountain units for TiO_2, Al_2O_3, FeO, MgO, CaO and Na_2O. SiO_2 in the Murrumbidgee units has lower variances than in the Rattlesnake Mountain units and K_2O has higher variances. The hornblende-quartz diorite of the Rattlesnake Mountain area has higher variances than the Murrumbidgee units for all constituents except K_2O. Baird et al. (1967) concluded that local variability accounted for a large proportion of variance of many elements in the individual rock units but, in contrast, the outcrop variance of the Shannons Flat Adamellite is very small compared with the total variance of the intrusion.

The variance data indicate that there is a difference in the style of variation between the contaminated granite group and the uncontaminated granite group. In the uncontaminated granites (the Shannons Flat Adamellite and Tharwa Adamellite) the variance of SiO_2 is at least nine times greater than the variance of any other chemical constituent, but in two of the five contaminated granites (the Stewartsfield Granodiorite and the Willoona Tonalite) the variance of K_2O exceeds that of SiO_2, and in another two intrusions (the Callemondah and Bolairo granodiorites) the variance of SiO_2 is only about twice as large as that of the next largest variance. These differences in the style of variation will be discussed more fully in connexion with variation of the batholith as a whole.

Regular variation within the largest intrusions

a) Shannons Flat Adamellite

In view of its large size compared with other intrusions in the batholith, its irregular shape, the presence of hornfels screens, and some variation in texture, the Shannons Flat Adamellite was suspected to be a composite intrusion. However, attempts to delineate separate intrusions in the field were unsuccessful. In consequence, sampling for chemical analysis was carried out on a predetermined geographical plan to allow analysis of variance in the hope of delineating subareas of homogeneity. An hierarchical system of subdivided rectangles was used to define sampling areas. Difficulties of access and outcrop hindered completion of the predetermined sampling in the central western area of the batholith (figure 4).

However, cluster analysis (Rhodes 1969a), offers an alternative approach by directly comparing all the samples analysed; furthermore it avoids the problem of sample groups straddling unrecognised compositional boundaries, a situation which could seriously weaken analysis of variance of arbitrary groups.

The method of cluster analysis used is described fully by Rhodes (1969a). Briefly, each sample is compared with every other sample, using all variables, by means of a distance coefficient which is a measure of the Euclidean distance between any pair of samples in m-dimensional space, where m is the number of variables used. The smaller the distance coefficient, the greater the similarity between samples.

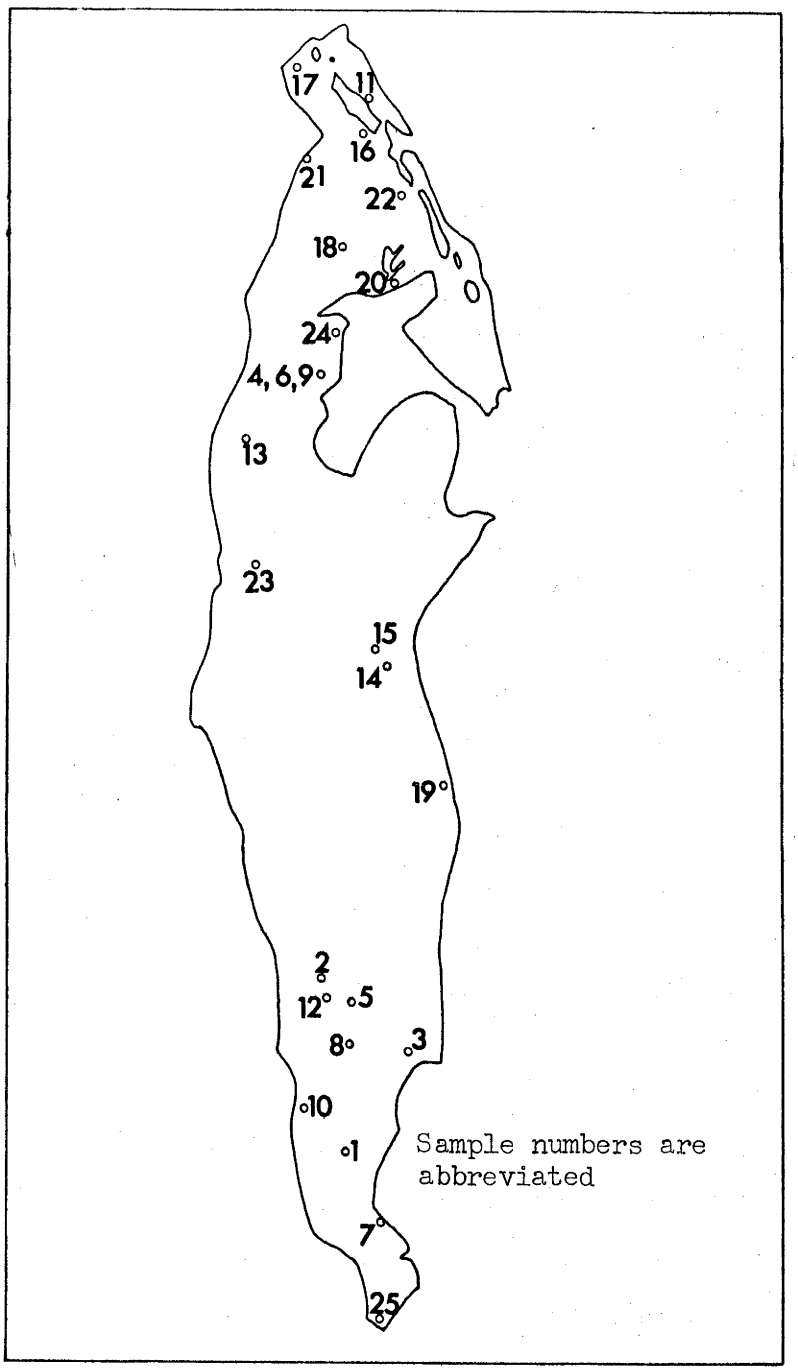

Figure 4. Distribution of samples analysed from the Shannons Flat Adamellite

The results of such a cluster analysis of the 25 samples of Shannons Flat Adamellite based on 32 chemical components (H_2O- and CO_2 were excluded arbitrarily) are presented in the form of a similarity matrix of the individual distance coefficients (table 21) and a dendrogram (figure 5) derived from it by an agglomerative, weighted-pair group method (Rhodes, 1969a). The dendrogram is the simplest presentation but, being a 2-dimensional representation of multidimensional relationships, it is subject to distortion and must be evaluated in conjunction with the similarity matrix. A measure of the degree of distortion is shown in table 21 in the form of a deviation matrix calculated as the differences between the distance coefficients of the similarity matrix and those of the dendrogram. It is apparent that the main distortion concerns the two samples 20524 and 20525 which individually show greater or lesser similarity to some samples of other groups than is obvious from the dendrogram where their attributes are aggregated.

It should be noted that strictly speaking uncorrelated variables should be applied in cluster analysis (Rhodes 1969a), a requirement not usually met by geochemical data, and use of correlated variables amounts to concealed weighting of the variables. Rhodes (1969b) tested the effect of meeting the conditions of orthogonality by first applying principal component analysis and then clustering the component scores (but without normalisation, in order to reduce the "noise" of lesser components) and the results were almost identical to those obtained using the raw chemical data, the distinction in method being principally

Table 21 Similarity and deviation matrices - Shannons Flat Adamellite

	17	16	22	18	11	20	21	9	4	6	2	12	10	13	1	19	23	3	14	15	7	5	8	24	25
17		.30	.31	.33	.28	.27	.26	.36	.38	.36	.39	.34	.40	.32	.39	.36	.32	.45	.32	.36	.42	.41	.44	.40	.52
16	.01		.30	.31	.23	.23	.27	.27	.32	.26	.34	.28	.36	.28	.36	.33	.32	.38	.39	.39	.39	.34	.39	.41	.58
22	.02	.03		.30	.25	.20	.24	.35	.37	.31	.35	.34	.35	.34	.41	.35	.34	.44	.39	.38	.38	.42	.46	.34	.52
18	.04	.04	.05		.24	.20	.18	.36	.36	.33	.38	.35	.38	.39	.40	.36	.34	.47	.37	.38	.43	.47	.53	.27	.46
11	.01	.04	.00	.03		.18	.19	.26	.28	.28	.32	.26	.33	.26	.35	.33	.28	.36	.37	.34	.36	.35	.41	.38	.55
20	.02	.04	.05	.01	.00		.15	.30	.34	.28	.32	.29	.34	.30	.36	.28	.26	.39	.35	.33	.33	.39	.47	.28	.48
21	.03	.00	.01	.03	.01	.00		.33	.37	.34	.38	.33	.37	.34	.38	.34	.26	.43	.38	.38	.39	.43	.46	.25	.43
9	.01	.08	.00	.01	.09	.05	.02		.14	.16	.16	.15	.21	.15	.20	.22	.23	.22	.28	.25	.32	.29	.33	.40	.54
4	.03	.03	.02	.01	.07	.01	.02	.00		.19	.18	.21	.23	.20	.20	.28	.30	.28	.31	.29	.38	.34	.35	.43	.58
6	.01	.09	.04	.02	.07	.07	.01	.01	.02		.17	.17	.22	.20	.25	.21	.28	.30	.26	.23	.34	.31	.38	.39	.54
2	.04	.01	.00	.03	.03	.03	.03	.01	.01	.00		.17	.17	.22	.19	.20	.28	.24	.30	.27	.32	.35	.38	.40	.54
12	.01	.07	.01	.00	.09	.06	.02	.04	.02	.02	.02		.16	.20	.22	.20	.23	.26	.28	.27	.29	.30	.33	.38	.49
10	.05	.01	.00	.03	.02	.01	.02	.02	.04	.03	.02	.00		.26	.21	.27	.27	.31	.29	.26	.32	.38	.35	.37	.46
13	.03	.07	.01	.04	.09	.05	.01	.06	.01	.01	.01	.01	.05		.26	.29	.23	.29	.33	.29	.35	.30	.32	.43	.58
1	.04	.01	.06	.05	.00	.01	.03	.02	.02	.03	.02	.02	.02	.04		.27	.29	.30	.33	.30	.33	.39	.36	.43	.53
19	.01	.02	.00	.01	.02	.07	.01	.02	.04	.03	.04	.04	.03	.05	.03		.27	.29	.31	.30	.34	.39	.45	.36	.49
23	.03	.03	.01	.01	.07	.09	.09	.03	.04	.02	.02	.03	.01	.03	.03	.01		.35	.27	.28	.33	.36	.38	.28	.41
3	.10	.03	.09	.12	.01	.04	.08	.06	.00	.02	.04	.02	.03	.01	.02	.01	.07		.41	.38	.35	.31	.40	.52	.65
14	.03	.04	.04	.02	.02	.00	.03	.02	.01	.04	.00	.02	.01	.03	.03	.01	.03	.11		.27	.39	.37	.44	.34	.45
15	.01	.04	.03	.03	.01	.02	.03	.05	.01	.07	.03	.03	.04	.01	.00	.00	.02	.08	.00		.35	.41	.47	.37	.52
7	.07	.04	.03	.08	.01	.02	.04	.02	.04	.00	.02	.05	.02	.01	.01	.00	.01	.01	.05	.01		.38	.44	.42	.53
5	.02	.05	.03	.08	.04	.00	.04	.10	.05	.08	.04	.09	.01	.09	.00	.00	.03	.08	.02	.02	.01		.27	.50	.64
8	.05	.00	.07	.14	.02	.08	.07	.06	.04	.01	.01	.06	.04	.07	.03	.06	.01	.01	.05	.08	.05	.01		.52	.61
24	.06	.05	.12	.19	.08	.18	.21	.06	.03	.07	.06	.08	.09	.03	.03	.10	.18	.06	.12	.09	.04	.04	.06		.26
25	.06	.12	.06	.00	.09	.02	.03	.09	.12	.09	.09	.03	.00	.12	.07	.03	.05	.19	.01	.06	.07	.18	.15	.00	

Similarity matrix is above, and deviation matrix below the diagonal (sample numbers abbreviated)

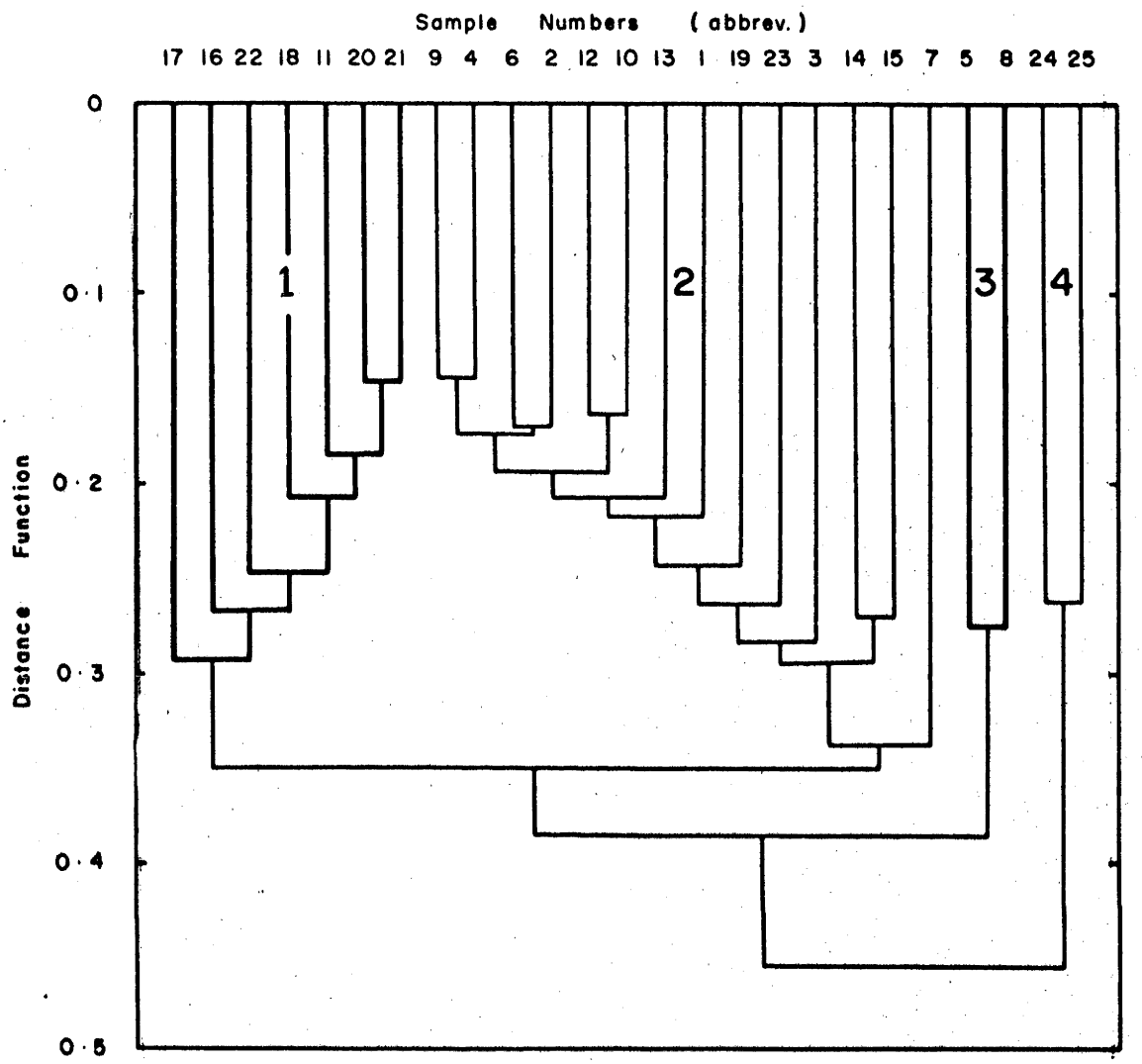

Figure 5. Dendrogram for the Shannons Flat Adamellite

one of deliberate, as distinct from "accidental", weighting of the variables. The direct approach of clustering raw chemical data is considered adequate for treating the Shannons Flat Adamellite.

Four primary groups are recognisable in figure 5, containing 7, 14, 2 and 2 analyses, respectively. The first group is composed solely of samples from an area north and east of Gibraltar Creek Falls, the second group consists of samples south and west of the first group, the third group consists of two samples from adjacent sampling locations west of Boboyan homestead, and the fourth group consists of two samples from opposite ends of the batholith, one from west of Gibraltar Creek Falls and one from south of Shannons Flat. Both samples of the fourth group are more acid than any other samples.

Statistical data for the four groups are recorded in table 22. Snedecor F tests of variables in the first and second groups indicate that the assumption that the variances of the two groups are independent estimates of the same population variance is unjustified for nine variables (FeO, MgO, CaO, Rb, Y, Pr, V, Ni, Cu) and Student's t tests indicate significant differences below the 5 per cent significance level for another 11 components (SiO_2, TiO_2, P_2O_5, Sr, Th, La, Ce, Nd, Cr, Mn, Zn). The differences in K_2O, Zr and Ga may be significant (10 per cent significance level). No significant differences between groups 1 and 2 were apparent for the remaining nine variables (Al_2O_3, Fe_2O_3, MnO, Na_2O, H_2O+, Ba, Pb, U, Nb).

In addition to their geographical dispositions and chemical differences, there is some textural evidence to indicate that groups 1,

Table 22 Statistical data for the four groups of samples of Shannons Flat Adamellite identified by cluster analysis

	Group 1		Group 2			Group 3	Group 4
	Mean	Std.Dev.	Mean	Std.Dev.	t*	Mean	Mean
SiO_2	72.59	0.42	71.80	0.73	2.69	71.62	74.40
TiO_2	0.33	0.02	0.39	0.03	5.81	0.36	0.25
Al_2O_3	13.97	0.17	13.98	0.23	0.04	13.51	13.56
Fe_2O_3	0.59	0.13	0.60	0.09	0.02	0.66	0.45
FeO	1.72	0.25	2.01	0.08	N.A.	2.22	1.37
MnO	0.04	0.004	0.05	0.006	0.57	0.06	0.04
MgO	0.77	0.17	0.90	0.07	N.A.	1.05	0.55
CaO	2.52	0.32	2.49	0.16	N.A.	2.34	1.74
Na_2O	2.67	0.08	2.62	0.08	1.39	2.46	2.80
K_2O	4.15	0.18	4.35	0.23	1.96	4.21	4.65
P_2O_5	0.08	0.01	0.10	0.01	4.36	0.09	0.07
H_2O^+	0.76	0.21	0.67	0.11	1.37	0.81	0.69
Ba	647	69	601	64	1.54	434	421
Rb	174	8.2	216	18	N.A.	253	224
Sr	162	12	148	12	2.50	149	108
Pb	28	1.6	27	2.9	0.61	31	31
Th	25	1.3	20	2.0	5.44	23	19
U	3.4	0.8	3.9	1.1	0.39	7.5	3.0
Zr	144	11	158	16	2.04	134	117
Nb	20	2.2	20	1.5	0.37	19	19
Y	42	2.9	50	44	N.A.	54	50
La	32	2.7	25	3.6	4.54	32	26
Ce	80	3.9	64	4.0	8.58	72	58
Pr	8.1	3.4	7.9	1.5	N.A.	8.5	5.0
Nd	27	1.9	22	2.9	4.34	30	20
V	37	7.0	48	3.3	N.A.	54	26
Cr	14	2.3	19	1.9	5.04	24	11
Mn	303	32	340	37	2.29	435	264
Ni	7.4	1.1	12	5.0	N.A.	17	9.5
Cu	1.3	1.0	3.1	3.7	N.A.	<1	<1
Zn	33	5.2	39	6.4	2.15	46	22
Ga	14	0.5	15	0.9	2.02	16	14

Oxides in per cent, elements in parts per million

$t_{99} = 2.86$, $t_{95} = 2.09$, $t_{90} = 1.73$

N.A. means t test not applied because variance ratio F exceeded that allowable at the 5% level.

* t value for test that means 1 and 2 do not differ

2 and 3 represent discrete intrusive phases. The rocks of group 1 are less conspicuously foliated than those of group 2, and those of group 3 are both finer grained and more massive than all other samples. Both samples of group 4, although chemically dissimilar, are texturally similar to adjacent analysed samples.

The structural state of the potassium feldspars is suggested as a possible additional test of the groupings. If the groups represent separate intrusive phases then the conditions of crystallisation in each case need not have been identical and a difference between groups in the degree of ordering of a mineral such as potassium feldspar would provide support for the existence of discrete intrusive phases. On the other hand, a lack of difference in structural state need not negate discrete intrusive phases, but merely imply similar conditions of crystallisation, especially since the degree of ordering of feldspars throughout the batholith is so high. Table 23 records the triclinicity (Δ) of potassium feldspars (Goldsmith & Laves, 1954) from each of the analysed rocks and the variation is shown graphically in figure 6. An F test indicates a significant difference in the variance of Δ between groups 1 and 2 at the 1 per cent level.

Thus, geographically reasonable variations in composition and texture of the rocks and in the degree of ordering of their potassium feldspars combine to suggest that the Shannons Flat Adamellite is a composite body, but conventional mapping techniques are inadequate to delineate separate phases.

Table 23 Triclinicity of potassium feldspars
Shannons Flat Adamellite

Group 1		Group 2		Group 3		Group 4	
Sample		Sample		Sample		Sample	
20517	.80	20509	.93	20505	.82	20524	.91
20516	.95	20504	.89	20508	.81	20525	.99
20522	.97	20506	.92				
20518	.90	20502	.95				
20511	.69	20512	.76				
20520	.95	20510	.92				
20521	.66	20513	.92				
		20501	.91				
		20519	.97				
		20523	.85				
		20503	.95				
		20514	.89				
		20515	.95				
		20507	.96				

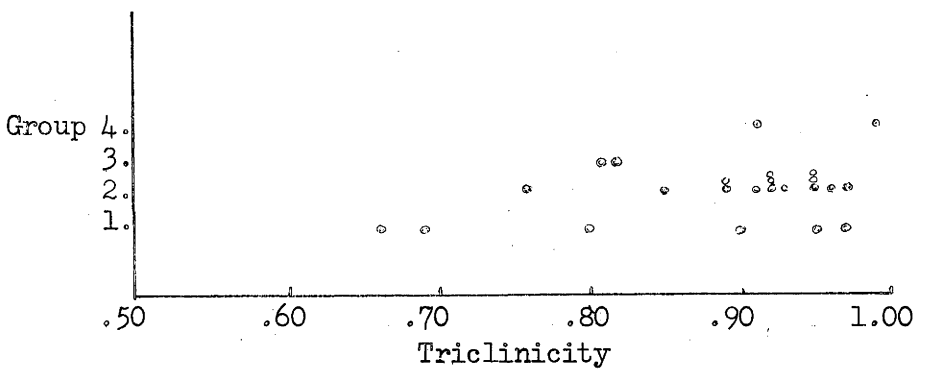

Figure 6 Graphical presentation of the variation in triclinicity of the potassium feldspars of the four groups of Shannons Flat Adamellite identified by cluster analysis

b) Clear Range Granodiorite

The relationship between the Clear Range Granodiorite and the south-eastern extension of the batholith described by Snelling (1957, 1960) as Murrumbucka Tonalite is problematical. Snelling (1960), speaking of the Clear Range Granodiorite, stated: 'South of Mt. Clear there is a gradual decrease in the content of potash feldspar and the rock grades into a tonalite - the Murrumbucka tonalite'. In contrast, the latest edition of the Canberra 1:250,000 Geological Sheet shows a definite geological boundary in the vicinity of Spring Vale Creek. Field examination has failed to substantiate a boundary and petrographic and chemical data support the hypothesis of a gradational relationship. To test this point more objectively and to test the possible existence of any other discontinuities in the Clear Range Granodiorite, cluster analysis, as described above for the Shannons Flat Adamellite, was performed on the 16 samples analysed from the Clear Range Granodiorite/ Murrumbucka Tonalite area (table 24, figure 7). The dendrogram shows five apparent clusters, one of which contains samples solely from the northern area whereas the remaining clusters consist of samples from central and southern areas. Geographically the latter clusters appear meaningless and reference to the similarity/deviation matrix (table 24) indicates considerable distortion of relationships in the central and southern samples. To avoid the difficulty of resorting to sample by sample examination of the similarity matrix to clarify the relationships, additional cluster analyses were performed using

(1) samples from the northern and central areas (table 25a, figure 8a)

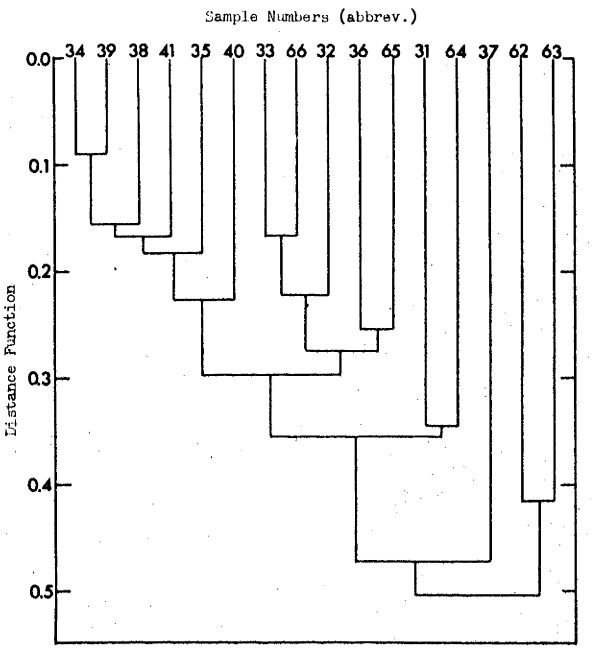

Figure 7 Dendrogram derived by cluster analysis of all samples of Clear Range Granodiorite

Table 24 Similarity and deviation matrices - Clear Range Granodiorite

	20562	20563	20564	20565	20566	20531	20532	20533	20534	20535	20536	20537	20538	20539	20540	20541
20562		0.42	0.50	0.43	0.52	0.48	0.35	0.51	0.58	0.60	0.49	0.67	0.54	0.65	0.71	0.70
20563	0.00		0.46	0.39	0.37	0.46	0.26	0.33	0.50	0.48	0.48	0.43	0.46	0.54	0.58	0.59
20564	0.00	0.04		0.35	0.31	0.34	0.32	0.34	0.36	0.35	0.33	0.51	0.35	0.39	0.45	0.43
20565	0.07	0.11	0.00		0.27	0.30	0.26	0.28	0.34	0.30	0.26	0.42	0.27	0.40	0.42	0.40
20566	0.02	0.13	0.04	0.01		0.31	0.23	0.17	0.22	0.24	0.29	0.39	0.19	0.25	0.26	0.30
20531	0.02	0.04	0.00	0.05	0.16		0.31	0.38	0.34	0.37	0.34	0.49	0.30	0.39	0.39	0.40
20532	0.15	0.24	0.03	0.02	0.01	0.04		0.21	0.31	0.34	0.29	0.42	0.28	0.36	0.42	0.42
20533	0.01	0.17	0.01	0.00	0.00	0.03	0.01		0.23	0.22	0.27	0.40	0.20	0.26	0.32	0.30
20534	0.08	0.00	0.01	0.04	0.08	0.01	0.01	0.07		0.17	0.24	0.50	0.13	0.09	0.22	0.16
20535	0.10	0.02	0.00	0.00	0.06	0.02	0.04	0.08	0.01		0.23	0.51	0.16	0.20	0.29	0.19
20536	0.01	0.02	0.02	0.00	0.01	0.01	0.01	0.01	0.06	0.07		0.50	0.22	0.28	0.40	0.31
20537	0.17	0.07	0.04	0.05	0.08	0.02	0.05	0.07	0.03	0.04	0.03		0.46	0.51	0.50	0.52
20538	0.04	0.04	0.00	0.03	0.11	0.05	0.02	0.10	0.03	0.02	0.08	0.01		0.18	0.23	0.18
20539	0.15	0.04	0.04	0.10	0.05	0.04	0.06	0.04	0.00	0.02	0.02	0.04	0.02		0.19	0.15
20540	0.21	0.08	0.10	0.12	0.04	0.04	0.12	0.02	0.01	0.06	0.10	0.03	0.00	0.04		0.21
20541	0.20	0.09	0.08	0.10	0.00	0.05	0.12	0.00	0.01	0.01	0.01	0.05	0.01	0.02	0.02	

The similarity matrix is above, and the deviation matrix is below the blank diagonal.

(ii) samples from the southern and central areas (table 25b, figure 8b) The deviation matrices indicate that distortion of the dendrograms has been reduced by this procedure and the relationships displayed are now simply stepwise, without significant clusters, consistent with gradational chemical relationships between the samples; figure 8a shows general gradational relationships between northern and central areas, and figure 8b shows gradational relationships between the central and southern areas.

As an additional check, principal component analysis (Harman, 1960; Cooley & Lohnes, 1962) was performed on the analyses. This procedure will be discussed more fully in a following section, but for present purposes it may be explained as a method which reduces the large number of variables to a smaller number of components which still account for most of the total variance of the system and which can be treated graphically without excessive distortion of relationships. Five components account for nearly 90 per cent of the total variance of the 16 samples; the first component accounts for 45 per cent of the variance and the next four components account for additional amounts of 21, 9, 8 and 6 per cent of the total variance. Component scores of the samples (derived by standardising the data such that each variable has a mean of zero and a variance of one, then multiplying by appropriate component loadings obtained from the component analysis) are listed in table 26 and selected two dimensional relationships are illustrated in figure 9. The spatial relationships projected onto the planes containing components I and II, I and III, and II and III,

Table 25 Similarity and deviation matrices - Clear Range Granodiorite

a) Dominantly northern samples

	20531	20532	20533	20534	20535	20536	20537	20538	20539	20540	20541
20531		0.42	0.49	0.48	0.49	0.49	0.65	0.41	0.57	0.52	0.61
20532	0.12		0.30	0.43	0.47	0.39	0.61	0.39	0.52	0.59	0.63
20533	0.01	0.00		0.29	0.30	0.35	0.51	0.28	0.33	0.43	0.43
20534	0.02	0.01	0.13		0.21	0.29	0.58	0.19	0.14	0.29	0.26
20535	0.01	0.05	0.12	0.03		0.32	0.59	0.19	0.27	0.33	0.26
20536	0.01	0.03	0.07	0.08	0.10		0.62	0.28	0.37	0.50	0.45
20537	0.10	0.02	0.08	0.01	0.00	0.03		0.55	0.60	0.58	0.60
20538	0.09	0.03	0.14	0.05	0.00	0.09	0.04		0.29	0.31	0.30
20539	0.07	0.10	0.09	0.00	0.03	0.00	0.01	0.05		0.28	0.24
20540	0.02	0.17	0.01	0.01	0.03	0.13	0.01	0.01	0.02		0.28
20541	0.11	0.21	0.01	0.01	0.01	0.08	0.01	0.03	0.03	0.02	

b) Dominantly southern samples

	20562	20563	20564	20565	20566	20531	20532	20533	20536	20537
20562		0.43	0.54	0.47	0.58	0.54	0.38	0.55	0.56	0.70
20563	0.00		0.50	0.44	0.44	0.52	0.30	0.40	0.55	0.47
20564	0.06	0.02		0.39	0.32	0.38	0.33	0.35	0.35	0.56
20565	0.01	0.04	0.04		0.31	0.35	0.30	0.30	0.31	0.48
20566	0.10	0.04	0.03	0.00		0.35	0.27	0.20	0.31	0.47
20531	0.06	0.06	0.01	0.02	0.02		0.34	0.41	0.40	0.54
20532	0.10	0.18	0.02	0.01	0.02	0.03		0.24	0.32	0.45
20533	0.07	0.08	0.00	0.01	0.00	0.04	0.01		0.28	0.47
20536	0.08	0.07	0.00	0.00	0.01	0.03	0.02	0.02		0.56
20537	0.18	0.05	0.04	0.04	0.05	0.02	0.07	0.05	0.04	

The similarity matrices are above, and the deviation matrices are below the blank diagonals.

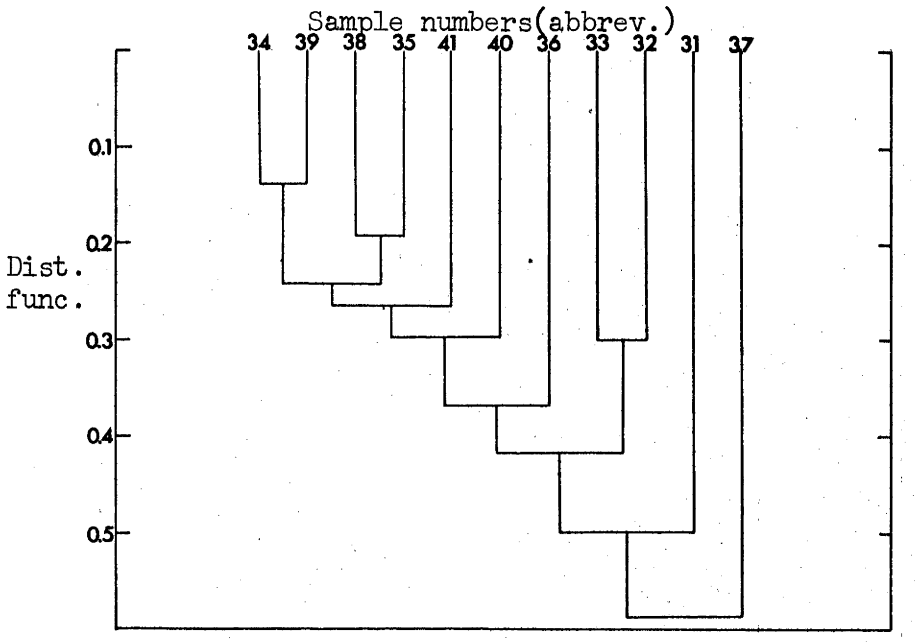

a) Mainly northern samples

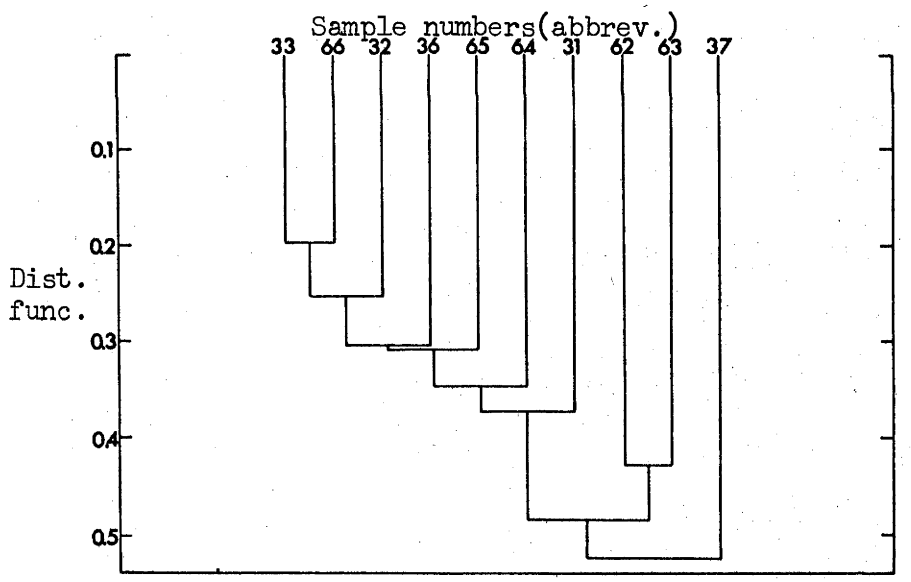

b) Mainly southern samples

Figure 8. Dendrograms derived by cluster analysis of two arbitrary groups of Clear Range Granodiorite

respectively, do not reveal any discontinuity between the southern samples and the northern samples and the disposition of samples relative to the component I axis in figures 9a and 9b indicates an apparent geographic gradation of this component. Figure 9d, showing component I plotted versus distance south of an arbitrary point (Mt Tennant) illustrates this geographic gradation. The correlation coefficient between component I and distance is -0.71.

It is concluded that the chemical data support the hypothesis of a gradational relationship between the Clear Range Granodiorite and the southern area previously designated as Murrumbucka Tonalite. Since the tonalite is not a mappable discrete unit, it is recommended that the use of the term "Murrumbucka Tonalite" be discontinued and that the rocks in the south be included under the formation name "Clear Range Granodiorite", granodiorite being the more abundant rock type.

Probably the tonalite variants are a result of assimilation of amphibolite xenoliths which are conspicuous in the southern region but absent from the northern areas. Such xenoliths are especially abundant in the vicinity of the most basic samples 20562 and 20563 from Murrumbucka Creek and Murrumbucka Gap. The reasons for the variation will be discussed more fully in the section dealing with petrogenesis.

Variation of the batholith as a whole

The rocks have been divided on the basis of field characteristics into three groups; namely, uncontaminated granites, contaminated granites and potassic leucogranites. In addition, the variance data

Table 26 Component scores of the Clear Range Granodiorite samples

		COMPONENT SCORES				
	d*	I	II	III	IV	V
20562	50.5	-7.61	-2.52	-0.77	0.74	-0.30
20563	51.7	-4.11	2.82	-1.63	-1.53	-0.54
20531	21.6	-0.98	-0.73	2.28	1.81	-2.20
20564	54.0	-1.02	-1.30	3.66	-2.92	0.72
20532	43.8	-2.42	0.05	-0.78	-0.38	-0.52
20565	54.5	-1.37	0.15	0.68	1.92	1.42
20533	35.6	0.17	0.68	-1.56	-1.01	0.49
20566	51.6	0.40	0.74	-0.08	-0.60	-0.68
20534	3.8	2.06	-1.25	-0.69	-0.13	-0.26
20535	10.5	2.02	-1.02	-0.59	-0.40	1.06
20536	48.8	0.23	-1.66	-0.02	1.04	2.14
20537	44.8	0.22	6.20	1.19	0.96	0.71
20538	8.4	1.49	-0.72	-0.47	0.65	0.06
20539	12.9	3.07	-0.85	-0.77	-0.49	-0.34
20540	7.0	3.71	0.06	-0.06	0.08	-2.00
20541	16.1	4.15	-0.63	-0.39	0.26	0.25

Samples arranged in order of increasing SiO_2 content down the table.

* d = distance of specimen south of Mt Tennant (kilometres).

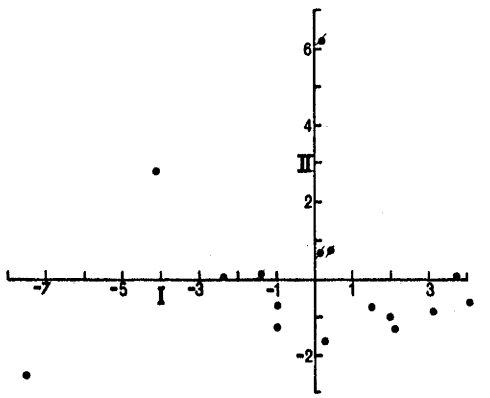

a) Component II vs I

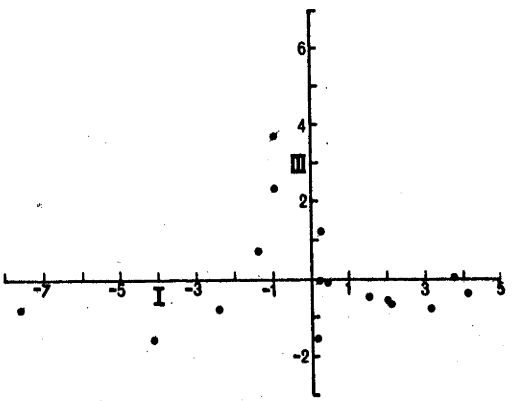

b) Component III vs I

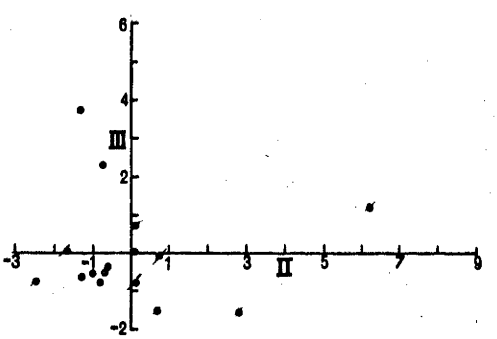

c) Component III vs II

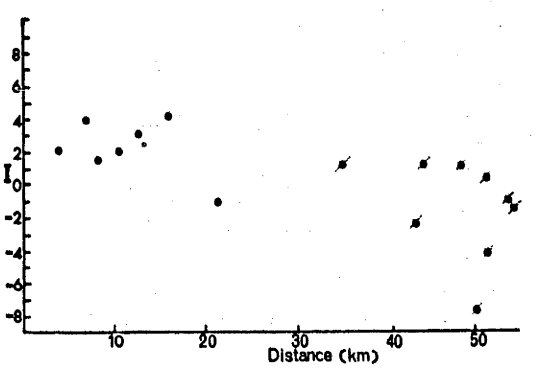

d) Component I vs distance south of Mt Tennent

Figure 9. Principal components diagrams for the Clear Range Granodiorite

for the individual intrusions indicated a difference in style of variation between the uncontaminated and contaminated granite groups. Attempts to define such differences in style of variation between groups of data with so many variables are difficult. One method of approach is to examine the intercorrelations of all the variables in each of the two groups and this can be achieved by inspection of the matrices of table 27 in which all the correlation coefficients of 31 chemical variables are shown separately for the contaminated granite group and the uncontaminated granite group. If the style of variation in the two groups is essentially similar then the pattern of interelement correlation (though not necessarily the absolute values of the correlation coefficients, in view of the limited numbers of samples) ought to be similar. Comparison of the two matrices indicates that this is not the case; variables such as FeO, MgO, CaO, K_2O, Rb, Th, U - to name but a few - show appreciably different sets of correlations in the two granite groups. The matrices contain a wealth of information on interrelationships of the variables (and will be referred to frequently in subsequent discussions) but direct comparison of the 465 pairs of correlation coefficients is extremely tedious.

A more refined method than visual comparison of the correlation matrices is afforded by factor analysis (Cattell, 1952), a mathematical procedure for comparing correlations among variables and grouping variables which vary together. Pertinent features of factor analyses of the two granite groups are summarised in table 28. Only 20 chemical variables were used in order to include as many of the samples as

Table 27 Correlation matrices for the uncontaminated granites (below the diagonal) and the contaminated granites (above the diagonal)

		CONTAMINATED GRANITES																												
		SiO_2	TiO_2	Al_2O_3	Fe_2O_3	FeO	MnO	MgO	CaO	Na_2O	K_2O	P_2O_5	Rb	Sr	Pb	Th	U	Zr	Nb	Y	Ga	Ba	La	Ce	Pr	Nd	V	Cr	Mn	Ni	Cu	Zn
	SiO_2		-0.43	-0.72	-0.45	-0.75	-0.58	-0.91	-0.79	0.63	0.37	-0.18	0.22	-0.42	0.47	0.25	0.14	0.13	-0.14	0.60	-0.36	0.24	-0.13	-0.15	0.07	-0.39	-0.93	-0.83	-0.33	-0.38	-0.32	-0.35
	TiO_2	-0.88		0.51	-0.04	0.78	0.36	0.38	0.12	-0.53	-0.29	0.31	-0.05	0.12	-0.21	-0.05	-0.08	0.64	0.59	-0.01	0.73	0.00	0.50	0.45	0.14	0.43	0.37	0.04	-0.12	0.10	0.13	0.53
	Al_2O_3	-0.40	0.33		0.20	0.82	0.55	0.74	0.55	-0.64	-0.26	0.11	-0.07	0.16	-0.19	-0.18	0.02	0.02	0.32	-0.35	0.51	-0.04	0.34	0.31	0.07	0.41	0.85	0.71	0.20	0.46	0.16	0.52
	Fe_2O_3	-0.71	0.63	0.13		-0.02	0.40	0.41	0.68	-0.15	-0.54	0.10	-0.56	0.55	-0.39	-0.04	-0.09	-0.21	-0.23	-0.52	-0.30	-0.43	0.25	0.17	0.01	0.46	0.70	0.81	0.42	0.32	0.32	0.04
U	FeO	-0.77	0.84	0.18	0.34		0.54	0.74	0.46	-0.74	-0.22	0.19	0.00	0.10	-0.23	-0.25	-0.15	0.24	0.52	-0.27	0.69	-0.03	0.38	0.33	0.05	0.42	0.89	0.57	0.07	0.29	0.34	0.63
N	MnO	-0.58	0.49	0.00	0.33	0.55		0.59	0.52	-0.63	-0.16	-0.35	-0.02	0.11	-0.27	-0.37	-0.06	0.11	-0.02	-0.50	0.17	-0.01	0.36	0.19	0.00	0.29	0.88	0.64	0.47	0.43	0.30	0.61
C	MgO	-0.80	0.81	0.12	0.62	0.80	0.46		0.76	-0.67	-0.31	0.11	-0.17	0.28	-0.35	-0.31	-0.28	-0.18	0.12	-0.59	0.30	-0.17	0.15	0.14	0.00	0.29	0.91	0.92	0.44	0.49	0.34	0.37
O	CaO	-0.64	0.58	0.57	0.43	0.47	0.33	0.30		-0.38	-0.56	0.05	-0.48	0.58	-0.46	-0.43	-0.21	-0.38	-0.07	-0.64	-0.03	-0.45	-0.05	-0.09	-0.14	0.21	0.86	0.80	0.29	0.12	0.22	0.02
N	Na_2O	0.71	-0.73	-0.03	-0.60	-0.62	-0.35	-0.67	-0.38		-0.16	-0.25	-0.28	0.22	0.05	0.15	0.17	-0.07	-0.21	0.46	-0.44	-0.42	-0.48	-0.28	-0.12	-0.20	-0.73	-0.53	-0.16	-0.56	-0.30	-0.72
T	K_2O	-0.30	0.38	0.03	0.30	0.14	0.16	0.30	-0.14	-0.62		-0.04	0.88	-0.84	0.57	0.09	-0.02	-0.08	-0.09	0.14	-0.03	0.85	0.06	-0.05	0.17	-0.43	-0.35	-0.32	-0.04	0.26	-0.05	0.33
A	P_2O_5	-0.53	0.69	0.14	0.34	0.70	0.10	0.54	0.32	-0.33	0.01		-0.03	0.00	-0.03	0.39	-0.06	0.03	0.28	0.06	0.26	0.22	0.44	0.57	0.14	0.46	0.00	-0.12	-0.35	0.22	0.04	0.43
M	Rb	-0.35	0.35	-0.22	0.18	0.42	0.40	0.40	-0.22	-0.46	0.62	0.28		-0.78	0.46	0.06	-0.05	0.05	0.08	0.04	0.16	0.80	0.18	0.00	0.13	-0.39	-0.28	-0.25	0.13	0.37	-0.10	0.44
I	Sr	0.19	-0.38	0.22	-0.28	-0.18	-0.16	-0.40	0.27	0.59	-0.83	-0.05	-0.58		-0.57	-0.10	0.21	0.04	0.06	-0.20	-0.06	-0.83	-0.14	0.05	-0.15	0.45	0.30	0.34	-0.02	-0.18	-0.12	-0.43
N	Pb	0.14	-0.11	0.12	-0.03	-0.06	-0.05	-0.11	-0.05	-0.23	0.39	-0.32	0.16	-0.33		-0.19	0.06	-0.03	-0.01	0.33	-0.06	0.54	-0.15	-0.14	0.15	-0.39	-0.58	-0.48	-0.29	-0.07	0.02	0.04
A	Th	-0.29	0.19	0.07	0.34	0.10	0.37	0.32	0.31	-0.28	0.11	-0.25	-0.12	-0.16	0.08		0.24	0.34	0.19	0.16	0.03	0.27	0.42	0.63	0.38	0.46	-0.42	-0.17	-0.12	0.34	0.09	0.12
T	U	-0.23	0.24	-0.17	0.25	0.42	-0.03	0.35	0.07	-0.35	-0.06	0.39	0.29	-0.03	0.14	-0.15		0.24	0.02	0.26	0.07	0.03	0.13	0.45	0.30	0.43	-0.22	-0.19	-0.11	0.04	-0.09	-0.13
E	Zr	-0.63	0.83	0.27	0.45	0.65	0.41	0.63	0.47	-0.45	0.25	0.54	0.13	-0.24	-0.23	0.26	0.04		0.61	0.22	0.44	0.06	0.49	0.60	0.30	0.45	-0.26	-0.38	-0.48	-0.02	-0.08	0.22
D	Nb	0.09	-0.03	0.21	-0.07	-0.06	0.04	-0.18	0.16	0.08	-0.12	-0.16	-0.16	0.19	0.07	0.04	-0.28	0.18		0.12	0.57	-0.05	0.55	0.66	0.34	0.61	-0.10	-0.13	-0.50	-0.02	0.36	0.01
	Y	-0.09	0.00	-0.19	-0.01	0.05	0.00	0.03	-0.06	-0.18	0.13	-0.11	0.18	0.02	-0.22	-0.11	0.02	0.00	0.17		0.17	0.09	-0.01	-0.03	-0.01	-0.12	-0.72	-0.66	-0.26	-0.30	-0.24	-0.11
	Ga	-0.45	0.35	0.09	0.23	0.45	0.49	0.29	0.25	-0.07	-0.08	0.49	0.32	0.15	-0.41	0.08	0.27	0.25	-0.17	0.03		0.22	0.53	0.54	0.18	0.37	0.34	0.07	-0.12	0.28	0.04	0.60
G	Ba	-0.36	0.40	0.60	0.30	0.16	0.04	0.05	0.68	-0.19	0.04	0.22	0.27	-0.16	0.30	-0.23	0.52	0.29	0.06	0.27	0.11		0.24	0.15	0.30	-0.25	-0.16	-0.08	0.00	0.51	0.18	0.51
R	La	-0.03	-0.01	-0.03	0.07	0.00	0.35	0.07	0.24	0.02	-0.18	-0.35	-0.35	0.17	-0.06	0.60	-0.05	0.14	0.11	0.08	0.09	0.27		0.76	0.43	0.59	0.26	0.25	-0.01	0.47	0.28	0.52
A	Ce	-0.15	0.08	0.16	0.24	0.02	0.27	0.14	0.40	-0.10	-0.16	-0.32	-0.42	0.17	0.03	0.86	-0.19	0.25	0.40	0.00	-0.05	0.45	0.78		0.62	0.79	0.17	0.21	-0.06	0.41	0.43	0.39
N	Pr	-0.19	0.12	0.01	0.29	0.10	0.07	0.07	0.27	-0.12	-0.17	0.16	-0.03	0.26	-0.23	0.00	0.20	0.16	0.56	0.00	0.21	0.21	-0.05	0.18		0.44	-0.07	0.09	0.01	0.25	0.53	0.09
I	Nd	-0.19	0.07	-0.13	0.24	0.14	0.38	0.18	0.31	-0.17	-0.23	-0.23	-0.24	0.22	-0.08	0.62	0.21	0.17	0.22	0.28	0.20	0.24	0.83	0.80	0.20		0.33	0.33	-0.01	0.20	0.40	0.15
T	V	-0.82	0.92	0.17	0.59	0.89	0.50	0.86	0.44	-0.78	0.36	0.64	0.50	-0.51	0.01	0.11	0.40	0.70	0.02	0.03	0.36	0.15	-0.01	0.03	0.22	0.13		0.78	0.29	0.32	0.28	0.47
E	Cr	-0.66	0.80	0.03	0.59	0.78	0.26	0.80	0.28	-0.70	0.32	0.73	0.52	-0.51	0.07	-0.02	0.61	0.52	-0.18	-0.02	0.31	0.02	-0.09	-0.11	0.13	0.03	0.90		0.44	0.65	0.39	0.32
S	Mn	-0.63	0.64	-0.03	0.45	0.74	0.58	0.70	0.19	-0.66	0.27	0.51	0.58	-0.38	0.12	0.19	0.43	0.37	-0.10	-0.20	0.39	-0.14	-0.15	-0.04	0.13	0.03	0.73	0.70		0.45	0.00	0.28
	Ni	-0.50	0.42	-0.21	0.32	0.47	0.35	0.52	0.01	-0.55	0.40	0.23	0.66	-0.32	-0.16	-0.04	0.30	0.23	-0.01	0.78	-0.08	0.32	-0.08	-0.13	0.09	0.20	0.51	0.45	0.35		0.18	0.61
	Cu	-0.11	0.21	0.12	0.06	0.23	0.04	0.17	0.17	-0.22	0.20	0.02	0.01	-0.19	0.44	0.02	-0.05	0.17	-0.16	-0.13	-0.18	0.08	-0.08	-0.07	-0.08	-0.19	0.28	0.18	0.05	-0.08		0.16
	Zn	-0.71	0.77	0.24	0.56	0.78	0.56	0.70	0.49	-0.59	0.13	0.56	0.33	-0.18	0.15	0.23	0.40	0.57	-0.07	-0.22	0.38	0.16	-0.06	0.09	0.09	0.11	0.76	0.70	0.84	0.23	0.22	

n	24	29	30	36
df	22	27	28	34
r_{99}	0.515	0.471	0.463	0.424
r_{95}	0.404	0.367	0.361	0.330
r_{90}	0.344	0.311	0.306	0.279

For the contaminated granites, no. of analyses equals 36 for SiO_2-Ga and 24 for Ba-Zn
For the uncontaminated granites, no. of analyses equals 30 for SiO_2-Ga and 29 for Ba-Zn

possible.

The particular method of factor analysis employed is that of calculating principal components, details of which are well described by Rao (1965) and Cooley & Lohnes (1962). A brief, clear outline of the method is given by Le Maitre (1968) who used principal component analysis to distinguish a difference in the style of chemical variation between alkali and subalkali volcanic rock series. The analyses may be considered as an ellipsoidal cluster of points in hyperspace with n orthogonal axes each representing one of n original chemical variables. Principal component analysis finds the principal axes of this ellipsoid and projects the old axes (these projections are called loadings) and the scores of the original analyses onto these new axes (the scores on each axis are calculated to equal standard deviations since by definition a factor, or principal component, has unit variance).

Although this procedure substitutes an equal number of new variables (principal components) for the initial variables, usually far fewer components are required to account for most of the variance of the data. This is the case for the granite data, eight components accounting for 88.8 per cent of the total variance of the uncontaminated granites and 91.9 per cent of the variance of the contaminated granites. The factor matrices presented in table 28 highlight the differences in nature of variation between the two groups; whereas SiO_2, FeO, MnO, MgO, and Ga are loaded to similar extents in component I in both groups, the remaining 15 variables show considerable differences in their respective loadings, K_2O, Rb, Sr, Th, U, Nb and Y even showing opposite

Table 28 Factor matrices derived by principal component analyses of the contaminated and uncontaminated granite groups

a) Factor matrix for the contaminated granites (36 samples)

	FACTORS							
	I	II	III	IV	V	VI	VII	VIII
SiO_2	0.93	-0.02	0.12	-0.12	0.00	0.13	0.14	0.03
TiO_2	-0.58	-0.60	0.36	-0.09	-0.07	0.20	0.13	0.21
Al_2O_3	-0.79	-0.29	-0.08	-0.05	-0.01	-0.31	-0.04	-0.08
Fe_2O_3	-0.52	0.62	0.03	0.20	0.25	0.05	0.39	0.10
FeO	-0.82	-0.52	-0.01	-0.08	-0.15	-0.03	-0.09	-0.01
MnO	-0.68	-0.04	-0.32	-0.41	0.38	0.11	0.12	0.18
MgO	-0.89	-0.01	-0.25	0.10	-0.08	-0.05	-0.09	-0.05
CaO	-0.83	0.44	-0.15	0.05	-0.12	-0.08	0.04	-0.10
Na_2O	0.66	0.47	0.40	-0.16	-0.19	0.04	-0.15	-0.15
K_2O	0.53	-0.49	-0.60	0.13	0.17	-0.07	-0.04	-0.04
P_2O_5	-0.14	-0.25	0.28	0.82	-0.18	-0.17	0.22	0.12
Rb	0.34	-0.63	-0.56	0.07	0.20	0.00	-0.11	-0.12
Sr	-0.48	0.57	0.56	-0.13	-0.05	-0.10	-0.02	-0.15
Pb	0.51	-0.33	-0.36	-0.12	-0.26	-0.23	0.53	-0.15
Th	0.29	-0.16	0.45	0.55	0.52	0.01	-0.15	-0.01
U	0.18	-0.03	0.37	-0.27	0.42	-0.74	0.04	-0.03
Zr	-0.02	-0.55	0.58	-0.26	0.34	0.29	0.20	-0.04
Nb	-0.25	-0.62	0.45	0.02	-0.09	0.13	0.09	-0.49
Y	0.59	-0.27	0.41	-0.17	-0.34	-0.19	-0.02	0.32
Ga	-0.39	-0.73	0.26	-0.06	-0.15	-0.12	-0.18	0.14
Cumulative proportion of total variance explained by factors								
	0.36	0.53	0.68	0.75	0.81	0.86	0.89	0.92

(continued on next page)

Table 28 Factor matrices derived by principal component analyses of the contaminated and uncontaminated granite groups

b) Factor matrix for the uncontaminated granites (30 samples)

	FACTORS							
	I	II	III	IV	V	VI	VII	VIII
SiO_2	0.93	0.17	-0.08	0.03	-0.02	-0.07	-0.02	0.21
TiO_2	-0.96	-0.09	0.06	0.08	-0.15	-0.10	-0.11	0.05
Al_2O_3	-0.23	-0.46	0.47	0.36	-0.23	-0.24	0.19	-0.39
Fe_2O_3	-0.69	0.00	0.18	0.04	0.19	0.24	-0.26	-0.16
FeO	-0.86	-0.14	-0.20	0.07	-0.08	0.00	0.19	0.23
MnO	-0.59	-0.05	0.09	-0.48	0.29	-0.14	0.42	0.12
MgO	-0.88	0.06	-0.07	0.00	0.10	0.06	-0.17	0.13
CaO	-0.53	-0.59	0.36	0.16	0.00	0.19	0.12	-0.13
Na_2O	0.79	-0.37	-0.16	-0.09	0.07	-0.30	0.04	0.02
K_2O	-0.42	0.76	0.25	-0.03	-0.18	-0.19	-0.03	-0.26
P_2O_5	-0.64	-0.27	-0.49	0.27	-0.21	-0.21	-0.15	0.09
Rb	-0.48	0.60	-0.34	-0.16	-0.11	-0.16	0.36	-0.07
Sr	0.40	-0.82	-0.13	0.01	0.01	0.20	0.19	-0.07
Pb	0.06	0.51	0.43	0.49	0.06	0.11	0.47	0.10
Th	-0.29	-0.03	0.56	-0.29	0.56	0.16	-0.10	0.10
U	-0.34	0.09	-0.53	0.45	0.14	0.48	0.17	0.14
Zr	-0.75	-0.22	0.17	-0.10	-0.22	-0.21	-0.24	0.27
Nb	0.10	-0.24	0.45	-0.23	-0.54	0.09	0.25	0.40
Y	-0.04	0.12	-0.15	-0.52	-0.51	0.55	-0.02	-0.26
Ga	-0.46	-0.34	-0.46	-0.28	0.23	-0.17	0.31	-0.23
Cumulative proportion of total variance explained by factors								
	0.35	0.50	0.61	0.68	0.74	0.80	0.85	0.89

(continued from previous page)

signs on their loadings. Likewise, the pattern of loadings on the second and subsequent components differs between the two groups; for example, CaO, K_2O, Rb, Sr and Pb show appreciable loadings in component II of the uncontaminated granites whereas TiO_2, FeO, Rb, Sr, Nb and Ga show the heaviest loadings of component II of the contaminated granites (Rb and Sr having opposite signed loadings to the uncontaminated granites).

Clearly the patterns of variation in the two granite groups differ and it remains to be resolved whether this is a result of independent origins of the two groups or whether there is a common origin from which the two groups have evolved by different mechanisms. The petrogenetic relationships of the third group, the leucogranites, which are intimately associated in the field especially with the uncontaminated granites, also require examination.

In order to consider as much of the variance as possible at the one time, principal component analysis again is a logical tool. Unlike the above application, where separate analyses of the two granite groups were desirable to provide a measure of the influences of each chemical variable on the location of the principal components in each of the granite groups, the interrelationships of the various rock types are best examined by principal component analysis of the whole batholith and this has been done using 31 chemical variables in 62 samples, representing xenoliths, contaminated granites, uncontaminated granites and leucogranites. In this case, seven components explain nearly 90 per cent of the total variance. Some relationships of the individual

samples are illustrated in figure 10 as projections onto three planes containing components I and II, I and III, and II and III, respectively. The separation of the uncontaminated granites from the contaminated granites, an association of the two xenoliths, 20576 and 20577, with the contaminated granites, and an association of the leucogranites with the uncontaminated granites, are conspicuous in plots of components I versus II and I versus III. The plot of components II and III shows some overlap of the two main granite groups.

One of the problems of using principal component analysis is the uncertainty of what each principal component represents in terms of geological variables. A less comprehensive but more conventional approach is to examine the interrelationships of the three groups using two dimensional variation diagrams of known variables. The most suitable diagrams commonly used are Harker diagrams representing the abundance of particular chemical constituents plotted against SiO_2 as the independent variable. SiO_2 is a logical independent variable since it accounts for about 57 per cent of the total variance of the contaminated granites and 74 per cent of that of the uncontaminated granites. Also its use is a partial compromise with principal component analysis since it approximates to the first principal component of both the contaminated and uncontaminated granites, with loadings of 0.926 in both cases (table 26). The merits of using SiO_2 as an independent variable in variation diagrams have been commented upon by Le Maitre (1968) in connexion with the variation of volcanic rock series. He found that of the commonly used parameters SiO_2 lay

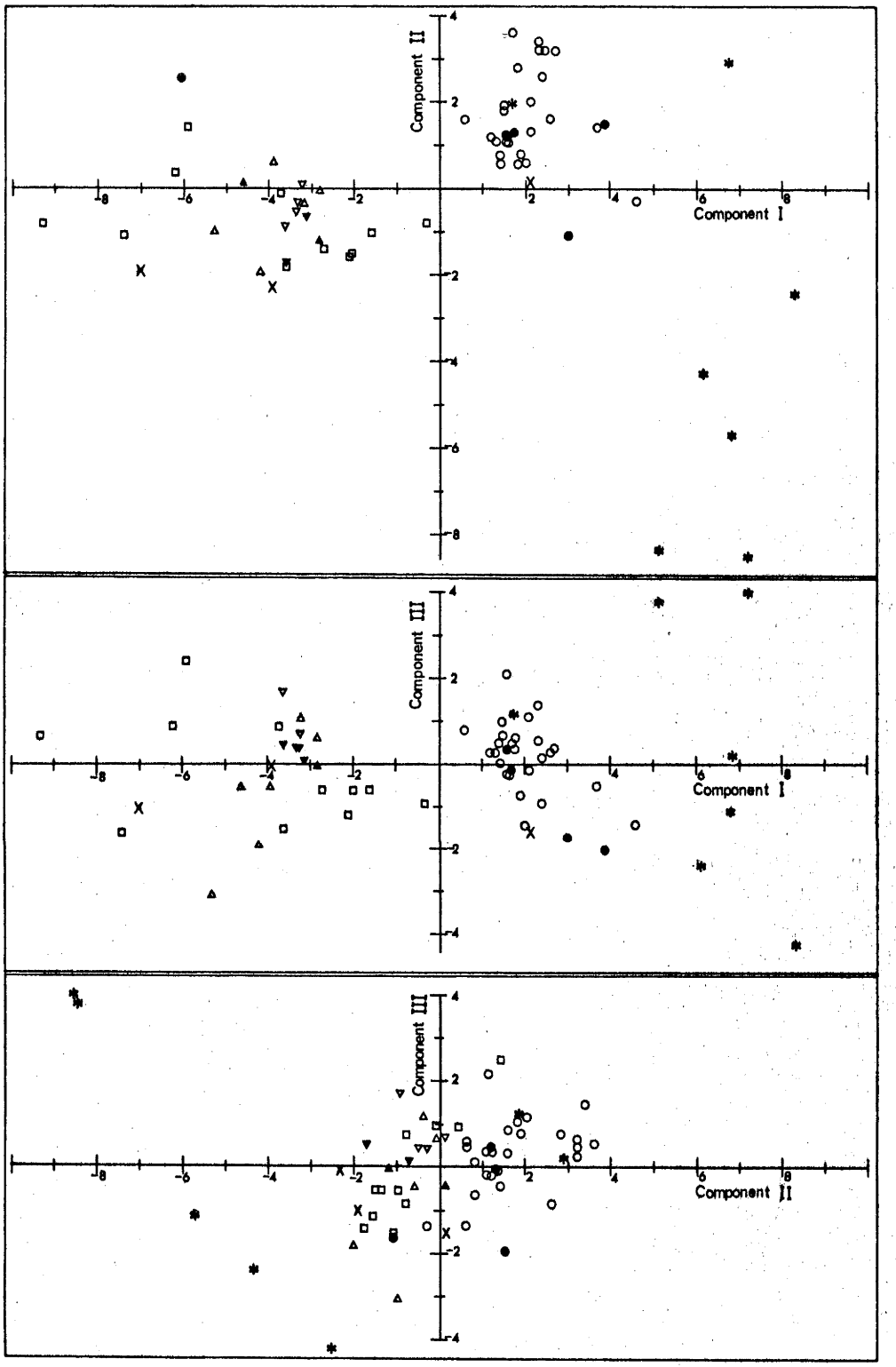

Figure 10. Principal components diagrams for the Murrumbidgee Batholith

closest to the first principal component. Certainly a simple variable such as SiO_2 is preferable to composite variables such as the Larsen index in which the problem of closure inherent in all percentage data is intensified (Chayes, 1960, 1962). An additional, but less important, benefit in using SiO_2 variation diagrams is that direct comparison of results can be made with many published studies.

The variation diagrams are presented in figures 11 - 19. Linear regression equations of the form

$$\text{variable} = b \cdot SiO_2 + a$$

for both the uncontaminated and contaminated granite groups are presented in table 29 along with significance tests, and significant regression lines are shown in figures 11 - 19. Some variables are essentially independent of SiO_2, since t tests indicate that their calculated regression lines do not have significant slopes and their coefficients of determination are correspondingly trivial. Regressions in this category refer to variables (e.g. Th and U) identified previously by principal component analysis of the individual granite groups (table 28) as having low factor loadings on component I, in which SiO_2 showed the highest loading. Many of the other regressions which do have slopes differing significantly from zero, also have rather low coefficients of determination. However, no regular curvilinear trends or groups of separate linear trends are apparent so simple linear regression is considered adequate for descriptive purposes. The lines must be considered only as "average" variation trends in the groups since it would be naive to assume that a single

Table 29 Regression data (in the form : variable = $bSiO_2$ + a) for both the uncontaminated and contaminated granite groups
(continued on next page)

Variable		Slope b	n	t value from test that b does not differ from zero (df = n-2)	t value from test that b_c does not differ from b_u (df = n_c+n_u-4)	Intercept a	Std. error of estimate	Coefficient of determination	Intersection of the two regressions (% SiO_2)
TiO_2	C	-0.017	36	-2.7	3.9	1.780	0.062	18.1	65.5
	U	-0.049	30	-9.6		3.876	0.031	76.8	
Al_2O_3	C	-0.138	36	-6.1	-0.9	23.876	0.223	52.3	73.5
	U	-0.094	30	-2.3		20.645	0.250	16.0	
Fe_2O_3	C	-0.084	36	-2.9	-0.3	6.414	0.282	20.2	-43.1
	U	-0.075	30	-5.3		6.026	0.088	49.8	
FeO	C	-0.251	36	-6.6	-1.4	20.920	0.378	55.9	85.2
	U	-0.182	30	-6.5		15.037	0.173	59.9	
MnO	C	-0.005	36	-4.1	0.0	0.405	0.012	33.2	
	U	-0.005	30	-3.8		0.415	0.008	33.7	
MgO	C	-0.268	36	-12.5	-4.9	20.592	0.211	82.2	75.1
	U	-0.130	30	-7.1		10.218	0.113	64.2	
CaO	C	-0.396	36	-7.5	-3.3	29.920	0.516	62.6	67.3
	U	-0.179	30	-4.4		15.321	0.249	41.1	
Na_2O	C	0.092	36	4.7	-1.0	-4.136	0.193	39.6	68.4
	U	0.121	30	5.3		-6.117	0.140	50.3	
K_2O	C	0.160	36	2.3	2.8	-7.866	0.683	13.6	74.5
	U	-0.087	30	-1.7		10.561	0.324	8.9	
P_2O_5	C	-0.006	36	-1.1	0.0	0.530	0.052	3.2	
	U	-0.006	30	-3.3		0.527	0.011	27.9	
Ba	C	15.049	24	1.1	2.3	-504.6	116.5	5.6	72.4
	U	-29.622	29	-2.0		2724.4	89.2	13.2	
Rb	C	5.553	36	1.3	2.4	-229.3	41.0	5.0	74.7
	U	-9.108	30	-2.0		865.5	28.1	12.4	
Sr	C	-12.101	36	-2.7	-2.7	996.8	43.5	18.0	70.7
	U	4.753	30	1.0		-193.7	28.1	3.7	
Pb	C	1.784	36	3.1	2.0	-99.3	5.7	22.0	71.0
	U	0.338	30	0.8		3.3	2.8	2.0	
Th	C	0.458	36	1.5	2.1	-13.3	3.0	6.3	73.4
	U	-0.775	30	-1.6		77.2	3.0	8.5	

C = contaminated granites
U = uncontaminated granites

df =	22	27	28	34	49	62
t_{90}	1.711	1.703	1.701	1.693		
t_{95}	2.074	2.052	2.048	2.032	2.009	1.999
t_{99}	2.819	2.711	2.763	2.728	2.679	2.657

Table 29 Regression data (in the form : variable = $bSiO_2 + a$) for both the uncontaminated and contaminated granite groups
(continued from previous page)

Variable		Slope b	n	t value from test that b does not differ from zero (df = n-2)	t value from test that b_c does not differ from b_u (df = n_b+n_u-4)	Intercept a	Std. error of estimate	Coefficient of determination	Intersection of the two regressions (% SiO_2)
U	C	0.101	36	0.9	1.5	-3.9	1.2	2.1	73.0
	U	-0.315	30	-1.3		26.9	1.5	5.3	
Zr	C	1.409	36	0.8	4.0	71.8	18.3	1.7	70.4
	U	-11.367	30	-4.3		970.9	16.1	40.3	
Nb	C	-0.141	36	-0.8	-0.8	26.6	1.7	1.9	60.8
	U	0.132	30	0.8		10.0	1.7	0.8	
Y	C	1.855	36	4.3	0.8	-97.3	4.2	35.4	74.6
	U	-2.315	30	-0.5		213.8	30.2	0.8	
La	C	-0.399	24	-0.6	-0.2	49.3	5.7	1.7	43.8
	U	-0.164	29	-0.2		39.0	5.6	0.1	
Ce	C	-0.800	24	-0.7	0.2	114.5	10.0	2.2	97.5
	U	-1.233	29	-0.8		156.7	9.3	2.4	
Pr	C	0.102	24	0.3	1.0	0.3	2.6	0.6	72.3
	U	-0.363	29	-1.0		33.9	2.2	3.7	
Nd	C	-0.816	24	-2.0	-0.1	75.0	3.6	15.4	113.0
	U	-0.701	29	-1.0		73.7	4.2	3.7	
V	C	-9.855	24	-12.2	-1.4	764.7	7.1	87.1	77.0
	U	-7.998	29	-7.5		621.9	6.5	67.9	
Cr	C	-11.007	24	-6.9	-5.0	819.3	14.0	68.7	73.0
	U	-2.600	29	-4.5		205.6	3.5	43.2	
Mn	C	-12.8	24	-1.7	1.75	1392.8	68.3	11.1	65.2
	U	-31.6	29	-4.2		2618.1	45.6	39.9	
Ni	C	-0.935	24	-1.9	1.3	84.8	4.3	14.3	66.1
	U	-2.000	29	-3.0		155.2	4.1	24.7	
Cu	C	-0.812	24	-1.1	-0.6	67.0	6.7	5.0	83.0
	U	-0.282	29	-0.6		22.5	2.9	1.3	
Zn	C	-2.776	24	-1.7	1.2	264.2	14.1	12.1	60.0
	U	-4.982	29	-5.3		396.7	5.8	50.8	
Ga	C	-0.241	36	-2.3	0.5	33.3	1.0	13.1	56.6
	U	-0.310	30	-2.6		37.2	0.7	20.0	

C = contaminated granites
U = uncontaminated granites

df =	22	27	28	34	49	62
t_{90}	1.711	1.703	1.701	1.693		
t_{95}	2.074	2.052	2.048	2.032	2.009	1.999
t_{99}	2.819	2.711	2.763	2.728	2.679	2.657

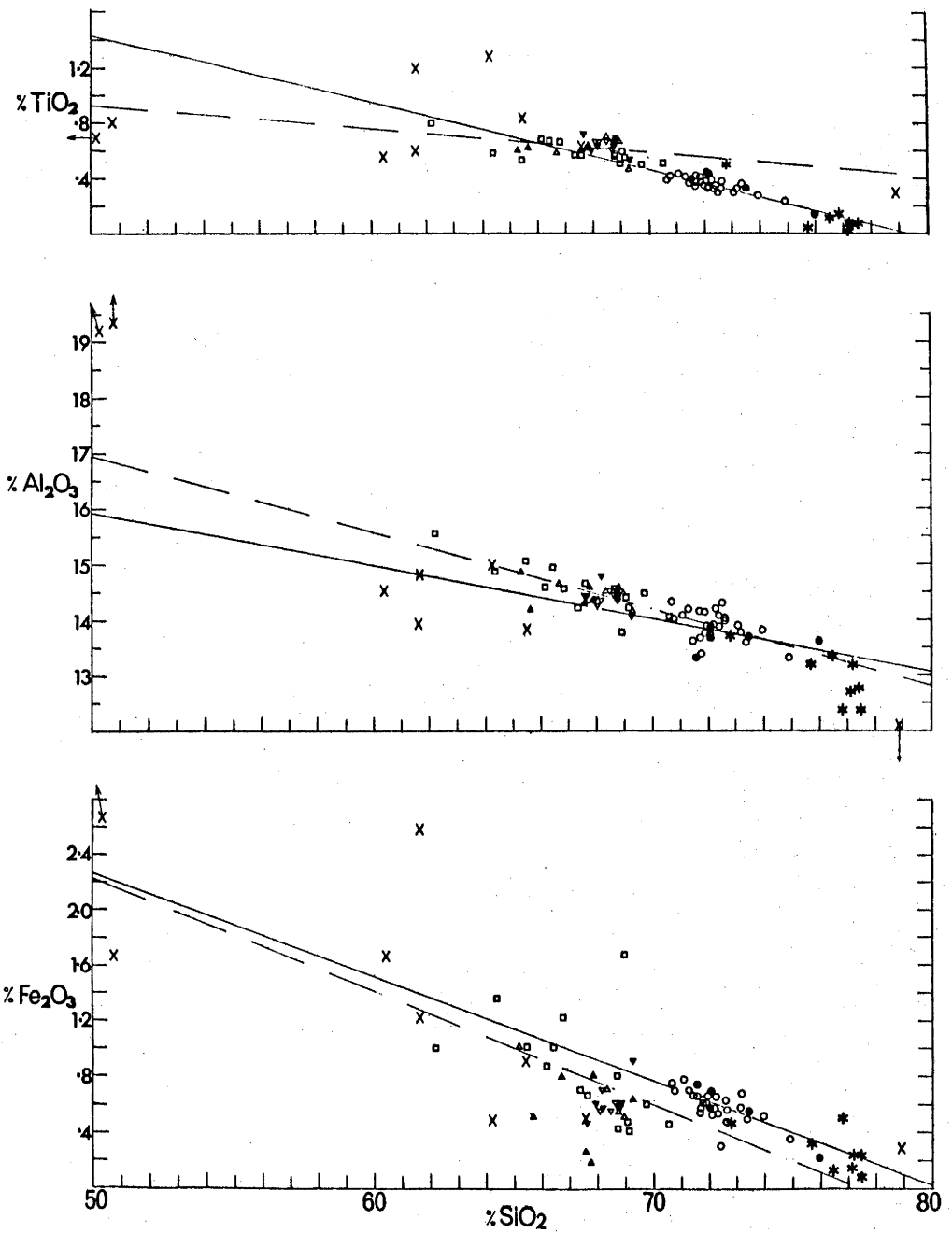

Figure 11. Harker variation diagrams for TiO_2, Al_2O_3 and Fe_2O_3

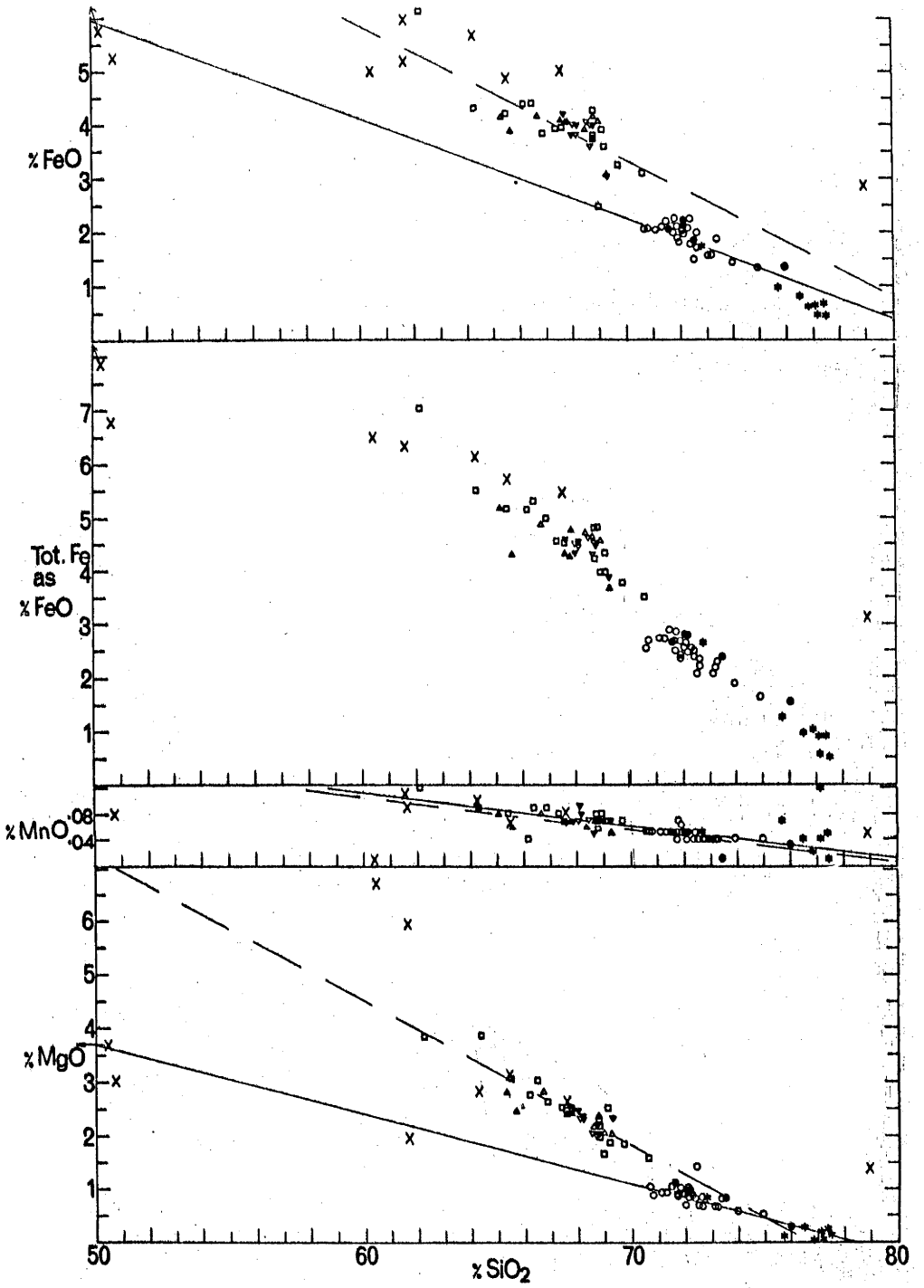

Figure 12. Harker variation diagrams for FeO, total Fe as FeO, MnO and MgO

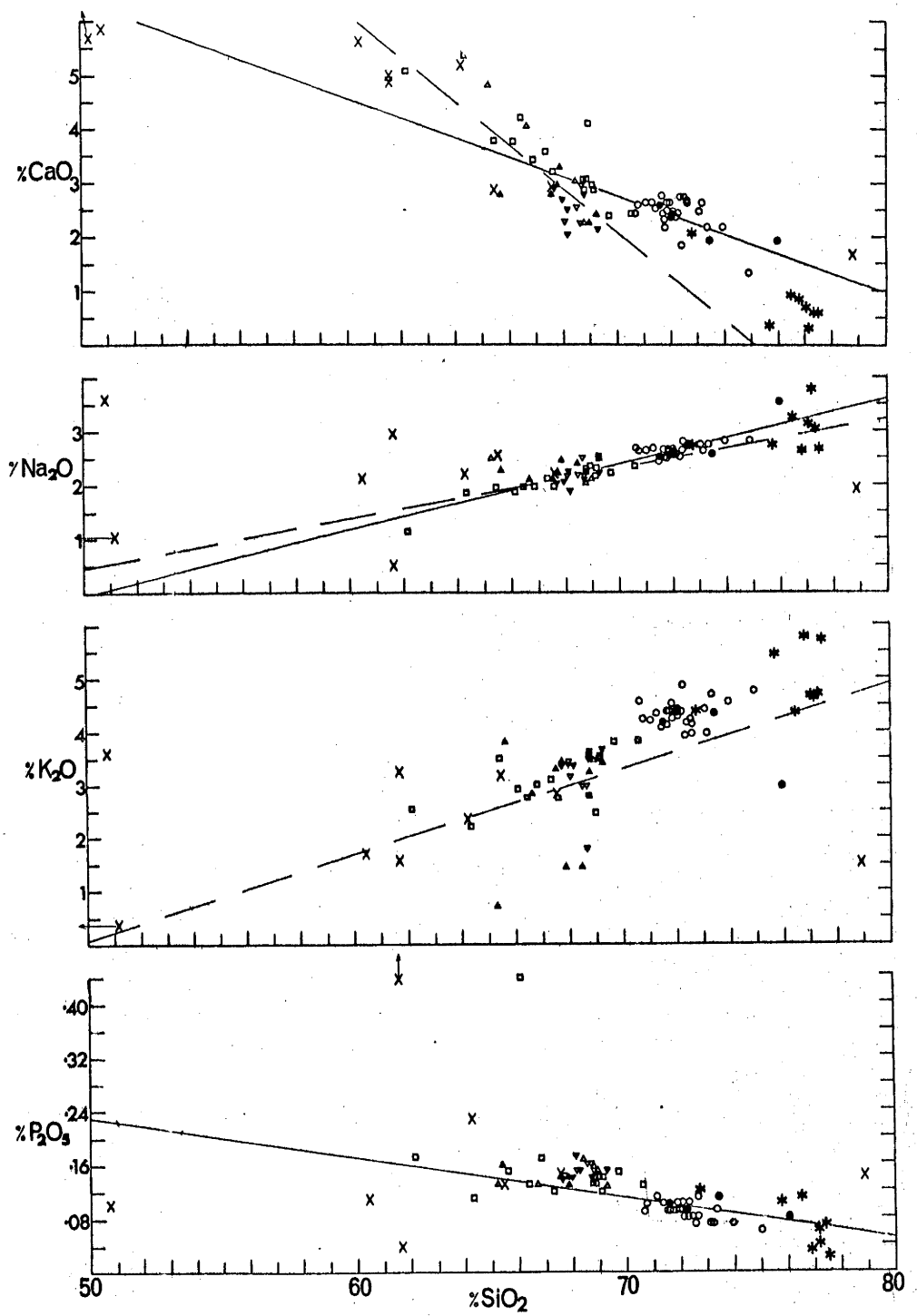

Figure 13. Harker variation diagrams for CaO, Na_2O, K_2O and P_2O_5

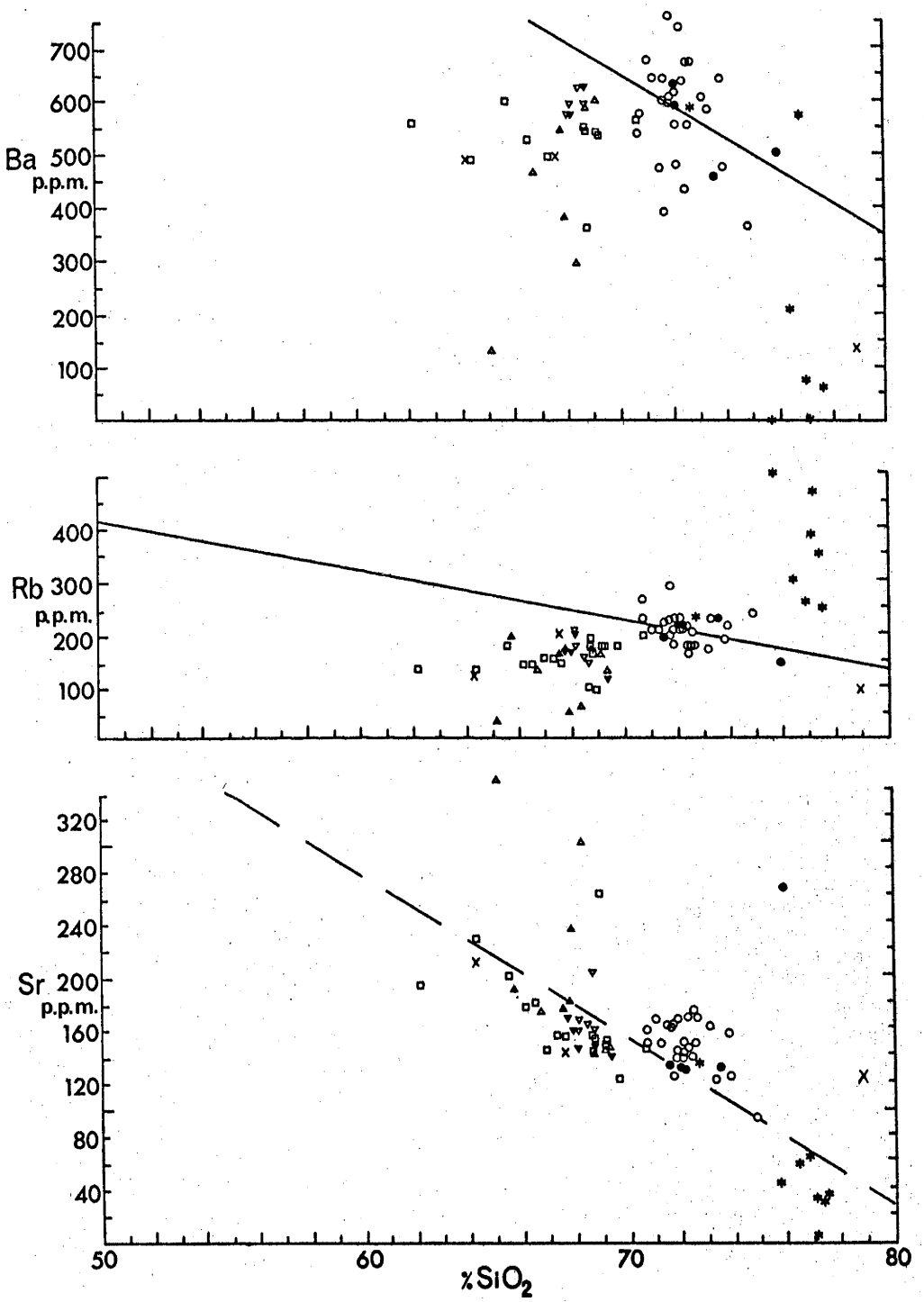

Figure 14. Harker variation diagrams for Ba, Rb and Sr

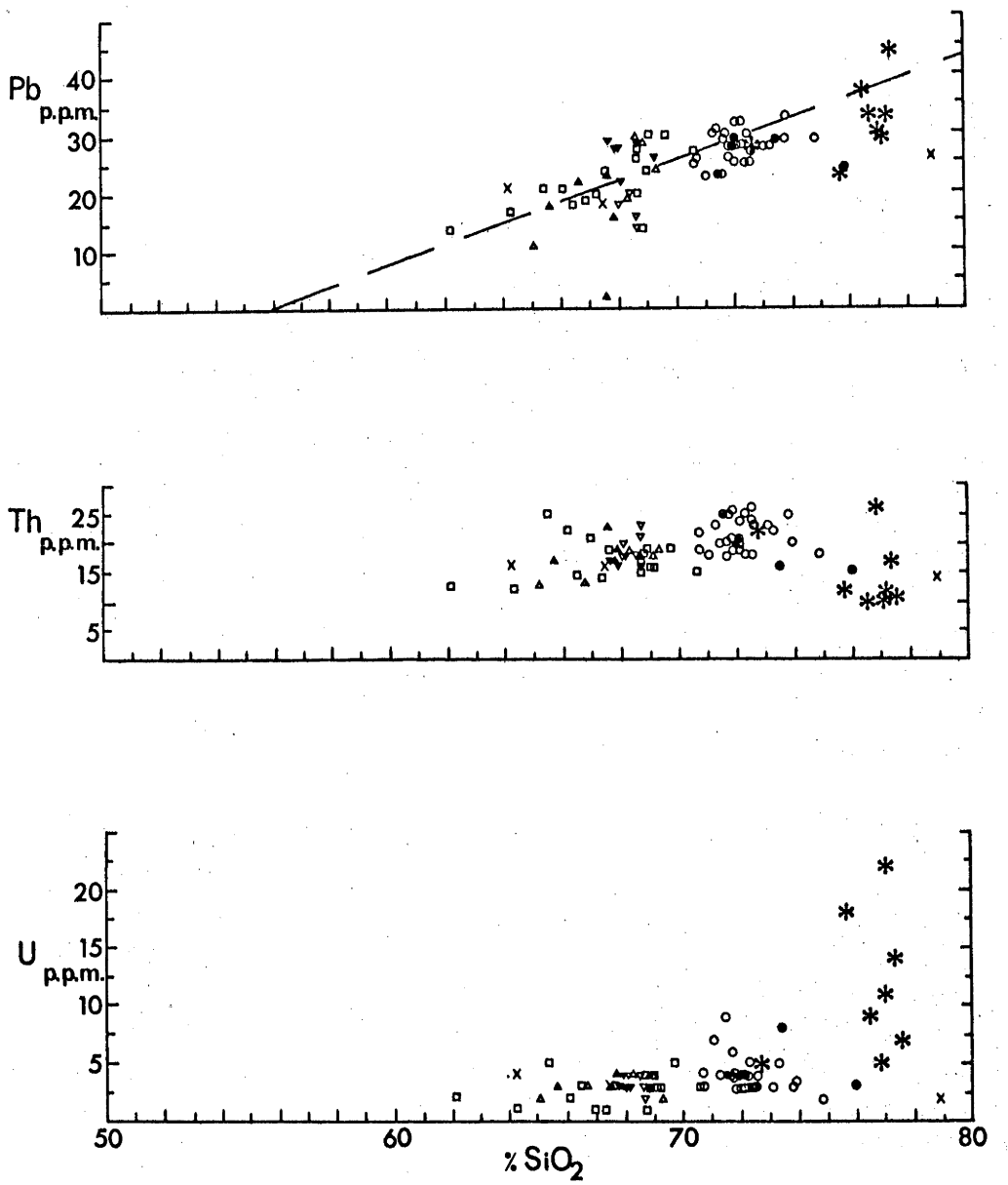

Figure 15. Harker variation diagrams for Pb, Th and U

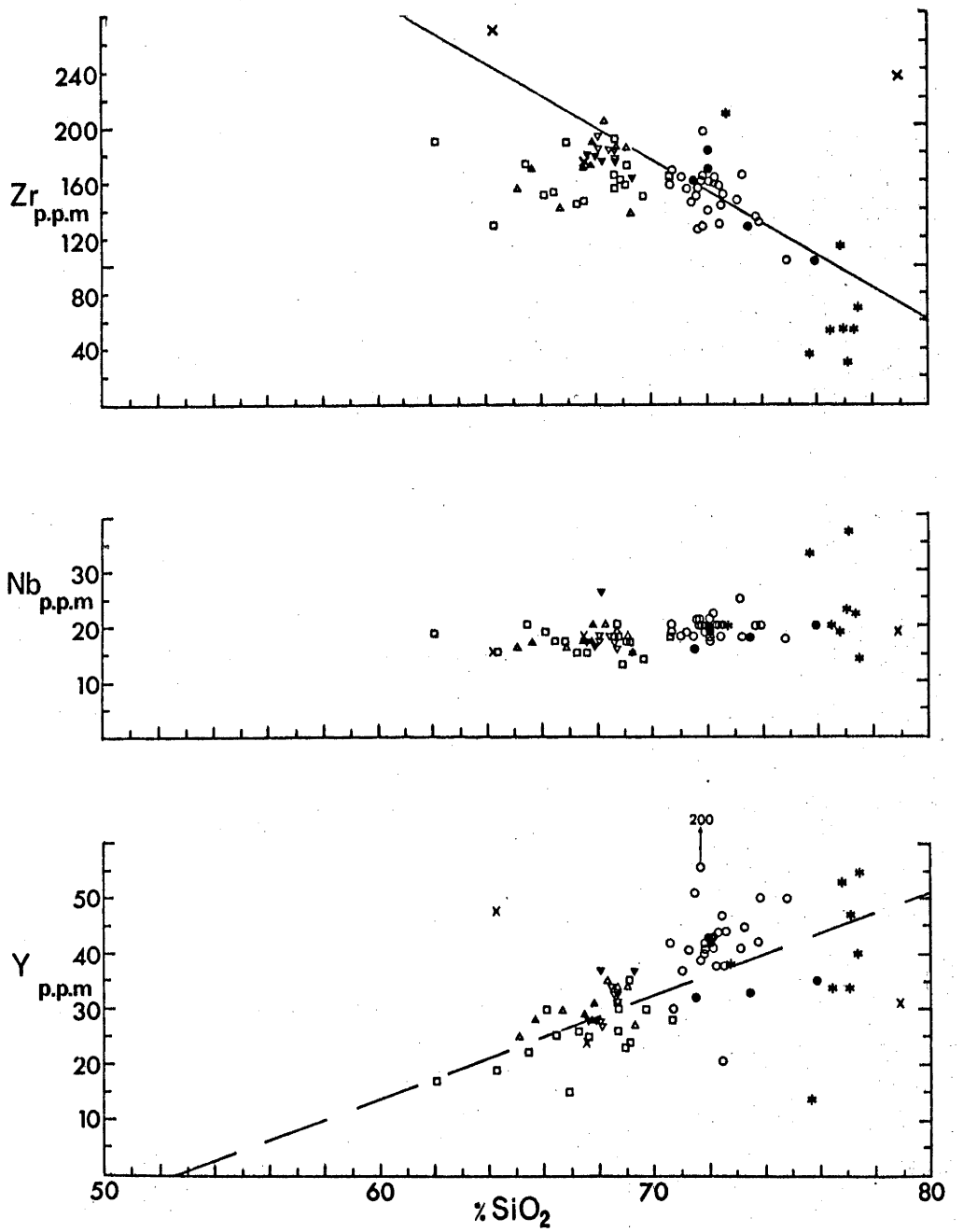

Figure 16. Harker variation diagrams for Zr, Nb and Y

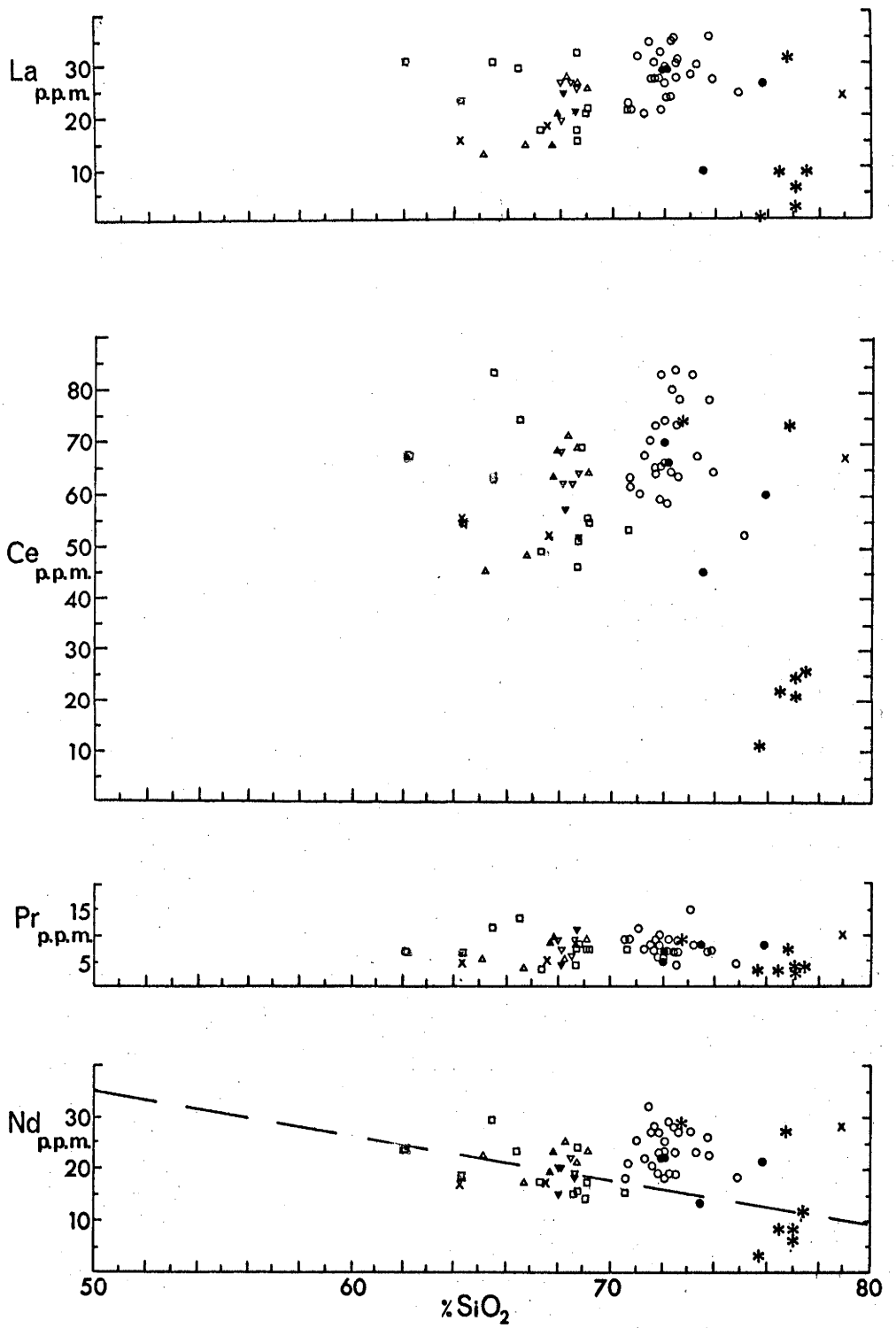

Figure 17. Harker variation diagrams for La, Ce, Pr and Nd

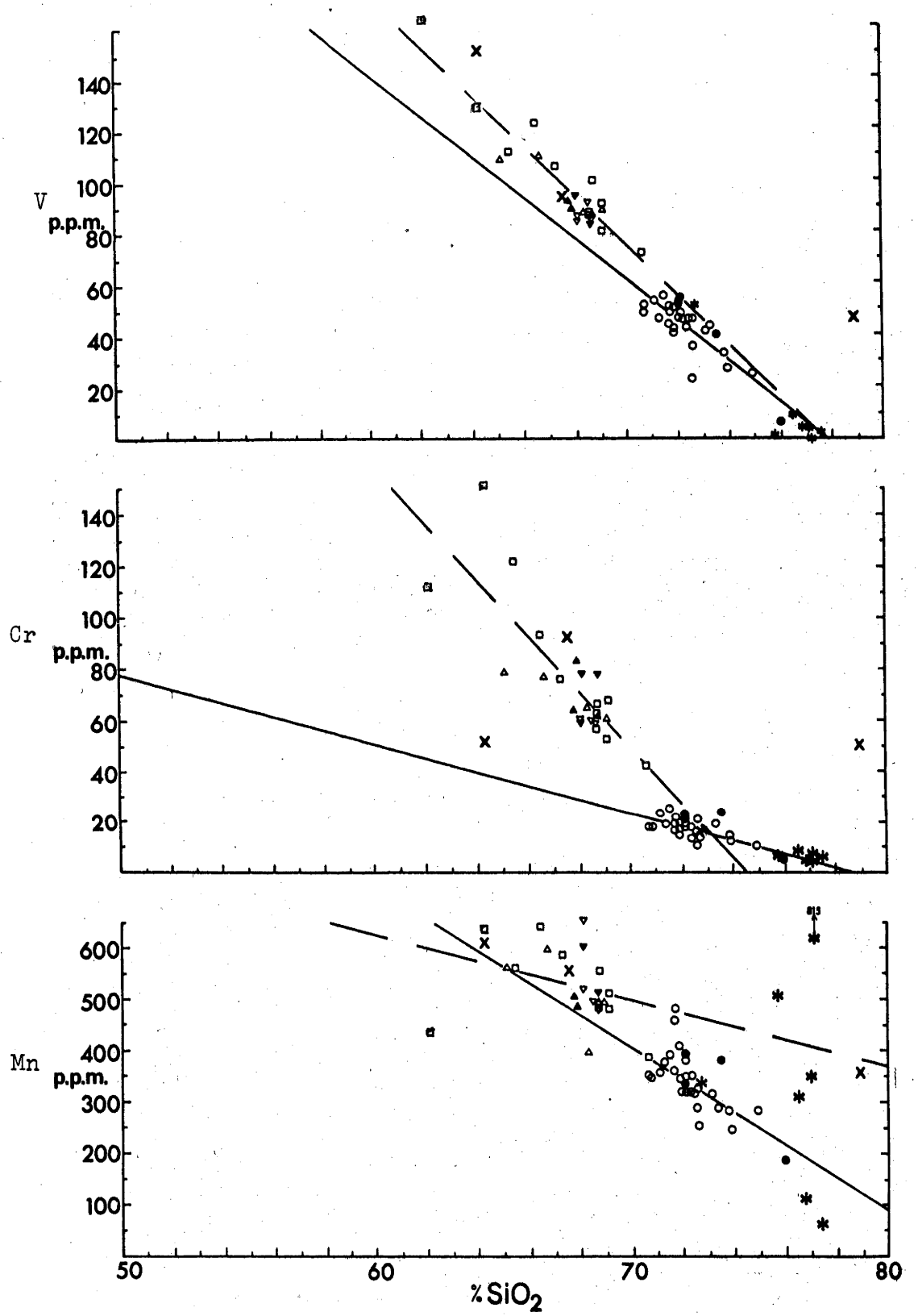

Figure 18. Harker variation diagrams for V, Cr and Mn

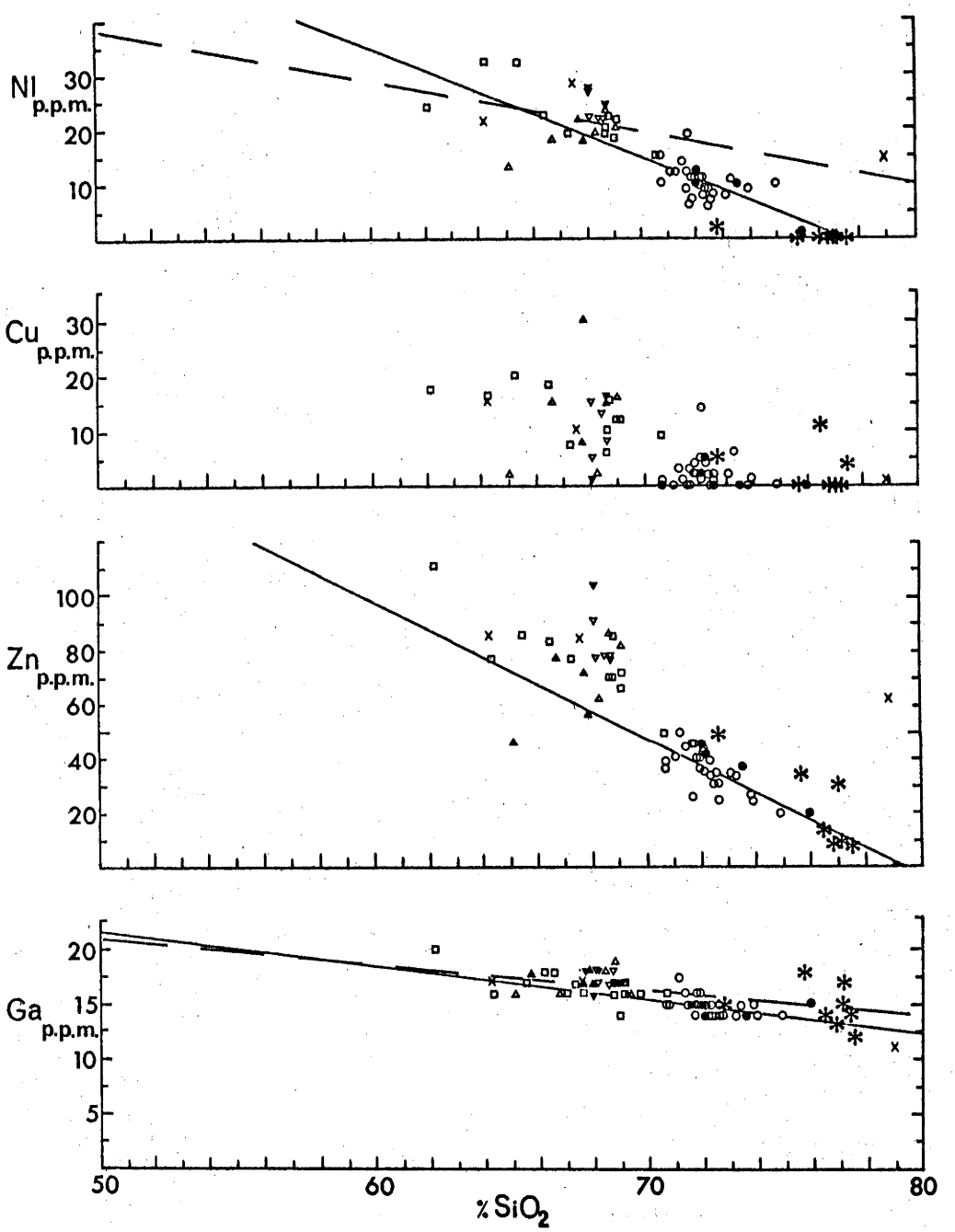

Figure 19. Harker variation diagrams for Ni, Cu, Zn and Ga

simple mechanism (e.g. the addition or subtraction of a single mineral phase or a unique bulk composition) was responsible for all the variation of a particular group of granites.

The chemical variables of the two groups can be summarised from table 29 and figures 11 - 19 into five classes.

1. constituents which increase with increasing SiO_2 in both the uncontaminated and the contaminated granite groups.

Na_2O is the only constituent to behave in this fashion and a t test indicates no significant difference in slope between the two regression lines. However, there is a significant difference in intercept.

2. constituents which increase with increasing SiO_2 in the contaminated granites but do not vary significantly in the uncontaminated granites.

K_2O, Y and Pb increase with increasing SiO_2 in the contaminated granites but do not vary significantly in the uncontaminated granites.

3. constituents which decrease in one granite group with increasing SiO_2 but do not vary significantly in the other.

a) P_2O_5, Ba, Rb, Zr, Mn and Zn do not vary significantly in the contaminated group but decrease in the uncontaminated group. However, P_2O_5 and Zn show no significant difference in slope between the regression lines for the two groups; nevertheless they differ significantly in intercept.

b) Sr and Nd do not vary significantly in the uncontaminated

granites but decrease in the contaminated group. The slopes of the regression lines of the two groups do not differ significantly for Nd and nor do the intercepts.

4. constituents which decrease with increasing SiO_2 in both groups.

TiO_2, Al_2O_3, Fe_2O_3, FeO, MnO, MgO, CaO, V, Cr, Ni and Ga all decrease with increasing SiO_2 in both groups. Although Al_2O_3, FeO, Fe_2O_3, MnO, V, Ni and Ga show no significant difference in slope between the regression lines for the two groups, all show significant differences in intercept. TiO_2, MgO, CaO and Cr show highly significant differences in both slope and intercept.

5. constituents which do not vary significantly in relation to SiO_2 in both groups.

Regression trends calculated for Th, U, Nb, La, Ce, Pr and Cu do not differ significantly from zero slope but all have significant differences in intercept for the pairs of regression lines.

Thus, only 19 out of 30 chemical constituents show similar regression trends in both granite groups and of these 19, four show significant differences in slope and the remainder except Nd show significant differences in intercept. These differences are consistent with the earlier conclusions from the correlation matrices and factor analyses.

When the intersections of the pairs of regression lines (table 29) are plotted as a histogram (figure 20), it is apparent that there is a frequency maximum at about 73.9 per cent SiO_2. This suggests that

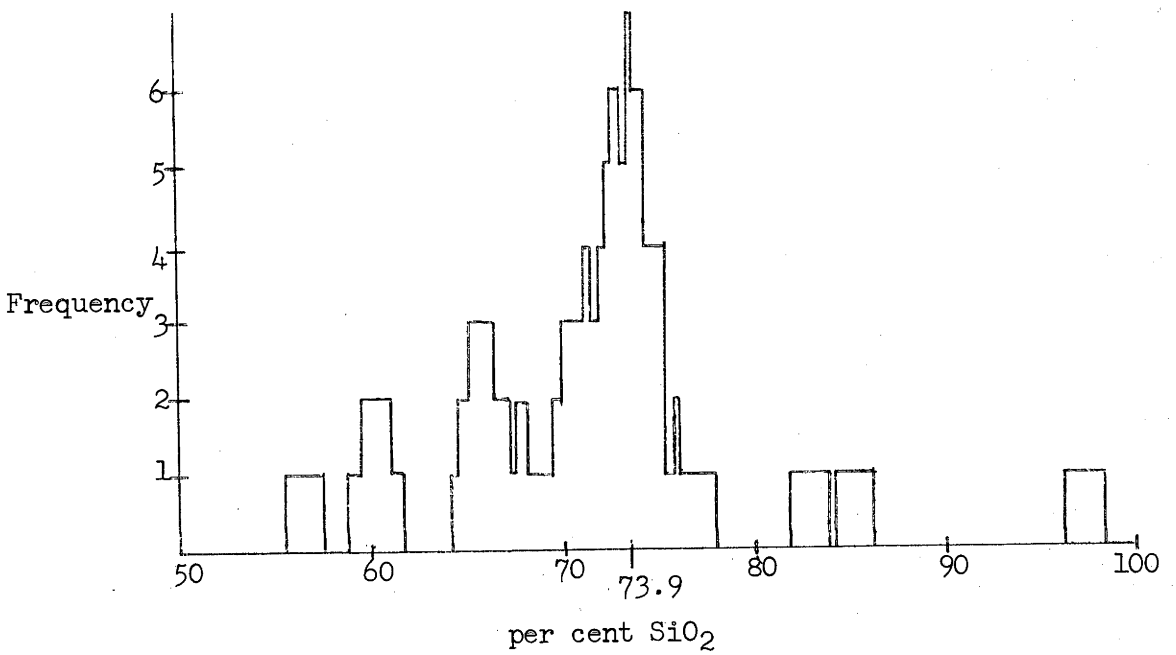

(histogram drawn using an integration method)

Figure 20 Histogram of the intersections of the regression lines calculated for the contaminated and uncontaminated granite groups.

there is a particular rock composition with about 73.9 per cent SiO_2 common to the variation trends of both granite groups, thereby implying a possible petrogenetic link. Table 30 records an estimate of this common composition calculated from the regression equations of table 29. An analysis of Tharwa Adamellite with 73.44 per cent SiO_2 and one of Shannons Flat Adamellite with 73.91 per cent SiO_2, listed for comparison, are similar to the theoretical composition. No recognised member of the contaminated granite group richer in SiO_2 than 70.61 per cent SiO_2 has been analysed. Most members of the uncontaminated granite group have SiO_2 contents below 73.9 per cent.

The leucogranites appear to show a systematic relationship to the uncontaminated granites since they plot close to the calculated regression lines of the uncontaminated granites on all the silica variation diagrams except those for Rb and U (in which the leucogranites are enriched relative to all the granites) and CaO, Ba, Sr, La, Ce, Pr and Nd (in which the leucogranites are depleted relative to the uncontaminated granite trends). The frequency of concordance implies that the leucogranites are related to the uncontaminated granites. A closer relationship of the leucogranites with the uncontaminated granites than with contaminated granites was also apparent from the principal component diagrams of figure 10.

The two xenoliths 20576 and 20577 from the Clear Range Granodiorite plot among the contaminated granites on the principal component diagrams (figure 10), but the SiO_2-rich xenolith 20578 plots near the uncontaminated granites. The same samples together with six previous

analyses of xenoliths from the contaminated granites are shown also on the SiO_2 variation diagrams. With the exception of 20578, the xenolith analyses are poorer in SiO_2 than most of the granites, and five of the nine samples are poorer in SiO_2 than any of the analysed granites. The xenolithe do not coincide closely with any of the calculated granite regression lines. Individual constituents of some xenoliths plot close to the contaminated granite regression trend, but there is no overall concordance of the xenoliths with the contaminated regression trends, nor is there a concordance of all chemical constituents of any one xenolith with the regression trends.

These relationships rule out any possibility that the variation of the contaminated granites can be attributed to a simple assimilation mechanism between some granite composition and a unique contaminant bulk composition corresponding closely with any of the nine analysed xenoliths. Indeed, the most conspicuous feature of the analysed xenoliths is their wide range of composition and it is exceedingly improbable that they represent variously altered versions of any originally homogeneous source material. They appear to have been derived from a variety of sedimentary, and possibly some igneous, rock types (possible origins of individual samples were discussed in Chapter 4).

If reaction between the xenoliths and some granite magma is the dominating mechanism responsible for variation in the contaminated granites, as proposed by Snelling (1957, 1960), then simple regression analysis is inadequate to describe the variation, which could consist of

numerous trends linking specific contaminant compositions with appropriate host magma compositions, which themselves would probably be members of other discrete variation trends. Only in a situation where a unique parental magma is contaminated by a unique contaminant composition, would simple linear variation result. In cases where several contaminant compositions were involved, variation in an infinite number of directions may occur. This is illustrated in figure 21 : mixtures of two end member compositions A and B are restricted to the line AB, whether projected onto a two dimensional plane such as y-SiO_2 (figure 21a) or considered in multidimensional hyperspace with axes corresponding to any chosen number of chemical variables. In the case of three end member compositions, A, B, and C, possible mixtures are restricted to the triangle ABC, again, whether considered as a projection on the plane y-SiO_2 (figure 21b) or as the true triangular area in the plane containing A, B, and C in multidimensional hyperspace. Some of the infinite possible variation trends in a three component hybrid rock series are illustrated as projections on the y-SiO_2 plane of figure 21b, where y is some chemical variable. Extrapolating this relationship further, possible mixtures resulting from m end members composed of n chemical constituents are restricted to a polyhedron whose corners are defined by the location of the m end members in n dimensional space. The linear hybrid model of rock series (Chayes, 1956; Chappell, 1966; Rhodes, 1969) is simply a special case of this general relationship.

Referring back to the principal components diagrams, the

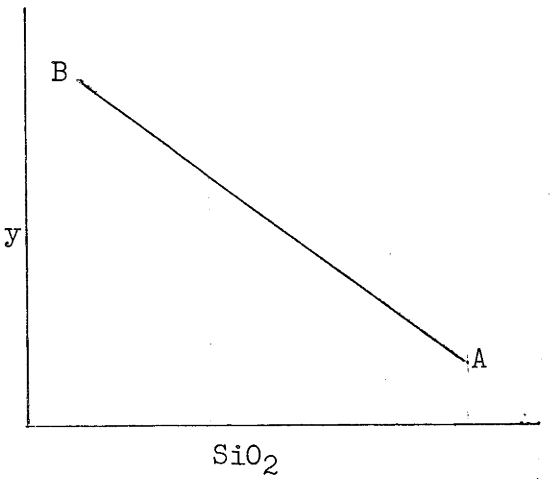

Mixtures of the unique compositions A and B are restricted to the line AB

a) Variation of mixtures of two end members

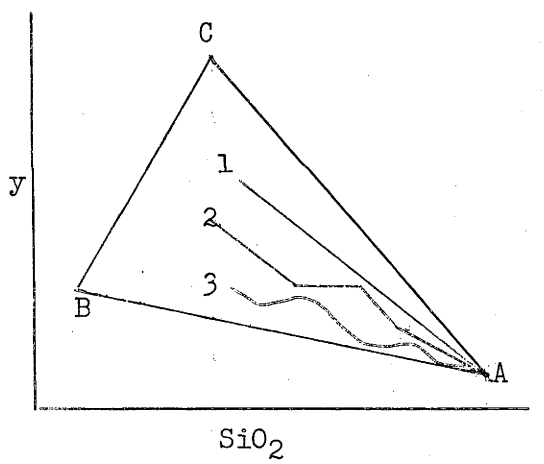

Mixtures of A, B and C are restricted to the triangular area ABC.

Four main types of "variation trend" resulting from mixing B and C with A are:

1. linear variation by addition of constant proportions of B and C.
2. angular variation trends caused by addition of intermittently varying proportions of B and C.
3. curvilinear trends resulting from addition of continuously varying proportions of B and C.
4. random variation, restricted to the field ABC, resulting from addition of random proportions of B and C to A.

b) Variation of mixtures of three end members

Figure 21 Geometrical relationships of variation diagrams of rock series formed by mixing specific end members

projections on planes I-II and I-III show a strong tendency to a fan-shaped distribution of contaminated granite analyses focussing towards the uncontaminated granites. A few SiO_2 variation diagrams also show a tendency to a fan-shaped distribution of contaminated granite analyses; for example, K_2O, Rb, Th, Cr and Ni. This may explain why regression lines with significant slopes but low coefficients of determination are obtained for many constituents: the calculated regression lines may represent "average" trends of fields, similar to the hypothetical example in figure 21b, extending between a reasonably homogeneous SiO_2-rich end member and several end members poorer in SiO_2.

Comparison of the chemistry of the Murrumbidgee granites with other granitic rocks

No benefit is anticipated in close comparison with granitic rocks of other areas, but some general comparisons are warranted in order to show that the compositions of the Murrumbidgee rocks are not unique and that, therefore, deduced features of their petrogenesis may be relevant to some other areas.

Kolbe & Taylor (1966) analysed 32 samples of granitic rocks from the Snowy Mountains region of New South Wales. These included mainly samples from the Kosciusko, Berridale and Maragle batholiths but also single leucogranite samples from the Bogong Granite and from the Yaouk Leucogranite. Mainly on chemical criteria the rocks were classified into three groups, constituting 4 "gneissic granites", 20 "granodiorites and adamellites" and 8 leucogranites". The "gneissic granites"

(consisting of one sample of Cooma granite and three samples of Boomerang Creek granitic gneiss) do not resemble any Murrumbidgee granites closely, being notably poorer in CaO, Na_2O and richer in K_2O than Murrumbidgee granites of comparable SiO_2 content. The "granodiorites and adamellites" show general similarities to the tonalites, granodiorites and adamellites of the Murrumbidgee Batholith but many individual samples are not closely comparable. The analyses most similar to analyses of Murrumbidgee granites are granodiorites from the Kosciusko and Happy Valley granites and an adamellite from the Gingera granite. The leucogranite analyses recorded by Kolbe & Taylor (1966) are similar to leucogranite analyses from the Murrumbidgee Batholith.

General comparison may be made between the average compositions of individual Murrumbidgee intrusions listed in table 19 and various average granite analyses compiled by Nockolds (1954) and listed in table 31. The Stewartsfield, Clear Range, Callemondah and Bolairo granodiorites and the Willoona Tonalite have remarkably similar average compositions but the Willoona Tonalite and the Callemondah Granodiorite, of which several individual specimens qualify modally as tonalite, have slightly lower K_2O contents than the other granodiorites. Compared with Nockolds' (1954) average biotite granodiorite and average muscovite-biotite granodiorite (table 31), all five intrusions have higher TiO_2, total Fe and MgO and lower Al_2O_3, Na_2O and Fe_2O_3/FeO. The high MgO and total Fe contents are more comparable with those of Nockolds' average tonalites but K_2O is higher and Na_2O is lower.

Table 31 Selected average analyses of Nockolds (1954) listed for comparison with the Murrumbidgee Batholith

	1	2	3	4	5	6	7
SiO_2	64.41	69.35	70.63	68.97	70.47	71.03	71.86
TiO_2	0.62	0.48	0.37	0.45	0.30	0.39	0.30
Al_2O_3	15.95	14.93	15.69	15.47	15.50	14.31	14.73
Fe_2O_3	1.46	1.19	0.86	1.12	0.63	0.95	0.64
FeO	3.81	3.07	1.40	2.05	2.12	1.96	1.61
MnO	0.10	0.06	0.04	0.06	0.03	0.06	0.04
MgO	2.45	0.94	0.83	1.15	0.65	0.75	0.67
CaO	5.36	3.04	2.82	2.99	1.91	1.89	1.51
Na_2O	3.39	4.67	4.91	3.69	4.12	3.33	3.18
K_2O	1.45	1.48	1.68	3.16	3.59	4.66	4.64
H_2O+	0.80	0.64	0.62	0.70	0.52	0.50	0.66
P_2O_5	0.20	0.15	0.15	0.19	0.16	0.17	0.16

1. Average hornblende-biotite tonalite
2. Average biotite tonalite
3. Average muscovite-biotite tonalite
4. Average biotite granodiorite
5. Average muscovite-biotite granodiorite
6. Average biotite granite
7. Average muscovite-biotite granite

Individual specimens classified as tonalite on modal criteria, for example hornblende-biotite tonalites 20562 and 20563 from Murrumbucka, are also lower in Na_2O and higher in K_2O than Nockolds (1954) average tonalites listed in table 31, and their total Fe and MgO contents are higher.

The Shannons Flat and Tharwa adamellites are similar to one another and compared with Nockolds' (1954) average biotite granite and average muscovite-biotite granite (table 31) they are both slightly poorer in Al_2O_3, Na_2O and K_2O and richer in CaO.

Comparison with other granite "series" can also be made utilising the familiar MFA diagram (figure 22). The Murrumbidgee granites conform with the classical "calc-alkaline" trend (Tilley, 1950).

The most acid granites, those containing greater than 80 per cent CIPW normative quartz + albite + orthoclase, can be discussed in relation to the synthetic system $NaAlSi_3O_8$ - $KAlSi_3O_8$ - SiO_2 - H_2O (Tuttle & Bowen, 1958). In figure 23 it can be seen that the granites cluster on the quartz-rich side of the "ternary" minimum at 500kg/cm^2 water vapour pressure. Two leucogranites plot very close to "ternary" minima, 20571 close to the minimum at 500kg/cm^2 water vapour pressure, and 20573 between the minima at 500 kg/cm^2 and 1000kg/cm^2.

The synthetic system is particularly relevant to the leucogranites since their individual sums of CIPW normative quartz + albite + orthoclase range from 92.7 to 95.9 per cent of the total rock. Plotting the uncontaminated granites is more questionable, since the sum of quartz, albite and orthoclase only just exceeds 80 per cent

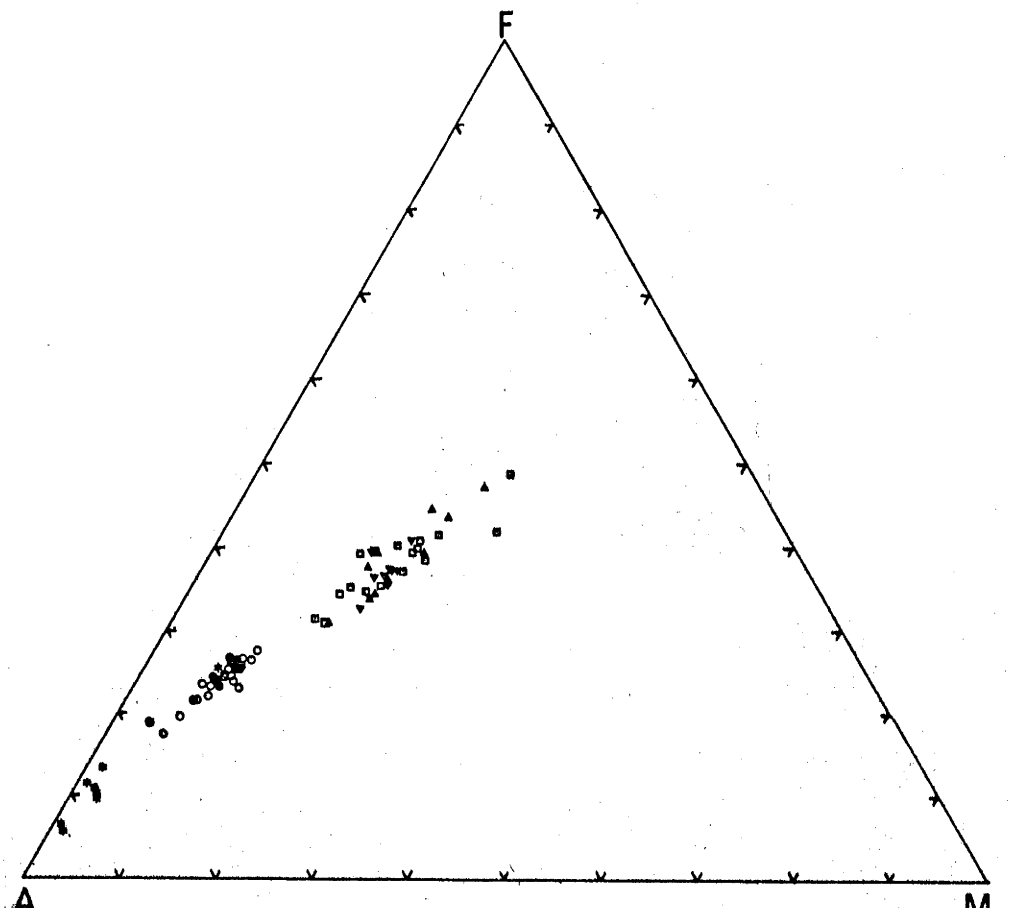

F = FeO + Fe_2O_3
A = Na_2O + K_2O
M = MgO

Figure 22. MFA diagram for the Murrumbidgee Batholith

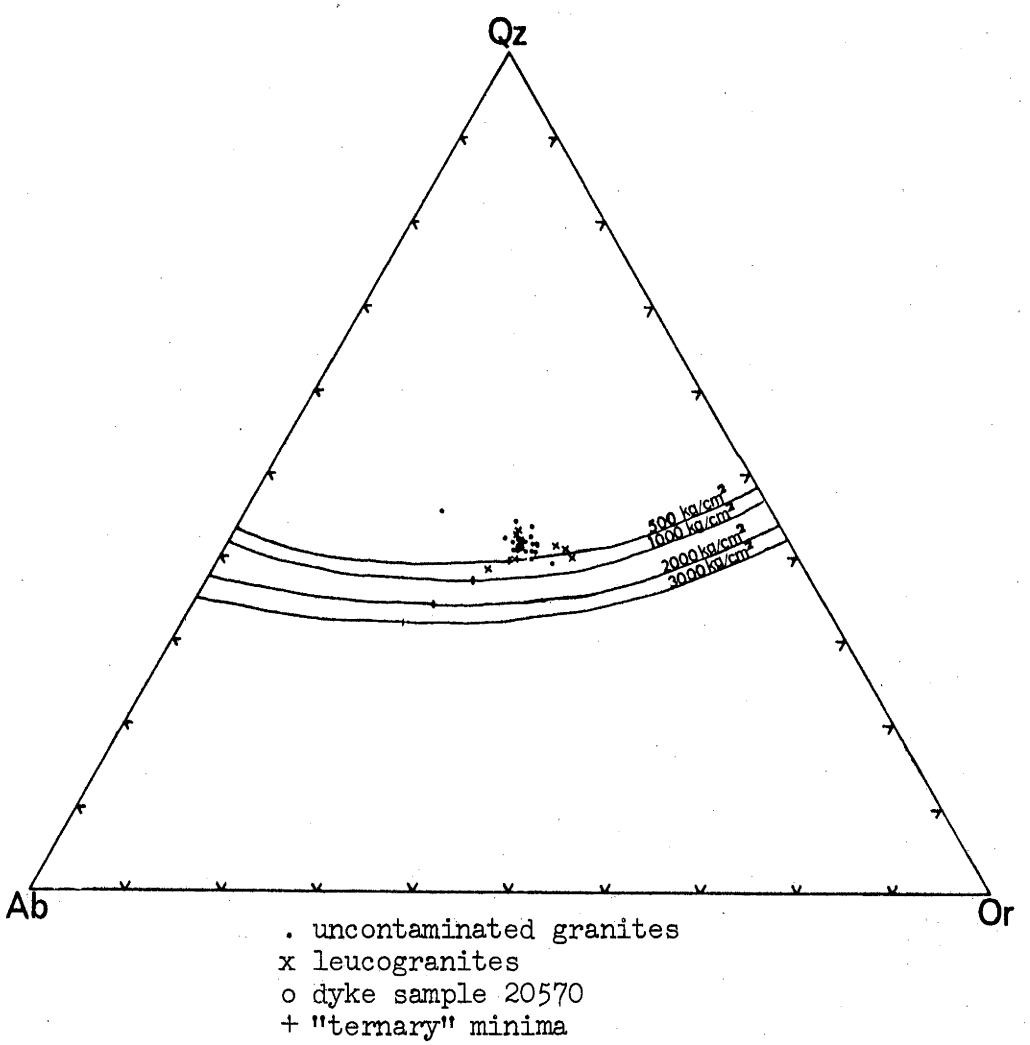

Figure 23. Normative composition of the leucogranites and most acid uncontaminated granites in relation to the synthetic "granite" system, Ab-Or-SiO_2-H_2O (Tuttle & Bowen, 1958)

(eight samples of Shannons Flat Adamellite contain less than 80 per cent and are not shown in figure 23). Other constituents may lead to appreciable displacement of projections on the quartz-albite-orthoclase plane, for example, CaO is considered to displace the isobaric minima towards the quartz-orthoclase join (Kleeman, 1965; Von Platen, 1965).

Variation of individual chemical constituents relative to SiO_2 recorded in many other granitic batholiths or groups of related granites may be summarised as follows (Bailey, 1969; Chao & Fleischer, 1960; Chappell, 1966; Gulson, 1968; Hall, 1967; Kolbe & Taylor, 1966; Larsen, 1948; Larsen & Gottfried, 1960; Nockolds, 1940; Nockolds & Allen, 1953, 1956; Nockolds & Mitchell, 1948; Rhodes, 1969b; Rogers & Ragland, 1961; Towell et al., 1965; Whitfield et al.,1959)

1. constituents which generally decrease with increasing SiO_2.

   TiO_2, Al_2O_3, Fe_2O_3, FeO, MnO, CaO, P_2O_5, Ba, Sr, Zr, V, Cr, Ni, Zn, Ga.

2. constituents which generally increase in abundance with increasing SiO_2.

   K_2O, Rb, Pb, Th, Nb.

3. constituents which generally show no apparent systematic relationship to SiO_2.

   La, Ce, Cu.

4. constituents which may increase, decrease, or show no significant variation in relation to increasing SiO_2 content of individual granite suites.

   Na_2O, U, Y, Pr, Nd.

The variation of the Murrumbidgee granites illustrated in figures 11 - 19, shows no important departure from the above generalised pattern of bahaviour in granitic rocks. In the uncontaminated granites the calculated regression for Sr suggests an increase with increasing SiO_2 content and those for K_2O and Rb indicate decreases but none of the slopes differ significantly from zero even at the 90 per cent confidence level. In the contaminated granites Zr and Ba contradict the generalisations by apparent increases with increasing SiO_2, but the slopes of their regression lines do not differ significantly from zero at the 90 per cent confidence level; Nb shows an apparent negative correlation, which is also not significant.

Geochemical coherence

Certain elements show close geochemical coherence; in some cases both their chemical and crystallochemical properties are similar (for example, K and Rb), in other cases they are not (for example, K and Th). Relative abundances and variation of coherent elements can suggest information on the source and evolution of rocks (Taylor, 1966). Covariant behaviour of particular pairs or groups of elements can be checked readily by referring to the correlation matrices of table 27.

One of the most frequently discussed coherences is that of K and Rb (Taubeneck, 1965; Shaw, 1968). The correlation matrices of table 27 show highly significant correlations between K_2O and Rb of 0.88 and 0.62 for the contaminated and uncontaminated granites, respectively.

According to Taylor (1968), the average K/Rb ratio for granites

is 240 and for granodiorites 230, but the relationships displayed in figure 24 indicate that all the Murrumbidgee granites are well below these figures and five contaminated granites, two uncontaminated granites and four leucogranites have K/Rb ratios below 150, the limit below which Taylor (1966) considers that special explanation is required. Two of three xenoliths for which data are available also have K/Rb ratios below 150. Similar low K/Rb values of leucogranites in the Snowy Mountains region (including a sample of Yaouk Leucogranite) have been interpreted by Kolbe & Taylor (1966) as indicating (along with other evidence) that the rocks originated by differentiation. Alternatively, Hall (1967) has interpreted low K/Rb ratios in the most acid rocks of the Rosses granite complex as being consistent with an origin of the rocks by partial melting. A third explanation invoked by Hall (1966) and Chappell (1966), in specific cases, is assimilation of material of low K/Rb ratios.

A plot of K against Rb (figure 24a) shows a similar pattern in the uncontaminated and contaminated granite groups to the main trend demonstrated by Shaw (1968) for a wide variety of continental and oceanic rock types - namely, a gradual decrease in K/Rb with increasing K and Rb. However, the trend of the leucogranites displays enrichment in Rb relative to almost constant K and resembles the trend of pegmatites and hydrothermal deposits (Shaw, 1968).

The group IIA elements Ca, Sr and Ba closely resemble each other chemically but their occurrences in igneous rocks differ; Sr largely accompanies Ca but Ba mainly accompanies K and a close coherence between Ba and K has been demonstrated in several calc-alkaline associations

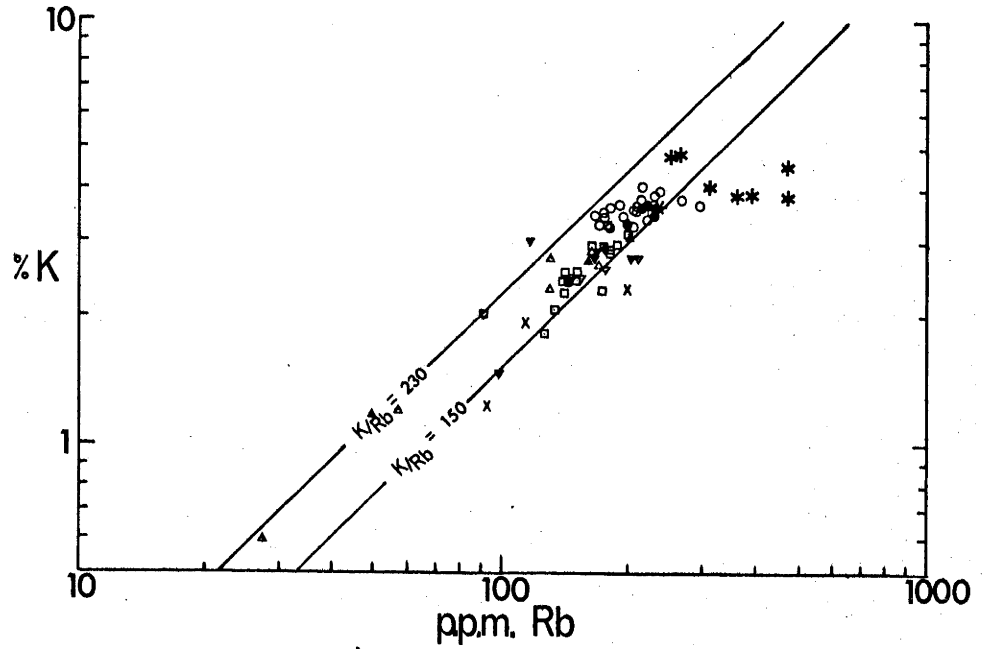

a) K versus Rb

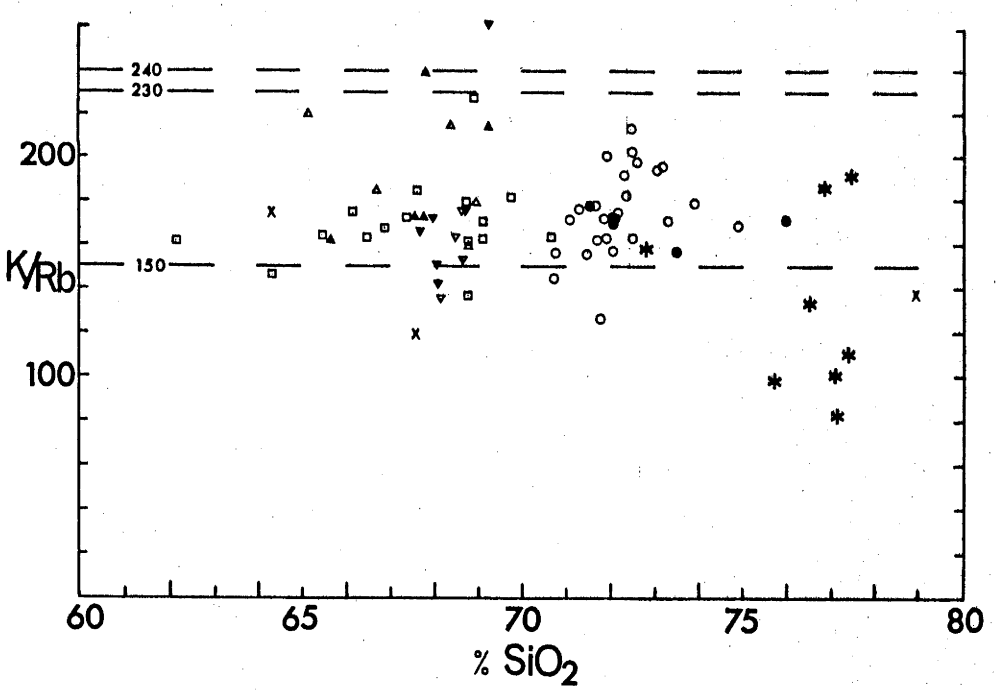

b) K/Rb versus SiO_2

Figure 24. Variation of K/Rb

(Taylor, 1966; Ewart et al., 1968). However, relationships in figure 25a are more complex and serve to emphasize yet again the distinctions between the three granite groups in the batholith. The contaminated granites show an increase in Ba concurrent with increasing K whereas the uncontaminated granites show a moderate variation in Ba independent of K. The leucogranites show an extreme range of Ba independent of K content. Referring to table 27, Ba shows its highest positive correlation with CaO (0.68) and its correlation with K_2O is negligible (0.04).

In contrast to Ba and K, the relationship between Sr and Ca (figure 25b) is a simple one of strong coherence in all the granites. Surprisingly, the correlation between CaO and Sr in the uncontaminated granites is not significant (0.27, table 25) and the highest positive correlation of Sr with a major component is with Na_2O (0.59). However, the range of Sr and Ca in the uncontaminated granites is small and the ratio remains constant and essentially equal to that of the contaminated granites. The xenoliths show similar Sr/Ca ratios to the granites.

Strong coherences between K, U and Th, particularly in basic and intermediate rocks, have been emphasised by Heier & Rogers (1963) and Clark et al., (1966). However, the intercorrelations of all three of these elements in table 27 are very low and some are even negative. The relationships are illustrated in figure 26. Th/U values are similar in the uncontaminated and contaminated granites, varying between about 10 and 1.7, but the leucogranites are richer in U and poorer in Th and thus have much lower Th/U ratios. From a theoretical point of view Taylor

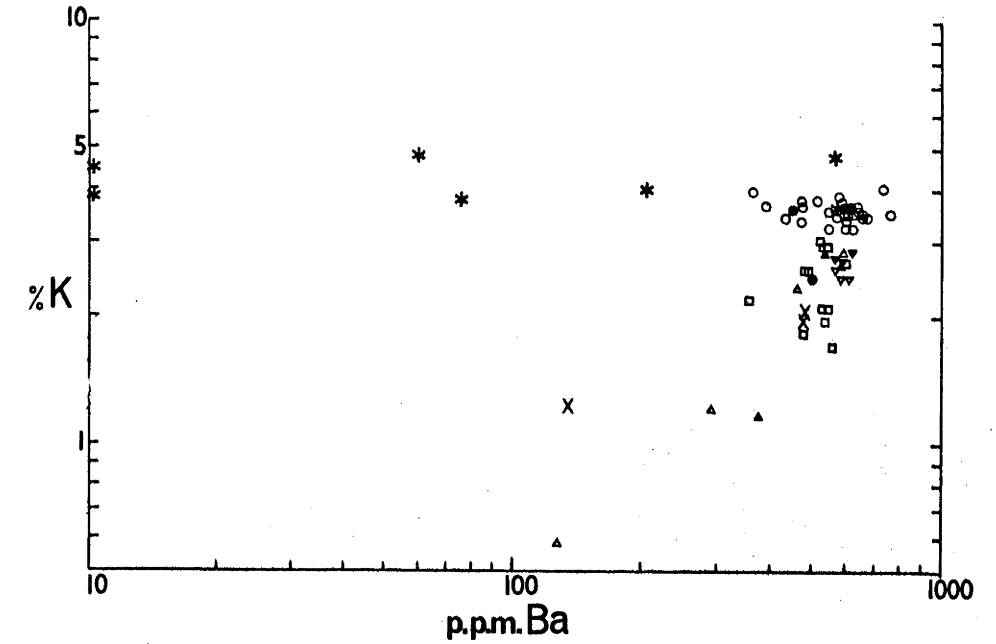

a) K versus Ba

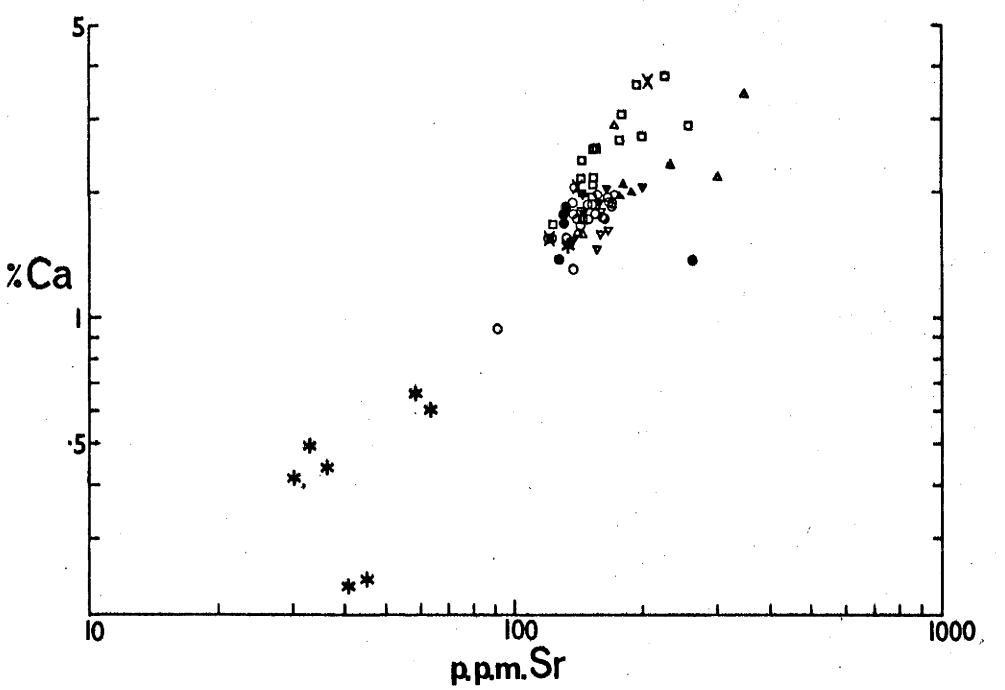

b) Ca versus Sr

Figure 25. Variation of K/Ba and Ca/Sr

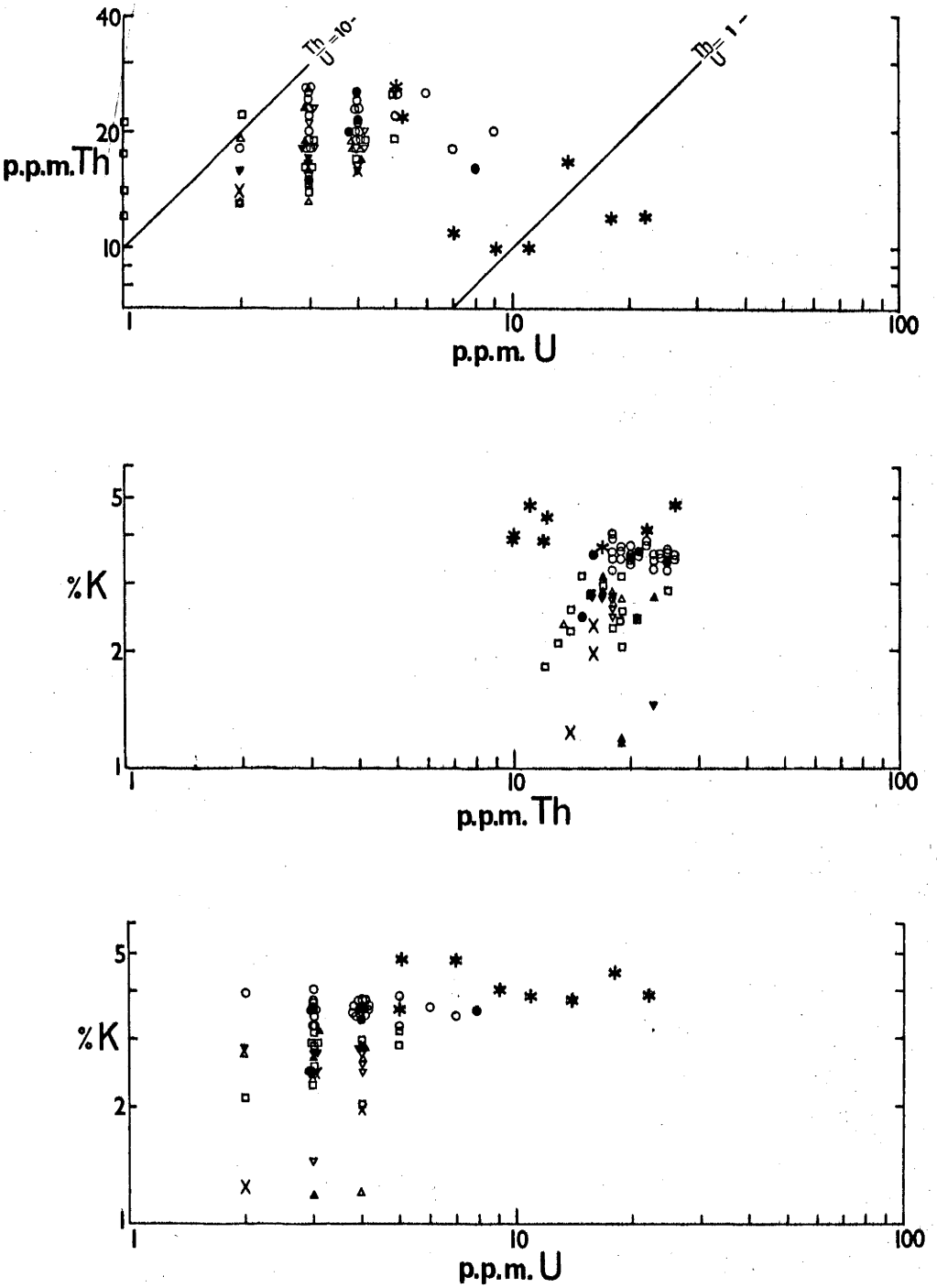

Figure 26. Variation of U, K and Th

(1966) predicted that fractional crystallisation should produce a decrease in Th/U and so the lower ratios of the leucogranites could be interpreted as indicating an origin by differentiation from either the contaminated or uncontaminated granite groups. However, the formation of U and Th complexes should lead to enrichment of both elements in residual magmas (Ringwood, 1955), whereas Th is low in the leucogranites relative to the other granites.

The ratios of K/Th and K/U show similar groupings to those for Th/U, the uncontaminated and contaminated groups showing comparable ratios but the leucogranites having higher K/Th and lower K/U.

The rare earth elements La to Lu form a group of very similar elements differing primarily in decreasing ionic radius with increasing atomic number (the "lanthanide contraction"). The lighter element Y resembles the heavy rare earths and is distributed coherently with them. The chemical properties of the rare earths are so similar that their separation from one another is difficult. However, the differences in their ionic radii imply that the large, light rare earths may be enriched by strong fractionation and this effect has been noted in crustal rocks (Haskin et al., 1966). The abundance of rare earths in chondritic meteorites may be regarded as an estimate of the "primordial" abundance (Haskin et al., 1966). Accordingly, one method of examining the fractionation of rare earths relative to their "primordial" abundances is to divide the absolute abundance of each element by the average abundance of that element in chondritic meteorites (Haskin et al., 1966) and to plot the resultant ratios against ionic radius of the rare

earths. Figure 27 shows the results of this procedure for selected Murrumbidgee rocks. The fractionated variation pattern of a composite of 40 North American Shales (Haskin et al., 1966) is also shown. Haskin et al. considered that the composite North American shale represents a reasonable approximation to the distribution of rare earths in crustal rocks.

The Shannons Flat Adamellite, Clear Range Granodiorite and quartz-rich metasedimentary xenolith (20567) plotted on Figure 27 resemble the "crustal" pattern of the composite North American shale in both relative and absolute rare earth abundances (as do other intrusions and individual samples not plotted on Figure 27). The pattern for the Yaouk Leucogranite (and other leucogranites) differs in having lower absolute abundances of La, Ce, Pr and Nd and notable depletion of La and Nd relative to Pr and Y. No rare earth patterns of Murrumbidgee granites or xenoliths resemble the "primordial" chondritic pattern.

Ga is commonly considered to show close coherence with Al (Nockolds & Allen, 1953; Burton et al., 1959) but Taylor (1966) pointed out that it may also enter zinc sulphide or substitute for Fe^{3+} in minerals. Mineral analyses of the Murrumbidgee rocks indicate that Ga is most abundant in muscovite and biotite but is also present in appreciable amounts in the feldspars. Thus, it appears to be substituting mainly for Al. Ga does not correlate well with Al in table 27 but since Ga and Al both show only slight variation, the ratio Al/Ga is essentially constant throughout the batholith. The Al/Ga ratios of the xenoliths are similar to those of the granites.

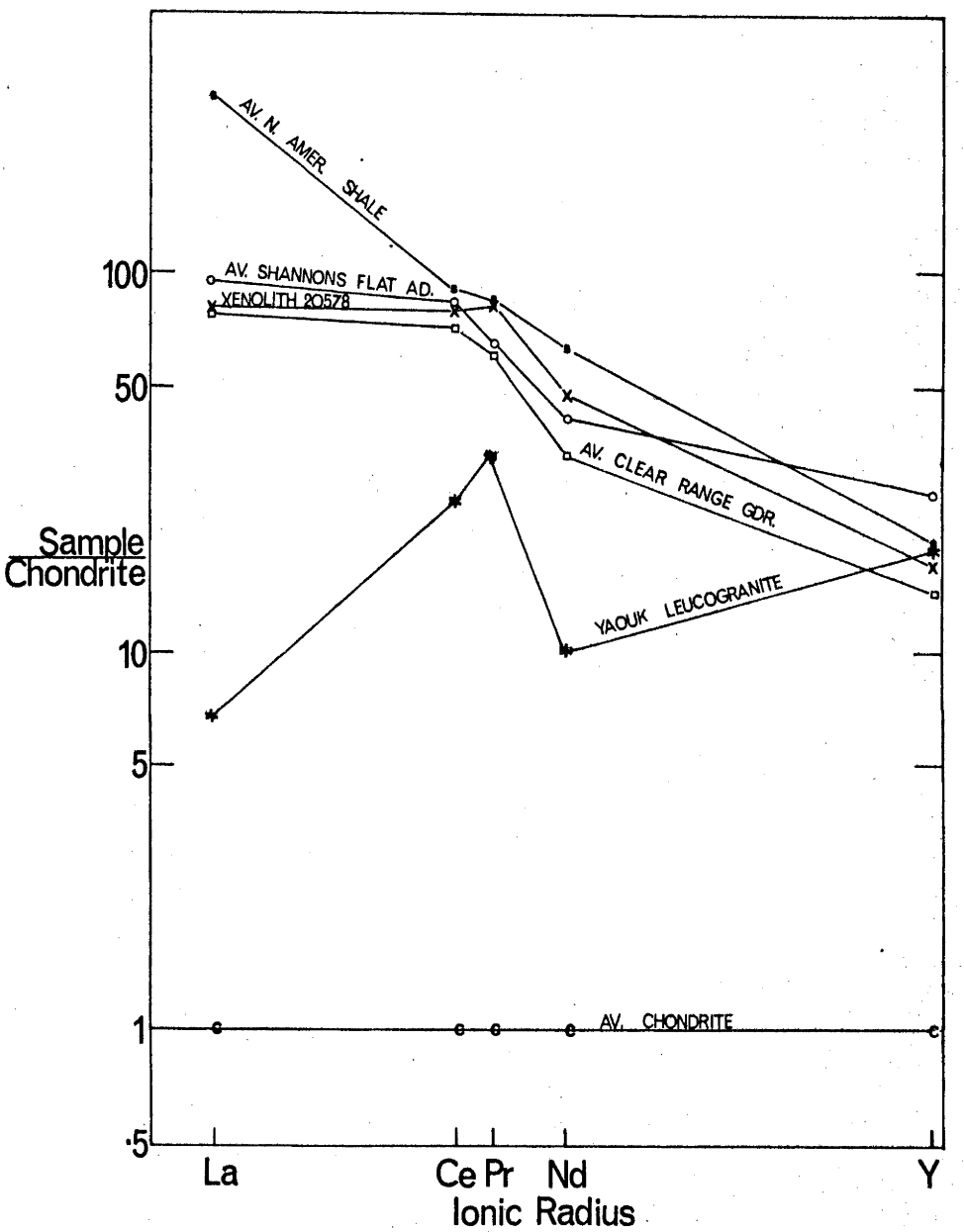

Figure 27. Variation of rare earth elements in relation to "average chondrite" and "average North American shale" (Haskin et al., 1966)

Nb can substitute for both Ti and Zr and it is interesting to note the high correlation with TiO_2 (0.59) and Zr (0.61) in the contaminated granites in contrast to the low correlations (0.21 and 0.18, respectively) in the uncontaminated granites.

Two other trace elements show notable correlations with mineral-forming elements for which they may substitute. Pb shows correlations of 0.57 and 0.39 with K_2O and Zn shows correlations of 0.63 and 0.78 with FeO (table 25) for the contaminated and uncontaminated granites, respectively.

6. MINERALOGY

In order to provide information on the distribution of elements within the rocks, 22 biotites, 22 plagioclases, 18 potassium feldspars, 2 muscovites, 1 hornblende and a garnet were separated by heavy liquids and magnetic separation techniques and analysed for selected major and trace elements using the same methods described for the whole rock analyses. Some biotite samples were analysed for lithium by atomic absorption.

Chappell (1966) and Gulson (1968) have shown that, with the exception of plagioclase, granitic minerals are essentially homogeneous with regard to major elements so the use of separated mineral samples is regarded as a valid method of studying the coexisting phases of these rocks. In order to minimise selective separation of plagioclase compositions no attempt was made to separate quartz from plagioclase considered from optical data to be close to andesine, but quartz was crudely separated from albite and from weakly zoned labradorite samples to permit better chemical analysis. Purity of all other minerals is estimated to exceed at least 98 per cent.

Mineral analyses typically record variable, but appreciable, contents of P_2O_5 but Koritnig (1965) and Corlett & Ribbe (1967) have shown that P is usually below 100ppm in granitic minerals confirming the petrographic evidence that most of the P_2O_5 is present in apatite inclusions. Accordingly, all analyses were corrected by removing P_2O_5 and requisite amounts of CaO to form apatite, then recalculated to their original totals.

Potassium feldspars

Chemical analyses of 18 potassium feldspars, their structural formulae and molecular proportions are recorded in table 32, along with their triclinicities (Goldsmith & Laves, 1954).

The triclinicity, defined as $\Delta = 12.5\ (d_{131} - d_{1\bar{3}1})$, gives a measure of the degree of ordering in potassium feldspars, ranging from 0.0 in monoclinic feldspars to 1.0 in maximum microcline (Goldsmith & Laves, 1954). Only five of the analysed feldspars have triclinicities below 0.90, so the dominant potassium feldspar throughout the batholith is highly ordered microcline. This is consistent with petrographic observations that the potassium feldspars of all thin sections from the batholith show, to varying degrees, cross-hatched twinning, a feature typical of microcline. Triclinicities of additional feldspars from the Shannons Flat Adamellite were presented in table23 and several of those are less ordered than the analysed samples, the range of triclinicity in the Shannons Flat Adamellite being from 0.52 to 0.97.

The structural states of 15 feldspars are shown also in graphical form in figure28 using 2θ (060) and 2θ ($\bar{2}04$) on a diagram given by Wright (1968) and showing the variation of these parameters (related to the b and c cell parameters respectively) for natural and synthetic feldspars of various structural states. The diffraction patterns were recorded at a scanning speed of $\frac{1}{2}^{o}$ 2θ /min for Cu K_{α} radiation following the procedure recommended by Wright & Stewart (1968). The feldspars cluster close to the maximum microcline of Wright's (1968) diagram except for samples 20559 and 20517 which lie between the

Table **32** Chemical analyses, structural formulae, molecular proportions and triclinicity of potassium feldspars from the Murrumbidgee Batholith

	Stewartsfield Granodiorite	Clear Range Granodiorite		Callemondah Granodiorite		Bolairo Granodiorite	Shannons Flat Adamellite							Tharwa Adamellite	Westerly Muscovite Granite	Yaouk Leucogranite	Unnamed Leucogranites	
	20559	20535	20541	20543	20546	20551	20502	20507	20510	20511	20513	20515	20521	20528	20569	20567	20571	20574
SiO_2	65.41	64.95	65.14	66.31	66.52	66.39	65.12	65.08	65.33	65.60	65.11	65.02	65.29	64.92	65.71	65.52	65.71	65.50
Al_2O_3	18.17	18.56	18.76	18.49	18.52	18.93	18.52	18.51	18.31	18.52	18.42	18.44	18.46	18.34	18.42	18.75	18.51	18.39
Fe_2O_3	0.11	0.11	0.12	0.18	0.20	0.14	0.09	0.09	0.13	0.09	0.12	0.10	0.07	0.10	0.10	0.06	0.08	0.07
CaO	0.12	0.00	0.00	0.19	0.28	0.00	0.00	0.00	0.00	0.06	0.06	0.01	0.02	0.00	0.00	0.00	0.00	0.00
Na_2O	1.24	0.95	1.85	1.92	1.92	1.25	1.53	1.36	1.32	1.90	2.25	1.19	1.95	1.16	1.23	3.16	3.20	1.87
K_2O	14.18	14.88	13.94	14.12	13.12	14.72	14.44	14.53	14.48	13.84	12.97	14.39	13.65	14.88	14.78	12.19	11.87	13.81
BaO	0.16	0.20	0.15			0.20	0.14	0.17	0.18	0.19	0.17	0.15	0.16	0.20	0.01	0.03	0.07	0.01
SrO	0.02	0.02	0.02			0.02	0.01	0.02	0.01	0.02	0.01	0.02	0.01	0.01	0.00	0.01	0.01	0.01
Rb_2O	0.05	0.03	0.04			0.03	0.05	0.05	0.05	0.05	0.05	0.05	0.06	0.05	0.12	0.09	0.07	0.06
Total	99.46	99.70	100.02	101.21	100.56	101.68	99.90	99.81	99.81	100.27	99.16	99.37	99.67	99.66	100.37	99.81	99.52	99.72
Trace elements (parts per million)																		
Ba	1440	1790	1355			1790	1215	1535	1615	1725	1540	1300	1440	1800	65	290	605	105
Sr	143	165	162			165	114	132	97	128	107	123	110	82	7	50	86	39
Rb	491	295	384			234	497	473	491	492	467	452	572	419	1094	825	646	554
Pb	20	34	26			36	18	16	17	15	15	17	15	17	14	20	23	24
Y	9	1	1			4	1	14	1	1	1	1	1	1	1	1	2	4
Ga	8	8	10			8	12	12	11	12	13	12	13	11	17	14	14	14
Structural formulae on the basis of 32 oxygen atoms																		
Z Si	12.061	11.990	11.955	12.016	12.057	11.995	11.986	11.992	12.028	12.003	12.006	12.013	12.006	12.002	12.031	11.970	12.017	12.029
Z Al	3.951	4.038	4.059	3.950	3.958	4.033	4.018	4.020	3.974	3.995	4.004	4.018	4.003	3.997	3.977	4.039	3.991	3.981
Z Fe	0.015	0.016	0.016	0.024	0.028	0.019	0.012	0.013	0.018	0.013	0.017	0.014	0.009	0.013	0.014	0.009	0.011	0.009
X Ca	0.024	0.000	0.000	0.037	0.054	0.001	0.000	0.000	0.000	0.012	0.012	0.002	0.003	0.000	0.000	0.000	0.000	0.000
X Na	0.442	0.339	0.660	0.673	0.674	0.437	0.546	0.486	0.472	0.673	0.804	0.427	0.696	0.414	0.437	1.120	1.135	0.667
X K	3.335	3.504	3.264	3.265	3.034	3.392	3.392	3.416	3.402	3.231	3.052	3.392	3.203	3.509	3.452	2.842	2.770	3.235
X Ba	0.012	0.014	0.011			0.014	0.010	0.012	0.013	0.014	0.012	0.011	0.012	0.015	0.001	0.002	0.005	0.001
X Sr	0.002	0.002	0.002			0.002	0.001	0.002	0.001	0.002	0.001	0.002	0.001	0.001	0.000	0.001	0.001	0.000
X Rb	0.006	0.004	0.005			0.003	0.006	0.006	0.006	0.006	0.006	0.006	0.007	0.005	0.014	0.011	0.008	0.007
Tot.Z	16.027	16.044	16.030	15.990	16.043	16.047	16.016	16.025	16.020	16.011	16.027	16.045	16.018	16.012	16.022	16.018	16.019	16.019
Tot.X	3.821	3.863	3.942	3.975	3.762	3.849	3.955	3.922	3.894	3.938	3.887	3.840	3.922	3.944	3.904	3.976	3.919	3.910
Percentages of the feldspar molecules (R = $RbAlSi_3O_8$, S = $SrAl_2Si_2O_8$)																		
An	0.64	0.00	0.00	0.93	1.44	0.02	0.00	0.00	0.00	0.29	0.31	0.05	0.08	0.00	0.00	0.00	0.00	0.00
Ab	11.57	8.77	16.73	16.93	17.92	11.35	13.81	12.39	12.13	17.09	20.69	11.12	17.74	10.50	11.20	28.17	28.96	17.05
Or	87.28	90.70	82.81	82.14	80.65	88.13	85.74	87.10	87.34	82.06	78.50	88.36	81.67	88.97	88.42	71.49	70.67	82.73
Cs	0.30	0.38	0.28			0.37	0.25	0.32	0.33	0.35	0.32	0.27	0.30	0.37	0.01	0.06	0.12	0.02
S	0.05	0.05	0.05			0.05	0.04	0.04	0.03	0.04	0.04	0.04	0.04	0.03	0.00	0.02	0.03	0.01
R	0.17	0.10	0.13			0.08	0.16	0.16	0.16	0.16	0.16	0.15	0.19	0.14	0.36	0.27	0.21	0.18
Triclinicity																		
	0.67	0.91	0.93	0.91	0.94	0.92	0.95	0.96	0.92	0.69	0.92	0.95	0.66	0.97	0.87	0.94	0.88	0.97
Calculated apatite content of the concentrate																		
	0.25	0.21	0.25	0.10	0.22	0.27	0.10	0.09	0.10	0.10	0.09	0.08	0.10	0.08	0.41	0.23	0.37	0.09

feldspars Spencer B and SH 1070. The Spencer B feldspar is considered by Wright & Stewart (1968) to be probably as highly ordered as any natural potassium feldspar still retaining a monoclinic symmetry and the feldspar SH 1070 is considered to be less ordered than Spencer B. The feldspars 20559 and 20517 have lower triclinicities (0.67 and 0.80) than any of the other feldspars from the Murrumbidgee Batholith shown on figure 28.

Wright (1968) claimed that the position of the ($\bar{2}01$) reflection, which is related to the a cell parameter, can be used to estimate the content of orthoclase component (Or) of potassium feldspars once their sturctural states have been identified using figure 28, provided their cell dimensions are not "anomalous". The recognition of "anomalous" cell dimensions is based on comparison of the measured 2θ $\bar{2}01$ and the value of 2θ $\bar{2}01$ read from figure 28, a difference of 0.1° 2θ being regarded as "anamolous". Eight of the plotted feldspars, including 20559 and 20517 are "anomalous" and, therefore, their Or content cannot be calculated from 2θ $\bar{2}01$. Wright & Stewart (1968) state that a large number of natural alkali feldspars are "anomalous" and the effect of the discrepancies in cell dimensions upon the estimation of their structural states from figure 28 is unknown. Calculation of the Or contents of the Murrumbidgee feldspars not qualifying as "anomalous", using the regression equation appropriate to the maximum microcline-low albite series (Wright, 1968), gave a range of values from 93.0 to 97.6 per cent (similar to the range of invalid Or contents calculated for the "anomalous" feldspars) which is substantially higher than the range of

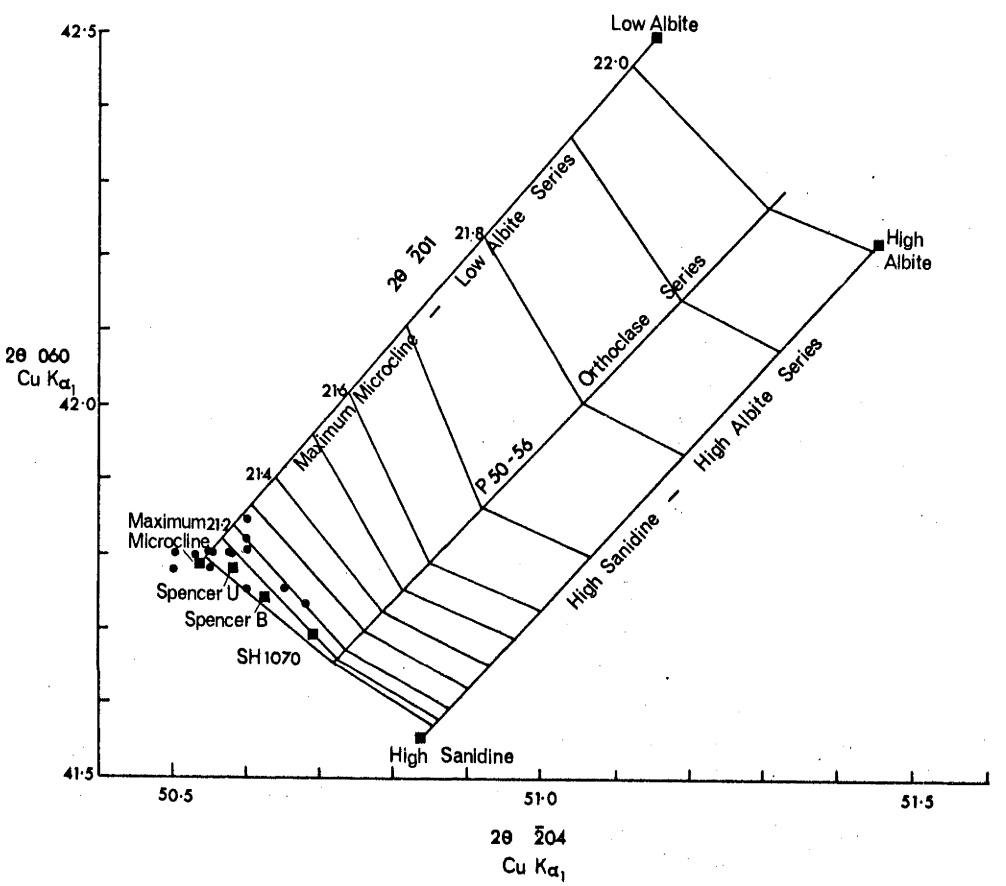

Figure 28. Structural state of potassium feldspars (diagram after Wright, 1968)

Or contents, from 71.49 to 90.70 per cent, calculated for the same group of feldspars from their chemical analyses.

The structural formulae, based on 32 oxygen atoms, show a very small excess of atoms in the Z sites (Z ranging from 16.011 to 16.045 atoms), except for sample 20543, but a notable deficiency in the X sites, which have a total occupancy of 3.763 to 3.975 atoms. There is a small amount of reciprocal variation between Si and Al in the Z sites, Si ranging from slightly below to slightly above its stoichiometric proportions of 12 atoms, and Al showing reciprocal departures from its stoichiometric proportions of 4 atoms in 15 out of the 18 analysed feldspars. The presence of divalent ions such as Ca, Ba and Sr in the X sites might be expected to lead to increased occupancy of Z sites by Al in order to compensate charge differences but the symmetrical range of Al about its stoichiometric proportion of 4 atoms reveals no evidence of this. It seems that charge differences are compensated mainly by vacancies in the X site. Excluding samples 20543 and 20546, for which data are incomplete, the average occupancy of X sites is 3.898 atoms in the feldspars of the contaminated and uncontaminated granites in which divalent elements are abundant, in contrast to an average of 3.927 X atoms in the leucogranite feldspars in which divalent elements are less abundant.

All the feldspars contain Fe to the extent of about 0.01 to 0.02 atoms per formula unit, considered to represent ferric ions replacing Al in Z sites. The amounts of Fe in the feldspars is essentially constant and since Fe, unlike other trace elements in the feldspars, is

a major constituent of minerals coexisting with the feldspars, its abundance probably represents the maximum permissible substitution of Fe in the feldspars under the physical conditions prevailing during crystallisation of the intrusions of the Murrumbidgee Batholith.

K and Na, the major occupants of the X sites, vary in reciprocal fashion, K ranging between 3.504 and 2.770 atoms per formula unit and Na between 0.339 and 1.135 atoms. There is no relationship between the variation of Na and K in the feldspars and the composition of their host rocks. The two concentrates, 20567 and 20571, which contain the highest proportion of Na, may be contaminated since the coexisting plagioclase is albite and, therefore, removal of all composite grains is difficult.

Calcium, other than that attributable to apatite inclusions, is very low in all the concentrates and ten of the feldspars, including all concentrates from the leucogranites contain no An component. The number of Ca atoms in the remaining eight feldspars ranges from 0.001 to 0.054 atoms per formula unit with no apparent regularity.

Ba, Sr, Rb and Ga vary in a regular manner which can be correlated with changes in bulk rock composition but Pb and Y show no significant correlation with host rock compositions. Ba decreases in the range from 1790 to 65 parts per million with increasing acidity of the host rock (correlation of -0.55 with SiO_2 of host rock) and Sr varies concomitantly in the range 165 to 7 parts per million (correlation of 0.85 with Ba content of the feldspar and -0.51 with increasing SiO_2 content of the host rock). Rb increases in abundance with increasing SiO_2 content of the host rock (correlation of 0.71) in the range 234 to

1094 parts per million and Ga also increases (correlation of 0.75 with host rock SiO_2) in the range 8 to 17 parts per million. Pb varies between 14 and 36 parts per million and shows no correlation with increasing acidity of the host rocks. However, it is generally highest in microclines from the contaminated granites, lowest in microclines from the uncontaminated granites and intermediate in abundance in microclines of the leucogranites. Y varies from below detection (about 1 part per million) in most samples to a maximum of 14 parts per million in microcline from a Shannons Flat Adamellite sample which has an unusually high Y content of 200 parts per million.

All six of these trace elements vary independently of the major element composition of the feldspar and similar independence has been noted elsewhere (Heier, 1962; Rhodes, 1969b,c). Regular changes in the abundance of Ba, Sr, Rb and Ga with changes in host rock composition, similar to the changes in Murrumbidgee feldspars, also have been recorded elsewhere (Sen et al., 1959; Heier, 1962; Chappell, 1966; Rhodes, 1969b,c).

The abundance of Sr in the potassium feldspars shows a highly significant correlation ($r = 0.67$) with the abundance of Sr in the host rocks and the abundances of Rb show a similarly high correlation between the content of the feldspars and the content of their hosts ($r = 0.87$). None of the other elements show significant correlations.

Plagioclase

Granitic plagioclase is a difficult mineral to examine chemically

because of its typical complicated zoning, but heavy liquid separation is regarded as a valid method of obtaining a reasonable "average" composition provided care is taken to minimise selective separation of extremes in composition. Complete separation of microcline without selective removal of albite in the sodic plagioclases is also a problem since, despite the use of fine fractions, composite grains of microcline and quartz or more calcic plagioclase, with specific gravities close to that of the bulk feldspar persist in the concentrates. However, within its limitations, the method is considered adequate to provide information on the plagioclases and this is desirable in order to make fullest use of the data obtained on the coexisting microcline and ferromagnesian minerals.

A summary of the plagioclase data is given in table 33. The analyses have been recalculated to their original totals on a quartz-free (and apatite-free) basis by allocating appropriate amounts of SiO_2 to satisfy the stoichiometric requirements of total Ca, Na, K, Ba, Sr and Rb. The resultant analyses have been used to calculate molecular proportions of the various feldspar components and structural formulae on the basis of 32 oxygen atoms.

Samples 20559, 20569, 20574 and 20571, ranging in Or content from 11.96 to 24.17 per cent are probably contaminated to an appreciable extent by microcline but the remainder, ranging in Or content from 1.29 to 8.22 per cent, are probably not appreciably contaminated, since sample 20555 which does not coexist with microcline contains 6.65 per cent Or. Comparable amounts of Or in plagioclases are recorded by

Table 33 Chemical analyses, structural formulae and molecular proportions of plagioclase feldspars from the Murrumbidgee Batholith

	Stewartsfield Granodiorite	Clear Range Granodiorite				Xenolith	Callemondah Granodiorite		Bolairo Granodiorite	Willoona Tonalite	Shannons Flat Adamellite							Tharwa Adamellite	Westerly Muscovite Granite	Yaouk Leucogranite	Unnamed Leucogranites	
	20559	20562	20563	20535	20541	20576	20543	20546	20551	20555	20502	20507	20510	20511	20513	20515	20521	20528	20569	20567	20571	20574
SiO_2	58.52	50.90	53.89	56.12	57.89	52.55	54.21	56.73	56.82	56.89	59.43	58.89	58.56	59.22	58.60	59.90	58.65	59.23	66.43	65.39	63.89	63.58
Al_2O_3	26.50	31.03	29.29	27.75	26.81	29.57	28.63	27.05	27.17	27.07	25.50	25.73	25.58	25.71	25.90	25.15	25.39	25.74	19.75	22.11	21.20	22.64
Fe_2O_3	0.31	0.23	0.12	0.31	0.33	0.61	0.36	0.26	0.28	0.34	0.25	0.36	0.37	0.36	0.38	0.27	0.36	0.42	0.22	0.19	0.21	0.40
CaO	7.30	13.88	11.41	9.16	7.40	12.11	10.62	7.95	8.49	8.09	6.72	6.90	6.45	6.80	7.52	6.32	7.34	6.80	0.40	2.05	1.81	3.67
Na_2O	5.99	3.44	4.90	5.87	6.54	4.29	4.86	6.07	6.06	6.03	7.26	6.99	6.81	6.94	6.62	7.19	6.59	6.89	8.87	9.53	7.57	8.16
K_2O	2.08	0.28	0.22	0.59	1.03	0.41	0.82	1.13	0.86	1.14	0.72	0.88	1.33	1.10	1.02	1.18	1.17	1.17	3.63	1.45	4.16	2.15
BaO	0.03	0.00	0.01	0.01	0.01	0.01	0.02	0.01	0.02	0.02	0.00	0.00	0.01	0.02	0.00	0.00	0.01	0.01	0.00	0.00	0.00	0.01
SrO	0.05	0.06	0.06	0.05	0.04	0.06	0.01	0.06	0.05	0.06	0.04	0.04	0.04	0.05	0.05	0.03	0.05	0.04	0.00	0.01	0.01	0.01
Rb_2O	0.01	0.00	0.00	0.00	0.01	0.00	0.00	0.00	0.01	0.00	0.00	0.00	0.01	0.01	0.01	0.00	0.00	0.01	0.03	0.01	0.03	0.01
Total	100.79	99.82	99.90	99.76	100.06	99.61	99.53	99.26	99.76	99.64	99.92	99.79	99.16	100.21	100.10	100.04	99.56	100.31	99.33	100.74	98.88	100.63
Trace elements (parts per million)																						
Ba	260	30	95	100	75	85	135	180	135	200	10	25	65	170	55	30	105	115	<7	<7	<5	<10
Sr	436	529	541	434	368	537	56	492	438	516	314	331	310	381	377	270	380	340	5	44	89	81
Rb	90	10	6	30	43	17	29	38	64	38	20	24	72	65	47	38	41	51	295	114	246	106
Pb	37	36	39	45	33	36	34	53	43	44	27	24	21	25	24	27	25	32	29	24	37	40
Y	17	6	7	15	13	37	10	17	16	15	7	178	24	12	11	11	19	11	7	13	16	33
Ga	27	29	27	29	26	30	26	28	27	29	27	28	27	28	26	23	27	27	19	24	20	22
Structural formulae on the basis of 32 oxygen atoms																						
Z Si	10.447	9.289	9.751	10.113	10.377	9.581	9.852	10.272	10.240	10.266	10.626	10.584	10.578	10.584	10.500	10.704	10.565	10.576	11.850	11.468	11.521	11.249
Z Al	5.577	6.675	6.247	5.896	5.666	6.356	6.134	5.773	5.773	5.759	5.376	5.452	5.448	5.417	5.471	5.298	5.392	5.420	4.154	4.572	4.508	4.722
Z Fe	0.042	0.031	0.016	0.042	0.044	0.083	0.049	0.036	0.038	0.046	0.034	0.048	0.050	0.048	0.052	0.036	0.049	0.057	0.030	0.025	0.028	0.053
X Ca	1.396	2.714	2.211	1.768	1.422	2.367	2.068	1.542	1.639	1.564	1.288	1.329	1.248	1.302	1.445	1.209	1.418	1.301	0.076	0.386	0.349	0.695
X Na	2.073	1.217	1.720	2.052	2.272	1.515	1.714	2.130	2.118	2.111	2.516	2.437	2.384	2.404	2.300	2.490	2.303	2.387	3.069	3.239	2.648	2.800
X K	0.473	0.065	0.051	0.135	0.235	0.096	0.190	0.261	0.198	0.263	0.164	0.202	0.306	0.251	0.234	0.269	0.269	0.267	0.826	0.325	0.956	0.484
X Ba	0.002	0.000	0.001	0.001	0.001	0.001	0.001	0.001	0.001	0.002	0.000	0.000	0.000	0.001	0.000	0.000	0.001	0.001	0.000	0.000	0.000	0.000
X Sr	0.005	0.007	0.007	0.005	0.005	0.007	0.001	0.006	0.005	0.006	0.004	0.004	0.004	0.005	0.005	0.003	0.005	0.004	0.000	0.001	0.001	0.001
X Rb	0.001	0.000	0.000	0.000	0.001	0.000	0.000	0.000	0.001	0.000	0.000	0.000	0.001	0.001	0.001	0.000	0.001	0.001	0.004	0.001	0.003	0.001
Tot. Z	16.066	15.995	16.014	16.051	16.087	16.020	16.035	16.081	16.051	16.071	16.036	16.084	16.076	16.049	16.023	16.038	16.006	16.053	16.034	16.065	16.057	16.024
Tot. X	3.950	4.003	3.990	3.961	3.936	3.986	3.974	3.940	3.962	3.946	3.972	3.972	3.943	3.964	3.985	3.971	3.997	3.961	3.975	3.952	3.957	3.981
Percentages of the feldspar molecules (R = $RbAlSi_3O_8$, S = $SrAl_2Si_2O_8$)																						
An	35.35	67.80	55.42	44.62	36.14	59.39	52.04	39.14	41.37	39.64	32.43	33.46	31.66	32.85	36.27	30.45	35.48	32.85	1.91	9.76	8.82	17.47
Ab	52.47	30.41	43.10	51.80	57.74	38.02	43.13	54.07	53.45	53.49	63.35	61.34	60.45	60.66	57.73	62.69	57.63	60.26	77.21	81.97	66.91	70.32
Or	11.96	1.62	1.29	3.42	5.97	2.40	4.78	6.62	5.00	6.65	4.13	5.09	7.76	6.33	5.87	6.76	6.74	6.75	20.79	8.22	24.17	12.16
Cs	0.05	0.01	0.02	0.02	0.02	0.02	0.03	0.03	0.03	0.04	0.00	0.01	0.01	0.03	0.01	0.01	0.02	0.02	0.00	0.00	0.00	0.00
S	0.14	0.17	0.17	0.14	0.12	0.17	0.02	0.16	0.14	0.16	0.10	0.10	0.10	0.12	0.12	0.08	0.12	0.11	0.00	0.01	0.03	0.02
R	0.03	0.00	0.00	0.01	0.01	0.01	0.01	0.01	0.02	0.01	0.01	0.01	0.02	0.02	0.02	0.01	0.01	0.02	0.09	0.04	0.08	0.03
Percentage An/(An + Ab)																						
	40	69	56	46	39	61	55	42	44	43	34	35	34	35	39	33	38	35	2	12	12	20
Normative percentage An/(An + Ab) in host rock																						
	41	70	62	38	35	56	52	36	42	37	34	34	33	36	34	34	33	33	3	10	11	10
Calculated percentage of quartz in the concentrate																						
	70.5	24.7	5.0	15.5	69.5	35.1	19.5	39.6	55.7	51.6	70.2	70.9	66.1	67.8	62.0	73.7	63.0	62.8	40.5	45.7	22.7	72.3
Calculated percentage of apatite in the concentrate																						
	0.10	2.96	0.63	0.24	0.09	0.47	0.17	0.19	0.11	0.12	0.06	0.05	0.07	0.06	0.09	0.05	0.08	0.06	0.26	0.18	0.29	0.06

Rhodes (1969b) from the Hartley granites, including 6.90 per cent Or in plagioclase from a diorite which contains no potassium feldspar phase. Amounts of 2-5 per cent in plagioclases considered to be free of significant potassium feldspar contamination are recorded by Chappell (1966) from the Moonbi granites. Data presented by Heier (1962) and Corlett & Ribbe (1967) indicate that maximum concentrations of potassium occur in plagioclases of andesine composition and it is interesting to note that the labradorite samples in table 33 average 2.52 per cent Or and range from 1.29 to 4.78 compared with an average of 5.93 per cent Or and a range of 3.42 to 7.76 for the andesine samples (excluding the suspect sample 20559).

The An content of the plagioclases ranged from 67.8 to 1.9 per cent of the total feldspar and is correlated closely with decreasing Ca content of the rocks concomitant with increasing acidity. The An/(Ab + An) ratios calculated from the chemical analyses agree closely with the same ratio calculated from the CIPW norms of the host rocks and since potassium feldspar (and hornblende in two cases) is the only natural mineral in the rocks which contains a significant amount of the Na (and Ca) allocated to plagioclase in the CIPW norm calculations, this agreement may be taken as proof that no significant fractionation of the plagioclase was incurred during gravity separation.

Ba ranges from below detection (5-7 parts per million) in the sodic plagioclases of the leucogranites to a maximum of 260 parts per million in andesine of the Stewartsfield Granodiorite. The abundance of Ba in the plagioclases shows a highly significant correlation ($r = 0.64$)

with the abundance of Ba in the host rocks. Corlett & Ribbe (1967) and Rhodes (1969b) claim an association between Ba and K in plagioclase but the data of table33 show an insignificant negative correlation ($r = -0.25$) between these two elements. There is a significant correlation ($r = 0.54$) between Ba and Sr in the plagioclases.

Sr is highly correlated ($r = 0.76$) with Ca content of the feldspars and, therefore, shows a regular decrease with increasing acidity of the host rocks, ranging from a maximum of 541 parts per million in labradorite of the most basic Clear Range Granodiorite to 5 parts per million in albite of the Westerly Muscovite Granite. There is a high correlation ($r = 0.81$) between the abundances of Sr in the plagioclases and their host rocks.

Rb ranges from 6 to 65 parts per million in those plagioclases of the contaminated and uncontaminated granites thought to be free of significant contamination by microcline, in contrast to 106 to 295 parts per million in the leucogranite plagioclases where contamination by the Rb-rich mineral microcline is thought to be significant.

Pb is not well correlated with the abundance of any other element in either the plagioclases or their host rocks, nor is it significantly correlated with the abundance of Pb in the host rock. It is most abundant in plagioclases from the contaminated granites, ranging from 33 to 53 parts per million, less abundant in plagioclase of the uncontaminated granites, ranging from 21 to 32 parts per million, and moderately abundant in the leucogranite plagioclases. This is a similar pattern of variation to that noted for Pb in the potassium feldspars.

Y varies from 7 to 37 parts per million in 21 of the plagioclases but sample 20507 contains 178 parts per million. This sample contains correspondingly high Sr in the bulk rock analysis (200 parts per million) and it was noted above that the potassium feldspar also contained more Sr than any of the other feldspars. The abundance of Y in the plagioclases is uncorrelated with any other element in the plagioclases or in their host rocks but is highly correlated with the content of Y in the host rocks ($r = 0.98$).

Ga ranges from 30 to 19 parts per million and decreases in abundance with increasing acidity of the host rock, which is paralleled by increasing Ab content of the plagioclase and consequent decreasing Al content. This is the reverse of the variation in Ga noted by Rhodes (1969b) in the Hartley granites where the Ga content of the plagioclases increases with increasing acidity of the host rocks. The correlation between Ga and Al in the plagioclases is 0.84 in contrast to the insignificant negative correlation of -0.17 between Ga and Al in the potassium feldspars. There is no significant correlation with the Ga content of the host rocks.

Biotite

Brown biotite is ubiquitous in the Murrumbidgee granites and xenoliths and some general chemical features were presented by Snelling (1957, 1960) on the basis of two biotites separated from uncontaminated granites, six from contaminated granites and one from a hornblende-bearing xenolith. No analyses of biotite from the leucogranites were

presented. The main features commented upon by Snelling are that all the biotites have more than two atoms of Al in tetrahedral sites and some Al in octahedral sites.

New analyses of 22 biotites from the batholith are presented in table 34 and their structural formulae, calculated on the basis of 22 oxygen atoms, water free, are listed in table 35 . The original analyses contained 0.01 to 0.70 per cent CaO but microprobe analyses by Chappell (1966) and Gulson (1968) on granitic biotites indicate that Ca is absent from the biotite structure and the amounts recorded in biotite analyses are present mainly in apatite inclusions. Accordingly, the analyses were recalculated on a CaO-free as well as a P_2O_5-free basis (the reasons for neglecting P_2O_5 were discussed above).

Satisfactory H_2O analysis of biotites is complicated by redox reactions during decomposition of the biotite, so calculation of the structural formulae on an anhydrous basis is preferred in order to avoid possible errors in H_2O being reflected throughout the calculated formulae. Theoretical H_2O contents have been estimated on the basis of four OH groups per unit formula calculated for 22 oxygen atoms, water-free and these are shown in brackets in table 34. Measured H_2O on samples 20507 and 20513 are substantially lower than the theoretical contents, despite decomposition in the presence of dry O_2 in an effort to overcome the redox problem. Many of the predicted totals of the analyses are low and this is probably due to the lack of F analyses.

All of the biotites contain more than enough Si and Al to provide the theoretical eight atoms in tetrahedral sites. The number of atoms

Table 34 Chemical analyses of biotites from the Murrumbidgee Batholith (continued on next two pages)

	Stewartsfield Granodiorite	Clear Range Granodiorite				Xenolith	Callemondah Granodiorite	
	20559	20562	20563	20535	20541	20576	20543	20546
SiO_2	34.39	36.43	36.44	35.44	35.33	37.26	36.59	35.32
TiO_2	3.95	1.58	2.09	2.88	3.16	3.52	2.52	3.24
Al_2O_3	16.68	17.25	16.57	17.60	17.45	16.60	16.68	17.98
Fe_2O_3	5.03	2.80	2.85	0.48	2.36	0.79	1.37	2.70
FeO	16.78	16.75	14.78	18.66	19.20	18.60	17.36	17.62
MnO	0.25	0.19	0.24	0.30	0.27	0.22	0.31	0.28
MgO	10.37	11.82	8.80	9.43	9.23	9.41	11.53	8.85
Na_2O	0.14	0.19	0.11	0.10	0.08	0.30	0.10	0.12
K_2O	8.12	9.05	9.52	9.63	9.13	8.96	9.57	9.39
H_2O	(3.96)+	(4.00)+	(3.83)+	(3.91)+	(3.96)+	(3.98)+	(3.99)+	(3.95)+
T*	0.67	0.47	0.46	0.51	0.55	0.54	0.48	0.60
Total	(100.34)	(100.53)	(95.69)	(98.94)	(100.72)	(100.18)	(100.50)	(100.05)
Ba	3151	1910	1898	2230	2461	2738	2153	2867
Rb	476	443	456	643	686	413	476	599
Sr	6	4	7	4	11	23	6	4
Pb	5	9	4	5	5	8	8	6
Zr	64	50	28	108	151	77	39	129
Nb	50	27	22	58	61	32	41	59
Y	11	1	<1	8	7	17	11	4
V	745	482	397	473	457	668	502	489
Cr	421	322	476	301	261	152	320	336
Mn		1291			1834			1891
Co	48	59	58	52	48	52	53	55
Ni	107	83	119	92	97	69	71	109
Cu	<1	12	31	1	6	4	10	7
Zn	298	335	272	309	276	280	285	317
Ga	38	31	26	35	38	27	28	31
Li	35	75			120			70

Oxides in per cent, elements in parts per million

\+ Calculated from structural formula

* T = $BaO + Rb_2O + Nb_2O_5 + V_2O_5 + Cr_2O_3 + NiO + ZnO + Li_2O$

Table 34 Chemical analyses of biotites from the Murrumbidgee Batholith (see also preceeding and succeeding pages)

	Bolairo Granodiorite	Willoona Tonalite	Shannons Flat Adamellite					
	20551	20555	20502	20507	20510	20511	20513	20515
SiO_2	36.43	34.91	35.12	36.11	35.62	34.73	35.78	35.45
TiO_2	2.94	3.41	3.25	3.53	3.20	3.95	4.02	3.27
Al_2O_3	18.16	17.67	16.28	16.27	16.51	15.50	15.62	16.13
Fe_2O_3	1.87	2.06	1.85	2.75	1.95	1.00	2.74	1.39
FeO	17.43	19.45	19.67	19.39	20.11	20.78	19.74	20.00
MnO	0.28	0.29	0.36	0.27	0.44	0.34	0.36	0.38
MgO	10.04	8.86	8.48	8.42	8.19	9.07	8.23	8.67
Na_2O	0.10	0.08	0.08	0.13	0.18	0.11	0.11	0.11
K_2O	9.55	8.94	9.41	9.43	9.10	8.01	9.36	9.46
H_2O	(4.03)+	(3.94)+	(3.87)+	3.31[1]	(3.90)+	(3.84)+	2.78[2]	(3.88)+
T*	0.57	0.62	0.66	0.60	0.58	0.71	0.79	0.63
Total	(101.40)	(100.23)	(99.03)	100.21	(99.78)	(98.04)	99.53	(99.37)
Ba	2433	2918	2953	3041	3034	3786	4193	2779
Rb	590	613	872	875	901	498	708	863
Sr	6	5	6	6	10	7	11	9
Pb	11	5	7	9	10	12	10	11
Zr	107	153	53	114	54	20	91	86
Nb	51	58	100	92	102	90	82	98
Y	11	13	5	98	11	11	12	7
V	448	496	436	424	470	398	484	453
Cr	348	332	101	120	77	73	155	101
Mn	1885	2038		1833			2529	
Co	50	51	42	53	43	42	50	39
Ni	109	109	49	95	24	92	74	55
Cu	6	1	6	4	5	121	14	24
Zn	304	344	349	215	218	444	378	330
Ga	34	32	44	42	45	39	39	40
Li	185	130	350	85		350	300	305

Oxides in per cent, elements in parts per million

\+ Calculated from structural formula

* $T = BaO + Rb_2O + Nb_2O_5 + V_2O_5 + Cr_2O_3 + NiO + ZnO + Li_2O$

1. Calculated $H_2O = 3.95$

2. Calculated $H_2O = 3.92$

Table 34 Chemical analyses of biotites from the Murrumbidgee Batholith (continued from previous two pages)

	Shannons Flat Adamellite		Tharwa Adamellite	Westerly Muscovite Granite	Yaouk Leucogranite	Unnamed Leucogranite
	20521	20523	20528	20569	20567	20571
SiO_2	34.88	35.36	36.06	32.65	33.95	34.21
TiO_2	3.82	3.95	3.26	1.22	2.51	3.45
Al_2O_3	15.80	15.45	16.07	20.19	18.88	17.84
Fe_2O_3	2.27	1.83	3.11	2.42	3.52	2.93
FeO	20.66	20.09	19.27	27.22	22.61	21.85
MnO	0.37	0.38	0.33	0.72	1.01	0.97
MgO	8.89	7.71	8.66	0.53	3.52	6.10
Na_2O	0.10	0.10	0.12	0.07	0.05	0.09
K_2O	7.97	9.28	9.40	8.71	8.33	8.61
H_2O	(3.88)+	(3.84)+	(3.95)+	(3.70)+	(3.82)+	(3.89)+
T*	0.80	0.59	0.67	0.60	0.57	0.93
Total	(99.44)	(98.58)	(100.80)	(98.03)	(98.77)	(100.97)
Ba	4287	3000	3377	<4	195	4682
Rb	483	663	738	2447	1393	1698
Sr	9	12	5	4	6	12
Pb	15	10	6	9	34	17
Zr	53	187	82	14	102	227
Nb	79	85	72	398	319	255
Y	26	38	8	<1	45	43
V	436	501	507	13	181	391
Cr	82	131	162	<1	25	191
Mn			2216	4612		6596
Co	47	42	45	13	15	24
Ni	25	50	76	9	30	49
Cu	62	6	9	1	21	11
Zn	855	323	350	762	561	316
Ga	28	39	40	52	72	45
Li	290	95	150	770	1060	130

Oxides in per cent, elements in parts per million

\+ Calculated from structural formula

* $T = BaO + Rb_2O + Nb_2O_5 + V_2O_5 + Cr_2O_3 + NiO + ZnO + Li_2O$

Table 35 Structural formulae of biotites from the Murrumbidgee Batholith (continued on next two pages)

		Stewartsfield Granodiorite	Clear Range Granodiorite				Xenolith	Callemondah Granodiorite	
		20559	20562	20563	20535	20541	20576	20543	20546
Z	Si	5.203	5.452	5.696	5.438	5.351	5.607	5.494	5.358
	Al	2.797	2.548	2.304	2.562	2.649	2.393	2.506	2.642
Y	Al	0.177	0.494	0.749	0.621	0.465	0.551	0.445	0.571
	Ti	0.449	0.178	0.246	0.333	0.360	0.398	0.284	0.370
	Fe^{3+}	0.573	0.315	0.3335	0.056	0.269	0.090	0.155	0.308
	Fe^{2+}	2.123	2.096	1.932	2.395	2.432	2.341	2.180	2.235
	Mn	0.032	0.024	0.032	0.039	0.035	0.028	0.039	0.036
	Mg	2.339	2.637	2.051	2.156	2.084	2.110	2.580	2.001
	V	0.013	0.009	0.007	0.009	0.008	0.012	0.009	0.009
	Cr	0.007	0.006	0.009	0.005	0.005	0.003	0.006	0.006
	Ni	0.002	0.001	0.002	0.001	0.002	0.001	0.001	0.002
	Zn	0.004	0.005	0.004	0.004	0.004	0.004	0.004	0.004
	Li	0.005	0.009			0.016			0.009
X	Na	0.041	0.055	0.035	0.030	0.023	0.086	0.030	0.035
	K	1.568	1.728	1.899	1.885	1.764	1.721	1.834	1.818
	Ba	0.021	0.012	0.013	0.015	0.016	0.018	0.014	0.019
	Rb	0.005	0.005	0.005	0.007	0.007	0.004	0.005	0.006
Z		8.000	8.000	8.000	8.000	8.000	8.000	8.000	8.000
Y		5.724	5.773	5.367	5.619	5.680	5.538	5.703	5.551
X		1.635	1.800	1.952	1.937	1.810	1.829	1.883	1.878
Tetrahedral charge		-2.797	-2.548	-2.304	-2.562	-2.649	-2.393	-2.506	-2.642
Octahedral charge		+1.137	+0.737	+0.340	+0.613	+0.827	+0.552	+0.607	+0.745
Inherent layer charge		-1.660	-1.811	-1.964	-1.949	-1.822	-1.841	-1.899	-1.897
Interlayer charge		+1.656	+1.812	+1.965	+1.952	+1.826	+1.847	+1.897	+1.897

Table 35 Structural formulae of biotites from the Murrumbidgee Batholith (see also preceeding and succeeding pages)

		Bolairo Granodiorite	Willoona Tonalite	Shannons Flat Adamellite					
		20551	20555	20502	20507	20510	20511	20513	20515
Z	Si	5.419	5.317	5.443	5.482	5.474	5.426	5.466	5.474
	Al	2.581	2.683	2.557	2.518	2.526	2.574	2.534	2.526
Y	Al	0.602	0.488	0.416	0.392	0.464	0.278	0.278	0.409
	Ti	0.329	0.390	0.378	0.403	0.369	0.464	0.462	0.380
	Fe^{3+}	0.209	0.236	0.215	0.314	0.226	0.117	0.315	0.162
	Fe^{2+}	2.168	2.477	2.550	2.462	2.584	2.714	2.522	2.582
	Mn	0.035	0.037	0.047	0.035	0.057	0.045	0.047	0.050
	Mg	2.226	2.011	1.960	1.906	1.874	2.111	1.873	1.995
	V	0.008	0.009	0.008	0.008	0.009	0.007	0.009	0.008
	Cr	0.006	0.006	0.002	0.002	0.001	0.001	0.003	0.002
	Ni	0.002	0.002	0.001	0.001	0.000	0.001	0.001	0.001
	Zn	0.004	0.005	0.005	0.003	0.003	0.006	0.005	0.005
	Li	0.024	0.017	0.047	0.011		0.047	0.039	0.041
X	Na	0.029	0.024	0.024	0.038	0.054	0.032	0.033	0.032
	K	1.813	1.737	1.860	1.827	1.785	1.597	1.825	1.863
	Ba	0.016	0.019	0.020	0.020	0.020	0.026	0.028	0.019
	Rb	0.006	0.007	0.010	0.009	0.010	0.005	0.008	0.009
Z		8.000	8.000	8.000	8.000	8.000	8.000	8.000	8.000
Y		5.613	5.678	5.629	5.538	5.590	5.791	5.554	5.635
X		1.864	1.787	1.914	1.894	1.869	1.660	1.894	1.923
Tetrahedral charge		-2.581	-2.683	-2.557	-2.518	-2.526	-2.574	-2.534	-2.526
Octahedral charge		+0.701	+0.876	+0.624	+0.601	+0.636	+0.880	+0.616	+0.586
Inherent layer charge		-1.880	-1.807	-1.933	-1.917	-1.890	-1.694	-1.918	-1.940
Interlayer charge		+1.880	+1.806	+1.934	+1.914	+1.889	+1.686	+1.922	+1.942

Table 35 Structural formulae of biotites from the Murrumbidgee Batholith (continued from previous two pages)

		Shannons Flat Adamellite 20521	Shannons Flat Adamellite 20523	Tharwa Adamellite 20528	Westerly Muscovite Granite 20569	Yaouk Leucogranite 20567	Unnamed Leucogranite 20571
Z	Si	5.383	5.514	5.478	5.287	5.333	5.273
	Al	2.617	2.486	2.522	2.713	2.667	2.727
Y	Al	0.256	0.354	0.354	1.139	0.828	0.513
	Ti^{3+}	0.443	0.463	0.373	0.149	0.297	0.400
	Fe^{3+}	0.264	0.215	0.356	0.295	0.417	0.340
	Fe^{2+}	2.665	2.621	2.448	3.687	2.970	2.816
	Mn	0.048	0.050	0.043	0.099	0.135	0.127
	Mg	2.044	1.793	1.961	0.128	0.825	1.400
	Nb	0.000	0.000	0.000	0.001	0.001	0.001
	V	0.008	0.009	0.009	0.000	0.003	0.007
	Cr	0.001	0.002	0.003	0.000	0.000	0.003
	Ni	0.000	0.001	0.001	0.002	0.002	0.002
	Zn	0.012	0.005	0.005	0.011	0.008	0.004
	Li	0.039	0.013	0.020	0.108	0.145	0.017
X	Na	0.030	0.030	0.035	0.022	0.015	0.027
	K	1.569	1.846	1.823	1.799	1.670	1.692
	Ba	0.029	0.020	0.022	0.000	0.001	0.032
	Rb	0.005	0.007	0.008	0.028	0.015	0.018
Z		8.000	8.000	8.000	8.000	8.000	8.000
Y		5.780	5.526	5.573	5.619	5.631	5.630
X		1.633	1.903	1.888	1.849	1.701	1.769
Tetrahedral charge		-2.617	-2.486	-2.522	-2.713	-2.667	-2.727
Octahedral charge		+0.952	+0.563	+0.612	+0.865	+0.968	+0.923
Inherent layer charge		-1.665	-1.923	-1.910	-1.848	-1.699	-1.804
Interlayer charge		+1.662	+1.923	+1.910	+1.849	+1.702	+1.801

in octahedral sites ranges from 5.367 to 5.791 in contrast with the theoretical 6 atoms of tri-octahedral micas. This range is within the general range of octahedral occupancy of biotites (Deer et al., 1962b; Foster, 1960) and suggests a state intermediate between that of strict tri-octahedral (Y= 6) and di-octahedral (Y = 4) micas. The number of interlayer cations is less than two atoms in all cases, ranging from 1.633 to 1.952.

Al is abundant in all the biotites ranging from 2.304 to 2.797 atoms in tetrahedral sites, and from 0.177 to 1.139 atoms in octahedral sites. The biotites from the leucogranites, in which they coexist with muscovite, are noticeably richer in both tetrahedral and octahedral Al (average 2.702 and 0.827 atoms, respectively) than biotites from the uncontaminated granites (average 2.542 and 0.356 atoms, respectively) where biotite coexists only with feldspars and quartz. Al in biotites from the contaminated granites, in which muscovite coexists with the biotite (except samples 20562 and 20563 in which hornblende occurs with the biotite), is more variable and ranges from 2.304 to 2.797 atoms in tetrahedral sites and from 0.177 to 0.749 atoms in octahedral sites.

Nockolds (1947) demonstrated that biotites coexisting with muscovite have higher Al_2O_3 contents than biotites coexisting with hornblende. Chappell (1966), on the basis of a survey of 52 published granitic biotite analyses of known paragenesis and 12 analyses of biotites from the Moonbi granites, suggested that biotites coexisting with muscovite or hornblende in granitic rocks normally contain close to 2.5 atoms of Al per formula unit in tetrahedral sites but in the octahedral sites,

those biotites coexisting with muscovite contain about 0.6 atoms of Al whereas those associated with hornblende contain small or negligible amounts of Al. Chappell (1966) regarded the Al in octahedral coordination as representing solid solution of muscovite in biotite free of octahedral Al, therefore attaining its maximum abundance in biotites coexisting with muscovite. There is general agreement (Deer et al., 1962b)that a complete solid solution series does not exist between biotite and muscovite. On the basis of the restricted solid solution hypothesis, Chappell (1966) suggested that granitic biotites existing in the absence of hornblende and muscovite and occurring in rocks intermediate in composition between hornblende-bearing and muscovite-bearing granites might be expected to contain about 2.5 atoms of Al in tetrahedral sites and between 0.0 and 0.6 atoms of Al in octahedral sites; this representing varying degrees of solid solution of muscovite up to the saturation point at which muscovite would appear as a coexisting phase. Fourteen published analyses of biotites existing in the absence of hornblende and muscovite listed by Chappell (1966) provided only general support for this hypothesis because, although octahedral Al varied between zero and 0.813 atoms, tetrahedral Al varied between 2.095 and 2.721 atoms.

The nine biotites analysed from the uncontaminated granites (table 35) all exist in rocks devoid of amphibole or primary muscovite and their range of 2.486 to 2.617 atoms of Al in tetrahedral sites together with a range of 0.256 to 0.464 atoms of Al in octahedral sites is consistent with Chappell's (1966) hypothesis. However, the three biotites

coexisting with muscovite in the leucogranites are richer in tetrahedral Al than the 2.5 atoms postulated by Chappell, as are six of the eight analyses of biotite coexisting with muscovites listed by Chappell (1966) and it is possible that changes in the proportions of Al in tetrahedral coordination do accompany changes in bulk rock composition (and resultant paragenesis).

It also seems likely that Chappell's estimate of the upper limit of octahedral occupancy of 0.6 atoms is too low, especially in cases in which garnet, as well as muscovite, coexists with the biotite since the biotite from the Westerly Muscovite Granite contains 1.139 atoms of Al in octahedral sites. Four of the eight analyses of biotites coexisting with muscovite recorded by Chappell (1966) also contain about 1 atom (0.997 to 1.267 atoms) of Al in octahedral sites and whereas Chappell (1966) considered that errors in classical Al analyses uncorrected for P_2O_5 might explain these high values, this is not the case in the analysis of the biotite from the Westerly Muscovite Granite. Three of the biotites come from Dartmoor granites (Brammall & Harwood, 1932) and it is considered significant that the host rocks of all three contain small amounts of garnet, as well as muscovite, a feature which is shared by the Westerly Muscovite Granite which contains 0.7 per cent garnet.

The biotites analysed from the contaminated granites, with the exception of 20562 and 20563, also coexist with muscovite and are mainly richer in tetrahedral Al (average 2.631, range 2.506 to 2.797) than the biotites of the uncontaminated granites, but poorer than those of the leucogranites. Their octahedral Al contents, although generally

greater than those of the uncontaminated granite biotites, range from 0.621 to as low as 0.177 atoms per formula unit.

The biotites occurring with hornblende, 20562 and 20563, do not conform well with Chappell's (1966) hypothesis since they contain appreciable amounts of octahedral Al (0.494 and 0.749 atoms, respectively). The 0.749 atoms of octahedral Al exceeds the amount present in any of the analysed Murrumbidgee biotites except those from the Yaouk Leucogranite and the Westerly Muscovite Granite. The large amount of octahedral Al in these two biotites, 20562 and 20563, sets them apart from the 41 analyses of granitic biotites coexisting with hornblende recorded by Chappell (1966) except for three analyses of biotites from tonalites in the Southern California Batholith (Larsen & Draisin, 1948) and one from an adamellite-porphyrite from Dundee, N.S.W. (Wilkinson et al., 1964). On the basis of their Al contents, the two biotites are indistinguishable from biotites coexisting with muscovite in other contaminated granites. On field relationships and chemistry the tonalite hosts of the two biotites are gradationally related to muscovite-biotite granodiorites of the Clear Range Granodiorite. It is possible that the hornblende of the tonalites is xenocrystal and not coexisting stably with the biotite, but textural evidence is indecisive.

Harry (1950) presented data on the substitution of Al for Si in tetrahedral sites of ferromagnesian minerals which indicated that Al increases relative to Si in tetrahedral sites with increasing metamorphic temperatures (using amphibole as an example). Although not discussed by Harry, accompanying figures for Al in octahedral sites in the amphiboles

also show an apparent increase. However, average figures compiled by Nockolds (1947) and listed by Harry (1950) for biotites from igneous rocks contradict any hypothesis of increasing Al occupancy of tetrahedral sites with increasing temperature. Nockolds' (1947) average Al contents of igneous biotites are as follows:

	Associated Mineral	Topaz	Muscovite	Biotite alone	Hornblende
Biotite	Al^{IV}	2.11	2.70	2.51	2.47
	Al^{VI}	1.42	0.78	0.38	0.15

On the basis of the associated minerals these averages are interpreted to represent an increasing temperature environment from left to right, out of harmony with a postulate of increasing Al content with increasing temperature.

On the basis of data from the Murrumbidgee Batholith and contributions by Nockolds (1947) and Chappell (1966), it is concluded that the Al occupancy of both tetrahedral and octahedral sites of biotites is related to the paragenesis of the host rock and, therefore, to the the bulk rock composition. Although order-disorder relationships associated with differences in pressure and temperature of formation may be expected to influence variations from stoichiometry, such variations are apparently less important controls than bulk rock chemistry and paragenesis. Some generalisations on the abundance of Al in biotites of various parageneses are as follows:

1. biotites coexisting with hornblende tend to have the lowest total Al content, reflected mainly as a low content of Al in octahedral coordination; tetrahedrally coordinated Al ranges from 2.1 to 2.7 atoms

per formula unit and is usually enough, together with Si to ensure total occupancy of the tetrahedral sites. Biotites of this paragenesis which have unusually high contents of Al are recorded from tonalites in the Southern California and Murrumbidgee batholiths.

2. biotites existing in the absence of hornblende or muscovite tend to have higher abundances of Al, reflected mainly as increased Al occupancy of octahedral sites since tetrahedral sites occupied by Al show a similar range to that of biotites coexisting with hornblende (2.1 to 2.7 atoms per formula unit). The Al occupancy of octahedral sites ranges from 0 to 0.8 atoms.

3. biotites coexisting with muscovite contain more Al than both of the preceding groups, represented by high abundance in either octahedral or tetrahedral sites, or both. Al is invariably present in octahedral sites and ranges from 0.2 to 0.8 atoms per formula unit. Al in tetrahedral sites ranges from 2.5 to nearly 3 atoms.

4. biotites coexisting with muscovite and garnet contain the greatest abundance of Al, expressed by increased occupancy of both tetrahedral and octahedral sites. Four analyses of biotites from this paragenesis (Brammall & Harwood, 1932, and this thesis) range in tetrahedrally coordinated Al from 2.6 to 2.7 atoms per formula unit and in octahedrally coordinated Al from 1.0 to 1.1 atoms.

These differing parageneses are closely linked with changes in the ratio (Fe + Mn)/Mg, which is lowest in rocks containing hornblende and highest in rocks containing muscovite and garnet. These changing ratios are reflected in the biotites by corresponding increases in the amount of

Fe and Mn substituting for Mg in octahedral sites. Fe^{2+}(0.75Å) is larger than Mg^{2+}(0.66Å) and it seems likely that the increases in octahedral Al associated with increases in Fe and Mn may be compensation for distortion of the layers caused by the larger ions, since Al^{3+}(0.51Å) is even smaller than Mg^{2+}(0.66Å). Increased substitution of trivalent ions in the octahedral layer gives rise to charge imbalances favouring increased substitution of Al for Si in the tetrahedral layer.

Structural considerations led Radoslovich & Norrish (1962) to conclude that the octahedral layer dominates the tetrahedral layer in micas. Regression calculations by Radoslovich (1962) indicate that the ratio of partial cell dimensions $\frac{b_{oct}}{b_{tet}}$ is approximated by the expression

$$\frac{Fe^{2+} + 0.853Fe^{3+} + 0.455Mg + 0.43Ti}{Al_{tetrahedral}} ,$$

where Fe^{2+}, etc. are ionic proportions in the structural formulae. Clearly changes in Fe^{2+} have a marked effect on b_{oct} and since the octahedral layer dominates the tetrahedral layer, increases in Fe^{2+} have a large effect on the ratio $\frac{b_{oct}}{b_{tet}}$. Significant substitution of Al in octahedral sites may be expected to offset the effect of Fe^{2+} and stabilise the ratio $\frac{b_{oct}}{b_{tet}}$ since the b dimensions of layer lattices containing only Al in octahedral sites are always a minimum.

Radoslovich considers that tetrahedral Al has no significant effect on cell dimensions so its abundance is probably influenced mainly by charge balancing requirements. Some of the apparent variation in abundance of Al in tetrahedral sites may be caused by analytical difficulties. Biotites from the most acid parageneses appear to contain

the greatest abundance of tetrahedral Al, but these biotites may also contain the greatest abundance of F. The presence of F would lead to loss of Si during analysis. Since the allocation of tetrahedral Al is dependent upon Si, any loss of Si during analysis would lead to increased apparent occupancy of tetrahedral sites by Al.

The other elements occupying octahedral sites in the biotites, show regular variation with changing composition of the host rocks except for Ti and Fe^{3+}. Ti ranges from 0.178 to 0.464 and Fe^{3+} from 0.056 to 0.573, with no apparent regular difference between biotites of the three granite groups. The range in Ti is consistent with the conclusion reached by Chappell (1966) from a survey of granitic biotites that the upper limit of Ti occupancy of biotites is close to 0.46 atoms per formula unit. Published analyses of granitic biotites record Fe^{3+} as high as 1.16 atoms per formula unit, but Fe_2O_3 analyses, being determined by difference from large amounts of FeO, are liable to large errors. However, most analyses examined by Chappell (1966) contain less than 0.55 atoms of Fe^{3+} and Chappell suggested that the range of 0.36 to 0.50 atoms per formula unit obtained for biotites coexisting with magnetite in Moonbi granites probably corresponds with the maximum permissable entry of Fe^{3+} into the octahedral sites of biotites. Biotites not coexisting with magnetite could be expected to contain less than this maximum amount. The data of table 35 are quite consistent with this hypothesis since none of the analysed biotites are considered to coexist with primary magnetite and all contain considerably less than 0.5 atoms per formula unit except for sample 20559 which contains 0.573 atoms.

As would be expected, since biotite is the dominant ferromagnesian phase in the batholith, other analysed elements in the biotites thought to substitute for Fe and Mg in octahedral sites show variation which can be correlated with changes in bulk composition. The relationships are exemplified in table 36 in which correlations between biotite composition and host rock composition are recorded in terms of correlations between biotite composition and SiO_2 content of the host rock (a suitable index of "acidity" of the host rock) and correlations between the abundances of each oxide or element in both biotite and host rock. FeO, MnO, Li_2O, Nb and Zn increase with increasing acidity of the host rock and MgO, V, Cr and Co decrease. MnO, V and Zn content of the biotites and their host rocks do not show high correlations but this is attributable to contrasts in the rate of change of the abundance of biotite (related to changes in total Fe + Mg of the host rocks) and the abundance of the particular trace element. For example, if an element, such as Mn, is accommodated almost entirely in biotite and decreases more slowly with increasing acidity than does the modal content of biotite then biotites of the most acid rocks must be enriched in this element. This type of behaviour emphasises the need to take into account all the chemical and related mineralogical variables in deducing the geochemical regularities or otherwise in rock series; mathematical correlations considered without reference to associated variables can be misleading.

Cu in the biotites has no significant correlation with acidity or Cu content of the host rocks. Since Cu is a strongly sulphophile element and rare pyrite is observed occasionally in the rocks, the apparently

Table 36 Correlation between composition of the biotites and composition of their host rocks

	Correlation between abundance of particular constituent in biotite and abundance of SiO_2 in the host rock	Correlation between abundance of particular constituent in biotite and abundance of the same constituent in the host rock
SiO_2	-0.74	-0.74
TiO_2	0.17	0.09
Al_2O_3	0.22	-0.24
Al(tet.)	0.27	
Al(oct.)	0.15	
Fe_2O_3	0.15	-0.28
FeO	0.81	-0.75
MnO	0.78	-0.44
MgO	-0.75	0.67
Na_2O	-0.60	-0.44
K_2O	-0.36	-0.27
Ba	0.05	0.21
Rb	0.72	0.95
Sr	-0.08	0.17
Pb	0.60	0.43
Nb	0.77	0.84
Y	0.37	0.87
V	-0.61	0.39
Cr	-0.72	0.73
Co	-0.80	
Ni	0.02	0.38
Cu	0.16	-0.24
Zn	0.48	-0.28
Ga	0.76	-0.31

20 degrees of freedom

$r_{90} = 0.360$

$r_{95} = 0.423$

$r_{99} = 0.537$

irregular distribution of Cu may be attributable to the existence of traces of copper sulphide minerals in some or all of the rocks.

Ga, the location of which is uncertain since it probably substitutes for Al and may be in either or both octahedral and tetrahedral sites, shows a significant correlation with increasing acidity of the host rock but an insignificant negative correlation with Ga abundance of the host rock. Appreciable amounts of Ga substitute in the coexisting feldspars and in muscovite.

Among the interlayer cations, K and Ba appear to show no significant variation with change in host rock composition. Rb and Pb show significant increases in abundance with increasing acidity and host rock content of these elements. Na shows a significant decrease with increasing acidity and Na content of the rocks. The role of the interlayer cations is to maintain electrical neutrality in the biotites and the total interlayer occupancy shows no significant variation with increasing acidity of the host rocks. Rb increases in the biotites with increasing acidity (and Rb content) of the host rocks, so the decrease in Na in the biotites may be compensation for increases in the more favourable Rb ion.

Layer charge relationships calculated in the manner described by Foster (1960), but using full cell formulae, are included in table 35 and it can be seen that charge balance has been maintained in the same fashion deduced by Foster (1960) for most biotites; trivalent and tetravalent substitutions in the octahedral layer are compensated partly by increased occupancy of tetrahedral sites by Al and partly by vacant

sites in the octahedral layer.

The biotites of the xenoliths appear similar to biotites of their enclosing host rocks and this similarity is exemplified by comparison between the biotite 20576, separated from a fine-grained discoid xenolith about 40 cm in maximum diameter, and biotite 20535 separated from Clear Range Granodiorite immediately adjacent to the xenolith. The xenolithic biotite is slightly poorer in Al, K, Rb Nb, Cr, Ga and richer in Na, Ba, and V than the biotite of the host granodiorite but the differences are small and the structural formula of the xenolithic biotite does not depart noticeably from that typical of the contaminated granites. A previous analysis of biotite from a quartz-feldspar-biotite xenolith in the Callemondah Granodiorite (Snelling,1960) also conforms closely with the compositions typical of the contaminated granites. This may be interpreted as additional support for the field and petrographic observations that reaction between xenoliths and the host granites has proceeded to an advanced stage and minerals in the xenoliths have approached equilibrium with those crystallising in the enclosing magma. The plagioclases of the xenoliths are an exception to this generalisation, but the persistence in the granites of relict basic cores of xenocrystal or early magmatic origin, commented upon by Snelling (1957, 1960) and indeed, the typical zoning of plagioclase in all igneous rocks, testify to the slowness with which plagioclase equilibrates with its surroundings.

An analysis of biotite from a hornblende-bearing xenolith in the Murrumbucka area presented by Snelling (1957, 1960) does not resemble the contaminated granite biotites at all closely, being notably poorer

in Al and Fe^{2+} and richer in Fe^{3+} and Mg.

Muscovites

Muscovite is present in the granodiorites and tonalites as well as in the leucogranites and analyses of muscovite from these contrasting hosts would be of interest. However, the presence of secondary muscovite renders dubious any separation of primary muscovite from the granodiorites. Only two muscovites, both from leucogranites essentially devoid of secondary muscovite, have been separated. Their analyses and structural formulae calculated on the basis of 22 oxygen atoms, water free are presented in table 37 . The analyses are very similar except that 20567 contains four times as much Mg as 20569. The host rock of 20567 contains twice as much Mg as the host of 20569 and biotite is the coexisting phase whereas the muscovite 20569 coexists with both biotite and garnet.

Nb and Ga are more abundant in both muscovites than in any of the other mineral phases analysed and the Rb contents are similar to the high contents of the coexisting biotites. The abundances of all other trace elements are low relative to the bulk rock composition.

The relationship between the pressure temperature stability curve of muscovite (Yoder & Eugster, 1955) and the minimum melting curve of granite (Tuttle & Bowen, 1958) indicates that muscovite can crystallise from a granitic liquid only at water vapour pressures in excess of about 1500 atmospheres and temperatures in excess of 700°C.

All of the Murrumbidgee rocks have high Al_2O_3 contents relative to alkalis and CaO, as evidenced by normative corundum in all samples (Appendix B) and it is this feature which is responsible for the rather

Table 37 Chemical analyses and structural formulae of muscovites from the Murrumbidgee Batholith

Westerly Muscovite Granite (20569)					Yaouk Leucogranite (20567)				
Analysis		Structural formula (22 O atoms, water free)			Analysis		Structural formula (22 O atoms, water free)		
SiO_2	45.77				SiO_2	46.09			
TiO_2	0.10				TiO_2	0.18			
Al_2O_3	34.05	Z	Si	6.147	Al_2O_3	32.65	Z	Si	6.205
Fe_2O_3	1.73		Al	1.853	Fe_2O_3	1.94		Al	1.795
FeO	2.54				FeO	2.20			
MnO	0.09		Al	3.536	MnO	0.13		Al	3.385
MgO	0.27		Ti^{3+}	0.010	MgO	1.18		Ti^{3+}	0.018
Na_2O	0.73		Fe^{3+}	0.175	Na_2O	0.69		Fe^{3+}	0.197
K_2O	10.35	Y	Fe^{2+}	0.285	K_2O	10.35	Y	Fe^{2+}	0.248
Rb_2O	0.16		Mn	0.010	Rb_2O	0.20		Mn	0.015
H_2O	(4.46)*		Mg	0.054	H_2O	(4.45)*		Mg	0.237
			Zn	0.001				Zn	0.001
Total	(100.25)				Total	(100.06)			
			Na	0.190				Na	0.180
Ba	<4		K	1.774	Ba	31	X	K	1.777
Rb	1454		Ba	0.000	Rb	1821		Ba	0.000
Sr	3		Rb	0.014	Sr	5		Rb	0.017
Pb	8				Pb	6			
Zr	13	Z		8.000	Zr	6	Z		8.000
Nb	106	Y		4.072	Nb	102	Y		4.100
Y	7	X		1.978	Y	13	X		1.975
La	<2				La	<2			
Ce	7				Ce	14			
Pr	3				Pr	4			
Nd	<5				Nd	<5			
V	3				V	17			
Cr	3				Cr	4			
Mn	655				Mn	954			
Co	<2				Co	<2			
Ni	4				Ni	5			
Cu	5				Cu	<1			
Zn	98				Zn	59			
Ga	102				Ga	84			

Oxides in per cent, elements in parts per million.

* Calculated from structural formula

unusual abundance of muscovite throughout the batholith, even in granodiorites and tonalites. In the case of the uncontaminated granites this excess of Al_2O_3 is sufficiently small to be able to be accommodated by substitution in the biotites but the potential formation of muscovite is evident by the common reaction rims, consisting of muscovite, ilmenite and magnetite, on biotites throughout the uncontaminated granites.

Probably these reaction rims represent expulsion of excess Al (which may be regarded as solid solution of muscovite in biotite) incorporated in the earlier formed crystals and released by ordering processes accompanying decreasing temperature conditions. Since, as discussed above, Ti and Fe^{3+} are present in the biotite in amounts approaching the maximum permissible occupancy, exsolution of muscovite would increase the abundance of Ti and Fe^{3+} above that which can be tolerated in the biotite structure leading to their expulsion as additional phases - ilmenite and magnetite. The reason for restriction of the alteration to the rims of the biotite grains is thought to lie in the general sluggishness of reactions within solid media compared with reactions at the interface between biotite and late hydrothermal fluids, which would also provide the additional H_2O required to form muscovite. The coarse texture of the uncontaminated granites indicates a slower cooling history than that of the contaminated granites in which similar reaction rims are not a conspicuous feature.

Hornblende

The chemical analysis and structural formula of hornblende separated from a tonalite variant of the Clear Range Granodiorite at Murrumbucka (sample 20563) is presented in table 38, along with data for hornblende from a xenolith collected in the same area (Snelling, 1960). The two analyses are similar and the hornblende of the tonalite may be derived by disintegration of hornblende-bearing xenoliths unique to this area of the batholith.

Garnet

Garnet is an accessory mineral in the fine-grained Westerly Muscovite Granite east of Bolairo Homestead, constituting 0.7 volume per cent of the rock from which garnet was separated for partial analysis. The mineral is a spessartine-rich almandine and results of the analysis are recorded in table 39. The garnet is disseminated throughout the rock and the textures suggest that the garnet represents a primary mineral phase.

Almandine-spessartine garnets are uncommon but not rare constituents of granitic rocks and their presence has been ascribed to argillaceous contamination (Brammall & Harwood, 1932; Deer et al., 1963a). No xenoliths, argillaceous or otherwise, have been observed in the Westerly Muscovite Granite but metasedimentary contamination is conspicuous in the associated contaminated granites.

Hsu (1968) examined selected phase relationships in the system Al-Mn-Fe-Si-O-H and presented models for garnet equilibria. He found that

Table 38 Chemical analyses and structural formulae of hornblendes from the Murrumbidgee Batholith

Clear Range Granodiorite (20563)					Xenolith from Clear Range Granodiorite (Snelling, 1960 Analysis 10, Table III)			
Analysis*		Structural formula (23 O atoms, water free)			Analysis*		Structural formula (23 O atoms, water free)	
SiO_2	47.39				SiO_2	48.12		
TiO_2	0.50				TiO_2	0.66		
Al_2O_3	8.51	Z	Si	6.936	Al_2O_3	7.79	Z Si	7.000
Fe_2O_3	4.21		Al	1.064	Fe_2O_3	3.46	Al	1.000
FeO	11.09				FeO	11.68		
MnO	0.40		Al	0.403	MnO	0.15	Al	0.335
MgO	12.16		Ti	0.055	MgO	12.73	Ti	0.072
CaO	11.92		Fe^{3+}	0.463	CaO	12.30	Fe^{3+}	0.379
Na_2O	0.81		Fe^{2+}	1.357	Na_2O	0.93	Fe^{2+}	1.420
K_2O	0.52	Y	Mn	0.050	K_2O	0.67	Y Mn	0.019
H_2O+			Mg	2.652	H_2O+	2.10	Mg	2.670
Total			V	0.008	Total	100.59		
			Cr	0.005				
Ba	< 4		Zn	0.003				
Rb	4							
Sr	15		Ca	1.869			Ca	1.913
Pb	7	X	Na	0.230			X Na	0.262
Zr	53		K	0.097			K	0.124
Nb	13							
Y	162	Z		8.000			Z	8.000
V	438	Y		4.996			Y	4.895
Cr	328	X		2.196			X	2.299
Co	49							
Ni	59							
Cu	1							
Zn	185							
Ga	17							

* Oxides in per cent, elements in parts per million

Table 39 Partial chemical analysis and structural formula of garnet from the Westerly Muscovite Granite (20569)

Analysis		Structural formula on the basis of 24 oxygen atoms		
SiO_2	35.52	Si	5.988	6.000
TiO_2	0.10	Al	0.012	
Al_2O_3	20.05	Al	3.972	4.204
Fe_2O_3	1.73	Fe^{3+}	0.219	
FeO	27.46	Ti	0.013	
MnO	11.99			
MgO	0.09	Mg	0.022	5.701
CaO	0.38	Fe^{2+}	3.872	
K_2O	0.12	Mn	1.712	
P_2O_5	0.06	Ca	0.069	
		K	0.026	
Total	97.50			

Molecular per cent end members

Almandine	68.2
Andradite	1.2
Pyrope	0.4
Spessartine	30.2

almandine stability is sensitive to oxygen fugacity but spessartine is essentially independent of oxygen fugacity. The pressure-temperature stability fields of the two garnets overlap those of granitic magmas but the high oxygen fugacities generally associated with increasing SiO_2 content of magmas severely restrict the overlap for pure almandine. However, the stability field of spessartine is much broader, considerably overlapping that of felsic magmas, so that spessartine-almandine solid solutions are stable in granitic magmas even at high oxygen fugacities.

In view of the lack of physical restriction to inhibit the crystallisation of spessartine in granites, Hsu (1968) concluded that the controlling factor must be the abundance of Mn. The influence of Mn on the formation of almandine-rich garnets in metamorphic rocks was suggested by Tilley as long ago as 1926 and stressed also by Brammall & Harwood (1926) in connexion with the garnets of the Dartmoor granites.

The Westerly Muscovite Granite sample 20569 is richer in Mn than any of the uncontaminated granites or leucogranites except the leucogranite sample 20573 which is richer in Mn than any analysed granite from the batholith. It is significant that this sample also contains accessory garnet, although its abundance is much less than that of the Westerly Muscovite Granite sample. The Mn content of these two samples is very high in relation to Fe and Mg which determine the biotite content of the rocks. It seems that the Mn abundance has exceeded that which can be accommodated by substitution in the biotite thereby necessitating the formation of an additional Mn-rich phase. This implies that the Mn content of 0.099 atoms per formula unit in biotite from sample 20569

must be close to the maximum permissible substitution of this element in biotites of this composition. However, Mn is richer in two other leucogranite biotites not coexisting with garnet and, although all the leucogranite biotites are much richer in Mn than the biotites of the other granites, it is doubtful whether an upper limit of Mn occupancy can be predicted without taking into account mutual effects of Fe, Mg and Al variations on the octahedral layer (see earlier discussion regarding octahedral Al in biotites).

Partition coefficients

Various workers have shown that the partition of trace elements between coexisting minerals is a tool which can be applied to geological thermometry, barometry and assessment of equilibrum (McIntyre, 1963).

The simplest distribution constant is defined according to the Berthelot-Nernst distribution law as $k = \frac{C_A}{C_B}$, where C_A is the concentration of a particular trace element in mineral phase A and C_B is the concentration of the same element in a coexisting mineral phase B. The distribution constant k depends only on temperature and pressure provided:

1. equilibrium is maintained between the coexisting phases.
2. the concentration of the trace element is small (i.e. the coexisting minerals may be considered as dilute solid solutions).
3. the presence of the trace is due to solid solution formation (not surface absorption nor occlusion).

A more convenient form of the distribution law, applicable in cases

involving the substitution of a trace element for a particular lattice element in both mineral phases is given by the expression

Partition coefficient $D = \frac{(Tr/Cr)A}{(Tr/Cr)B}$, where $(Tr/Cr)A$ is the ratio of trace to carrier element in mineral phase A and $(Tr/Cr)B$ is the ratio in mineral phase B (McIntyre, 1963). This partition coefficient D depends only on pressure, temperature and the composition of the solid phases. It is not applicable in cases where the trace element substitutes for a certain major element in one of the coexisting pair of minerals but for a different major element in the second mineral. In such cases the distribution constant k can be used, subject to the previously stated conditions.

Partition coefficients are independent of the presence of other trace elements but are influenced by major changes in the composition of either coexisting phase. If the major components of the minerals form an ideal mixture then relationships are somewhat simplified and the effect of major compositional changes on the partition coefficient can be predicted. Where major compositional changes occur in only one of a pair of coexisting minerals and are the result of ideal solution of two macro-components, the problem can be treated in terms of two end member partition coefficients and it can be shown that the log of the partition coefficients is linearly related to the mole fraction of an end member of the macro-variable phase. Cases of coexisting phases each consisting of solid solutions of macrocomponents become increasingly complicated even when the solid solutions can be considered ideal.

Under most circumstances the substitution of an ion of different

valency from the lattice ion can be expected to require any or all of the following circumstances in order to maintain charge balance:

1. substitution of another element elsewhere in the lattice.
2. addition of another trace element interstitially.
3. development of lattice vacancies.

These requirements place such constraints on the partition theory that they may be too difficult to treat in terms of the simple Berthelot-Nernst distribution law.

To summarise the forgoing, partition coefficients can contribute information on the following points:

1. the state of equilibrium between coexisting mineral phases.

   Coexisting mineral phases of restricted macrocomposition and considered to have formed under restricted pressure and temperature conditions should possess constant partition coefficients for those trace elements fulfilling the conditions required by the Berthelot-Nernst distribution law. Departure from constancy implies either disequilibrium between the coexisting mineral phases at the time of their formation, subsequent chemical redistribution, or failure to satisfy some basic assumption of the distribution law.

2. temperature and pressure

   Experimentally determined partition coefficients are rare for coexisting mineral phases so estimation of absolute temperatures and pressures is generally not possible. However, constancy of partition coefficients implies severely restricted temperature

and pressure variation whereas geographically gradational changes in distribution coefficients or abrupt variation with change in lithology would imply variation in the temperature or pressure at the time of establishment of the distributions.

Distribution of elements between potassium feldspar and plagioclase

The simple Berthelot-Nernst distribution constant k is appropriate for assessing the distribution of Ba, Sr, Rb, Y and Pb in the feldspars, although the substitution of divalent Ba, Sr and Pb and trivalent Y for univalent ions in potassium feldspars and either univalent or divalent ions in plagioclase imposes additional and uncertain restrictions on the distribution law. The values of k for the five elements in 16 coexisting pairs of potassium feldspar and plagioclase are recorded in table 40.

The Ba distribution coefficients are variable but strongly favour potassium feldspar. In view of the strong enrichment of Ba in the potassium feldspars, even small amounts of potassium feldspar contaminating the plagioclase concentrates would produce large variations in the calculated distribution coefficients, so no particular significance is attributed to the variation in values.

The Sr distribution coefficient is fairly constant in the contaminated and uncontaminated granite feldspars, with an average of 0.35 and a range from 0.241 to 0.456, but the distribution is substantially different in the leucogranites, with a range of 0.5 to 1.4, two of the 4 pairs showing a slight enrichment of Sr in potassium feldspars over that in the plagioclase.

Table 40 Partition coefficients
(continued on next page)

	Ba_{Kf}/Ba_{Pl}	Sr_{Kf}/Sr_{Pl}	Rb_{Kf}/Rb_{Pl}	Y_{Kf}/Y_{Pl}	Pb_{Kf}/Pb_{Pl}	$\frac{(Ga/Al)_{Kf}}{(Ga/Al)_{Pl}}$
Contaminated granites						
20559	5.523	0.328	5.468	0.529	0.541	0.432
20535	4.127	0.381	9.933		0.756	0.412
20541	18.067	0.441	8.993		0.788	0.549
20551	13.274	0.376	3.679	0.250	0.837	0.425
Uncontaminated granites						
20502	18.708	0.364	24.850		0.667	0.611
20507	61.360	0.399	19.385	0.078	0.667	0.596
20510	24.831	0.313	6.819		0.810	0.568
20511	10.141	0.336	7.569		0.600	0.594
20513	22.945	0.284	9.936		0.625	0.703
20515	43.267	0.456	11.895		0.630	0.711
20521	13.695	0.290	13.951		0.600	0.662
20528	15.626	0.241	8.216		0.531	0.571
Leucogranites						
20569		1.373	3.708		0.483	0.959
20567		1.136	7.256		0.833	0.687
20571		0.970	2.622	0.125	0.622	0.802
20574	0.242	0.404	5.217	0.121	0.596	0.784

Table 40 Partition coefficients
(continued from previous page)

	$\frac{(Ba/K)_{Kf}}{(Ba/K)_{Bi}}$	$\frac{(Sr/K)_{Kf}}{(Sr/K)_{Bi}}$	$\frac{(Rb/K)_{Kf}}{(Rb/K)_{Bi}}$	$\frac{(Pb/K)_{Kf}}{(Pb/K)_{Bi}}$	$\frac{(Ga/Al)_{Kf}}{(Ga/Al)_{Bi}}$
Contaminated granites					
20559	0.261	13.648	0.591	2.291	0.193
20535	0.520	26.700	0.297	4.402	0.218
20541	0.361	9.648	0.367	3.408	0.245
20551	0.478	17.860	0.257	2.123	0.225
Uncontaminated granites					
20502	0.268	12.379	0.371	1.674	0.239
20507	0.327	14.281	0.351	1.154	0.251
20510	0.334	6.098	0.343	1.069	0.220
20511	0.261	10.500	0.567	0.717	0.257
20513	0.264	7.021	0.476	1.082	0.282
20515	0.307	8.984	0.344	1.015	0.263
20521	0.196	7.138	0.692	0.583	0.398
20528	0.336	10.370	0.359	1.790	0.241
Leucogranites					
20569		1.029	0.263	0.092	0.358
20567	1.007	5.698	0.405	0.402	0.196
20571	0.094	5.195	0.276	0.980	0.300

	$(Ga/Al)_{Pl}/(Ga/Al)_{Bi}$
Contaminated granites	
20559	0.447
20562	0.521
20563	0.593
20535	0.528
20541	0.446
20576	0.627
20543	0.544
20546	0.600
20551	0.833
20555	0.592

	$(Ga/Al)_{Pl}/(Ga/Al)_{Bi}$
Uncontaminated granites	
20502	0.392
20507	0.421
20510	0.388
20511	0.434
20513	0.402
20515	0.369
20521	0.601
20528	0.421
Leucogranites	
20569	0.374
20567	0.285
20571	0.374

Enrichment of Sr in plagioclase relative to coexisting potassium feldspar is recorded in other granitic rocks (Sen et al., 1959; Chappell, 1966; Rhodes, 1969b) but feldspars from igneous and metamorphic rocks of Langøy (Heier, 1960) show enrichment of Sr in potassium feldspar relative to coexisting plagioclase.

Although the distribution coefficients of Rb between the feldspars all show marked enrichment of Rb in the potassium feldspars, actual values of the coefficient are variable, probably mainly because of contamination of some or all of the plagioclase concentrates by Rb-rich microcline. The highest distribution constant is 24.9 for sample 20502, the plagioclase of which contains the lowest orthoclase content (4.13 per cent) of any of the analysed plagioclases coexisting with potassium feldspar.

Y is below detection in 11 of the potassium feldspars but its abundance in the coexisting plagioclases ranges from 7 to 178 parts per million. The five pairs for which distribution coefficients can be calculated, range in k from 0.078 to 0.529 and are inadequate for recognition of any regular pattern.

The distribution coefficients of Pb are fairly constant for all the feldspar pairs, averaging 0.65 and ranging from 0.5 to 0.8. This distribution is opposite to that found by Doe & Tilling (1967) in 12 feldspar pairs from plutonic, volcanic and metamorphic environments. The distribution constants determined by these authors were commonly within 10 per cent of 2.4 and no example was found where Pb is enriched in plagioclase relative to potassium feldspar. However, data presented

by Howie (1955) and Heier (1960) suggested that plagioclase is the more favourable host of Pb and give similar values of the distribution coefficient to those found in the Murrumbidgee rocks. The constancy of the distribution coefficients determined by Doe & Tilling (1967) in widely differing environments was interpreted as implying that either the Pb distribution is not temperature dependent, that all the feldspar pairs formed at nearly the same temperature, or that Pb in minerals exchanges rapidly with their surroundings upon cooling to some minimum temperature, and similar interpretations are necessary to explain the constancy of the Murrumbidgee data.

Ga substitutes for Al in both feldspars so the partition coefficient $D = \frac{(Ga/Al)Kf}{(Ga/Al)Pl}$ is appropriate for studying its distribution. There is a regular variation in the partition coefficient, values ranging from 0.4 to 0.5 in the contaminated granites, from 0.6 to 0.7 in the uncontaminated granites and 0.7 to nearly 1.0 in the leucogranites. Other studies (Heier, 1960; Sen et al., 1959; Rhodes, 1969b) also show an enrichment of Ga in plagioclase relative to coexisting potassium feldspar.

Distribution of elements between potassium feldspar and biotite

The partition coefficient D defined above is appropriate for discussing the distributions of Ba, Sr, Rb and Pb which substitute for K in both minerals, and the distribution of Ga which substitutes for Al.

The partition coefficient for Ba ranges from 0.3 to 0.5 in the contaminated granites and from 0.2 to 0.3 in the uncontaminated granites, strongly favouring biotite in both cases. Values for the three

leucogranite biotites differ widely from each other and from those of the other biotites; two coefficients exceed a value of one.

The Sr distribution favours potassium feldspar over biotite in all the granites and the partition coefficient decreases from the contaminated granites (range 10 to 27) through the uncontaminated granites (range 6 to 14) to a minimum in the leucogranites (range 1 to 6).

Rb is enriched in biotite and no regular variation of the partition coefficient is apparent, the overall range being 0.3 to 0.6.

Pb partition coefficients vary regularly with rock type, ranging from 2.1 to 4.4 in the contaminated granites, from 0.6 to 1.8 in the uncontaminated granites and from 0.1 to 1.0 in the leucogranites.

Ga is enriched in biotite relative to potassium feldspar. The partition coefficient ranges from 0.2 to 0.4 and does not appear to be related to rock type.

Distribution of Ga between plagioclase and biotite

Ga substitutes for Al in both mineral phases and although the partition coefficient D indicates relative enrichment of Ga in biotite, there are regular variations in the partition coefficient which can be correlated with the nature of the host rock. D ranges from 0.4 to 0.8 in the contaminated granites, 0.4 to 0.6 in the uncontaminated granites and 0.3 to 0.4 in the leucogranites.

Significance of the partition coefficients

The regular patterns of partition coefficients deduced for a number of trace elements are interpreted as indicating a close approach to

equilibrium within the rocks.

The constancy of partition coefficients of some elements in some mineral pairs, for example Pb between the feldspars and Ga between potassium feldspars and biotite, independent of the nature of the host rocks indicates either that the distribution of these elements is not greatly temperature dependent, that the temperatures of crystallisation of the mineral pairs in the various rock types did not differ significantly, or that these mineral pairs have exchanged efficiently with each other in the solid state during cooling until some constant limiting temperature was attained.

On the other hand, regular changes of partition coefficients of other elements correlated with differences in the nature of the host rocks are reasonable evidence for a difference in temperature and/or pressure conditions at which the minerals equilibrated in the different rock types. Ga distribution between microcline and plagioclase and between plagioclase and biotite and Sr and Pb distributions between potassium feldspars and biotite vary regularly from one granite type to another. The Ga partition coefficient between microcline and plagioclase increases from the contaminated granites through the uncontaminated granites to a maximum in the leucogranites. The Ga partition coefficient between plagioclase and biotite and the Sr and Pb coefficients between microcline and biotite behave conversely. In view of the intimate association of these three rock types, appreciable pressure differences are considered unlikely and the variation of the partition coefficient is most probably attributable to temperature variation. In any case,

temperature exercises a far greater influence on distribution coefficients than pressure (McIntyre, 1963). The field relationships, textures and composition of the leucogranites are such that they may be considered to have crystallised at lower temperatures than the more calcic and mafic uncontaminated and contaminated granites. Therefore, the lowest temperatures of crystallisation appear to be associated with high Ga partition coefficients between potassium feldspar and plagioclase, low Sr and Pb partition coefficients between potassium feldspars and biotite, and low Ga partition coefficients between plagioclase and biotite. The corollary of this is the implication that the contaminated granites, which have the lowest partition coefficients of Ga between potassium feldspar and plagioclase, the highest of Sr and Pb between potassium feldspar and biotites, and the highest of Ga between plagioclase and biotite, equilibrated at higher temperatures than either the uncontaminated granites or the leucogranites.

However, the distribution coefficients of Sr between potassium feldspar and plagioclase show a large difference between the leucogranites and the other two granite groups, but no discernible difference between the contaminated and uncontaminated granites. This may indicate that any temperature difference between the latter granite groups at the time of equilibration of the mineral phases was much less than the difference between either of these groups and the leucogranites.

7. PETROGENESIS

In this section the most significant features of the batholith are summarised and the probable origins of the rocks are discussed:-

1. Magmatic features

There are abrupt contacts between granites and country rock. There is a lack of associated high grade regional metamorphism, but a development of limited contact metamorphism immediately adjacent to granite contacts. Indisputable dilational dyke features are characteristic of many aplitic granites on outcrop scale. There is textural evidence of marginal chilling in several localities, the most notable of which is the margin of the Bolairo Granodiorite near "Greenbank" Homestead where a chilled porphyritic texture is developed and the quartz phenocrysts have features indicating that they originally crystallised as β-quartz. All of these features are interpreted as evidence of a magmatic origin of the rocks and no further consideration will be given to metasomatic formation of the granites in situ.

2. Natural three-fold division of the rocks tempered by common features

The most conspicuous feature of the batholith is a natural three-fold division into granite groups, which have been designated contaminated granites, uncontaminated granites and leucogranites. Although the three groups are sufficiently distinct to allow positive classification of any granite from the batholith into one of the three groups on any one of a number of macroscopic, chemical or mineralogical criteria, even in an isolated hand specimen, the three types are intimately associated in the field and there is no evidence to indicate

that any large time differences separate their emplacement.

Some mineralogical and chemical features are shared by all the granites. All are rich in quartz and consist of quartz, plagioclase, biotite and generally microcline and muscovite. Hornblende, common in many granitic rocks elsewhere is a minor constituent of only one local area of the batholith. All the rocks are characterised by a notable excess of Al over that required to form feldspars. This is apparent as ubiquitous corundum in calculated CIPW norms and is accommodated in the actual granites by a high degree of Al substitution in biotites in all the rocks and by formation of muscovite in many rocks, including tonalites and granodiorites as well as more acid granites.

The close temporal and spatial association of the three groups coupled with the shared features of chemistry and mineralogy suggest that the rocks may be petrogenetically related despite their present modal, chemical and textural differences.

3. Textures

The contaminated granites have a well developed foliation which is recognised as partly primary, on the basis of aligned xenoliths, and partly secondary, on the basis of conspicuous strain phenomena. This is interpreted as indicating final emplacement of the contaminated granites in a largely or wholly solid state, an interpretation consistent with the very limited metamorphic effects associated with the intrusions.

The coarse, fairly massive texture of much of the uncontaminated granite contrasts sharply with the finer grained, conspicuously foliated texture of the contaminated granites and indicates more passive

emplacement and a more prolonged period of crystallisation. Although contact metamorphic effects are also very limited, metasomatic reactions with limestones adjacent to the northeastern margin of the Shannons Flat Adamellite have produced one fairly large and several small skarns. Foliation is a conspicuous feature in the uncontaminated granites on the eastern and western margins of the batholith where it is at least largely secondary and probably formed in response to post-emplacement movement on the Cotter and Murrumbidgee faults.

Textures of the leucogranites vary from medium-grained porphyritic to aplitic, indicating that crystallisation occurred fairly rapidly due either to cooling or loss of pressure. Foliation is inconspicuous except in the coarsest leucogranite (the Yaouk Leucogranite) in which a secondary foliation is developed, probably related to post-emplacement shearing associated with the Cotter Fault. Shearing is not conspicuous in the aplitic Westerly Muscovite Granite which lies between the Yaouk Leucogranite and the Cotter Fault but this may be a result of the higher resistance of the aplitic texture to shearing stresses. In short, the textures of the leucogranites are consistent with emplacement as liquids which quenched fairly rapidly, with the exception of the Yaouk Leucogranite, the coarse grainsize of which indicates more prolonged crystallisation.

4. Presence of xenoliths

Xenoliths are very abundant in the contaminated granites, ranging in size from single xenocrysts to a usual maximum dimension of about 40 cm, although rare larger xenoliths are encountered. There are a few

xenoliths in the uncontaminated granites but none have been recognised in the leucogranites.

Any proposed origin of the rocks must explain the abundance of xenoliths in the contaminated granites and their virtual exclusion from the other two granite groups.

5. Composition of the xenoliths

Most of the xenoliths are poor in SiO_2 and rich in mafic and aluminous constituents compared with the granites of the batholith and these features are shared by their host rocks (the contaminated granites) in comparison with the uncontaminated granites and leucogranites. Coupled with the rounded, corroded nature of the xenoliths, the existence of microxenoliths, xenocrysts and "ghost" xenoliths and the extent to which the mineral phases in the xenoliths appear to have been made over to phases in equilibrium with those existing in the host rocks,this suggests that the present composition of the contaminated granites is a result of modification of a more acid magma by incorporation of xenolithic material.

The coincidence of more calcic and mafic-rich, hornblende-bearing phases of the Clear Range Granodiorite with an abundance of amphibolite xenoliths at Murrumbucka is further evidence of a close link between xenolithic composition and host rock composition.

The compositions of the xenoliths indicate that most are of sedimentary origin (psammites and pelites) but some may be derived from basic or ultrabasic igneous rocks.

6. Average compositions and variances of the contaminated granites

With the exception of the Clear Range Granodiorite, the contaminated granites have similar average compositions and similar variances, implying that they originated from a common source, since it is unlikely that magmas originating separately would assimilate similar amounts of similar xenoliths and react with them to similar extent.

The Clear Range Granodiorite, the largest body of contaminated granite, is more variable, though similar to the other contaminated granites in average composition. It contains more basic phases in its southern extremity and these are associated with and,by implication, caused by assimilated amphibolite xenoliths. These xenoliths presumably result from lithological variation in the rocks which are the source of the more typical quartz-rich metasedimentary xenoliths since they are associated with the more typical xenoliths and show a similar extent of reaction with their enclosing hosts.

7. Field association of the leucogranites with the uncontaminated granites

Most of the leucogranites show a close spatial association with the uncontaminated granites. The Shannons Flat Adamellite contains numerous bosses, dilational dykes and irregularly shaped "pockets" of aplitic and porphyritic leucogranites, indicating a genetic link. The only leucogranites occurring within the contaminated granites are occasional aplite veins.

8. Patterns of chemical variation

Variation patterns for the two main granite groups are different,

as evidenced by the variance data, factor analysis and the variation diagrams. However, the frequency with which the separate variation trends for the two groups intersect at about 73.9 per cent SiO_2 on Harker diagrams suggests that there may be a common rock composition from which the two groups diverge by different processes, thereby giving rise to different styles of variation. Several samples of uncontaminated granites have compositions closely similar to the hypothetical common member but no recognised member of the contaminated granites is sufficiently acid to approach its composition closely.

Field and microscopic observations point to assimilation of xenoliths as the factor probably responsible for variation in the contaminated granites. The chemistry of the most abundant xenoliths is such that combining their compositions with acid magma similar to the hypothetical common member of the main granite groups would give compositions varying in a similar general fashion to those recorded in the contaminated granites.

However, the xenoliths vary appreciably in composition, being derived apparently from a variety of psammitic and pelitic sedimentary rock types and to a much lesser degree, basic or ultrabasic igneous rocks. Addition of varying amounts of any single xenolith composition is inadequate to explain all the variance of the rocks. Nor is the situation improved by postulating addition of varying amounts of some constant mixture of xenolith compositions (or the compositions of their inferred source rocks) since the small amount of variance explained by the calculated linear regression equations for the contaminated granites

implies that the variation cannot be ascribed to simple mixing of varying proportions of two end member compositions, as would be required to fit an hypothesis of contamination of a unique acid melt by varying amounts of unique contaminant. Variation of other granite groups ascribed to formation by simple hybrid processes involving two unique (or at least restricted) end members (Chappell, 1966; Rhodes, 1969b; Bailey, 1969) possess variation patterns which fit linear regressions much more closely than do the contaminated granites.

Similarities between the variation diagrams and a hypothetical model proposed in figure 21 for mixing several relatively SiO_2-poor contaminants with a single SiO_2-rich end member, suggests that the variation of the contaminated granites is more correctly described in terms of variation fields rather than in terms of unique trends, and may be explained by mixing an acid melt of fairly restricted composition (such as the hypothetical common member) with various sedimentary and basic igneous rock types which are mainly poorer in Si and K and richer in Fe, Mg and Al than the resultant contaminated granites.

The regression trends for the uncontaminated granites explain even less of the observed variance. It has been stressed that the field evidence points to a genetic link between the leucogranites and the uncontaminated granites. The field relationships, the composition of the leucogranites in relation to the "ternary" minima of the Ab-Or-SiO_2-H_2O system(Tuttle & Bowen, 1958) and the pattern of Rb enrichment relative to K in the leucogranites, collectively suggest derivation of the leucogranites by fractionation of the uncontaminated

granites. On similar evidence Kolbe & Taylor (1966) concluded that comparable leucogranites occurring throughout the Snowy Mountains region also originated by fractionation of associated granitic magmas.

In view of the suggestion that a magma containing about 73.9 per cent SiO_2, and shared by the uncontaminated granites, might be the acid "parent" of the contaminated granites, it is constructive to consider whether this composition might also be the initial magma from which the uncontaminated granites (SiO_2 generally less than 73.9 per cent) and leucogranites (SiO_2 greater than 73.9 per cent) evolved. The area of outcrop of the uncontaminated granites is about 700km^2 and that of the leucogranites is about 205km^2. On the bold assumption that these areas may be equated approximately with original volume relationships of the rocks, and that the arithmetic mean of the uncontaminated granite analyses (which are fairly well distributed areally) approximates to the overall composition of the uncontaminated granites, the composition of a leucogranite fraction required to produce these present volume relationships by fractionation from the hypothetical magma of 73.9 per cent SiO_2 to leave a crystalline residue with a bulk composition equivalent to that calculated for the uncontaminated granites has been calculated (table 41). The results indicate that either the hypothetical magma is too acid or that much larger volumes of acid differentiate are formed than are indicated by present outcrop areas. However, one rock which is similar to the hypothetical parent and is known to have been entirely liquid immediately prior to rapid crystallisation has been analysed. This is sample 20570 from a narrow

Table 41 Theoretical leucogranite compositions (see text for explanation)

Average uncontaminated granite		Parental magma estimated from variation diagrams	Calculated leucogranite fraction	Composition of quenched dyke specimen 20570	Calculated leucogranite fraction
SiO_2	72.34	73.9	79.22	72.73	74.06
TiO_2	0.36	0.39	0.49	0.50	0.98
Al_2O_3	13.86	13.69	13.11	13.70	13.15
Fe_2O_3	0.59	0.35	-	0.46	0.02
FeO	1.90	1.98	2.25	2.24	3.40
MnO	0.04	0.05	0.08	0.05	0.08
MgO	0.85	0.70	0.19	0.82	0.72
CaO	2.40	1.38	-	2.08	0.99
Na_2O	2.66	2.75	3.06	2.70	2.84
K_2O	4.26	4.11	3.60	4.36	4.70
P_2O_5	0.09	0.11	0.18	0.12	0.22
Ba	586	525	317	590	604
Rb	207	170	44	229	304
Sr	150	127	48	133	75
Pb	28	31	41	28	28
Th	21	19	12	22	25
U	4	4	4	5	8
Zr	149	149	149	210	418
Nb	20	19	16	20	20
Y	46	43	33	38	11
La	26	24	17	30	44
Ce	67	64	54	74	98
Pr	8	8	8	9	12
Nd	23	19	5	29	50
V	44	34	-	52	79
Cr	17	10	-	16	13
Mn	331	404	653	330	327
Ni	11	12	15	2	-
Cu	2	7	24	5	15
Zn	36	53	111	49	93
Ga	15	15	15	15	15

Oxides in per cent, elements in parts per million

fine-grained adamellite dyke exposed in a road cutting in Honeysuckle Valley. Calculations repeated using the same volume relationships but substituting this natural liquid composition for the hypothetical composition, give a leucogranite fraction (table 41) which corresponds quite well with natural leucogranites analysed from the batholith. In view of the numerous assumptions required for the calculation, and the lack of a satisfactory estimate of the bulk composition of the total leucogranite fraction, close comparison is unwarranted. However, the exercise serves to demonstrate semiquantitatively that fractionation of a granite liquid with a composition close to that suggested as a parental liquid of the contaminated granites and similar to a natural liquid indentified in the batholith (sample 20570) could produce leucogranite liquids in similar abundance and with similar composition to the observed leucogranites.

9. Distribution coefficients

Regular patterns of some of the distribution coefficients of trace elements between coexisting pairs of minerals related to their occurrence in the three granite groups were interpreted as indicating a decreasing temperature sequence from the contaminated granites, through the uncontaminated granites to the leucogranites. However, the difference in temperature between the contaminated granites and uncontaminated granites was inferred to be less than that between the leucogranites and the other granites.

The inferred higher temperature of the contaminated granites compared with the uncontaminated granites may, at first appearance, seem

at variance with their proposed derivation by contamination of probably the same magma crystallising to form the uncontaminated granites and the leucogranites. However, the diffusion of Fe, Mg and Ca from the xenoliths into contaminated granite magma and the loss of alkalis from the magma to the xenoliths would raise the solidus of the magma appreciably, causing it to solidify at higher temperatures than uncontaminated magma. The difference in temperature at which the minerals equilibrated may also be affected by contrasting cooling histories of the two main granite types. The contaminated granites have textures indicating emplacement as almost solid bodies and their textures are consistent with fairly rapid crystallisation, whereas the uncontaminated granites have textures indicating a slow cooling history which would be more conducive to equilibration of the mineral phases at temperatures even below the liquidus - an annealing process. The likely reason for a difference in cooling rates is the effect of endothermic reactions associated with assimilation of xenolithic minerals superimposed on natural conduction losses, in the contaminated granites, in contrast to simply exothermic reactions associated with crystallisation to offset conduction losses in the uncontaminated granites.

10. Significance of muscovite

The contaminated granites and the leucogranites contain muscovite and this has two implications; firstly that there is an excess of Al in the rocks over that required to combine with Na, K and Ca to form feldspars and, secondly, that the water vapour pressure has been high

during crystallisation if the muscovite precipitated from granitic magma, as its texture, at least in the leucogranites, would imply. The relationship between the pressure-temperature stability curve of muscovite (Yoder & Eugster, 1955) and the minimum melting curve of granite (Tuttle & Bowen, 1958) suggest that the muscovite could crystallise from granitic magmas only at water pressures in excess of 1500 atmospheres and temperatures in excess of about 700°C, although it could form by metasomatic or metamorphic reactions below these limits.

11. Significance of the leucogranites in relation to synthetic granite systems

The normative quartz, albite and orthoclase proportions of the leucogranites lie close to the "ternary" minima for low water vapour pressures in the system $NaAlSi_3O_8$-$KAlSi_3O_8$-SiO_2-H_2O (Tuttle & Bowen, 1958), in contradiction to the water vapour pressures inferred by the existence of muscovite. The composition of the proposed parental magma of the granites (taking the composition of the natural liquid represented by the dyke specimen 20570 as a reasonable approximation) plots in the quartz field of the system, near the "ternary" minima for low water vapour pressures.

However, contributions by Kleeman (1965) and von Platen (1965) indicate that additions of even small amounts of anorthite have a marked effect on the location of the phase boundaries and the "ternary" minima. The effect of anorthite is to displace the minima towards the SiO_2-$KAlSi_3O_8$ join, so the position of the Murrumbidgee granites in the Ca-free granite system could be seriously influenced by Ca, especially

the uncontaminated granites and the proposed parental magma which contain about 2 per cent CaO. Comparison with diagrams presented by von Platen (1965) suggest that Ca-rich compositions plotting near the "ternary" minima for low water vapour pressures could be clustering near projected minima for high water vapour pressures displaced by the effect of anorthite components towards the SiO_2-$KAlSi_3O_8$ join.

Kleeman (1965) published tentative phase diagrams for the SiO_2-saturated surface of the Or-Ab-An-SiO_2-H_2O system based on limited experimental data. This system is more relevant to natural granites than the Ab-Or-Qz-H_2O system since most granites contain significant proportions of normative anorthite. Figure29 shows the proposed parental magma and the leucogranites (including four previously published analyses) plotted on Kleeman's (1965) diagram. The proposed parental magma plots well clear of the low temperature trough, in the plagioclase field, but the leucogranites plot in the trough delineated for water pressures between 10,000 and 1000 bars, except two samples of Westerly Muscovite Granite and a dyke sample (20574) which plot on the orthoclase side of the 1000 bars cotectic; however, all three samples plot near the trough within the limits of analytical uncertainty suggested by Kleeman (1965). The leucogranites scatter across the lowest water vapour pressure area of the cotectic region of the diagram but mainly concentrate close to the 1000 bar cotectic. Provided the postulated positions of the cotectics are reasonably accurate, this supports the hypothesis of low water vapour pressures involved during fractionation of the leucogranites inferred from the Ab-Or-SiO_2-H_2O

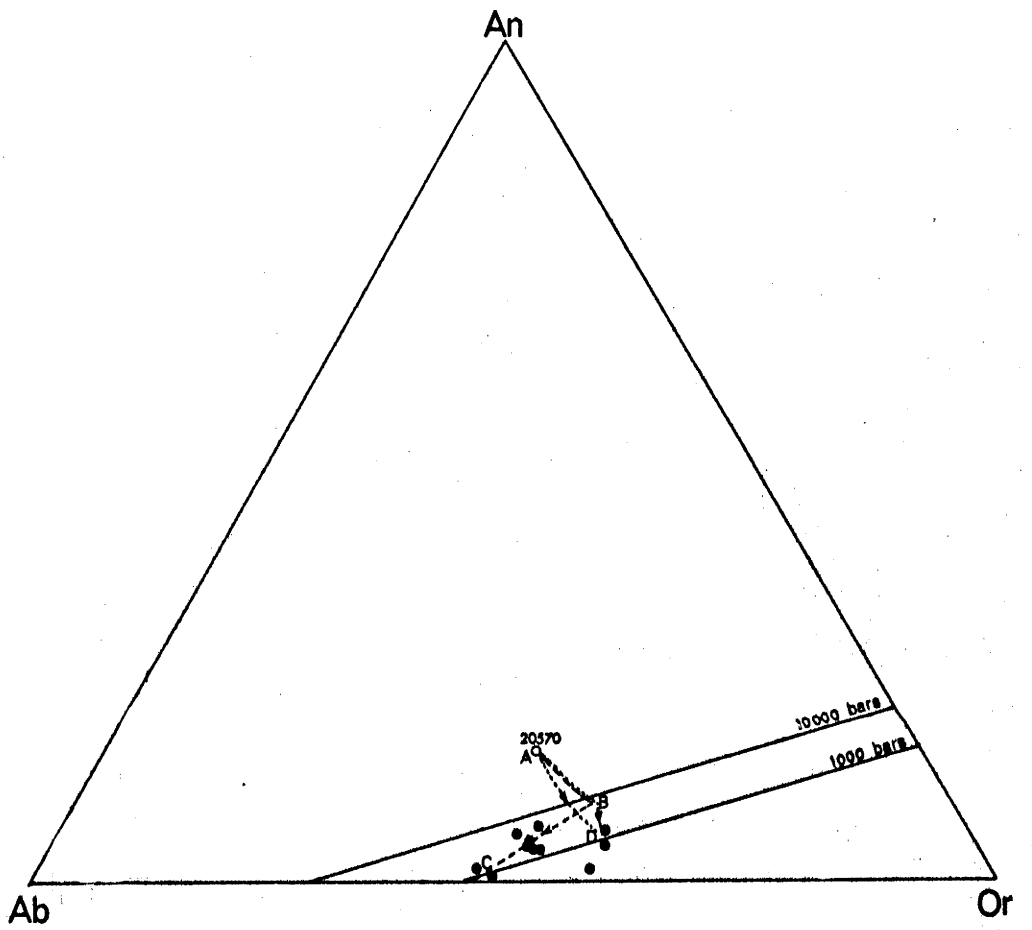

Figure 29. Normative composition of Murrumbidgee leucogranites and proposed parental magma projected onto the plane Or-Ab-An in the system Or-Ab-An-SiO_2-H_2O (Kleeman, 1965)

system. The implication of this is that either the minimum water vapour pressure required for muscovite to crystallise from granitic magmas has been wrongly assessed or that the muscovite has crystallised under conditions of higher water vapour pressure than those prevailing during final crystallisation, surviving as a metastable phase during decreasing temperature and/or water vapour pressure.

The distribution of the leucogranites in the low temperature trough of the Or-Ab-An diagram (figure 29) suggests that loss of water vapour pressure, and consequent raising of the solidus may have been a factor in the fractionation of the parental magma to produce the leucogranites. With the exception of two dyke specimens (20572 and 20574) the leucogranites plot in a band which crosses the low temperature trough diagonally and an inferred general path of fractionated liquids is shown on figure29 as ABC. If fractionation occurred at fairly constant water vapour pressures a pattern of liquids within the low temperature trough roughly parallel to the limits of the trough might be anticipated; that is, a pattern of liquids falling along a cotectic curve for a specific water vapour pressure. A diagonal path such as ABC implies decreasing water vapour pressure simultaneously with decreasing temperature.

Samples 20572 (a narrow aplite dyke) and 20574 (a porphyritic dyke) straddle the 1000 bars cotectic in such a position relative to the parental magma that little or no movement of liquids down a cotectic curve could be involved in their fractionation and paths such as AD or ABD (figure 29) are inferred for the progressive liquid compositions.

A path such as AD could result from decreasing temperature with low prevailing water pressure whereas a path such as ABD infers decreasing temperature and rapidly decreasing pressure.

The position of the proposed parental magma in the diagram indicates that it is not a "minimum temperature" granite melt and it is enriched in plagioclase components relative to lowest temperature granitic liquids. The other granites of the batholith are not plotted in the diagram since their proposed origins render it unlikely that any of them can be safely regarded as actual liquid compositions. The field in which the uncontaminated granites would lie, if they were shown, overlaps the position of the proposed parental magma and extends towards the anorthite-rich end of the Ab-An join, a field compatible with the proposal that they are the solid residue of fractionated parental magma.

12. Source of the proposed parental magma

The abundance of metasedimentary xenoliths in the contaminated granites and the extent of their corrosion by the enclosing magma gives an obvious clue to the origin of the magma. There is no evidence of extensive incorporation of local country rock at the margins of any of the granites. The few recognisable xenoliths rafted from the enclosing hornfels contrast markedly with the typical xenoliths of the contaminated granites in possessing angular shapes and displaying little evidence of appreciable chemical exchange with the enclosing granite. A similar lack of significant incorporation of local wall rock is a general feature of most granites. It would seem unlikely, if

the xenoliths of the contaminated granites are locally derived, or even derived at some intermediate level during their emplacement, that the equally voluminous, and apparently comagmatic, uncontaminated granites shoud escape incorporating similar amounts of comparable xenoliths during emplacement in the same environment. The obvious conclusion is that the xenoliths of the contaminated granites were incorporated at the source of magma generation and the absence of xenoliths in the uncontaminated granites must reflect some fundamentally different process of generation or a different magma source.

The composition of most of the xenoliths indicates their derivation from psammitic and pelitic rocks generally similar to the Ordovician metasediments exposed over wide areas of Victoria and south-eastern New South Wales. The amphibolite xenoliths in the Murrumbucka area are not at variance with derivation from Ordovician rocks; igneous members are not abundant but sparse occurrences of metamorphosed rocks of basic and ultrabasic composition are known (Joplin 1942) and probably represent minor flows, sills and dykes.

Experimental work on synthetic and natural rocks (see summary by Piwinskii & Wyllie, 1968) has indicated that granitic magmas can be generated within diverse crustal rock types by acceptable increases in pressures and temperatures. The most relevant studies in connexion with the origin of Murrumbidgee granites are those by:

1. Winkler (1957) and Winkler & von Platen (1958, 1960, 1961a) who examined the melting of greywackes, clays and calcite-bearing clays around 700°C at 2 kilobars water pressure.

2. Wyllie & Tuttle (1958, 1961) who partially melted shales at water pressures ranging from 690 bars to 2.76 kilobars.

3. Wyart & Sabatier (1959) who partially melted pelitic sediments.

4. Oja (1959) and Kranck & Oja (1960) who partially melted greywackes.

5. Brown (1963) who partially melted arkose at 1 kilobar water pressure and 750°C.

6. Winkler (1960), Winkler & von Platen (1961b) and Steuhl (1962) who partially melted paragneisses.

All to these studies indicate that granitic liquids commence to form from sedimentary material usually at temperatures 20-30 centigrade degrees above the solidus for "normal" granites at corresponding water pressures. Generally at temperatures 50 degrees above the solidus liquid constitutes about 50 per cent of the charge and changes progessively in composition towards an intermediate range of igneous rocks.

The field characteristics and mineralogy of locally developed high-grade "regional" metamorphic rocks associated with the Cooma granite (Joplin, 1942) indicate that conditions suitable for melting of the Ordovician metasediments were attained and indications are that the Cooma granite formed more-or-less in situ by anatexis, although Joplin (1962) maintains that at least some granitic material was contributed from below the present exposures '....possibly sediments differentially melted at a still lower level....'. Sr isotope investigations by Pidgeon & Compston (1965) are compatible with formation of the granite

essentially in situ by anatexis of the high-grade metsedimentary rocks. They found an unusually high Sr^{87}/Sr^{86} ratio of 0.7179 ± 0.005 for the Cooma granite (Rb/Sr age, 415 ± 12 m.y.) and a very similar ratio and age for the surrounding high-grade metasediments, in contrast to a lower initial Sr^{87}/Sr^{86} ratio (0.710 ± 0.002) and greater age (460 ± 11 m.y.) for more distant greenschist facies metasediments.

Other similar granites, grouped under the term "gneissic granites" (Joplin, 1962), associated with locally developed high-grade "regional" metamorphism in the generally low-grade Ordovician psammopelitic rocks, occur throughout southern New South Wales and northern Victoria (Joplin, 1947, 1962; Vallance, 1953, 1954, 1969). All of the so-called "gneissic granites" (Joplin, 1962) occur within the widespread psammopelitic sequence regarded as Ordovician, prompting Browne (1929, 1931) to regard them as Ordovician in age. In places they are intruded by rocks designated "foliated granites" by Joplin (1962) and regarded as Silurian by Browne (1929, 1931). The intrusive relationship between the southern extension of the foliated Clear Range Granodiorite and the gneissic Cooma granite is one example of this relationship. However, K/Ar and Rb/Sr age dating have failed to substantiate a significant age difference between these two granite types and it is likely that they represent two stages of a common process.

The "gneissic granites", such as the Cooma granite appear to represent the earliest stages of anatexis of psammopelitic metasediments within local "hot spots" developed at relatively high levels in the crust. Individual areas of these granites within their high-grade

metamorphic envelopes are small compared with the area of associated granites, such as the Murrumbidgee Batholith, occurring in low-grade regional metamorphic environments. The fact that the Cooma-type granites have not migrated appreciably from the site of their generation is probably related to the feature that such small bodies of magma would have little ability to withstand the heat losses by conduction consequent upon migration from their source. In contrast larger bodies of magma, generated in more extensive tracts of high grade metamorphic rocks, could accommodate conduction losses (and pressure losses) involved in migrating through "cold" country rocks by crystallisation of relatively small amounts of the total volume of magma. No large tracts of high-grade metamorphic rocks are exposed in south-eastern New South Wales but this is compatible with the expectation that the lower region of the crust,well below the present exposed level of the granites, is the logical location of such an environment. The local high-grade metamorphic regions undoubtedly represent local upward perturbations in the isogeotherms, perhaps even related to transfer of heat into higher levels of the crust by movement of large bodies of magma generated at depth.

If this is the case, the Cooma-type "gneissic granites" might be expected to represent lower temperature melting fractions than the larger bodies of magma responsible for contributing the heat to melt them. There is some evidence provided to support this hypothesis by Joplin's (1962) comparison of the composition of the "gneissic granites" with the other granite types of the Tasman Geosyncline.

Joplin (1962) states that no "gneissic" types are known to contain less than 69.79 per cent SiO_2 and that 'The gneissic granites therefore appear to have no basic differentiates and these features clearly distinguish them from both foliated and massive types...'.

Therefore, extensive partial melting of psammopelitic metasediments and reaction with relict unmelted metasedimentary material, followed by migration to higher crustal levels, is a reasonable explanation of the contaminated granites of the Murrumbidgee Batholith. A notable objection to extending this explanation to the uncontaminated granites is the lack of appreciable cognate "xenolithic" material in contrast to its abundance in the contaminated granites. This could imply that the uncontaminated granites represent a total melt of some other crustal or upper mantle material or a differentiate of some other liquid, since it is difficult to perceive of a mechanism of stripping all the abundant relict "xenoliths" from one body of magma but not from another generated in the same environment. However, chemical and mineralogical evidence was presented to indicate that the actual magmas involved in generating both the uncontaminated and contaminated granites were probably very similar. Furthermore, Sr isotope data obtained by Pidgeon & Compston (1965) on a sample of uncontaminated granite (Shannons Flat Adamellite) gave a Sr^{87}/Sr^{86} ratio of 0.707 which is similar to the average value of 0.710 obtained by them for the low-grade psammopelitic metasediments surrounding the higher grade metamorphic rocks at Cooma. Thus, it seems that there is no reason to believe that the magma responsible for the uncontaminated granites was

generated in different source rocks to those of the contaminated granites. The age relationship of the main bulk of the uncontaminated granites to the contaminated granites may have some relevance to the lack of xenoliths. The Shannons Flat Adamellite appears to have been emplaced first, and therefore may represent the first liquid tapped from the region of melting. Since an initial influx of heat would produce only relatively small volumes of liquid in a largely solid matrix, the question of relict material being transported by the magma would not arise, since the anatectic melt would literally filter through a matrix of solid rock before collecting into sufficiently large volumes to move upwards on a large scale. Lacy (1960) has proposed a similar mechanism as the general explanation of the paucity of relict material in anatectic melts. The abundance of cognate material in the contaminated granites may reflect a stage in anatexis at which the amount of melt exceeded the amount of solid relict material so that the fabric of the metasediments collapsed and the whole region became fluid and capable of being squeezed upwards.

The deduced source of magmas in the Murrumbidgee Batholith is similar to that proposed by Kolbe & Taylor (1966) for the "gneissic granites" and "granodiorites and adamellites" of the whole Snowy Mountains region. However, the mechanisms invoked to explain the compositional variation differ.

Evolution of the Murrumbidgee Batholith

The preceding observations and interpretations may be summarised into a unified model along the following lines.

During Silurian or early Devonian times temperatures in the deepest parts of the Tasman Geosyncline rose sufficiently to partially melt psammopelitic rocks belong to, or similar to, Ordovician strata now exposed in Victoria and south-eastern New South Wales. In the shallowest and coolest regions melting occurred on very limited scales and the bodies of acid magma generated were too small to withstand heat losses involved in migrating far from their source. Therefore, granites of this type, of which the Cooma granite is a good example, are found within locally developed high-grade "regionally" metamorphosed rocks, and reveal field evidence of derivation by local anatexis.

Within more extensive tracts of heated metasediments, below the region of incipient melting, larger bodies of granitic melt coalesced and rose under tectonic and gravitational impulses to higher levels in the crust where they crystallised slowly to form complementary adamellites and leucogranites. Decreasing water pressures as well as decreasing temperatures seem to have played a part in the fractionation process resulting in formation of the leucogranites. Since faulting appears to have played an important part in emplacement of the batholith, and major faults are common in and around the batholith, progressive loss of volatiles by leaking along faults is feasible.

The composition of the apparent parental magma initially emplaced is not a minimum temperature granitic melt in relation to the An-Ab-Or-Qz-H_2O system and indicates that melting proceeded above temperatures required for incipient melting, probably until some critical proportion of the source rock was melted and the dispersed fluids could coalesce

and migrate upwards en masse. This elevated temperature above the minimum granite liquids for even very high water vapour pressures was no doubt important in maintaining a sufficient proportion of the melt in a liquid state at the time of its emplacement at higher levels in the crust, despite losses of heat by conduction and raising of the granite solidus in response to decreased water vapour pressures, so that relatively slow cooling in situ was able to produce the leucogranite fractions.

With disintegration of the remnant solid rocks in the zone of melting, either because of increased proportions of melt, or because of collapse caused by the migration of the first bulk of magma, the remaining relict solid material and anatectic melt reacted extensively by metamorphic, metasomatic and anatectic means. In response to tectonic pressures they were finally squeezed upwards along overlying zones of weakness to similar levels as the first magma fraction, perhaps partly guided by ruptures initiated by the initial pulse of magma. Raising of the solidus, in response to decreasing pressure, and normal loss of heat by conduction were enhanced by continued interaction between melt and incorporated solid residue ensuring that final solidification of these rocks occurred prior to, or soon after reaching their present level of exposure, so that fractionation to form more acid liquids is not a common feature of these rocks.

Relevance of the Murrumbidgee Batholith to other granitic intrusions in the Tasman Geosyncline

Several attempts have been made to classify the granites of south-

eastern Australia on the basis of their field characteristics with overtones of age implications (Browne 1929; Browne in David, 1950; Joplin, 1962).

The three main types distinguished in these classifications are listed below, along with examples from the Murrumbidgee Batholith region.

Browne (1929)	Joplin (1962)	Example
Ordovician type	gneissic granite	Cooma granite
Silurian type	foliated granite	Clear Range Granodiorite
Post-Silurian type	massive granite	Shannons Flat Adamellite

The revision of Browne's (1929) terminology by Joplin (1962) was prompted by the discovery by Evernden & Richards (1962) that "Ordovician" and "Silurian" types overlap significantly in age and range from Middle Silurian to Middle Devonian. The "post-Silurian types" range from Silurian-Devonian to Mesozoic. Browne's (1929) classification was based on inferred age relationships whereas Joplin (1962) considered that the three types represented different phases in the development of granitic magma within the geosyncline and that they were therefore correlated to some extent with time and with depth, but most importantly with tectonic environments and the intensity of movement during their emplacement. The results of the present investigation, coupled with contributions by Chappell (1966) and Rhodes (1969b)and various studies, published and unpublished, in the New England region indicate that relationships are more complicated than a three-fold division would imply. Of the three types, the "gneissic

granites" probably have the most consistent petrogenetic implication, usually being consistent with formation essentially in situ, but nonethe-less these would be more positively distinguished by some terminology stressing their high-grade metamorphic environment (e.g. the "regional-aureole granites" of White et al., (1964). "Foliated granites" may be foliated because of forcible emplacement in a partly solid state or because of subsequent deformation not necessarily associated with their emplacement. Massive types can develop in a wide variety of tectonic environments and the various origins inferred for the leucogranites and uncontaminated granites of the Murrumbidgee Batholith, abundant massive granites in the New England region (Chappell, 1966; Wilkinson, 1969) and massive granites in the Hartley region (Rhodes, 1969b)serve to illustrate the looseness of such a grouping.

More meaningful petrogenetic classification would be achieved by distinguishing granites on the basis of their surrounding pressure-temperature environment and xenolith content. The granites containing mainly metasedimentary xenoliths, or associated with other granites containing such xenoliths, appear to be generally surrounded by low-grade regionally metamorphosed rocks (with a superimposed hornfels zone) or less commonly, high-grade regionally metamorphosed rocks. Thus they are mesozonal and catazonal (Buddington, 1959). In contrast, granites containing basic igneous xenoliths or associated with granites containing such xenoliths, generally occur in low-grade regionally metamorphosed environments or in unmetamorphosed terrains; that is, in mesozonal and epizonal environments (Buddington, 1959).

These contrasting environments may be directly related to the contrasting origins (Chappell, 1966; Rhodes, 1969b; this thesis) deduced for representatives of these two granite types. It is likely that water-rich magmas generated by melting sedimentary rocks would be seriously restrained from reaching high levels in the crust because of large increases in the temperature of solidification brought about by sudden release of water pressure when the water pressure exceeded the load pressure at some relatively early stage during transit through the crust. In contrast, granitic magmas generated by partial melting of basic material might be expected to have lower initial water contents and therefore be less affected by changes in water pressure associated with transit through the crust.

APPENDIX A

ANALYTICAL METHODS

About 15 kg of rock were collected from each locality, and from each bulk sample about 2 kg of small rock fragments were obtained using a hydraulic rock splitter. These fragments were crushed to coarse sand size in a tungsten carbide Siebtechnik swing mill. The sample was homogenised and successively split to yield about 200g, then reduced to pass 120 mesh nylon sieving cloth either by grinding in a mechanical agate pestle and mortar or by additional crushing in the swing mill. The lengthier process of grinding in the agate pestle and mortar was discontinued when it became apparent that appreciable contamination from the swing mill is restricted to tungsten, carbon and cobalt. For trace element analysis it was necessary to crush 10g of each powdered sample for as additional four minutes in a small tungsten carbide ball mill.

With the exception of Na_2O, FeO, H_2O+, H_2O-, CO_2, and Li_2O , all analyses were performed by X-ray fluroescence spectrometry. All analyses were performed at least in duplicate, except for H_2O+, H_2O-, CO_2 and Li_2O.

The major elements (Si, Ti, Al, total Fe, Mg, Mn, Ca, K, P) were measured on glass discs prepared by fusing the sample with a flux of lithium borate and lanthanum oxide, in order to eliminate grain-size effects and reduce matrix effects (which were corrected finally by applying matrix correction coefficients). The analytical method closely follows that described by Norrish & Chappell (1967) and Norrish & Hutton

(1969).

Trace elements were measured on undiluted pelletised powdered samples, and mass absorption coefficients were measured directly (Sweatman et al., 1963; Norrish & Chappell, 1967). Only four absorption coefficients were measured : the rubidium and strontium coefficients for the short wavelength radiations (0.7-1Å), the zinc coefficient for wavelengths shorter than the iron K absorption edge (1.744Å) and the iron coefficient for longer wavelengths (table A1). Other absorption coefficients can be adequately obtained by interpolation from these four. The undiluted rock powder was used for measuring the rubidium and strontium coefficients; in the case of the iron and zinc coefficients a cellulose diluent was used to allow satisfactory intensities of the attenuated X-ray beam.

Matrix and interference effects were calculated directly (Norrish & Chappell, 1967; Chappell et al., 1969) and calibration was made against primary synthetic standards, thus eliminating uncertainties introduced by using "recommended" or "preferred" values of natural standards. The high degree of precision and accuracy obtainable using these methods can be assessed from several recent publications dealing with both major and trace element analysis (Norrish & Chappell, 1967; Norrish & Hutton, 1969; Compston et al., 1969; Chappell et al., 1969).

All rock analyses were made in duplicate on separately prepared discs and pellets. Trace element analyses of all mineral samples were performed in duplicate on single pellets; some major element analyses of minerals were performed in duplicate on single discs. A summary of

analytical conditions is presented in table A1 and analyses of international rock standards analysed using the same methods are presented in table A2.

Sodium was determined by flame photometry, using a Baird-Atomic double-beam flame photometer with a propane-air flame, and lithium as an internal standard. The method is analogous to that described by Cooper (1963) for potassium determinations.

Ferrous iron was measured by dissolving the sample in hydrofluroric acid in the presence of excess ammonium metavanadate, then titrating the excess metavanadate against ferrous ammonium sulphate solution, previously standardised against B.D.H. standard ceric sulphate solution. Ferric iron was obtained by difference between total iron, measured by X-ray fluroescence, and ferrous iron, measured by titration.

Combined water and carbon dioxide were determined by heating the sample in a tube furnace for two hours at 1200°C in a stream of dry, carbon dioxide-free nitrogen. The water and carbon dioxide given off were collected in micro-absorption tubes filled with phosphorus pentoxide and 'carbosorb' soda asbestos.

Hygroscopic water was obtained by loss after heating for two hours at 110°C.

Lithium in biotites was measured by atomic absorption.

Table A1 Summary of analytical conditions for X-ray spectrometry

	X-ray tube	Analytical line	Crystal	Collimator	Detector	Abs. coeff.	Lower limit detection
SiO_2	Cr	K_α	P.E.	Coarse	F.C.		0.05
TiO_2	Cr	K_α	LiF(200)	Coarse	F.C.		0.002
Al_2O_3	Cr	K_α	P.E.	Coarse	F.C.		0.05
Fe_2O_3*	W	K_α	LiF(200)	Coarse	F.C.		0.002
MnO	W	K_α	LiF(200)	Coarse	F.C.		0.002
MgO	Cr	K_α	A.D.P.	Coarse	F.C.		0.05
CaO	Cr	K_α	LiF(200)	Coarse	F.C.		0.002
K_2O	Cr	K_α	LiF(200)	Coarse	F.C.		0.002
P_2O_5	Cr	K_α	Ge	Coarse	F.C.		0.003
Ba	W	L_{β_1}	LiF(220)	Coarse	F.C.	Fe	4
Rb	Mo	K_α	LiF(200)	Fine	S.C.	Rb	0.5
Sr	Mo	K_α	LiF(200)	Coarse	S.C.	Sr	0.5
Pb	Mo	L_{β_1}	LiF(200)	Fine	S.C.	Rb	1
Th	Mo	L_{α_1}	LiF(200)	Fine	S.C.	Rb	1
U	Mo	L_{α_1}	LiF(220)	Fine	S.C.	Rb	0.5
Zr	Ag	K_α	LiF(200)	Coarse	S.C.	Sr	1
Nb	Ag	K_α	LiF(200)	Fine	S.C.	Sr	1
Y	Mo	K_α	LiF(200)	Coarse	S.C.	Sr	1
La	Au	L_{α_1}	LiF(200)	Coarse	F.C.	Fe	2
Ce	W	L_{β_1}	LiF(200)	Fine	F.C.	Fe	5
Pr	W	L_{α_1}	LiF(220)	Coarse	F.C.	Fe	2
Nd	W	L_{β_1}	LiF(220)	Coarse	F.C.	Fe	5
V	W	K_α	LiF(220)	Fine	F.C.	Fe	1
Cr	W	K_α	LiF(200)	Fine	F.C.	Fe	1
Mn	Au	K_α	LiF(200)	Fine	F.C.	Fe	1
Ni	Au	K_α	LiF(200)	Coarse	S.C.	Zn	1
Cu	Au	K_α	LiF(200)	Coarse	S.C.	Zn	1
Zn	Au	K_α	LiF(200)	Coarse	S.C.	Zn	1
Ga	Mo	K_α	LiF(200)	Coarse	S.C.	Zn	1

Oxides expressed in per cent, elements in parts per million

* Total Fe expressed as Fe_2O_3

Table A2 X-ray fluorescence analyses of three international rock standards (results obtained by A.N.U. Geology Department, X-ray Laboratory during 1968, 1969)

	G-2	GSP-1	BCR-1
SiO_2	69.08	67.40	54.38
TiO_2	0.48	0.66	2.25
Al_2O_3	15.12	15.00	13.51
Fe_2O_3*	2.62	4.23	13.32
MnO	0.03	0.04	0.19
MgO	0.77	0.95	3.40
CaO	1.91	2.00	7.01
K_2O	4.48	5.53	1.71
P_2O_5	0.13	0.28	0.37
Ba	2125	1427	801
Rb	170	253	47
Sr	484	235	330
Pb	31	55	15
Th	24	90	6
U	2.1	1.7	2.2
Zr	321	538	191
Nb	12	25	13
Y	10	24	34
La	82	119	(9)
Ce	171	319	57
Pr	18	42	8
Nd	45	125	23
V	30	41	364
Cr	12	13	13
Mn	213	248	1190
Ni	3	7	9
Cu	10	30	16
Zn	99	115	128
Ga	23	22	21

Oxides in per cent, elements in parts per million

* Total Fe expressed as Fe_2O_3

Calibration based on synthetic standards

APPENDIX B

CIPW NORMS

	Qz	Or	Ab	An	Co	En	Fs	Mt	Il	Ap	Cc	H_2O
Stewartsfield Granodiorite												
20558	26.39	22.33	19.20	12.34	1.84	6.12	5.66	0.74	1.18	0.36	0.20	1.99
20559	31.13	19.50	17.59	12.23	2.83	6.00	6.29	0.38	1.14	0.33	0.25	1.92
20560	29.57	20.56	18.69	13.01	2.42	6.02	6.23	0.26	1.18	0.31	0.30	1.64
20561	35.49	8.33	20.55	15.09	3.29	6.22	5.71	1.17	1.22	0.33	0.11	1.67
Clear Range Granodiorite												
20562	26.15	14.95	9.64	22.87	2.56	9.56	9.09	1.45	1.52	0.40	0.45	1.52
20563	25.87	13.00	15.65	25.17	0.23	9.66	5.77	1.99	1.10	0.26	0.25	1.27
20531	26.06	20.62	16.41	17.32	1.76	7.62	5.93	1.55	1.01	0.38	0.14	1.24
20564	30.49	17.19	15.65	15.73	2.63	6.95	6.17	1.28	1.29	1.04		
20532	28.80	16.19	16.58	19.65	1.57	7.52	6.08	1.54	1.27	0.31	0.14	1.27
20565	31.01	17.72	16.58	15.75	2.33	6.57	4.94	1.78	1.25	0.40		
20533	29.79	18.20	17.85	16.54	1.34	6.30	5.65	1.03	1.08	0.28	0.14	0.96
20566	32.93	16.31	16.58	14.91	2.96	6.12	5.74	0.97	1.08	0.33		
20534	30.71	20.86	18.86	13.95	1.94	4.95	5.64	0.64	1.10	0.31	0.14	1.30
20535	31.29	21.03	18.95	11.65	2.68	5.50	5.44	0.78	1.10	0.33	0.39	1.11
20536	33.32	16.48	18.35	13.71	2.79	5.73	6.18	0.90	1.27	0.31	0.20	1.03
20537	33.97	14.48	19.88	19.42	0.15	4.13	2.34	2.44	0.95	0.33		
20538	31.41	20.38	18.18	13.01	2.37	6.25	5.79	0.70	1.12	0.33	0.27	0.67
20539	31.72	20.80	19.37	12.57	2.02	4.63	5.32	0.61	1.04	0.28	0.32	1.17
20540	32.87	22.45	18.61	10.78	2.81	4.63	4.61	0.87	0.95	0.36		
20541	33.66	22.51	19.62	10.41	2.31	3.96	4.45	0.67	0.97	0.31	0.25	1.18
Callemondah Granodiorite												
20542	31.42	4.19	21.06	22.77	1.61	6.95	5.63	1.68	1.14	0.31	0.07	2.25
20543	28.54	16.72	17.59	19.16	1.15	7.02	6.04	1.16	1.10	0.31	0.05	1.04
20544	37.42	8.57	20.13	13.60	4.02	5.45	5.31	1.25	1.33	0.40	0.11	2.03
20545	34.88	19.14	17.00	9.23	4.39	5.08	6.04	0.80	1.29	0.38	0.32	1.02
20546	33.58	20.44	17.59	9.89	3.70	5.08	5.94	0.75	1.25	0.36	0.07	1.08
20547	31.90	20.32	20.97	11.06	2.34	5.05	4.37	0.93	0.89	0.31		
Bolairo Granodiorite												
20548	31.33	19.73	17.08	11.88	3.16	6.32	6.29	0.67	1.20	0.33	0.59	1.24
20549	31.64	20.09	17.42	11.99	2.92	6.15	5.46	0.88	1.14	0.31	0.18	1.45
20550	31.62	19.85	18.86	10.79	3.53	5.75	5.81	0.84	1.20	0.36	0.23	1.50
20551	32.04	20.56	17.25	12.34	2.73	5.93	5.80	0.81	1.20	0.33	0.23	1.34
20552	32.91	21.62	18.78	9.64	2.93	5.78	4.01	1.32	1.01	0.36		

	Qz	Or	Ab	An	Co	En	Fs	Mt	Il	Ap	Cc	H_2O
Willoona Tonalite												
20553	33.18	18.61	18.18	9.69	3.75	5.85	5.78	0.81	1.27	0.40	0.18	1.61
20554	34.70	19.85	15.90	8.65	4.46	5.80	5.32	1.03	1.25	0.36	0.16	1.62
20555	34.01	17.61	18.44	10.81	3.76	5.13	5.87	0.81	1.27	0.38	0.25	1.73
20556	36.29	10.28	21.06	13.39	3.60	5.40	4.88	1.17	1.16	0.38		
20557	35.00	17.67	18.10	9.82	4.24	4.98	5.70	0.88	1.27	0.36	0.11	1.04
Shannons Flat Adamellite												
20501	30.31	26.88	22.41	11.00	1.03	2.64	2.66	0.81	0.74	0.21	0.11	0.93
20502	31.32	24.87	23.00	11.62	0.72	2.19	2.51	1.01	0.78	0.24	0.20	0.80
20503	32.17	24.81	22.07	11.90	0.87	2.34	2.36	1.15	0.82	0.26	0.14	0.63
20504	31.67	25.46	22.50	11.82	0.83	2.34	2.55	1.01	0.78	0.24	0.20	0.94
20505	34.05	23.99	20.47	11.42	1.06	2.64	2.86	0.97	0.70	0.21	0.16	0.87
20506	32.58	24.28	22.16	12.74	0.74	2.29	2.72	0.80	0.78	0.21	0.11	0.83
20507	33.10	25.82	21.23	11.15	0.74	2.17	2.55	0.84	0.70	0.21	0.11	0.73
20508	33.54	25.76	21.06	9.67	1.03	2.56	3.00	0.94	0.66	0.21	0.18	0.88
20509	32.71	25.05	21.99	12.01	0.86	2.27	2.70	0.90	0.78	0.24	0.14	0.70
20510	32.75	26.59	21.82	10.74	0.71	1.99	2.33	0.90	0.70	0.21	0.05	0.81
20511	33.27	25.46	21.57	12.27	0.53	1.77	2.18	0.96	0.66	0.21	0.07	0.85
20512	33.42	25.29	21.65	11.41	0.71	2.09	2.59	0.77	0.74	0.24	0.07	0.77
20513	32.60	25.52	22.33	11.33	0.67	2.51	2.56	0.96	0.80	0.24	0.11	0.77
20514	33.31	25.70	21.57	11.21	0.91	2.27	2.56	0.84	0.65	0.19	0.05	0.78
20515	31.88	28.65	21.14	11.03	0.80	2.22	2.69	0.78	0.74	0.24	0.11	0.46
20516	34.01	23.10	22.24	12.53	0.93	2.07	3.24	0.45	0.68	0.19	0.16	0.75
20517	34.28	24.52	23.60	7.86	1.93	2.84	2.14	0.97	0.65	0.19	0.25	1.42
20518	33.29	24.93	23.00	12.70	0.60	1.69	1.67	0.94	0.57	0.17	0.14	0.78
20519	33.80	23.22	23.51	11.90	0.82	2.12	2.60	0.71	0.72	0.26	0.14	0.79
20520	33.91	24.40	22.75	12.19	0.62	1.72	2.11	0.83	0.63	0.19	0.14	0.69
20521	33.68	26.00	23.09	11.26	0.52	1.67	1.84	0.86	0.57	0.17	0.16	0.75
20522	35.77	23.40	22.07	12.14	0.74	1.69	1.77	0.99	0.61	0.17	0.16	0.79
20523	33.20	27.59	23.09	9.44	0.60	2.07	2.39	0.72	0.68	0.21	0.23	0.68
20524	34.43	26.82	23.68	9.75	0.71	1.42	1.71	0.77	0.51	0.17	0.18	0.57
20525	36.40	28.06	23.68	5.71	1.48	1.29	1.75	0.52	0.44	0.14	0.16	0.95
Tharwa Adamellite												
20526	33.17	24.40	21.14	12.19	0.27	2.81	2.42	1.07	0.76	0.24		
20527	32.60	26.11	21.91	11.20	0.77	2.44	2.55	1.01	0.82	0.21	0.11	0.70
20528	33.42	25.76	21.40	10.56	0.94	2.29	2.89	0.84	0.80	0.24	0.16	0.77
20529	36.15	25.58	21.57	8.36	1.76	2.04	2.35	0.81	0.63	0.26	0.16	0.76
20530	39.06	17.43	29.94	8.51	1.50	0.75	2.08	0.33	0.27	0.19	0.16	0.64

Leucogranites and minor intrusions

	Qz	Or	Ab	An	Co	En	Fs	Mt	Il	Ap	Cc	H_2O
20569	38.54	31.96	23.00	0.66	2.92	0.27	1.45	0.46	0.08	0.24	0.14	0.80
20567	39.37	27.59	26.05	2.74	1.56	0.50	0.88	0.35	0.15	0.14	0.11	0.61
20568	40.07	27.21	25.54	2.42	1.81	0.55	0.93	0.36	0.13	0.17		
20570	33.91	25.76	22.84	9.03	1.23	2.04	2.91	0.67	0.95	0.28	0.18	0.62
20571	36.72	28.48	27.49	3.40	1.55	0.67	1.16	0.19	0.21	0.26	0.16	0.64
20572	37.54	34.15	22.24	3.59	0.45	0.15	0.48	0.72	0.27	0.07	0.14	0.39
20573	36.76	27.30	31.80	1.01	1.66	0.12	0.68	0.20	0.06	0.09	0.11	0.60
20574	38.66	33.85	22.33	2.52	0.91	0.27	0.58	0.13	0.15	0.05	0.14	0.44

Xenoliths*

	Qz	Or	Ab	An	Co	En	Fs	Mt	Il	Ap	Cc	H_2O
1.	30.11	2.19	8.71	1.59	19.08	8.99	12.07	4.99	1.31			0.76
2.	0.00	21.51	30.12	28.17	2.87	0.00	0.00	2.41	1.52	0.24	0.07	1.57
3.	17.11	10.28	17.93	24.99	0.00	16.19	6.69	2.41	1.04	0.26		1.59
4.	23.29	9.39	24.87	21.10	0.52	4.85	6.88	3.76	2.26	1.26	0.07	1.49
5.	23.86	19.44	4.06	23.48	0.96	14.79	7.55	1.77	1.14	0.09	0.11	2.58
6.	24.84	13.88	18.44	23.13	0.39	7.00	7.91	0.71	2.41	0.55	0.36	1.05
7.	30.77	16.66	18.69	13.29	2.84	6.55	7.74	0.72	1.18	0.33	0.05	1.26
8.	25.27	18.67	21.40	13.37	1.37	7.62	6.79	1.33	1.60	0.31	0.02	1.62
9.	53.99	8.86	16.24	9.36	1.30	3.46	4.23	0.41	0.97	0.33	0.16	0.85

* Sample numbers are the same as in table 7

2. also contains 0.32 Ne, 5.25 Fo, 5.39 Fa.

3. also contains 0.78 Di-Wo, 0.51 Di-En, 0.21 Di-Fs.

REFERENCES

Bailey, J.C., 1969: Geochemistry and petrogenesis of volcano-plutonic formations in the Georgetown Inlier, North Queensland. Aust. Nat. Univ., Ph.D. Thesis (unpub.).

Baird, A.K., McIntyre, D.B., & Welday, E.E., 1967: Geochemical and structural studies in batholithic rocks of Southern California: Part II, sampling of the Rattlesnake Mountain pluton for chemical composition, variability and trend analysis. Bull. geol. Soc. Am., 78, pp. 191-222.

Brammall, A., & Harwood, H.F., 1932: The Dartmoor granites: their genetic relationships. Q. Jl. geol. Soc. Lond., 88, pp. 171-234.

Brown, G.M., 1963: Melting relationships of Tertiary granitic rocks in Skye and Rhum. Miner. Mag., 33, pp. 533-563.

Brown, I.A., 1933: The geology of the South Coast of N.S.W., with special reference to the origin and relationships of the igneous rocks. Proc. Linn. Soc. N.S.W., 58, pp. 334-362

Browne, W.R., 1914: The geology of the Cooma district, N.S.W. Part I. J. Proc. R. Soc. N.S.W., 48, pp.172-222.

Browne, W.R., 1929: An outline of the history of igneous action in N.S.W. till the close of the Palaeozoic Era. Proc. Linn. Soc. N.S.W., 54, pp. ix-xxxix.

Browne, W.R., 1931: Notes on bathyliths and some of their implications. J. Proc. R. Soc. N.S.W., 65, pp. 112-144.

Browne, W.R., 1943: The geology of the Cooma district, N.S.W. Part II. The country between Bunyan and Colinton. J. Proc. R. Soc. N.S.W., 77, pp. 156-172.

Buddington, A.F., 1959: Granite emplacement with special reference to North America. Bull. geol. Soc. Am., 70, pp. 671-748.

Burton, J.D., Culkin, F., & Riley, J.P., 1959: The abundances of gallium and germanium in terrestrial materials. Geochim. cosmochim. Acta, 16, pp. 151-180.

Cattell, R.B., 1952: Factor Analysis: an Introduction and Manual for the Psychologist and Social Scientist. Harper, New York.

Chao, E.C.T., & Fleischer, M., 1960: Abundance of zirconium in igneous rocks. Rep. 21 Int. geol. Congr., 1, pp.106-131.

Chappell, B.W., 1966: Petrogenesis of the granites at Moonbi, New South Wales. Aust. Nat. Univ., Ph.D. Thesis (unpub.)

Chappell, B.W., Arriens, P.A., Compston, W., & Vernon, M.J., 1969: Rubidium and strontium determinations by X-ray fluorescence spectrometry and isotope dilution below the part per million level. Geochim. cosmochim. Acta, 33, pp.

Chayes, F., 1956: Modal composition of the major members of the Southern California Batholith. Carnegie Institute of Washington Yearbook, 55, pp.214-216.

Chayes, F., 1960: On correlation between variables of constant sum. J. geophys. Res., 65, pp.4185-4193.

Chayes, F., 1962: Numerical correlation and petrographic variation. J. Geol., 70, pp. 440-452.

Clark, S.P., Peterman, Z.E., & Heier, K.S., 1966: Abundances of uranium, thorium and potassium. Mem. geol. Soc. Am., 97, pp. 521-541.

Compston, W., Chappell, B.W., Arriens, P.A., & Vernon, M.J., 1969: On the feasibility of NBS 70a K-feldspar as a Rb-Sr age reference sample. Geochim. cosmochim. Acta, 33, pp. 753-757.

Cooley, N.W., & Lohnes, P.R., 1962: Multivariate Procedures for the Behavioural Sciences. Wiley, New York.

Cooper, J.A., 1963: The flame photometric determination of potassium in geological materials used for potassium argon dating. Geochim. cosmochim. Acta, 27, pp. 525-546.

Corlett, M., & Ribbe, P.H., 1967: Electron probe microanalysis of minor elements in plagioclase feldspars. Schweiz. miner. petrogr. Mitt., 47, pp. 317-332.

David, T.W.E., 1950: (Ed. Browne, W.R.): The Geology of the Commonwealth of Australia. Arnold & Co., London.

Deer, W.A., Howie, R,A., & Zussman, J., 1962a: Rock-forming Minerals. Vol. 1. Ortho-and Ring Silicates. Longmans, London.

Deer, W.A., Howie, R.A., and Zussman, J., 1962b: Rock-forming Minerals. Vol. 3. Sheet Silicates. Longmans, London.

Doe, B.R., & Tilling, R.I., 1967: The distribution of lead between coexisting K-feldspar and plagioclase. Am. Miner., 52, pp. 805-816.

Evernden, J.F., & Richards, J.R., 1962: Potassium-argon ages in eastern Australia. J.geol. Soc. Aust., 9, pp. 1-49.

Ewart, A., Taylor, S.R., & Capp, A.C., 1968: Trace and minor element geochemistry of the rhyolitic volcanic rocks, Central North Island, New Zealand. Contr. Mineral. and Petrol., 18, pp. 76-104.

Foster, J.D., 1960: Interpretation of the composition of trioctahedral micas. Prof. Pap. U.S. geol. Surv., 354-B, pp. 11-49.

Goldsmith, J.R., & Laves, F., 1954: The microcline-sanidine stability relations. Geochim. cosmochim. Acta, 5, pp. 1-19.

Gulson, B.L., 1968: The evolution of dioritic rocks - with special reference to the high potassium diorites of the Yeovil igneous complex, N.S.W. Aust. Nat. Univ., Ph.D Thesis (unpub.).

Hall, A., 1966: A petrogenetic study of the Rosses granite complex, Donegal. J. Petrology, 7, pp. 202-220.

Hall, A., 1967: The variation of some trace elements in the Rosses granite complex, Donegal. Geol. Mag., 104, pp. 99-109.

Harman, H.H., 1960: Modern Factor Analysis. Univ. Chicago Press, Chicago.

Harry, W.T., 1950: Aluminium replacing silicon in some silicate lattices. Miner. Mag., 29, pp. 142-149.

Haskin, L.A., Frey, F.A., Schmitt, R.A., & Smith, R.H., 1966: Meteoritic, solar and terrestrial rare-earth abundances. Physics Chem. Earth, 7, pp. 167-321.

Hatch, F.H., Wells, A.K. & Wells, M.K., 1961: Petrology of the Igneous Rocks. Murby, London.

Heier, K.S., 1960: Petrology and geochemistry of high-grade metamorphic and igneous rocks on Langøy, Northern Norway. Norges Geologiske Undersøkelse, 207.

Heier, K.S., 1962: Trace elements in feldspars - a review. Norsk. geol. Tiddskr., 42 (Feldspar Volume), pp. 415-454.

Heier, K.S., & Rogers, J.J.W., 1963: Radiometric determination of thorium, uranium and potassium in basalts and in two magmatic differentiation series. Geochim. cosmochim. Acta, 27, pp. 137-154.

Howie, R.A., 1955: The geochemistry of the charnockite series of Madras, India. Trans R. Soc. Edinb., 62, pp. 725-768.

Hsu, L.C., 1968: Selected phase relationships in the system Al-Mn-Fe-Si-O-H: A model for garnet equilibria. J. Petrology, 9, pp. 40-83.

Joplin, Germaine A., 1939: Studies in metamorphism and assimilation in the Cooma district of New South Wales. Part I. The amphibolites and their metasomatism. J. Proc. R. Soc. N.S.W., 73, pp. 86-106.

Joplin, Germaine A., 1942: Petrological studies in the Ordovician of New South Wales. I. The Cooma complex. Proc. Linn. Soc. N.S.W., 67, pp. 156-196.

Joplin, Germaine A., 1943: Petrological studies in the Ordovician of New South Wales. II. The northern extension of the Cooma complex. Proc. Linn. Soc. N.S.W., 68, pp. 159-183.

Joplin, Germaine A., 1947: Petrological studies in the Ordovician of New South Wales. IV. The northern extension of the north-east Victorian metamorphic complex. Proc. Linn. Soc. N.S.W., 72, pp. 87-124.

Joplin, Germaine A., 1962: An apparent magmatic cycle in the Tasman Geosyncline. J.geol. Soc. Aust., 9, pp. 51-69.

Kleeman, A.W., 1965: The origin of granitic magmas. J.geol. Soc. Aust., 12, pp. 35-52.

Kolbe, P., & Taylor, S.R., 1966: Geochemical investigation of the granitic rocks of the Snowy Mountains area, New South Wales. J.geol. Soc. Aust., 13, pp. 1-25.

Koritnig, S., 1965: Geochemistry of phosphorus - I. The replacement of Si^{4+} by P^{5+} in rock forming silicate minerals. Geochim. cosmochim. Acta, 29, pp. 361-372.

Kranck, E., & Oja, R., 1960: Experimental studies in anatexis. Rep. 21 Int. geol. Congr., 14, pp. 16-29.

Lacey, E.D., 1960: Melts of granitic composition: their structure, properties and behaviour. Rep. 21 Int. geol. Congr., 14, pp. 7-15.

Larsen, E.S., 1948: Batholith and associated rocks of Corona, Elsinore, and San Luis Rey Quadrangles, Southern California. Geol. Soc. Am. Mem., 29.

Larsen, E.S., & Draisin, W.M., 1948: Composition of minerals in the rocks of the Southern California batholith. Rep. 21 Int. geol. Congr., 2, pp. 67-69.

Larsen, E.S., & Gottfried, D., 1960: Uranium and thorium in selected suites of igneous rocks. Am. J. Sci., 258A, pp. 151-169.

Legge, J.G., 1937: Notes on the physiography and geology of the Federal Capital Territory. Rep. Aust. N.Z. Ass. Advmt. Sci., 23, pp. 84-88

Le Maitre, R.W., 1968: Chemical variation within and between volcanic rock series - a statistical approach. J. Petrology, 9, pp. 220-252.

McIntyre, W.L., 1963: Trace element partition coefficients - a review of theory and applications to geology. Geochim. cosmochim. Acta, 27, pp. 1209-1264.

Moroney, M.J., 1958: Facts from Figures. Penguin, Middlesex.

Nockolds, S.R., 1940: The Garabal Hill - Glen Fyne igneous complex. Q. Jl. geol. Soc. Lond., 96, pp. 451-551.

Nockolds, S.R., 1947: The relation between chemical composition and paragenesis in the biotite micas of igneous rocks. Am. J. Sci., 245, pp. 40;-420.

Nockolds, S.R., 1954: Average chemical compositions of some igneous rocks. Bull. geol. Soc. Am., 65, pp. 1007-1032.

Nockolds, S.R., & Allen, R., 1953: The geochemistry of some igneous rock series. Geochim. cosmochim. Acta, 4, pp. 105-142.

Nockolds, S.R., & Allen, R., 1956: The geochemistry of some igneous rock series. III. Geochim. cosmochim. Acta, 9, pp. 34-37.

Nockolds, S.R., & Mitchell, R.L., 1948: The geochemistry of some Caledonian plutonic rocks: a study in the relationship between the major and trace elements of igneous rocks and their minerals. Trans. R. Soc. Edinb., 61, pp. 533-575.

Norrish, K., & Chappell, B.W., 1967: X-ray fluorescence spectrography, in Physical Methods in Determinative Mineralogy. (Ed. Zussman, J.). Academic Press, London.

Norrish, K., & Hutton, J.T., 1969: An accurate X-ray spectrographic method for the analysis of a wide range of geological samples. Geochim. cosmochim. Acta, 33, pp. 431-454.

Oja, R., 1959: Experiments in anatexis. Unpub. thesis, McGill Univ., cited in Piwinskii, A.J., & Wyllie, P.J., 1968.

Öpik, A.A., 1958: The geology of the Canberra City district. Bull. Bur. Miner. Resour. Geol. Geophys. Aust., 32.

Packjam, G.H., 1960: Sedimentary history of part of the Tasman Geosyncline in south-eastern Australia. Rep. 21 Int. geol. Congr., 12, pp. 74-83.

Pidgeon, R.T., & Compston, W., 1965: The age and origin of the Cooma Granite and its associated metamorphic Zones, New South Wales. J. Petrology, 6, pp. 193-222.

Piwinskii, A.J., & Wyllie, P.J., 1968: Experimental studies of igneous rock series: a zoned pluton in the Wallowa Batholith, Oregon. J. Geol., 76, pp. 205-234.

Radoslovich, E.W., 1962: The cell dimensions and symmetry of layer-lattice silicates. II. Regression relations. Am. Miner., 47, pp. 617-636.

Radoslovich, E.W., & Norrish, K, 1962: The cell dimensions and symmetry of layer lattice silicates. I. Some structural considerations. Am. Miner., 47, pp. 599-616.

Rao, C.R, 1965: Linear Statistical Inference and its Applications. Wiley, New York.

Rhodes, J.M., 1969a: The application of cluster and discriminatory analysis in mapping granite intrusions. Lithos, 2, (in press).

Rhodes, J.M., 1969b: The geochemistry of a granite-gabbro association at Hartley, New South Wales. Aust. Nat. Univ., Ph.D. Thesis (unpub.).

Rhodes, J.M., 1969c: The chemistry of potassium feldspars in granitic rocks. Chem. Geol. (in press).

Ringwood, A.E., 1955: The principles governing trace element behaviour during magmatic crystallisation. Part II. The role of complex formation. Geochim. cosmochim. Acta, 7, pp. 242-254.

Rogers, J.J.W., & Ragland, P.C., 1961: Variation in thorium and uranium in selected granitic rocks. Geochim. cosmochim. Acta, 25, pp. 99-109

Sen, N., Nockolds, S.R., & Allen, R., 1959: Trace elements in minerals from rocks of the Southern California batholith. Geochim. cosmochim. Acta, 16, pp. 58-78.

Shaw, D.M., 1968: A review of K-Rb fractionation trends by covariance analysis. Geochim. cosmochim. Acta, 32, pp. 573-602.

Snelling, N.J., 1957: The geology and petrology of the Murrumbidgee Bathylith and its relation to the Palaeozoic igneous activity of the Tasman Geosynsline. Aust.Nat. Univ., Ph.D. Thesis (unpub.).

Snelling, N.J., 1960: The geology and petrology of the Murrumbidgee Batholith. Q. Jl. geol. Soc. Lond., 116, pp. 187-215.

Steuhl, H., 1962: Die experimentelle Metamorphose und Anatexis eines Parabiotitgneises aus dem Schwarzwald. Chem. Erde, 21, pp. 413-449.

Sweatman, T.R., Norrish, K., & Durie, R.A., 1963: An assessment of X-ray spectrometry for the determination of inorganic constituents in brown coals. Mic. Rep. Div. Coal Research C.S.I.R.O., 177.

Taubeneck, W.H., 1965: An appraisal of some K-Rb ratios in igneous rocks. J. geophys. Res., 70, pp. 475-478.

Taylor, S.R., 1966: The application of trace element data to problems in petrology. Physics Chem. Earth, 6, pp. 133-213.

Taylor, S.R., 1968: Geochemistry of andesites, in Origin and Distribution of the Elements. (Ed. Ahrens, L.H.) Pergamon Press, Oxford & New York.

Tilley, C.E., 1926: On garnet in pelitic contact zones. Miner. Mag., 21, pp. 47-50.

Tilley, C.E., 1950: Some aspects of magmatic evolution. Q. Jl. geol. Soc. Lond., 106, pp. 37-61.

Towell, D.G., Volforsky, R., & Winchester, J.W., 1965: Rare earth distributions in some rocks and associated minerals of the batholith of Southern California. J. geophys. Res., 70, pp. 3485-3496.

Tuttle, O.F., & Bowen, N.L., 1958: Origin of granite in the light of experimental studies in the system $NaAlSi_3O_8$ - $KAlSi_3O_8$ - SiO_2 - H_2O. Geol. Soc. Am. Mem., 74.

Vallance, T.G., 1953: Studies in the metamorphic and plutonic geology of the Wantabadgery-Adelong-Tumbarumba district, N.S.W. I. Introduction and metamorphism of the sedimentary rocks. Proc. Linn. Soc. N.S.W., 78, pp. 90-121.

Vallance, T.G., 1954: Studies in the metamorphic and plutonic geology of the Wantabadgery -Adelong-Tumbarumba district, N.S.W. III. The granitic rocks. Proc. Linn. Soc. N.S.W., 78, pp. 197-220.

Vallance, T.G., 1969: in The geology of New South Wales. (Ed. Packham, G.H.). J.geol. Soc. Aust., 16.

Vogel, T.A., & Seifert, K.E., 1965: Deformation twinning in ordered plagioclase. Am. Miner., 50, pp. 514-518.

von Platen, H., 1965: Experimental anatexis and genesis of migmatites, in Controls of Metamorphism. (Pitcher, W.S., & Flinn, G.W., eds). Oliver & Boyd, London.

White, A.J.R., Chappell, B.W., & Branch, C.D., 1964: Classification of granite types according to associated rocks. 37th A.N.Z.A.A.S. Congr. (Canberra)

Whitfield, J.J., Rogers, J.J.W., & Adams, J.A.S., 1959: The relationship between the petrology and the thorium and uranium contents of some granitic rocks. Geochim. cosmochim. Acta, 17, pp. 248-271.

Wilkinson, J.F.G., 1969, in Geology of New South Wales. (Ed. Packham, G.H.) J. geol. Soc. Aust., 16.

Wilkinson, J.F.G., Vernon, R.H., & Shaw, S.E., 1964: The petrology of an adamellite-porphyrite from the New England Bathylith (New South Wales). J. Petrology, 5, pp. 461-488.

Winkler, H., 1957: Experimentelle Gesteinsmetamorphose - I. Hydrothermale Metamorphose karbonatfreier Tone. Geochim. cosmochim. Acta, 13, pp. 42-69.

Winkler, H., 1960: La genèse du granite et des migmatites par anatexie expérimentale. Rev. géog. phys. et géol. dynamique, 3, pp. 67-76.

Winkler, H., & von Platen, H., 1958: Experimentelle Gesteinsmetamorphose - II. Bildung von anatektischen granitischen Schmelzen bei der Metamorphose von NaCl- führenden kalkfreien Tonen. Geochim. cosmochim. Acta, 15, pp. 91-112.

Winkler, H., & von Platen, H., 1960: Experimentelle Gesteinsmetamorphose -III. Anatektische Ultrametamorphose kalkhaltiger Tone. Geochim. cosmochim. Acta, 18, pp. 294-316.

Winkler, H., & von Platen, H., 1961a: Experimentelle Gesteinsmetamorphose - IV. Bildung anatektischer Schmelzen aus metamorphisierten Granwacken. Geochim. cosmochim. Acta, 24, pp. 48-69.

Winkler, H., & von Platen, H., 1961b: Experimentelle Gesteinsmetamorphose - V. Experimentelle anatektische Schmelzen und ihre petrogenetische Bedeutung. Geochim. cosmochim. Acta, 24, pp. 250-259.

Wright, T. L. , 1968: X-ray and optical study of alkali feldspar : II An X-ray method for determining the composition and structural state from measurements of 2θ values for three reflections. Am. Miner., 53, pp. 88-104.

Wright, T.L., & Stewart, D.B., 1968: X-ray and optical study of alkali feldspar : I. Determination of composition and structural state from refined unit-cell parameters and 2V. Am. Miner., 53, pp. 38-87

Wyart, J., & Sabatier, G., 1959: Transformation des sédiments pelitiques à 800°C. sous une pression d'eau de 1800 bars et granitisation. Soc. française minéralogie et crystallographie Bull., 82, pp. 201-210.

Wyllie, P.J. & Tuttle, O.F., 1958: Hydrothermal experiments on the melting of shales. Am. geophys. Union Trans., 39, p. 537.

Wyllie, P.J., & Tuttle, O.F., 1961: Hydrothermal melting of shales. Geol. Mag., 98, pp. 56-66.

Yoder, H.S., & Eugster, H.P., 1955: Synthetic and natural muscovites. Geochim. cosmochim. Acta, 8, pp. 266-269.